VOLUME 22 (1961) No. 2

NUCLEAR PHYSICS

JOURNAL DEVOTED TO THE EXPERIMENTAL AND THEORETICAL STUDY OF THE FUNDAMENTAL CONSTITUENTS OF MATTER AND THEIR INTERACTIONS

EDITOR: L. ROSENFELD - COPENHAGEN

H. KÜMMEL, Compound pair states in imperfect Fermi gases 177
A. DE-SHALIT and J. D. WALECKA, Spectra of odd nuclei 184
A. V. EFREMOV, V. A. MESHCHERYAKOV, D. V. SHIRKOV and H. Y. TZU, On deriving equations from the Mandelstam representation 202
J. E. E. BAGLIN, M. N. THOMPSON and B. M. SPICER, Photodisintegration of Al^{27}. (I). Photoneutron cross section 207
J. E. E. BAGLIN, M. N. THOMPSON and B. M. SPICER, Photodisintegration of Al^{27}. (II). Theoretical 216
YU. A. BUDAGOV, S. WIKTOR, V. P. DZHELEPOV, P. F. YERMOLOV and V. I. MOSKALEV, Elastic scattering of negative pions by protons at 128 and 162 MeV 226
S. L. ANDERSEN, O. DØRUM, E. GAUTVIK and T. HOLTEBEKK, Resonance energies and half-widths for proton capture in sodium and phosphorus 245
V. N. GRIBOV, Asymptotic behaviour of the scattering amplitude at high energies 249
H. UMEZAWA and A. VISCONTI, A new Majorana field theory 262
RICHARD E. PRANGE, The moment of inertia of large superfluid fermion systems 283
ROBERT F. CHRISTY, Corrections to nuclear Q values resulting from atomic binding and excitation 301
SÖLVE HULTBERG, TOM O'CONNOR and JOSEPH H. HAMILTON, Angular distributions of photoelectrons ejected from uranium by 1.118 MeV gamma rays . . 306
E. Z. SKURNIK, B. ELBEK and M. C. OLESEN, Inelastic scattering from Th^{232} and U^{238} 316
J. DĄBKOWSKI and J. SAWICKI, The high energy optical model and nuclear forces 318
A. H. WAPSTRA and D. W. CONNOR, The persistence of nuclear polarization produced by the capture of polarized thermal neutrons 336
Erratum 339
Addendum and erratum 340

January 1961

NORTH-HOLLAND PUBLISHING COMPANY - AMSTERDAM

EDITORIAL BOARD

AUSTRALIA & NEW ZEALAND:	H. Messel (Sydney), M. L. Oliphant (Canberra)
AUSTRIA:	B. Karlik (Vienna), H. Thirring (Vienna)
BELGIUM:	M. de Hemptinne (Louvain), J. Verhaeghe (Ghent)
CANADA:	G. Volkoff (Vancouver)
DENMARK:	C. Møller (Copenhagen), S. Rozental (Copenhagen), G. E. Brown (Copenhagen)
FINLAND:	L. Simons (Helsinki)
FRANCE:	A. Berthelot (Saclay), S. Gorodetzky (Strasbourg)
GERMANY (DEM. REP.):	G. Hertz (Leipzig)
GERMANY (FED. REP.):	W. Gentner (Freiburg i. B.), J. H. D. Jensen (Heidelberg)
GREAT BRITAIN:	W. E. Burcham (Birmingham), T. H. R. Skyrme (Harwell)
HUNGARY:	L. Janossy (Budapest)
INDIA:	H. Bhabha (Bombay), R. Ramanna (Trombay)
IRISH REPUBLIC:	J. McConnell (Maynooth)
ISRAEL:	G. Racah (Jerusalem)
ITALY:	E. Amaldi (Rome)
JAPAN:	S. Kikuchi (Tokay), S. Tomonaga (Tokyo)
MEXICO:	M. Moshinsky (Mexico)
NETHERLANDS:	H. Brinkman (Groningen), S. R. de Groot (Leiden)
NORWAY:	E. Hylleraas (Oslo), A. Lundby (Oslo), H. Wergeland (Trondheim)
POLAND:	L. Infeld (Warsaw), J. Werle (Warsaw)
PORTUGAL:	J. M. Araújo (Porto), J. R. de Almeida Santos (Coimbra)
SOUTH AMERICA:	G. Beck (Saõ Paulo), J. Leite Lopes (Rio de Janeiro)
SPAIN:	J. M. Otero (Madrid), C. Sanchez del Rio (Madrid)
SWEDEN:	O. Klein (Stockholm), K. Siegbahn (Uppsala), I. Waller (Uppsala)
SWITZERLAND:	P. Huber (Basel), P. Scherrer (Zürich)
U.A.R. & ARAB COUNTRIES:	F. El Bedewi (Cairo), M. G. Nooh (Cairo)
U.S.A.:	H. H. Barschall (Madison, Wisconsin), S. Devons (New York), V. F. Weisskopf (Cambridge, Mass.)
U.S.S.R.:	M. A. Markov (Moscow), I. S. Shapiro (Moscow), D. V. Skobeltzyn (Moscow)
YUGOSLAVIA:	I. Supek (Zagreb)

CONTRIBUTIONS may be sent to the Editor, Professor L. Rosenfeld, NORDITA, Blegdamsvej 17, Copenhagen Ø, either directly, or preferably through the intermediary of one of the members of the Editorial Board of the country or region in which the author is working. They may be written in English, French or German.

NUCLEAR PHYSICS is published in fortnightly issues. The subscription price per volume of 700 pages is fl 57.00; 114s; $ 15.00. Post-free.

SUBSCRIPTIONS should be sent to the publishers, NORTH-HOLLAND PUBLISHING COMPANY P.O. Box 103, Amsterdam or to any subscription-agent.

BOOKS FOR REVIEW should be sent to Professor Rosenfeld.

No part of this issue may be reproduced in any form, by print, photoprint, microfilm or any other means without permission from the publisher.

Printed in the Netherlands

1.C

Nuclear Physics **22** (1961) 177—183; ©*North-Holland Publishing Co., Amsterdam*

Not to be reproduced by photoprint of microfilm without written permission from the publisher

COMPOUND PAIR STATES IN IMPERFECT FERMI GASES

H. KÜMMEL

Max-Planck-Institut für Chemie (Otto Hahn-Institut), Mainz, Germany

Received 29 September 1960

Abstract: The Bethe-Goldstone-equation is replaced by a rigorous nonlinear integro-differential equation determining the two particle correlations and the interaction energy. This nonlinear equation has been solved for vanishing total momentum and separable potential. The hole-hole and particle-hole interactions as well as the three and four particle clusters have been neglected. There are no singularities in this more rigorous equation. For those values of the two particle energy for which singularities occur, if one neglects the quadratic terms, the solutions are of "compound type", i.e. the localized part has a large (but finite) amplitude compared with the unperturbed plane wave.

1. Introduction

A serious drawback of the present systematic many fermion theories is the occurrence of singularities in the expression for the interaction energy derived using one of the customary perturbation methods [1]). They are due to bound pairs caused by the presence of the filled Fermi sphere with sharp edge. There are some arguments that the inclusion of special higher order contributions may restore finite results [2]). Especially the "diagrams of the wrong statistics" (diagrams with more than one line of the same momentum at the same "time") seem to be important. We shall see that this is the case indeed: the inclusion of the self consistent single particle energies for holes and particles makes the singular localized solutions of the Bethe-Goldstone equation nonlocal and finite. These contributions are of the type mentioned above. The derivation is very simple once one has the correct two particle equation, which necessarily is nonlinear. The points, for which the solutions of the ordinary Bethe-Goldstone equation are singular, are points of special interest: The corresponding solutions of the improved nonlinear equation have a large amplitude of the localized part compared with the unperturbed plane wave. They are long lived compound states of pairs of particles.

We shall use a separable potential. Furthermore, we neglect the hole-particle and hole-hole interactions, as well as the higher correlations. This seems to be justified in view of the unsuccessful attempt by Mehta [3]) to throw out the singularities by considering these terms (corresponding to his generalized ladder approximation). Presumably, they can be treated also in a similar manner by including quadratic terms and we expect to get finite results, too.

2. Two Body Equation

The ground state energy of the N-fermion system with volume Ω and density $\rho = N/\Omega$ interacting via the spin independent potential $V(x_i - x_k)$ (with range r_0) can be written rigorously

$$E = \frac{\Omega}{5\pi^2} p_F^5 + \tfrac{1}{2} \sum_{mm'} \int \mathrm{d}x_1 \mathrm{d}x_2 \varphi_m^*(1) \varphi_{m'}^*(2) V(12) (12|\chi_2|mm'), \tag{1}$$

with

$$\rho = \frac{p_F^3}{3\pi^2}. \tag{2}$$

We put $\hbar = 2m = 1$, denote the single particle states

$$\varphi_{\mathbf{k}}(\mathbf{x}_1) \equiv \varphi_k(1) \equiv \frac{1}{\sqrt{\Omega}} \mathrm{e}^{\mathrm{i}\mathbf{k}\cdot\mathbf{x}} u(s) \tag{3}$$

inside the Fermi sphere by labels $\mathbf{m}(|\mathbf{m}| \leqq p_F)$, outside by labels $\mathbf{l}(|\mathbf{l}| > p_F)$. The spins are included in $\mathbf{k}$ and $\mathbf{x}$, if convenient. The function $(12|\chi_2|mm')$ is the rigorous two body wave function

$$(12|\chi_2|mm') = \mathscr{A} \varphi_m(1) \varphi_{m'}(2) + (12|S_2|mm'), \tag{4}$$

where $\mathscr{A}$ denotes the antisymmetrization and the two body cluster function S_2 is solution of the following equation (written in momentum space, i.e. for $(l_1 l_2|S_2|m_1 m_2) \equiv \int \mathrm{d}x_1 \mathrm{d}x_2 \varphi_{l_1}^*(1) \varphi_{l_2}^*(2) (12|S_2|m_1 m_2)$):

$$\begin{aligned}
&(\varepsilon_{l_1} + \varepsilon_{l_2} - \varepsilon_{m_1} - \varepsilon_{m_2}) (l_1 l_2|S_2|m_1 m_2) + (l_1 l_2|V\chi_2|m_1 m_2) && \text{(a)} \\
&+ \sum_{ll'm} \{(ll'|S_2|mm_2)(mm_2|V|ll') \\
&\qquad + (ll'|S_2|m_1 m)(m_1 m|V|ll')\} (l_1 l_2|S_2|m_1 m_2) && \text{(b)} \\
&- \sum_{lmm'} \{(ll_2|S_2|mm')(mm'|V|ll_2) \\
&\qquad + (l_1 l|S_2|mm')(mm'|V|l_1 l)\} (l_1 l_2|S_2|m_1 m_2) && \text{(c)} \quad (5) \\
&- \mathscr{A} \sum_{lm} (ml_2|V|lm_2)(l_1 l|S_2|m_1 m) && \text{(d)} \\
&+ \tfrac{1}{2} \sum_{mm'} (l_1 l_2|S_2|mm')(mm'|V\chi_2|m_1 m_2) && \text{(e)} \\
&+ \tfrac{1}{2} \mathscr{A} \sum_{mm'll'} (mm'|V|ll')(l_1 l'|S_2|mm')(ll_2|S_2|mm_2) && \text{(f)} \\
&+ \text{terms with } S_3 \text{ and } S_4 = 0, && \text{(g)}
\end{aligned}$$

with the single particle energies

$$\varepsilon_k = k^2 + \sum_m \{(km|V|km) - (km|V|mk)\}. \tag{6}$$

Eq. (5) is a special case of the rigorous equations for general cluster functions S_n derived by the author [4]). The functions S_n are related to the complete wave function of the N-fermion system by

$$\begin{aligned}\psi(1,\ldots,N) = \frac{1}{\sqrt{N!}}\mathcal{A}\{&\varphi_{m_1}(1)\ldots\varphi_{m_N}(N) + (12|S_2|m_1m_2)\varphi_{m_3}(3)\ldots\varphi_{m_N}(N)\\ &+ (12|S_2|m_1m_2)(34|S_2|m_3\,m_4)\varphi_{m_5}(5)\ldots\varphi_{m_N}(N)\\ &+ (123|S_3|m_1m_2m_3)\varphi_{m_4}(4)\ldots\varphi_{m_N}(N)\\ &+\ldots+(1\ldots N|S_N|m_1\ldots m_N)\}.\end{aligned} \tag{7}$$

They describe n-particle correlations (or clusters) and can be represented by linked diagrams in the ordinary perturbation theory. Their linked property can be defined and proven also without use of perturbation expansions. They are orthogonal to the occupied states φ_m.

We did not write down the terms with S_3 and S_4; in any case, one has to neglect them, since the functions S_3 and S_4 are solutions of higher order equations and one has no method at hand to solve them (except for the hard core interaction).

In the low density limit $\rho r_0^3 \to 0$ only the first line (5a) remains, which is the Bethe-Goldstone equation without selfconsistent single particle potential. The divergencies resulting from the use of this equation suggest that one has interchanged the limiting process $\rho r_0^3 \to 0$ with the infinite summation of perturbation terms. This can be repaired by the inclusion of the most important higher order terms. The question arises which terms should be neglected and which not.

The terms (5b) resp. (5c) are correlation corrections to ε_l resp. ε_m. (5d), (5e) and (5f) represent hole-particle, hole-hole and interactions with more intermediate particles and holes. We tend to neglect them by the reason we mentioned in the introduction. They would make the situation more complicated without yielding new insight.

Then we are left with eq. (5a, b, c). The self consistent contributions to single particle energies (5b) and (5c) are represented by the diagrams of fig. 1 and fig. 2 †.

† The self consistent single particle potentials outside the Fermi sphere are *not* identical with the corresponding K-matrix expression (for *particles*). However, we believe that one should express all things in terms of S_n-functions, since the S_n are defined independently of any perturbation expansion, whereas it is not always possible to express quantities in terms of the K-matrix without referring to perturbation theory. We add the remark that the contributions to (5b) are small by a factor $(hp_F)^3$ (h = healing distance) compared with the other terms. Therefore it is likely that one may drop the single particle energy corrections outside the Fermi sphere, i.e. we may drop the terms with $D^{lm}_{m'}$ in the third section.

After separation of the centre of mass motion we get for the special case $\mathbf{m}_1+\mathbf{m}_2=0$:

$$
\begin{aligned}
&2(\varepsilon_l-\varepsilon_m)(l|S|m;\,0)+(l|V|m)+\sum_{l'}(l|V|l')(l'|S_2|m;\,0)\\
&+\sum_{m'l'}\{(\mathbf{m}'-\tfrac{1}{2}(\mathbf{l}'+\mathbf{1})|V|\tfrac{1}{2}(\mathbf{l}-\mathbf{l}'))(\tfrac{1}{2}(\mathbf{l}-\mathbf{l}')|S_2|\mathbf{m}'-\tfrac{1}{2}(\mathbf{l}'+\mathbf{1});\mathbf{l}'+\mathbf{1})\\
&+(\mathbf{m}'-\tfrac{1}{2}(\mathbf{l}'-\mathbf{1})|V|\tfrac{1}{2}(\mathbf{l}+\mathbf{l}'))(\tfrac{1}{2}(\mathbf{l}+\mathbf{l}')|S_2|\mathbf{m}'-\tfrac{1}{2}(\mathbf{l}'-\mathbf{1});\mathbf{l}'-\mathbf{1})\}(l|S_2|m;\,0) \qquad (8)\\
&-\sum_{m'l'}\{(\tfrac{1}{2}(\mathbf{m}-\mathbf{m}')|V|\mathbf{l}'-\tfrac{1}{2}(\mathbf{m}'+\mathbf{m}))(\mathbf{l}'-\tfrac{1}{2}(\mathbf{m}+\mathbf{m}')|S_2|\tfrac{1}{2}(\mathbf{m}-\mathbf{m}');\mathbf{m}'+\mathbf{m}))\\
&+(\tfrac{1}{2}(\mathbf{m}'+\mathbf{m})|V|\mathbf{l}'-\tfrac{1}{2}(\mathbf{m}'-\mathbf{m}))(\mathbf{l}'-\tfrac{1}{2}(\mathbf{m}'-\mathbf{m})|S_2|\tfrac{1}{2}(\mathbf{m}'+\mathbf{m});\mathbf{m}'-\mathbf{m})\}(l|S_2|m;\,0)=0,
\end{aligned}
$$

with

$$(l_1l_2|S_2|m_1m_2)=\delta_{\mathbf{l}_1+\mathbf{l}_2-\mathbf{m}_1-\mathbf{m}_2}(\tfrac{1}{2}(\mathbf{l}_1-\mathbf{l}_2)|S_2|\tfrac{1}{2}(\mathbf{m}_1-\mathbf{m}_2);\mathbf{m}_1+\mathbf{m}_2) \qquad (9)$$

and

$$(k|S_2|m_j\,0)=0 \quad \text{for} \quad |\mathbf{k}|\leqq p_F. \qquad (10)$$

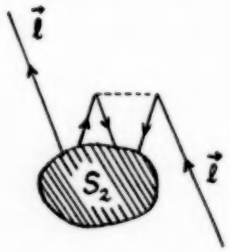

Fig. 1. Diagram contributing to eq. (5b).

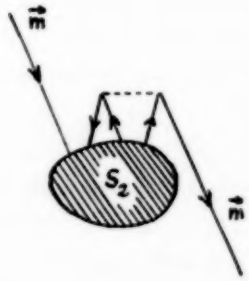

Fig. 2. Diagram contributing to eq. (5c).

Unfortunately, there are couplings to functions with total momentum different from zero. Several authors have assumed that the results do not change very much, if one always puts the total momentum equal to zero in the two particle functions. If we do so, we get

$$
\begin{aligned}
&2(\varepsilon_l-\varepsilon_m)(l|S_2|m;\,0)+(l|V|m)+\sum_{l'}(l|V|l')(l'|S_2|m;\,0)\\
&+\sum_{m'}\sum_{l'}\{(\mathbf{m}'-\tfrac{1}{2}(\mathbf{l}'+\mathbf{1})|V|\tfrac{1}{2}(\mathbf{l}-\mathbf{l}'))\\
&\qquad+(\mathbf{m}'-\tfrac{1}{2}(\mathbf{l}'-\mathbf{1})|V|\tfrac{1}{2}(\mathbf{l}-\mathbf{l}'))\}(l|S_2|m';\,0)(l|S_2|m;\,0) \qquad (11)\\
&-\sum_{l'}\sum_{m'}\{(\tfrac{1}{2}(\mathbf{m}-\mathbf{m}')|V|\mathbf{l}'-\tfrac{1}{2}(\mathbf{m}+\mathbf{m}'))\\
&\qquad+(\tfrac{1}{2}(\mathbf{m}-\mathbf{m}'|V|\mathbf{l}'-\tfrac{1}{2}(\mathbf{m}'-\mathbf{m}))\}(l'|S_2|m_j\,0)(l|S|m;\,0)=0.
\end{aligned}
$$

Here we have used the antisymmetry of S_2 in l_1l_2 and m_1m_2 (i.e. $(\mathbf{l}|S_2|\mathbf{m};\,0)=-(-\mathbf{l}|S_2|\mathbf{m};\,0)$ etc.). Finally, we introduce the separable

potential

$$(k_1 k_2|V|k'_1 k'_2) = \delta_{\mathbf{k}_1+\mathbf{k}_2-\mathbf{k}'_1-\mathbf{k}'_2}\lambda v(|\tfrac{1}{2}(\mathbf{k}_1-\mathbf{k}_2)|)v(|\tfrac{1}{2}(\mathbf{k}'_1-\mathbf{k}'_2)|), \tag{12}$$

with

$$v(|\mathbf{k}|) \geqq 0, \tag{13}$$

and have the following equation for S_2:

$$\begin{aligned} &2(\varepsilon_l-\varepsilon_m)(l|S|m)+\lambda v(l)v(m)+\lambda v(l)\sum_{l'} v(l')(l'|S|m) \\ &+\lambda\sum_{m'}\sum_{l'}\sum_{\pm}\{v(|\tfrac{1}{2}(\mathbf{l}-\mathbf{l}')|)v(|\mathbf{m}'-\tfrac{1}{2}(\mathbf{l}\pm\mathbf{l}')|)(l|S|m') \\ &-v(|\tfrac{1}{2}(\mathbf{m}-\mathbf{m}'|)v(|\mathbf{l}'-\tfrac{1}{2}(\mathbf{m}\pm\mathbf{m}'|)(l'|S|m)\{(l|S|m) = 0. \end{aligned} \tag{14}$$

Here we have dropped the dependence on the total momentum.

3. Solution of the Two Body Equation

Putting in (14)

$$(l|\hat{S}|m) \equiv 2(\varepsilon_l-\varepsilon_m)(l|S|m),$$

we have

$$\begin{aligned} &(l|\hat{S}|m)+\lambda v(l)v(m)+\lambda v(l)\sum_{l'} v(l')\frac{(l'|\hat{S}|m)}{2(\varepsilon_{l'}-\varepsilon_{m'})} \\ &+\lambda\sum_{l'm'\pm}\left\{v(|\tfrac{1}{2}(\mathbf{l}-\mathbf{l}')|)v(|\mathbf{m}'-\tfrac{1}{2}(\mathbf{l}\pm\mathbf{l}')|)\frac{(l|\hat{S}|m')}{\varepsilon_l-\varepsilon_{m'}}\right. \\ &\left.-v(|\tfrac{1}{2}(\mathbf{m}-\mathbf{m}')|)v(|\mathbf{l}'-\tfrac{1}{2}(\mathbf{m}\pm\mathbf{m}')|)\frac{(l'|\hat{S}|m)}{\varepsilon_{l'}-\varepsilon_m}\right\}\frac{(l|\hat{S}|m)}{2(\varepsilon_l-\varepsilon_m)} = 0. \end{aligned} \tag{15}$$

With the substitution

$$(l|\hat{S}|m) = C_{lm}v(l)v(m) \tag{16}$$

and the definitions

$$1+\tfrac{1}{2}\lambda\sum_{l'}\frac{v^2(l')}{\varepsilon_{l'}-\varepsilon_m} \equiv A_m, \tag{17}$$

$$\sum_{l'\pm}\frac{v(|\tfrac{1}{2}(\mathbf{l}-\mathbf{l}')|)v(|\mathbf{m}'-\tfrac{1}{2}(\mathbf{l}\pm\mathbf{l}')|)v(m')v(l)}{2(\varepsilon_l-\varepsilon_m)(\varepsilon_{l'}-\varepsilon_m)} \equiv D^{lm}_{m'}, \tag{18}$$

$$\sum_{m'\pm}\frac{v(|\tfrac{1}{2}(\mathbf{m}-\mathbf{m}')|)v(|\mathbf{l}'-\tfrac{1}{2}(\mathbf{m}\pm\mathbf{m}')|)v(l')v(m)}{2(\varepsilon_l-\varepsilon_m)(\varepsilon_l-\varepsilon_{m'})} \equiv B^{lm}_{l'}, \tag{19}$$

we have the coupled set of quadratic equations

$$A_m C_{lm}+\lambda+\lambda C_{lm}\{\sum_{m'} D^{lm}_{m'}C_{lm'}-\sum_{l'} B^{lm}_{l'}C_{l'm}\} = 0. \tag{20}$$

Presumably, it will be impossible to get the rigorous solution of (20). Therefore we propose the following approximation method, based on the fact that the quadratic terms are small in the low density limit. So, there is some hope that it suffices to handle them approximately. The main problem are the coupling terms. Therefore we consider all terms with $C_{lm'}$ and $C_{l'm}$ for $m' \neq m$ and $l' \neq l$ as small. The first order solution is

$$C_{lm}^{(1)} = \frac{A_m}{2\lambda(B_l{}^{lm} - D_m{}^{lm})} \pm \sqrt{\left(\frac{A_m}{2\lambda(B_l{}^{lm} - D_m{}^{lm})}\right)^2 + \frac{1}{B_l{}^{lm} - D_m{}^{lm}}}. \tag{21}$$

To get the second order, we use the eq. (20) in the approximate form

$$A_m C_{lm} + \lambda + \lambda C_{lm}^2 (D_m{}^{lm} - B_l{}^{lm}) + \lambda C_{lm}\{\sum_{m' \neq m} D_{m'}^{lm} C_{lm'}^{(1)} - \sum_{l' \neq l} B_{l'}^{lm} C_{l'm}^{(1)}\} = 0, \tag{22}$$

and have

$$C_{lm}^{(2)} = \frac{A_{lm}^{(1)}}{2\lambda(B_l{}^{lm} - D_m{}^{lm})} \pm \sqrt{\left(\frac{A_m{}^{(1)}}{2\lambda(B_l{}^{lm} - D_m{}^{lm})}\right)^2 + \frac{1}{B_l{}^{lm} - D_m{}^{lm}}}, \tag{23}$$

with

$$A_{lm}^{(1)} \equiv A_m + \lambda\{\sum_{m' \neq m} D_{m'}^{lm} C_{lm'}^{(1)} - \sum_{l' \neq l} B_{l'}^{lm} C_{l'm}^{(1)}\}. \tag{24}$$

In this manner we can proceed to any given order.

Let us discuss the solutions for the more critical attractive potential ($\lambda < 0$). In this case there always exists a value $|\mathbf{m}| = m_0$ for which

$$A_{m_0} = 0 \tag{25}$$

(in the limit $N \to \infty$, $\Omega \to \infty$ and ρ finite). Therefore, the Bethe-Goldstone equation resulting from (20) by neglecting the quadratic terms has the well known Cooper singularity for $|m| = m_0$, since then

$$C_{lm}^{(0)} = -\frac{\lambda}{A_m}. \tag{26}$$

The same cannot be said about our more rigorous equation. Apparently we must use the minus sign in order to get finite solutions for $\lambda \to -0$. In general, the solutions C_{lm} will not be singular: $C_{lm}^{(1)}$ is singular only if $A_m = 0$ *and* $B_l{}^{lm} - D_m{}^{lm} = 0$ (for the *same* $m = m_0$). *Two* conditions for $v(k)$ have to be satisfied and this will happen for very special potentials only. It never happens for $v(l) \neq v(m)$ or if the healing distance is small $(k_F)^3 \ll 1$). The same can be said — with slight changes — for all higher orders. If the function $v(k)$ is such, that $B_{l'}{}^{lm} \approx \delta_{ll'}$ and $D_{m'}^{lm} \approx \delta_{mm'}$ the set is decoupled and the discussion is even simpler.

On the other hand, the localized part S_2 of the two particle wave function is large for $|\mathbf{m}| \approx m_0$. This is why we may say that we have compound pair states instead of bound pair (Cooper) states. The probability for two particles

being near together is very large for $|\mathbf{m}| \approx m_0$, but the pair decays after a finite time.

4. Discussion of the Result

We have seen that the singularities arise indeed from an interchange of two limiting procedures. More precisely, the perturbation series does not exist. As is clear from (21), the rigorous expression for the wave function (and the energy) is a non analytic function of the coupling constant λ and the expansion into integral powers of λ does not converge. The same conclusion was reached by other authors for other problems [5, 6]). In these papers, the perturbation series is rearranged such that the results are finite and it is believed that this procedure yields meaningful answers. Also other papers dealing with the Fermi gas yield finite results. They either employ the Greens function method [7, 8]), which is more general, however more complicated than our method and does not yield the energy in a simple manner, or less systematic methods [9, 10]), which can be treated quite easily.

One must expect that in higher order calculations the singularities reappear again. But, in view of the success of our method, one should always be able to make the singularities finite, as we did. However, there is no guarantee that the approximations become better just by the inclusion of terms which help to get finite results. This point has been discussed by Martin and Schwinger [11]).

Unfortunately, our method, is not suitable for the investigation of the energy spectrum. The occurrence of compound states seems to favour the energy gap, although there may be a small finite density between the anomalous ground state and the normal states.

I wish to thank Dr. E. J. Squires for remarks concerning the first draft of this paper.

References

1) L. N. Cooper, Phys. Rev. **104** (1956) 1353;
A. Bohr, B. R. Mottelson and D. Pines, Phys. Rev. **110** (1958) 936;
J. Goldstone, Thesis, Cambridge University;
K. Gottfried, CERN report (unpublished);
L. Van Hove, Lecture at the Int. Spring School of Physics, Naples, 1960
2) C. Bloch and C. De Dominicis, Nuclear Physics **10** (1959) 509;
A. Katz, Lecture at the Int. Spring School of Phys., Naples, 1960
3) M. L. Mehta, preprint, 1960
4) H. Kümmel, Lecture at the Int. Spring School of Physics, Naples 1960;
F. Coester and H. Kümmel, Nuclear Physics **17** (1960) 477
5) List of references in T. D. Lee and C. N. Yang, Phys. Rev. **117** (1960) 12
6) M. Gell-Mann and K. A. Brueckner, Phys. Rev. **106** (1957) 364
7) R. Prange, preprint 1959
8) W. Wild, Z. Phys. **128** (1960) 322
9) N. N. Bogoliubov, V. V. Tolmacev and D. V. Shirkov, New method in the theory of superconductivity (Moscow, 1958)
10) J. Bardeen, L. Cooper and J. R. Schrieffer, Phys. Rev. **108** (1957) 1175
11) P. C. Martin and J. Schwinger, preprint 1960

1.D.1:
1.E.1

Nuclear Physics **22** (1961) 184—201; ©*North-Holland Publishing Co., Amsterdam*
Not to be reproduced by photoprint or microfilm without written permission from the publisher

SPECTRA OF ODD NUCLEI

A. DE-SHALIT † and J. D. WALECKA

Institute of Theoretical Physics, Department of Physics, Stanford University, Stanford, California ††

Received 31 August 1960

Abstract: A general discussion of the spectra of odd nuclei is presented. For this purpose it was found useful to develop a new method for the calculation of energy levels. An explicit expression is derived for the distribution of the relative angle of the two particles, properly weighted according to the spin-dependence of the interaction. With the help of these expressions the general structure of spectra of odd nuclei can be more clearly seen. In particular the modified Nordheim rules are seen to hold quite generally, and it is found that for configurations containing a half-filled shell the lowest state has an even or odd J according to whether its parity is odd or even.

1. Introduction

Odd nuclei have attained an increasing interest in recent years. Although they are slightly more difficult to produce, the amount of information one can obtain from them is considerably greater than from odd-mass or even nuclei. Thus, excitations in odd-mass nuclei are mostly associated with the transition of the odd particle from one state to another and consequently only its average interaction with the rest of the nucleons is involved. In even nuclei, one very rarely sees the complete set of excited states of the ground state configuration, and even when one does, the order of levels 0^+, 2^+ . . . hardly teaches us anything about the nature of the residual nuclear interaction. In addition, there is usually the difficulty of collective excitations whose energy is comparable to or even lower than that required to excite the ground state configuration.

The effective residual proton-neutron interaction is relatively weak. As a result, it takes relatively little energy to produce the excited states of the ground state configuration in an odd nucleus. In many cases this energy is even less than the energy required to excite an odd nucleon to the next single particle state. Under such circumstances the first few low-lying states in an odd nucleus all belong to the same configuration, and can supply us with valuable information.

The calculation of the energy of the low-lying nuclear states is usually done by estimating the diagonal part of the interaction taken with wave functions

† On leave from the Weizmann Institute of Science, Rehovoth, Israel.

†† Work supported in part by the United States Air Force through the Air Force Office of Scientific Research.

of a definite total angular momentum. For two-particle systems this amounts to the diagonalization of the Hamiltonian within a configuration $(j_1 j_2)$ and neglecting all configuration mixtures.

If $j_1 < j_2$ then the interaction between a proton, say, in j_1, and a neutron in j_2 is entirely determined in terms of $2j_1+1$ multipoles. In fact, every interaction can be decomposed into a sum of multipole-multipole interactions. However, for a nucleon in an orbit j all multipole moments of order $k > 2j+1$ vanish. Hence, at most $2j_1+1$ multipoles are effective in the interaction between the nucleons in j_1 and j_2 $(j_1 < j_2)$. The configuration (j_1, j_2) has also got $2j_1+1$ states with $J = j_2-j_1, \ldots, J = j_2+j_1$. Hence, if we know all the states of the configuration (j_1, j_2) we can generally determine the strength of all the relevant multipoles which play a role in the interaction between two such nucleons. Having done this, we can proceed to configurations like (j_1^3, j_2) or (j_1, j_2^3) etc. The proton-neutron interactions in these configurations are uniquely determined by the strength of the various multipoles deduced from (j_1, j_2), and the structure of such configurations can therefore give us a possibility of testing the underlying model.

Furthermore, the availability of experimental data on a number of states belonging to the same configuration enables us also to study the nature of the electro-magnetic moments of each of the nucleons. It is an easy matter to see that all static moments of order k, as well as the transition moments of the same order, are given in terms of two effective single-particle moments of that order as long as we confine ourselves to states of the same odd configuration. Thus, it ought to be possible, if the model we are using is valid, to express all M1 transition probabilities as well as magnetic moments, within the $2j_1+1$ states of the configuration (j_1, j_2) in terms of just two quantities: the effective magnetic moment of the nucleon in j_1 and that of the nucleon in j_2. Such tests, besides checking the validity of the underlying model, may perhaps lead to a better understanding of the nature of effective moments and charges.

With various such possibilities in mind, we try in this paper to analyze the structure of configurations of odd nuclei in order to see which of their features are more sensitive to the nature of the proton-neutron interaction, and which result from some general properties of these interactions.

To be able to do any simple calculation we shall have to specify our states more closely. For this purpose we shall use the odd-group model, in which states of the configuration (j_1^p, j_2^n) are specified not only by the total angular momentum J, but also by the total angular momentum J_p of the proton group and that of the neutrons, J_n. Some valid objections [1]) have been raised against this model pointing out its clear failure to predict the level structure of K^{42}. However, explicit calculations [2]) show that in many cases the lowest proton and neutron seniorities have a big amplitude in the wave function of a given nuclear state, whereas the admixtures of other values of J_p and J_n are quite

small. Also the modified Nordheim rule formulated by Brennan and Bernstein [3]) seems to indicate that the association of definite values of J_p and J_n with the ground states of odd nuclei is physically meaningful. We should expect J_p and J_n to be good quantum numbers for an odd nucleus if V_{pn} is much weaker than V_{pp} or V_{nn}. Although V_{pn} is certainly not weaker than V_{pp} or V_{pn}, by an order of magnitude, the spread in energy of odd configurations does seem to be smaller than that of odd-mass or even configurations. It seems, therefore, that V_{pn} is at least somewhat weaker than V_{pp} and V_{nn}, and this may explain the apparent validity of J_p and J_n as approximate quantum numbers in many cases. We shall, therefore, write our states as $|j_1^p(J_p)j_2^n(J_n)J\rangle$ and consider, in determining the energies, only matrix elements diagonal in J_p and J_n.

For the proton-neutron interaction we shall assume the general form

$$V_{pn} = V_0(r_1, r_2, \cos\omega_{12}) + \boldsymbol{\sigma}_1 \cdot \boldsymbol{\sigma}_2 V_1(r_1, r_2, \cos\omega_{12}). \tag{1}$$

Here V_0 and V_1 are not necessarily functions of $|\mathbf{r}_1 - \mathbf{r}_2|$, but we do require that their angular dependence will involve only the angle ω_{12} between $\mathbf{r}_1$ and $\mathbf{r}_2$ and not the directions of $\mathbf{r}_1$ and $\mathbf{r}_2$ separately. This ensures the spherical symmetry of the problem. We do not include charge and space exchange forces since, for heavy nuclei, when the protons and neutrons occupy different orbits, such forces lead to vanishing results.

Both V_0 and V_1 turn out to be attractive interactions when experimental results are compared with theoretical calculations. Although this resembles the free proton-neutron interaction, it should be stressed that the validity of this statement for the *residual* interaction V_{pn} is not an abvious consequence. V_{pn} takes into account the fact that a fair portion of the real proton-neutron interaction is taken up by the central field and possibly the single-particle spin-orbit interaction. It represents, therefore, only the difference between the actual interaction and the average single particle potentials.

For many purposes it is convenient to use Slater's method of calculating expectation values of V_{pn}. In this method V_{pn} is decomposed into its multipoles and each multipole is handled separately. For our purposes it will, however, be more convenient to use a new approach. Rather than separating V_{pn} into its multipoles, we derive the probability $a^J(\cos\omega_{12})$ for the angle variable ω_{12} in $|j_1^p(J_p)j_2^n(J_n)J\rangle$. The energy of the corresponding state is then given by

$$E_J = \tfrac{1}{2}\int a^J(\cos\omega_{12})\mathrm{d}(\cos\omega_{12}) \int R_1^2(r_1)R_2^2(r_2)V_{pn}\,\mathrm{d}r_1\,\mathrm{d}r_2.$$

Both methods are simply related to each other, the second method being sometimes more convenient for the derivation of more general results.

2. Odd Nuclei With One Half-Filled Shell

As was pointed out by Schwartz [4]), V_0 and $\boldsymbol{\sigma}_1 \cdot \boldsymbol{\sigma}_2 V_1$ contribute in a different way to the energy of a system of p protons and n neutrons. Because of parity conservation, expectation values of odd-spatial multipoles vanish. Thus, only the even spatial multipoles of V_0 and V_1 contribute to the interaction energy in the configuration $(j_1^p j_2^n)$. Since V_1 is multiplied by $\boldsymbol{\sigma}_1 \cdot \boldsymbol{\sigma}_2$, it turns out that $\boldsymbol{\sigma}_1 \cdot \boldsymbol{\sigma}_2 V_1$ contributes to the interaction only via *odd* tensors [5, 6]) (even space multipoles combined with the *odd* tensor $\boldsymbol{\sigma}$ to form an odd overall spin-space multipole). In the seniority scheme the expectation values of an odd tensor operator are independent of the number of particles (the magnetic moment operator is a well-known example, its expectation values $\langle j^n v J|\mu|j^n v J\rangle$ being independent of n for a given J and v). On the other hand, the expectation values of an even tensor change linearly with the number of particles, inverting its sign as it passes through the middle of the shell (the quadrupole moment operator is a well-known example, $\langle j^n v|Q|j^n v J\rangle$ being proportional to $2j+1-2n$ for a given v and J). The different p and n dependence of $\langle j_1^p j_2^n J|V_0|j_1^p j_2^n J\rangle$ and $\langle j_1^p j_2^n J|\boldsymbol{\sigma}_1 \cdot \boldsymbol{\sigma}_2 V_1|j_1^p j_2^n J\rangle$ stems from these properties of even and odd tensors.

If either p or n correspond to a half-filled shell, then expectation values of the corresponding even ($\neq 0$) tensors vanish. It follows that in this case $\langle j_1^p j_2^n J|V_0|j_1^p j_2^n J\rangle$ has a contribution only from the monopole part of the proton-neutron interaction. Monopoles, being spherically symmetric, lead to the same interaction for any value of J. Therefore if, say $p = \frac{1}{2}(2j_1+1)$ then V_0 does not contribute anything to the *splitting* between the different states of $(j_1^p j_2^n)$. In other words, the splitting of levels of a given configuration in odd nuclei with one half-filled shell is entirely due to the effect of $\boldsymbol{\sigma}_1 \cdot \boldsymbol{\sigma}_2 V_1$. Such nuclei form, therefore, a convenient sample for the study of the spin-dependent part of the interaction, completely separated from the effects of the spin-independent part.

The simplest of these cases is the one in which the proton or neutron is in $s_{\frac{1}{2}}$ and $p = 1$(or $n = 1$). In this case, the configuration (j_1, j_2), for instance, has two states, $J = j_2+\frac{1}{2}$ and $J = j_2-\frac{1}{2}$. The splitting of these two levels is determined by

$$\langle \tfrac{1}{2} j_2 J|\boldsymbol{\sigma}_1 \cdot \boldsymbol{\sigma}_2 V_1|\tfrac{1}{2} j_2 J\rangle.$$

Since a spin-independent interaction leads to no splitting in this case, we can calculate the splitting equally well by considering

$$\langle \tfrac{1}{2} j_2 J|(\boldsymbol{\sigma}_1 \cdot \boldsymbol{\sigma}_2 - 1) V_1|\tfrac{1}{2} j_2 J\rangle. \tag{2}$$

The operator $(\boldsymbol{\sigma}_1 \cdot \boldsymbol{\sigma}_2 - 1)$ is diagonal in the total spin $\mathbf{S} = \mathbf{s}_1+\mathbf{s}_2$, vanishes for $S = 1$, and equals -4 for $S = 0$. It is obvious that since $l_1 = 0$ we must have $\mathbf{l}_2+\mathbf{S} = \mathbf{J}$. Hence, if $J \neq l_2$ we cannot have $S = 0$. It follows that (2) vanishes

for $J \neq l_2$. Since $\boldsymbol{\sigma}_1 \cdot \boldsymbol{\sigma}_2 - 1$ is repulsive for $S = 0$, we see that, if V_1 is an attractive interaction, and if $l_1 = 0$, then

$$\langle \tfrac{1}{2} j_2 J | (\boldsymbol{\sigma}_1 \cdot \boldsymbol{\sigma}_2 - 1) V_1 | \tfrac{1}{2} j_2 J \rangle \begin{cases} > 0 & \text{if} \quad J = l_2, \\ = 0 & \text{if} \quad J \neq l_2. \end{cases} \tag{3}$$

The lowest of the two states $J = j_2 + \frac{1}{2}$ and $J = j_2 - \frac{1}{2}$ will therefore have $J \neq l_2$. The parity of this configuration is $(-1)^{l_1+l_2} = (-1)^{l_2}$; hence, the parity of the ground state of the configuration $(j_1 j_2)$ when $l_1 = 0$ is $(-1)^{J+1}$. For such configurations we therefore expect to find ground states with an odd value of J if the parity is positive and even value of J if the parity is negative.

As we shall see in the next sections, this rule holds for any odd number of particles in j_2 if they are coupled to lowest seniority. It is also fairly easy to see that if $l_1 = 1$, $j_1 = \frac{1}{2}$ (i.e., a proton in a $p_{\frac{1}{2}}$ orbit), the state with $J = l_2$ is the lowest one, so that again its parity is $(-1)^{J+1}$. Thus, with the sole assumption that V_1 in (1) is attractive we can formulate the following rule:

> In the odd configuration $(j_1, j_2^n[J_n = j_2])$ in which $j_1 = \frac{1}{2}$, the ground state total angular momentum has even or odd values of J according to whether the parity of the configuration is negative or positive.

There are many cases in which this rule can be checked. Practically no exceptions are known. In the region of $40 \leqq Z \leqq 50$ and $N \geqq 50$, for instance, it is expected that all low-lying odd configurations with negative parity involve a $p_{\frac{1}{2}}$ proton, since for $N \geqq 50$ the neutron states have positive parities and the available proton states for $40 \leqq Z \leqq 50$ are $p_{\frac{1}{2}}$ and $g_{\frac{9}{2}}$. Indeed, one finds that lowest states of odd parity in odd nuclei in this region all have even values of J. In another region, the low-lying states of the odd Tl isotopes most probably involve an $s_{\frac{1}{2}}$ proton coupled to various neutron orbits. Again we find that the lowest states of negative parity have even values of J, whereas the lowest states of positive parity have odd values of J.

The doublet splitting $\delta E = [E(J = j_2 + \frac{1}{2}) - E(J = j_2 - \frac{1}{2})]$ in the configuration $(j_1 j_2)$ with $j_1 = s_{\frac{1}{2}}$ can serve to estimate the strength of the spin-dependent interaction in (1). As can be very easily seen (see following section), this splitting is given by

$$\delta E = \frac{2j_2 + 1}{2l_2 + 1} \int R^2_{n_1 l_1}(r_1) R^2_{n_2 l_2}(r_2) V_1(r_1, r_2, \cos \omega_{12}) \mathrm{d}(\cos \omega_{12}) \mathrm{d}r_1 \, \mathrm{d}r_2. \tag{4}$$

In Tl^{208}, for instance, there is a good reason to believe [7]) that the ground state and the first excited state form the doublet $(s_{\frac{1}{2}} g_{\frac{9}{2}})$. Their splitting is 40 keV. In Tl^{198} and Tl^{196} a doublet was found [8]), composed of two levels with $J = 2^-$ and $J = 3^-$, 23 and 34 keV apart respectively. Since the M1 transition between these levels competes very favourably with the much more energetic M1 transition to the ground state, it is reasonable to assume that these doublets are the states of the configuration $(s_{\frac{1}{2}}, f_{\frac{5}{2}})$. The ground state would then belong

to the configuration $(s_{\frac{1}{2}} p_{\frac{3}{2}})$, and consequently the ground state M1 is Δl forbidden, whereas the M1 transition between the two states $(s_{\frac{1}{2}} f_{\frac{5}{2}})_{J=3}$ and $(s_{\frac{1}{2}} f_{\frac{5}{2}})_{J=2}$ can proceed without any hindrance.

Taking the above values for the doublet splittings in the even-mass isotopes of Tl we obtain from (4)

$$\int V_1 R_{3s}^2(r_1) R_{2g}^2(r_2) \mathrm{d}r_1 \mathrm{d}r_2 = 36 \text{ keV},$$

$$\int V_1 R_{3s}^2(r_1) R_{2f}^2(r_2) \mathrm{d}r_1 \mathrm{d}r_2 = 32 \text{ keV}.$$

The close fit between these two numbers is remarkable. If $V_1 = g_1 \delta(\mathbf{r}_1 - \mathbf{r}_2)$, then, using harmonic oscillator wave functions, one expects [9]), in arbitrary units,

$$\int V_1 R_{3s}^2(r_1) R_{2g}^2(r_2) \mathrm{d}r_1 \mathrm{d}r_2 = 8,$$

$$\int V_1 R_{3s}^2(r_1) R_{2f}^2(r_2) \mathrm{d}r_1 \mathrm{d}r_2 = 10.$$

For an infinite range, the two integrals reduce to the normalization integrals and are thus equal to each other.

The observed doublet splitting seems to be roughly the same also for very light nuclei. Thus, in Al^{28} we find the doublet $(d_{\frac{5}{2}} s_{\frac{1}{2}})$ with a splitting of 31 keV, and in P^{32} the doublet $(s_{\frac{1}{2}} d_{\frac{3}{2}})$ has a splitting of 77 keV. The full meaning of this approximate constancy of the doublet splitting † is not too clear. However, it is obvious from the observed values of these splittings that V_1, or at least its monopole part, is a very weak interaction. From binding energies of odd nuclei it is possible to estimate also V_0. It turns out [4, 6, 9]) that $V_0 \approx 10 V_1$, so that for the residual proton-neutron interaction we have $V_t \approx 1.6 V_s$.

In the following section we shall proceed to derive more detailed formulae for the energy levels of odd nuclei. Some of these relations were given previously [11]), in an attempt to explain the modified Nordheim Rule [3]). Here we shalll present a somewhat different approach which may indicate more clearly the general features obtained before [11]).

3. The Energy Levels Of Odd-Odd Nuclei

Let us consider the two-particle configuration $(j_1 j_2)$ with a Wigner interaction $V_0(r_1, r_2 \cos \omega_{12})$ between them. Expanding V_0 in Legendre polynomials we have, as is well known,

$$\langle j_1 j_2 J | V_0 | j_1 j_2 J \rangle = \sum_K (-1)^{j_1 + j_2 + J} \begin{Bmatrix} j_1 j_2 J \\ j_2 j_1 K \end{Bmatrix} F_K (j_1 \| C^{(K)} \| j_1)(j_2 \| C^{(K)} \| j_2). \quad (5)$$

† Cohen and Price [10]) find evidence for other doublets, with a splitting of ≈ 60 keV, in the mass region 85—135.

Here, F_K is the Slater integral

$$F_K = \frac{2K+1}{2}\int P_K(\cos\omega_{12})V_0(r_1, r_2, \cos\omega_{12})R^2_{n_1l_1}(r_1)R^2_{n_2l_2}(r_2)\mathrm{d}r_1\mathrm{d}r_2\mathrm{d}(\cos\omega_{12}) \quad (6)$$

and (see ref. [12]))

$$C_q^{(K)} = \sqrt{\frac{4\pi}{2K+1}}\,Y_{K,q}.$$

Eq. (5) is very convenient for the calculation of the energy levels of the configuration (j_1j_2). For the description of general properties of this configuration it may be more convenient to define new functions, to be called the angular-ordering functions:

$$\begin{aligned} a^J_{j_1j_2}(x) &= \sum_K (-1)^{j_1+j_2+J}(2K+1)\begin{Bmatrix} j_1 j_2 J \\ j_2 j_1 K\end{Bmatrix}(j_1\|C^{(K)}\|j_1)(j_2\|C^{(K)}\|j_2)P_K(x) \\ &= (-1)^{J+1}(2j_1+1)(2j_2+1)\sum_{\substack{\text{even } K \\ K\le \min(2j_1,\,2j_2)}}(2K+1)\begin{Bmatrix} j_1 j_2 J \\ j_2 j_1 K\end{Bmatrix} \\ &\quad\times\begin{pmatrix} j_1 K j_1 \\ \frac{1}{2}\,0\,-\frac{1}{2}\end{pmatrix}\begin{pmatrix} j_2 K j_2 \\ \frac{1}{2}\,0\,-\frac{1}{2}\end{pmatrix}P_K(x). \end{aligned} \quad (7)$$

The last step was obtained by using the explicit formulae [13]) for the reduced matrix elements of $C^{(K)}$. With the help of these functions (5) can be written as

$$\langle j_1j_2J|V_0|j_1j_2J\rangle = \tfrac{1}{2}\int_{-1}^{1} a^J_{j_1j_2}(\cos\omega_{12})\Omega_0(\cos\omega_{12})\mathrm{d}(\cos\omega_{12}), \quad (8)$$

where $\Omega_0(\cos\omega_{12})$, the reduced-angular interaction, is given by

$$\Omega_0(\cos\omega_{12}) = \int R^2_{n_1l_1}(r_1)R^2_{n_2l_2}(r_2)V_0(r_1, r_2, \cos\omega_{12})\mathrm{d}r_1\mathrm{d}r_2. \quad (9)$$

Very often we can make some general statement about the dependence on $\cos\omega_{12}$ of $\Omega_0(\cos\omega_{12})$. Thus, if V_0 is a monotonically decreasing function of the separation between the two particles, then $\Omega_0(\cos\omega_{12})$ decreases monotonically with $\cos\omega_{12}$. A glance at the angular-ordering functions can then indicate the expected order of levels. For short-range interactions, for instance, all we have to know is the behaviour of $a^J(x)$ near $x = 1$.

The angular ordering functions depend on the type of interaction considered, but not on its detailed r_1 and r_2 dependence. Thus, for an interaction of the type $\boldsymbol{\sigma}_1\cdot\boldsymbol{\sigma}_2V_1$ we define the appropriate functions by

$$\begin{aligned} b^J_{l_1j_1l_2j_2}(x) &= 6(2j_1+1)(2j_2+1)(2l_1+1)(2l_2+1)(-1)^{j_1+j_2+l_1+l_2+J} \\ &\times\sum_{\substack{K,K' \\ K\le \min(2l_1,\,2l_2) \\ K'=K\pm1}}(2K+1)(2K'+1)\begin{Bmatrix} j_1 j_2 J \\ j_2 j_1 K\end{Bmatrix}\begin{Bmatrix} \frac{1}{2} & \frac{1}{2} & 1 \\ l_1 & l_1 & K \\ j_1 & j_1 & K'\end{Bmatrix}\begin{Bmatrix} \frac{1}{2} & \frac{1}{2} & 1 \\ l_2 & l_2 & K \\ j_2 & j_2 & K'\end{Bmatrix}\begin{pmatrix} l_1 & K & l_1 \\ 0 & 0 & 0\end{pmatrix}\begin{pmatrix} l_2 & K & l_2 \\ 0 & 0 & 0\end{pmatrix}P_K(x). \end{aligned} \quad (10)$$

Only even values of K and odd values of K' contribute to this sum, since the 3-j symbols in (10) vanish for odd K and with an even K the 9-j symbols vanish for even K'. With these functions it can be easily seen that

$$\langle j_1 j_2 J|\boldsymbol{\sigma}_1 \cdot \boldsymbol{\sigma}_2 V_1|j_1 j_2 J\rangle = \tfrac{1}{2}\int_{-1}^{1} b^J_{l_1 j_1 l_2 j_2}(\cos\omega_{12})\Omega_1(\cos\omega_{12})\mathrm{d}(\cos\omega_{12}), \quad (11)$$

where $\Omega_1(x)$ is given by (9).

Thus, the angular-ordering functions contain in them all the "geometrical" information available about the system, including whatever is known on the explicit spin dependence of the forces.

For more-than-two-particle configurations a similar technique can be used. Considering the configuration $(j_n{}^p[J_p]j_2{}^n[J_n])$, the energy levels are obtained by

$$E(J) = \langle j_1{}^p(J_p)j_1{}^n(J_n)J|\sum V_{pn}|j_1{}^p(J_p)j_2{}^n(J_p)J\rangle, \quad (12)$$

where $\sum V_{pn}$ extends over all $p-n$ proton-neutron pairs. If the proton and neutron states are both of lowest seniority (i.e., $v_p = 1, J_p = j_1, v_n = 1, J_n = j_2$) then (12) is given very simply in terms of the energies in the two-particle configuration [4]). In fact, we obtain, for $v_p = v_n = 1$,

$$\langle j_1{}^p(j_1)j_2{}^n(j_2)J|\sum V_0(pn)|j_1{}^p(j_1)j_2{}^n(j_2)J\rangle = \frac{2j_1+1-2p}{2j_1-1}\,\frac{2j_2+1-2n}{2j_2-1}\langle j_1 j_2 J|V_0|j_1 j_2 J\rangle + \text{const.}, \quad (13)$$

and

$$\langle j_1{}^p(j_1)j_2{}^n(j_2)J|\sum \boldsymbol{\sigma}_p \cdot \boldsymbol{\sigma}_n V_1(pn)|j_1{}^p(j_1)j_2{}^n(j_2)J\rangle = \langle j_1 j_2 J|\boldsymbol{\sigma}_1 \cdot \boldsymbol{\sigma}_2 V_1|j_1 j_2 J\rangle. \quad (14)$$

The constant in (13) is independent of J and its explicit expression is given in ref. [4]).

If the protons, and/or the neutrons, are not in their lowest seniority state, the angular-ordering functions can be modified to take it into account. It was shown before [11]) that the energies in this case can be interpreted essentially as the energies in the two-particle system with, however, modified multipole moments. The modification factors $f_K{}^{(p)}$ are given by

$$f_K{}^{(p)} = \sum_{J'_p} (-1)^{J'_p+j_1+J_p+K} \begin{Bmatrix} j_1 & J_p & J'_p \\ J_p & j_1 & K \end{Bmatrix} |(j_1{}^{p-1}(J'_p)j_1 J_p|\}j_1{}^p J_p)|^2, \quad (15)$$

where $(j_1{}^{p-1}(J'_p)j_1 J_p|\}j_1{}^p J_p)$ is a fractional parentage coefficient [14]). The angular-ordering functions in this case will be given by

$$a^J_{J_p J_n}(x) = (-1)^{j_1+j_2+J_p+J_n+J+1}(2j_1+1)(2j_2+1)p(2J_p+1)n(2J_n+1) \times \sum_{\text{even } K}(2K+1)\begin{Bmatrix} J_p & J_n & J \\ J_n & J_p & K \end{Bmatrix}\begin{pmatrix} j_1 & K & j_1 \\ \frac{1}{2} & 0 & -\frac{1}{2} \end{pmatrix}\begin{pmatrix} j_2 & K & j_2 \\ \frac{1}{2} & 0 & -\frac{1}{2} \end{pmatrix} f_K{}^{(p)} f_K{}^{(n)} P_K(x), \quad (16)$$

$$b^J_{l_1 J_p l_2 J_n}(x) = (-1)^{l_1+l_2+J_p+J_n+J}(2j_1+1)(2j_2+1)(2l_1+1)(2l_2+1)p(2J_p+1)n(2J_n+1)$$

$$\times \sum_{K,K'} (2K+1)(2K'+1) \begin{Bmatrix} J_n & J_n & J \\ J_p & J_p & K' \end{Bmatrix} \begin{pmatrix} l_1 & K & l_1 \\ 0 & 0 & 0 \end{pmatrix} \begin{pmatrix} l_2 & K & l_2 \\ 0 & 0 & 0 \end{pmatrix} \begin{Bmatrix} \frac{1}{2} & \frac{1}{2} & 1 \\ l_1 & l_1 & K \\ j_1 & j_1 & K' \end{Bmatrix} \begin{Bmatrix} \frac{1}{2} & \frac{1}{2} & 1 \\ l_2 & l_2 & K \\ j_2 & j_2 & K' \end{Bmatrix} f^{(p)}_{K'} f^{(n)}_{K'} P_K(x). \quad (17)$$

Thus, again, the evaluation of the energies in these configurations is reduced to the "projection" of the reduced angular interaction $\Omega(\cos\omega_{12})$ on the known functions $a^J_{J_p J_n}(\cos\omega_{12})$ and $b^J_{l_1 J_p l_2 J_n}(\cos\omega_{12})$.

The angular-ordering functions were calculated for a number of simple cases. Table 1 gives the expansion coefficients χ_K of these functions in terms of Legendre polynomials. Other functions may be readily calculated using available tables of Racah coefficients [13]), and fractional parentage coefficients [15]).

4. Properties of the Angular-Ordering Functions and the Spectra of Odd Nuclei

If $V(r_1, r_2\cos\omega_{12})$ is an attractive interaction for all values of its variables then it follows from (9) that the reduced angular interaction $\Omega(\cos\omega_{12})$ is non-positive. Furthermore, on general physical grounds, we can expect $\Omega(\cos\omega_{12})$ to be a monotonically increasing function, leading to a reduced interaction between two particles whose angular separation is bigger and whose radial distribution is unaltered. We may try to approximate $\Omega(x)$ by the following function:

$$\Omega(x) = \begin{cases} -x^{2n} & \text{for } 0 \leqq x \leqq 1, \\ 0 & \text{for } x \leqq 0. \end{cases}$$

With $n = 0$ we have a long angular-range interaction; as n increases we are describing shorter angular-range interactions. It should be stressed that we may expect a long-range tail for the reduced angular interaction, since even for a large ω_{12} it includes contributions from the proton-neutron interaction when they are both close to the centre of the nucleus. Since, however, the bulk of interaction takes place when both particles are essentially at the nuclear surface, $\Omega(\cos\omega_{12})$ can be expected to become quite small by the time we reach an angle $\omega_{12} = 60°$. In this situation the range of the proton-neutron residual interaction should be comparable to the nuclear radius in order to obtain a significant contribution to Ω. Using the well-known identities:

$$x^0 = P_0(x), \quad x^2 = \tfrac{1}{3}[2P_2(x)+P_0(x)], \quad x^4 = \tfrac{1}{35}(8P_4(x)+20P_2(x)+7P_0(x)).$$

We see that as the angular range decreases we have contributions from higher multipoles. This is the content of the statement, often made, that the low multipoles take care of the long-range interaction, whereas the high multipoles represent the contribution from the short-range interaction.

TABLE 1

The coefficients χ_K in the expansion $a^J_{j_1 j_2}(x) = \Sigma_K \chi_K P_K(x)$

Configuration	J	$P_0(x)$	$P_2(x)$	$P_4(x)$	Configuration	J	$P_0(x)$	$P_2(x)$	$P_4(x)$
$(\frac{1}{2}, \frac{1}{2})$	0	1			$[(\frac{5}{2})^3_1 \frac{1}{2}]$	1	3		
	1	1				2	3		
$(\frac{1}{2}, \frac{3}{2})$	1	1			$[(\frac{5}{2})^3_1 \frac{3}{2}]$	0	3		
	2	1				1	3		
$(\frac{1}{2}, \frac{5}{2})$	2	1				2	3		
	3	1				3	3		
$(\frac{1}{2}, \frac{7}{2})$	3	1			$[(\frac{5}{2})^3_1 \frac{5}{2}]$	1	3		
	4	1				2	3		
$(\frac{3}{2}, \frac{3}{2})$	0	1	1			3	3		
	1	1	$\frac{1}{5}$			4	3		
	2	1	$-\frac{3}{5}$		$[(\frac{5}{2})^3_1 \frac{7}{2}]$	2	3		
	3	1	$\frac{1}{5}$			3	3		
$(\frac{3}{2}, \frac{5}{2})$	1	1	$\frac{4}{5}$			4	3		
	2	1	$-\frac{4}{35}$			5	3		
	3	1	$-\frac{22}{35}$		$[(\frac{7}{2})^3_1 \frac{1}{2}]$	2	3		
	4	1	$\frac{2}{7}$			3	3		
$(\frac{3}{2}, \frac{7}{2})$	2	1	$\frac{5}{7}$		$[(\frac{7}{2})^3_1 \frac{3}{2}]$	1	3	$\frac{13}{15}$	
	3	1	$-\frac{5}{21}$			2	3	$-\frac{13}{105}$	
	4	1	$-\frac{13}{21}$			3	3	$-\frac{143}{210}$	
	5	1	$\frac{1}{3}$			4	3	$\frac{13}{42}$	
$(\frac{5}{2}, \frac{5}{2})$	0	1	$\frac{8}{7}$	$\frac{6}{7}$	$[(\frac{7}{2})^3_1 \frac{5}{2}]$	0	3	$\frac{26}{21}$	$-\frac{51}{77}$
	1	1	$\frac{184}{245}$	$-\frac{6}{49}$		1	3	$\frac{598}{735}$	$\frac{51}{539}$
	2	1	$\frac{4}{35}$	$-\frac{3}{7}$		2	3	$\frac{13}{105}$	$\frac{51}{154}$
	3	1	$-\frac{106}{245}$	$\frac{19}{49}$		3	3	$-\frac{377}{735}$	$-\frac{323}{1078}$
	4	1	$-\frac{4}{7}$	$-\frac{3}{21}$		4	3	$-\frac{13}{21}$	$\frac{17}{154}$
	5	1	$\frac{20}{49}$	$\frac{1}{49}$		5	3	$\frac{65}{147}$	$-\frac{17}{1078}$
$(\frac{5}{2}, \frac{7}{2})$	1	1	$\frac{50}{49}$	$\frac{27}{49}$	$[(\frac{7}{2})^3_1 \frac{7}{2}]$	1	3	$\frac{325}{294}$	$-\frac{459}{1078}$
	2	1	$\frac{10}{21}$	$-\frac{3}{7}$		2	3	$\frac{65}{126}$	$\frac{51}{154}$
	3	1	$-\frac{20}{147}$	$-\frac{12}{49}$		3	3	$-\frac{65}{441}$	$\frac{102}{539}$
	4	1	$-\frac{4}{7}$	$\frac{36}{77}$		4	3	$-\frac{13}{21}$	$-\frac{306}{847}$
	5	1	$-\frac{74}{147}$	$-\frac{123}{539}$		5	3	$-\frac{481}{882}$	$\frac{2091}{11858}$
	6	1	$\frac{12}{21}$	$\frac{3}{77}$		6	3	$\frac{65}{126}$	$-\frac{51}{1694}$

TABLE 2

The coefficients χ_K in the expansion $b^J_{l_1 j_1 l_2 j_2}(x) = \Sigma_K \chi_K P_K(x)$

Configuration	J	$P_0(x)$	$P_2(x)$	$P_4(x)$	Configuration	J	$P_0(x)$	$P_2(x)$	$P_4(x)$
$(s_{\frac{1}{2}}\ s_{\frac{1}{2}})$	0	-3			$(d_{\frac{3}{2}}\ d_{\frac{3}{2}})$	0	$-\frac{3}{5}$	$-\frac{9}{7}$	$-\frac{144}{35}$
	1	1				1	$-\frac{11}{25}$	$-\frac{29}{35}$	$\frac{432}{175}$
$(s_{\frac{1}{2}}\ p_{\frac{1}{2}})$	0	1				2	$-\frac{3}{25}$	$-\frac{9}{35}$	$-\frac{144}{175}$
	1	$-\frac{1}{3}$				3	$\frac{9}{25}$	$\frac{177}{245}$	$\frac{144}{1225}$
$(s_{\frac{1}{2}}\ p_{\frac{3}{2}})$	1	$-\frac{5}{3}$			$(d_{\frac{3}{2}}\ d_{\frac{1}{2}})$	1	$\frac{21}{25}$	$\frac{24}{35}$	$\frac{48}{175}$
	2	1				2	$\frac{13}{25}$	$\frac{8}{245}$	$-\frac{432}{1225}$
$(s_{\frac{1}{2}}\ d_{\frac{3}{2}})$	1	1				3	$\frac{1}{25}$	$\frac{114}{735}$	$\frac{216}{1225}$
	2	$-\frac{3}{5}$				4	$-\frac{3}{5}$	$-\frac{18}{49}$	$-\frac{8}{245}$
$(s_{\frac{1}{2}}\ d_{\frac{5}{2}})$	2	$-\frac{7}{5}$			$(d_{\frac{5}{2}}\ d_{\frac{5}{2}})$	0	$-\frac{7}{5}$	$-\frac{16}{7}$	$-\frac{186}{35}$
	3	1				1	$-\frac{31}{25}$	$-\frac{208}{245}$	$\frac{4554}{1225}$
$(p_{\frac{1}{2}}\ p_{\frac{1}{2}})$	0	$-\frac{1}{3}$	$-\frac{8}{3}$			2	$-\frac{23}{25}$	$\frac{172}{245}$	$-\frac{6759}{3675}$
	1	$\frac{1}{9}$	$\frac{8}{9}$			3	$-\frac{11}{25}$	$\frac{172}{245}$	$\frac{799}{1225}$
$(p_{\frac{1}{2}}\ p_{\frac{3}{2}})$	1	$\frac{5}{9}$	$\frac{4}{9}$			4	$\frac{1}{5}$	$-\frac{44}{49}$	$-\frac{117}{735}$
	2	$-\frac{1}{3}$	$-\frac{4}{15}$			5	1	$\frac{20}{49}$	$\frac{1}{49}$
$(p_{\frac{1}{2}}\ d_{\frac{3}{2}})$	1	$-\frac{1}{3}$	$-\frac{4}{3}$		$[(d_{\frac{3}{2}})^3_{\frac{1}{2}}\ s_{\frac{1}{2}}]$	1	-1		
	2	$\frac{1}{5}$	$\frac{4}{5}$			2	$\frac{3}{5}$		
$(p_{\frac{1}{2}}\ d_{\frac{5}{2}})$	2	$\frac{7}{15}$	$\frac{8}{15}$		$[(d_{\frac{3}{2}})^3_{\frac{1}{2}}\ p_{\frac{1}{2}}]$	1	$\frac{1}{3}$	$\frac{8}{21}$	
	3	$-\frac{1}{3}$	$-\frac{8}{21}$			2	$-\frac{1}{5}$	$-\frac{8}{35}$	
$(p_{\frac{3}{2}}\ p_{\frac{3}{2}})$	0	$-\frac{5}{3}$	$-\frac{13}{3}$		$[(d_{\frac{3}{2}})^3_{\frac{3}{2}}\ p_{\frac{3}{2}}]$	0	-1	4	
	1	$-\frac{11}{9}$	$\frac{109}{45}$			1	$-\frac{11}{15}$	$-\frac{268}{105}$	
	2	$-\frac{1}{3}$	$-\frac{13}{15}$			2	$-\frac{1}{5}$	$\frac{4}{5}$	
	3	1	$\frac{1}{5}$			3	$\frac{3}{5}$	$-\frac{12}{245}$	
$(p_{\frac{3}{2}}\ d_{\frac{3}{2}})$	0	1	1		$[(d_{\frac{3}{2}})^3_{\frac{3}{2}}\ d_{\frac{3}{2}})$	0	$\frac{3}{5}$	$-\frac{12}{49}$	$-\frac{192}{245}$
	1	$\frac{11}{15}$	$-\frac{1}{15}$			1	$\frac{11}{25}$	$\frac{228}{245}$	$\frac{576}{1225}$
	2	$\frac{1}{5}$	$\frac{1}{5}$			2	$\frac{3}{25}$	$-\frac{12}{245}$	$-\frac{192}{1225}$
	3	$-\frac{3}{5}$	$-\frac{9}{35}$			3	$-\frac{9}{25}$	$-\frac{324}{1715}$	$-\frac{192}{8575}$
$(p_{\frac{3}{2}}\ d_{\frac{5}{2}})$	1	$-\frac{7}{5}$	$-\frac{8}{5}$		$[(d_{\frac{3}{2}})^3_{\frac{5}{2}}\ d_{\frac{5}{2}}]$	1	$-\frac{21}{25}$	$\frac{312}{245}$	$\frac{64}{1225}$
	2	$-\frac{13}{15}$	$\frac{184}{105}$			2	$-\frac{13}{25}$	$-\frac{3256}{1715}$	$-\frac{576}{8575}$
	3	$-\frac{1}{15}$	$-\frac{14}{15}$			3	$-\frac{1}{25}$	$\frac{1544}{1715}$	$\frac{288}{8575}$
	4	1	$\frac{2}{7}$			4	$\frac{3}{5}$	$-\frac{24}{343}$	$-\frac{32}{5145}$

We shall first consider interactions with a long angular range. In this case the splitting is entirely due to the spin-dependent forces. A similar situation occurs for a single half-filled shell. We will discuss the general case later.

For long range angular interactions the Wigner force does not contribute to the splitting since the coefficients of P_0 are independent of J, and P_K, $K \neq 0$ does not contribute in this limit. The whole contribution to the splitting in this case comes from the spin-dependent part of the interaction $\boldsymbol{\sigma}_1 \cdot \boldsymbol{\sigma}_2 V_1$. As we see from table 2, $b^J_{l_1 j_1 l_2 j_2}$ has its maximum value for $J = |j_1 - j_2|$ if $j_1 = l_1 \pm \frac{1}{2}$ and $j_2 = l_2 \mp \frac{1}{2}$, and for $J = j_1 + j_2$ if $j_1 = l_1 \pm \frac{1}{2}$, $j_2 = l_2 \pm \frac{1}{2}$. This is true both for cases when J_p is a state of lowest seniority as well as for the cases of seniority $v = 3$ and $J_p = j_1 - 1$. Thus, in the limit of long range Nordheim's strong rule [16]) is obeyed, and his weak rule prefers $J = j_1 + j_2$ to other values of J.

If the proton shell is half-filled, then the Wigner-force does not contribute to the splitting of the energy levels for any range. In fact, for such cases $a^J_{J_p J_n} = pn$, and the whole splitting is due to $\boldsymbol{\sigma}_1 \cdot \boldsymbol{\sigma}_2 V_1$. In the long range limit, as we have just seen, we have $J = |j_1 - j_2|$ or $J = j_1 + j_2$ as the lowest state, depending on whether the Nordheim number $N = j_1 + l_1 + \frac{1}{2} + j_2 + l_2 + \frac{1}{2}$, is odd or even, i.e., the lowest state is given by $J = |j_1 + (-1)^N j_2|$. However, we note in table 2 that if we confine ourselves to neutron and proton configurations of lowest seniority then the state with $J = |j_1 + (-1)^N j_2|$ is the only one for which all the coefficients χ_K are positive. It then follows that it will remain the lowest state also for somewhat shorter ranges. Furthermore, we notice that in the case of Nordheim's strong rule, $(-1)^N = -1$, it is generally true that $\chi_K{}^{|j_1 - j_2|} > \chi_K{}^J$ for any K. Thus, $J = |j_1 - j_2|$ remains the lowest state irrespective of the range of the angular interaction. For even N, other states may become lower than $J = j_1 + j_2$, but only for very short range. Even then the only competing states are with $J = j_1 + j_2 - 2$, $J = j_1 + j_2 - 4$ etc. Thus, if the protons fill half a shell we can say that, irrespective of the range of forces, but provided both protons and neutrons are in their lowest seniority state, the ground state spin is $J = |j_1 - j_2|$ if N is odd and it is $J = j_1 + j_2 - 2n$ if N is even. Since the parity of the configuration is $(-1)^{l_1 + l_2}$, it is seen that in both cases the ground state spin satisfies the relation

$$(-1)^{J+1} = (-1)^{l_1 + l_2}. \tag{18}$$

We therefore expect that whenever the protons or the neutrons fill half a shell the ground state will have an even J for odd parity configurations and odd J for even parity configurations.

For $j_1 = \frac{1}{2}$ this rule reduces to the rule derived in section 1. Since it is found to be so well obeyed in actual nuclei, it is interesting to see how this rule is affected by the introduction of tensor forces. A convenient general formula for the tensor force is derived in the appendix. For the case of $l_1 = 0$ one obtains a very simple expression. As shown in the appendix, our rule will continue to hold

even with a tensor force, provided $J(r_{12})$ is attractive and its angular range is either very short or very long.

If neither the protons nor the neutrons fill half a shell, we see from table 1 that the Wigner force alone would always lead to a lowest state with $J = |j_1 - j_2|$ if both the protons and the neutrons are in states of lowest seniority.

The same result holds for the spin-dependent force for odd Nordheim numbers N. Therefore, $J = |j_1 - j_2|$ is always the ground state for odd Nordheim numbers and *any attractive interaction* (the strong rule). For even Nordheim numbers, the spin-dependent forces tend to raise the state with $J = |j_1 - j_2|$ and lower $J = j_1 + j_2$. These two states, therefore, come closer to, and may even cross, each other. Thus, in this case either $J = j_1 + j_2$ or $J = |j_1 - j_2|$ is expected to be the ground state, the two states being at any rate close to each other. This agrees with the empirical rule formulated by Brennan and Bernstein [3]).

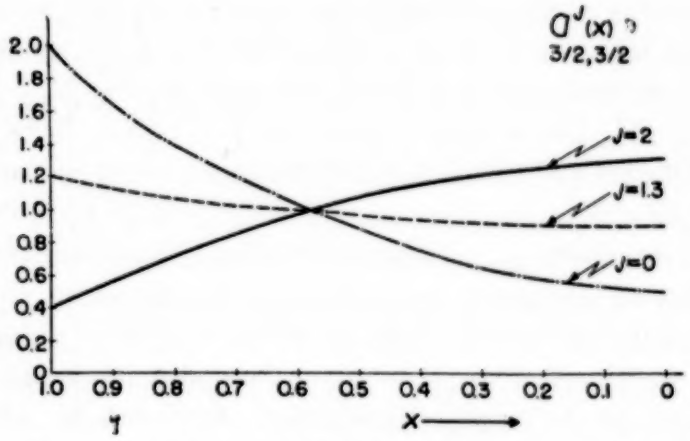

Fig. 1. The angular-ordering functions for Wigner forces and $j_1 = j_2 = \frac{3}{2}$. The abscissa is $x = \cos \omega_{12}$.

For the case of $([\frac{7}{2}]_{\frac{1}{2}}^3, \frac{5}{2})$ configuration, for instance, (see table 1) we notice a different situation. As long as P_0 and P_2 are the only important terms, $J = 0$ is the lowest state. As the angular range of the interaction is decreased, the contribution of P_4 becomes more important. Since P_4 appears in $J = 0$ with the most negative coefficient, it will be depressed relative to other levels as the range is made shorter. In fact, in the δ-limit $J = 1$ wins and becomes slightly more bound than $J = 0$, with $J = 2$ and $J = 5$ getting very close to $J = 0$. One has, of course, to add to this the effects of the spin-dependent forces before making final conclusions, and in Nordheim's strong-rule case even a weak $\boldsymbol{\sigma}_1 \cdot \boldsymbol{\sigma}_2 V_1$ force would push the $J = 1$ state high enough to assure that $J = 0$ is the ground state. However, we see already from this example how more detailed information on the spins of the low-lying states in odd nuclei could serve to pin down the angular range of the residual interaction.

In figs. 1 and 2 we have plotted the angular-ordering functions for $j_1 = j_2 = \frac{3}{2}$.

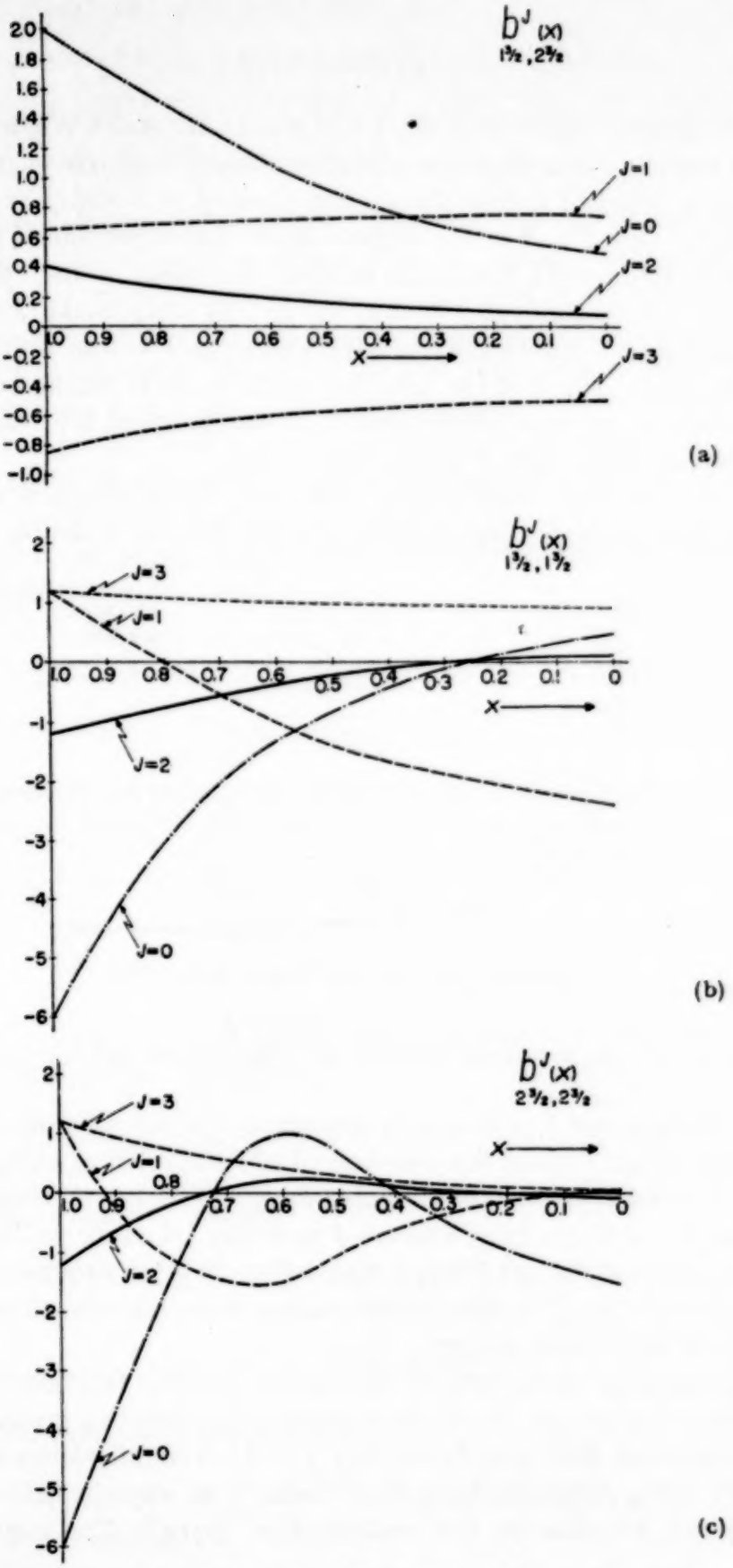

Fig. 2. The angular-ordering functions for the spin-dependent forces. The configurations are: $p_{\frac{1}{2}} d_{\frac{3}{2}}$ in fig. 2(a) (odd Nordheim number), $p_{\frac{1}{2}} p_{\frac{3}{2}}$ in fig. 2(b) and $d_{\frac{3}{2}} d_{\frac{5}{2}}$ in fig. 2(c) (even Nordheim number).

Since

$$\int_0^1 a^J(x)\mathrm{d}x = 1,$$

it is immediately evident from fig. 1 that a pure attractive Wigner force whose reduced angular interaction is a monotonic function of cos ω_{12} will lead to a spectrum in which $J = 0$ is the ground state, $J = 1$ and $J = 3$ come next (degenerate) and $J = 2$ is the highest state. An inspection of fig. 2(a) now shows that for an odd Nordheim number the effect of the spin-dependent interaction will be to leave $J = 0$ as the ground state, make $J = 1$ the next state, leave $J = 2$ practically unaltered and repel $J = 3$ so that it may even get to be above $J = 2$ if the spin-dependent force is strong enough. These conclusions are practically independent of the range of the reduced angular interaction as these figures show very clearly.

For even Nordheim number (figs. 2(b), (c)) the situation is slightly more complex. For $l_1 = l_2 = 1$ (fig. 2(b)) we see that the $J = 0$ state is very strongly

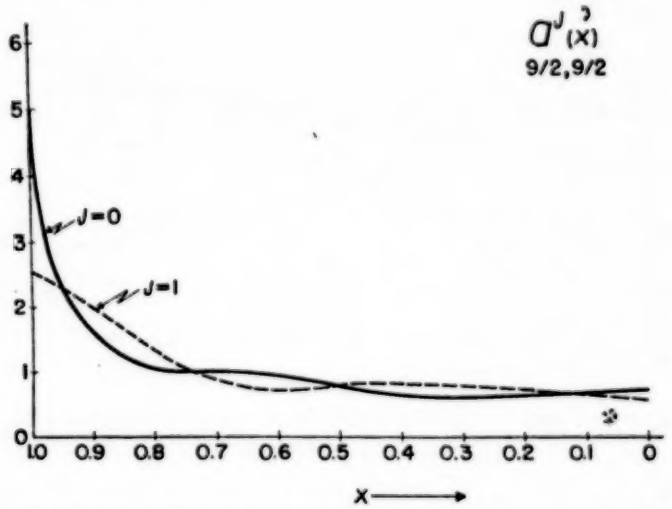

Fig. 3. The angular-ordering functions for Wigner forces and $j_1 = j_2 = \frac{9}{2}$.

repelled, whereas the $J = 3$ state is the only one which remains attractive for any angular range. Thus, if the spin-dependent force is strong enough compared with V_0, $J = 3$ will become the ground-state, $J = 1$ the next state if the range is short, and $J = 2$ if it is long, whereas $J = 0$ may even become the least bound state, if V_1 is strong enough. For $l_1 = l_2 = 2$ (fig. 2(c)) the situation is essentially the same except that $J = 0$ has better chances to remain fairly low if the angular range of Ω_1 is long enough.

Another example of the uses of the angular-ordering functions is offered by the configuration $(h_{\frac{9}{2}}g_{\frac{9}{2}})$. Nordheim's strong rule predicts a ground state with $J = 0$, whereas in Bi^{210} it is found that $J = 1^-$ is slightly lower than $J = 0^-$ (about 40 keV). Attempts have been made [17]) to explain this situation by ascribing the 1^- state to the configuration $(h_{\frac{9}{2}}i_{\frac{11}{2}})$. The angular-ordering

functions for $(h_{\frac{9}{2}}g_{\frac{9}{2}})$ and $J = 0$, are given by

$$a^0_{\frac{9}{2}\frac{9}{2}}(x) = 1 + \tfrac{40}{33}P_2(x) + \tfrac{162}{143}P_4(x) + \tfrac{32}{33}P_6(x) + \tfrac{98}{143}P_8(x),$$
$$a^1_{\frac{9}{2}\frac{9}{2}}(x) = 1 + \tfrac{1160}{1089}P_2(x) + \tfrac{1062}{1573}P_4(x) + \tfrac{160}{1089}P_6(x) - \tfrac{490}{1573}P_8(x),$$
$$b^0_{5\frac{1}{2}\,4\frac{1}{2}}(x) = a^0_{\frac{9}{2}\frac{9}{2}}(x), \quad b^1_{5\frac{1}{2}\,4\frac{1}{2}}(x) = a^1_{\frac{9}{2}\frac{9}{2}}(x) - \tfrac{4}{99}a^0_{\frac{9}{2}\frac{9}{2}}(x).$$

In fig. 3 we have plotted $a^0(x)$ and $a^1(x)$; $b^0(x)$ and $b^1(x)$ are practically identical. We see from this figure that although in the δ-limit $J = 0$ is much more bound than $J = 1$, even a slight increase in the range of the reduced angular interaction brings the two levels very close to each other. Thus, the approximate treatment of this system in the δ-limit may be very misleading as far as the separation between $J = 0$ and $J = 1$ is concerned.

It may be expected that the reduced angular interaction will be fairly independent of the detailed configuration. The angular-ordering functions will then be very useful in determining the sequence of energy levels in odd nuclei, or, conversely, if this sequence is experimentally determined the angular range of the interaction can be found.

Appendix

THE TENSOR FORCE

In this appendix we present the tensor interaction in a form conveniently suited to the j–j coupling [18]) model. The tensor interaction is

$$S_{12}(r_{12}) = J(r_{12})\mathbf{S}\cdot\mathbf{L}, \tag{A.1}$$

where

$$\mathbf{S} = [\boldsymbol{\sigma}_1\times\boldsymbol{\sigma}_2]^{(2)}, \quad \mathbf{L} = [\mathbf{r}_{12}\times\mathbf{r}_{12}]^{(2)} \tag{A.2}$$

are the irreducible tensors of second order constructed from the spins and relative position vector. Expanding

$$J(r_{12}) = \sum_K f_K(r_1, r_2)P_K(\cos\omega_{12}) = \sum_K f_K\,\mathbf{C}_1^{(K)}\cdot\mathbf{C}_2^{(K)} \tag{A.3}$$

and using the following relation:

$$(KK'|K'')C_1^{K''q''} = \sum_{q,q'}(KqK'q'|KK'K''q'')C_1^{Kq}C_1^{K'q'} \tag{A.4}$$

with

$$(KK'|K'') = (K0K'0|KK'K''0),$$

we can write, after some manipulation,

$$S_{12} = \sum_{l,K',K''} F_{K'K''}\begin{Bmatrix} K' & K'' & 2 \\ 1 & 1 & l \end{Bmatrix}\mathbf{X}_1^{(l)}(K')\cdot\mathbf{X}_2^{(l)}(K''), \tag{A.5}$$

where

$$F_{K'K''} = 5\sqrt{(2K'+1)(2K''+1)}\sum_K \left[\frac{(11|2)(K2|K')r_1^2}{\sqrt{5(2K+1)}}\delta_{K''K} + \frac{(11|2)(K2|K'')r_2^2}{\sqrt{5(2K+1)}}\delta_{K'K} + 2r_1r_2(K1|K')(K1|K'')\begin{Bmatrix} K' & K'' & 2 \\ 1 & 1 & K \end{Bmatrix}\right] f_K .$$

We have used

$$\mathbf{X}_1^{(1)}(K') = |\mathbf{C}_1^{(K')} \times \boldsymbol{\sigma}_1^{(1)}]^{(1)}.$$

The matrix elements of $\mathbf{X}_1 \cdot \mathbf{X}_2$ in the $j-j$ coupling scheme can immediately be written down

$$\langle j_1 j_2 J|\mathbf{X}_1^{(1)}(K') \cdot \mathbf{X}_2^{(1)}(K'')|j_1 j_2 J\rangle = |(\tfrac{1}{2}||\boldsymbol{\sigma}||\tfrac{1}{2})|^2 (l_1||C_1^{(K')}||l_1)(l_2||C_2^{(K'')}||l_2)$$
$$\times (2j_1+1)(2j_2+1)(2l+1)(-1)^{j_1+j_2+J}\begin{Bmatrix} J & j_2 & j_1 \\ l & j_1 & j_2 \end{Bmatrix}\begin{Bmatrix} \frac{1}{2} & \frac{1}{2} & 1 \\ l_1 & l_1 & K' \\ j_1 & j_1 & l \end{Bmatrix}\begin{Bmatrix} \frac{1}{2} & \frac{1}{2} & 1 \\ l_2 & l_2 & K'' \\ j_2 & j_2 & l \end{Bmatrix}. \quad \text{(A.6)}$$

From this last expression we note that K' and K'' must be even and hence l must be odd. These equations are still sufficiently complicated so that it is difficult to see the role of the tensor force in the general case. If, however, one of the l_i (say l_1) $= 0$, it simplifies considerably

$$\langle \tfrac{1}{2} j_2 J|S_{12}|\tfrac{1}{2} j_2 J\rangle = 2\sqrt{30}(-1)^{j_2+l_2+J+\frac{1}{2}}(2l_2+1)(2j_2+1)$$
$$\times \begin{pmatrix} l_2 & 2 & l_2 \\ 0 & 0 & 0 \end{pmatrix}\begin{Bmatrix} j_2 & j_2 & 1 \\ \frac{1}{2} & \frac{1}{2} & J \end{Bmatrix}\begin{Bmatrix} \frac{1}{2} & \frac{1}{2} & 1 \\ l_2 & l_2 & 2 \\ j_2 & j_2 & 1 \end{Bmatrix}\langle r_2^2 f_0 - \tfrac{2}{3}r_1r_2 f_1 + \tfrac{1}{5}r_1^2 f_2\rangle. \quad \text{(A.7)}$$

The overall phase of this expression is easily shown to be $(-1)^{J+l_2+1}$. Therefore, if

$$\langle r_2^2 f_0 - \tfrac{2}{3}r_1r_2 f_1 + \tfrac{1}{5}r_1^2 f_2\rangle \leqq 0, \quad \text{(A.8)}$$

then the ground state will be that with $J+l_2+1$ even and hence will have negative or positive parity as J is even or odd in accordance with our general rule. We also notice that if $J(r_{12}) = \delta(\mathbf{r}_1 - \mathbf{r}_2)$,

$$f_0 - \tfrac{2}{3}f_1 + \tfrac{1}{5}f_2 = 0,$$

and the tensor force vanishes as it must.

We note that the condition (A.8) is just

$$\tfrac{1}{2}\int R^2_{n_1 l_1}(r_1) R^2_{n_2 l_2}(r_2)\mathrm{d}r_1\mathrm{d}r_2 \int_{-1}^{1}\mathrm{d}x$$
$$\times [r_2^2 P_0(x) - 2r_1r_2 P_1(x) + r_1^2 P_2(x)]J(r_1, r_2, x) \leqq 0. \quad \text{(A.9)}$$

This equation is satisfied with a negative $J(r_1, r_2, x)$ as long as the angular range is either very long or very short.

References

1) S. Pandya, Phys. Rev. **108** (1957) 1312
2) B. Oquidam and B. Jancovici, Nuovo Cim. **11** (1959) 578
3) M. H. Brennan and A. M. Bernstein, to be published
4) C. Schwartz, Phys. Rev. **94** (1954) 95
5) G. Racah and I. Talmi, Physica **18** (1952) 1097
6) A. deShalit, Phys. Rev. **91** (1952) 1479
7) A. deShalit, Phys. Rev. **105** (1957) 1531
8) B. Jung and G. Anderson, Nuclear Physics **15** (1960) 108
9) H. Noya, A. Arima and H. Horie, Prog. Theor. Phys. Supp. **8** (1958) 31
10) B. L. Cohen and R. E. Price, Nuclear Physics **17** (1960) 129
11) A. deShalit and J. D. Walecka, Phys. Rev., to be published
12) See, for instance, ref. [4])
13) See, for instance, M. Rottenberg, R. Bivins, N. Metropolis and J. K. Wooten, Jr., The 3-j and 6-j symbols (The Technology Press, MIT, Cambridge, 1959)
14) G. Racah, Phys. Rev. **62** (1942) 438
15) A. R. Edmonds and B. H. Flowers, Proc. Roy. Soc. A **214** (1952) 515;
B. H. Flowers, Proc. Roy. Soc. A **215** (1952) 398;
C. Schwartz and A. deShalit, Phys. Rev. **94** (1954) 1257;
A. deShalit, Nuclear Physics **7** (1957) 225
16) L. W. Nordheim, Phys. Rev. **78** (1950) 294
17) N. Newby, Jr. and E. J. Konopinski, Phys. Rev. **115** (1959) 434;
P. Banerjee and H. D. Zeh, Z. Physik, **159** (1960) 170
18) See also I. Talmi, Phys. Rev. **89** (1953) 1065

8.B

Nuclear Physics **22** (1961) 202—206; © *North-Holland Publishing Co., Amsterdam*

Not to be reproduced by photoprint or microfilm without written permission from the publisher

ON DERIVING EQUATIONS FROM THE MANDELSTAM REPRESENTATION

A. V. EFREMOV, V. A. MESHCHERYAKOV, D. V. SHIRKOV and H. Y. TZU

Laboratory of Theoretical Physics, Joint Institute for Nuclear Research, Dubna, USSR

Received 1 July 1960

Abstract: A new recipe is proposed for deriving the integral equations for partial-wave scattering amplitudes on the basis of the dispersion relations at a fixed angle and the unitarity condition. The method is illustrated by applying it in the simplest case of $\pi\pi$-scattering. The results on the πN-scattering are summarized in brief.

A number of recent papers dealt with the derivation of integral equations for various scattering processes. All these papers [1–6]) have one feature in common: from the outset they make use of the analyty cal properties of partial wave amplitudes. Due to the spherical functions of the Mandelstam representation, this results in a restriction of the domain of convergence in the unphysical region.

Recently [7–9]) we derived a system of equations for πN-scattering using a different approach, viz., one based on the dispersion relations at a fixed scattering angle, which enabled us to make a detailed investigation of the analytical properties in the unphysical region. This provided us with a new method of deriving integral equations for partial-wave scattering amplitudes. Essentially, it reduces itself to the following.

In deriving integral equations from the dispersion relations and unitarity condition, two kinds of approximation are usually made:

1) Two-particle intermediate state approximation of the unitary condition is made, the contributions to the imaginary parts of the scattering amplitudes from intermediate states involving three or more particles usually being neglected.

2) States of low angular momenta alone are taken into account, the contributions from the waves of the higher angular momenta usually being neglected.

There are good grounds to hope that the first approximation holds for the low energy region. The second approximation is consistent with the first in the physical region. Care should be taken, however, in discarding the higher waves in the unphysical region. As will be shown below, in a number of important cases the second approximation leads to large errors in the unphysical region even at low energies. By way of illustration, we shall discuss in detail the simplest case of $\pi\pi$-scattering and present a short summary of the results on πN-scattering.

The dispersion relations for $\pi\pi$-scattering at a fixed value of $\cos\theta = c$ have the following form:

$$A(\nu, c) = \frac{1}{\pi}\int_0^\infty d\nu' \frac{\operatorname{Im}\mathscr{A}(\nu', c)}{\nu'-\nu} + \frac{1}{\pi}\int_\infty^a d\nu' \frac{\operatorname{Im}\mathscr{A}(\nu', c)}{\nu'-\nu}, \tag{1}$$

where $\nu = q^2$ is the square of momentum in the c.m.s. of reaction 1. The location of the point a depends on c and is shown in fig. 1. In the unphysical region $-\infty < \nu < a$, the quantity $\operatorname{Im}\mathscr{A}$ is usually expressed in terms of the

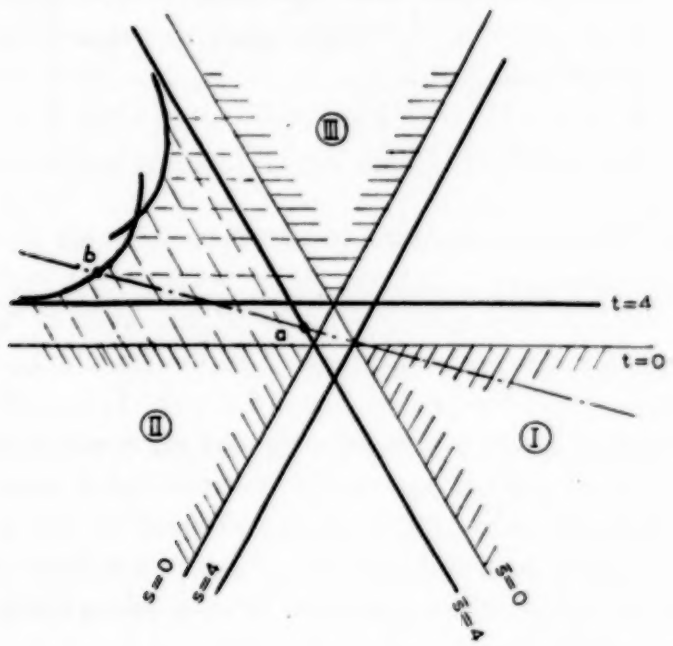

Fig. 1

partial wave amplitudes of reactions II and III through an analytical continuation of the Legendre expansion. The expansion fails at the point b on the boundary of the region where the spectral function does not vanish. But even before the point b is reached, there is a large region at a distance from the physical region comparable with that from the point b. It is unlikely that the scattering amplitude in this region could be approximated with reasonable accuracy by keeping only a few terms of the Legendre expansion. Using the spectral representation, the dependence of the imaginary part of the scattering amplitude on $\cos\bar{\theta} = \bar{c}$ can be expressed in explicit form. This dependence is determined by the denominators $\tau \pm \bar{c}$ appearing in the representation, where $\tau = 1 + s'/2\bar{\nu}$. According to the Heine theorem we have

$$\frac{1}{\tau+\bar{c}} = \sum_{l\geq 0} (2l+1) Q_l(\tau) P_l(\mp\bar{c}). \tag{2}$$

The accuracy of the usual approximation (representing the denominators by the first two terms of the above expansion) can be estimated as follows. Let us put $\tilde{\nu} = 3$, which corresponds to the threshold of the first inelastic process. Since the most important contribution comes from the neighbourhood of b, the value of s' is chosen so as to correspond to the point b. The quantity $\tilde{c}$ is determined by c and $\tilde{\nu}$. The results of calculation for the two different scattering angles $c = 1$ and $c = 0$ are given in table 1.

TABLE 1

Results of Calculation

c	$\tilde{c}$	$\frac{1}{\tau - \tilde{c}}$	$Q_0(\tau) + 3\tilde{c}Q_1(\tau)$	Error
1	1	0.281	0.273	3 %
0	$\frac{11}{3}$	1.125	0.405	

It is clear that this approximation can lead to large errors for $c = 0$.

The partial-wave dispersion relation can be obtained by integrating eq. (1) over c from -1 to $+1$ after multiplying by $P_l(c)$. Then it becomes evident that there is a large domain in the unphysical region for which this approximation does not hold even if the region beyond $\nu' = -L = -10$ is cut off.

To avoid introducing a new parameter, the cut off momentum L, Chew and Mandelstam let $L \to \infty$ after dropping the d- and higher waves. Actually, if we use eq. (1) after one subtraction, the coefficient of the d-wave behaves like $\ln L$ as $L \to \infty$. It is doubtful that the contribution from the high-energy unphysical region is sufficiently suppressed by one subtraction, rendering the solution of the equation insensitive to the value of L. As a matter of fact, Fraser and Fulco [2]) used a similar method to treat the problem of the nucleon structure and the $N\bar{N}$-annihilation. Some of their results proved sensitive to the value of the cut off momentum.

The case of πN-scattering is similar. Due to the peculiarity of the kinematics ($M \neq \mu$), the cosine of the reaction angle in $\pi + \pi \to + N\bar{N}$ takes on a complex value in the unphysical region. There also exists a region where the Legendre expansion converges but the first two terms of it yield a poor approximation.

To avoid these difficulties, inherent in various processes, we propose another general approach to the problem of deriving integral equations for low energy processes from the dispersion relations and unitary conditions.

It is known experimentally that only a few angular momentum states count at low energies. To determine these states theoretically, it is sufficient to have expressions for the scattering amplitude (and its derivatives) just at a few angles and there is no need to use dispersion relations for all scattering angles. It is evident from fig. 1 that the range in which the analytic continuation by the Legendre expansion is valid varies largely with different angles. In deriving

integral equations we propose to choose only those angles for which the Legendre expansion fails only at the distant part of the physical region. The forward and backward scattering are especially welcome in this case, since in these cases the path of the dispersion integral never intersects the boundary of the region where the spectral functions do not vanish, and the problem of divergence of the Legendre expansion does not arise at all.

This programme for the case of $\pi\pi$-scattering is carried out by Ho Tso-hsin *et al.* who employ the expansion in the neighbourhood of $\cos\theta = 1$. The equations obtained for the partial wave differ from that of Chew and Mandelstam as regards the structure of the integral over the unphysical region.

The numerical solution of these equations is now in progress. It is possible that the solution of the eqs. of ref. [10]) will differ essentially from that of Chew and Mandelstam, if there exist solutions with a large p-wave.

The above-mentioned method is also applied to the problem of πN-scattering in refs. [8,9]). It will be noted that Chew *et al.* [11]) actually employed this method in their work on the πN-scattering, using the expansion in the neighbourhood of $\cos\theta = 1$. If, however, the unitarity condition is limited to the two-particle intermediate state approximation, the process $\pi+\pi\to N+\bar{N}$ has no effect on πN-scattering for $\cos\theta = 1$. The effect of $\pi+\pi\to N+\bar{N}$ on πN-scattering is largest at $\cos\theta = -1$. Therefore the dispersion relations for both backward and forward scattering are employed in ref. [8]); the equations obtained for πN-scattering have to be solved simultaneously with those for the $\pi+\pi\to N+\bar{N}$ process.

In ref. [9]) an expansion in the neighbourhood of $\cos\theta = -1$ is used. Under certain assumptions a system of equations can be obtained for the πN-scattering partial waves, with $\pi\pi$-scattering phase-shifts appearing in the kernels. If the phase shifts of the $\pi\pi$-scattering are assumed to be equal to zero in the equation obtained in refs. [8,9]) then the principal terms (in an expansion in powers of $1/M$) coincide with those of Chew *et al.* [11]). Then it becomes possible to estimate the sign and the order of magnitude of the s-wave scattering length of $\pi\pi$-scattering from the p-phase shifts of πN-scattering near the threshold. This value obtained is $0.9/\mu$, which agrees with the results of ref. [12]). The same problem is discussed in ref. [4]). However, the effect of the s-wave ($\pi\pi$-scattering) was not taken into account at all in that paper, and the results obtained cannot be reliable.

Recently the method proposed in the present paper has been used for deriving integral equations for the partial waves of πK-scattering [13]) and KN-scattering [14]).

Note: After the present paper has been written, the authors received the copy of a recent paper by Chew and Mandelstam [15]) which stated that in the case of $\pi\pi$-scattering when the p-wave is large at low energies, the integral

equations previously formulated in ref. [1]) require a cut-off and the solution becomes unstable. Therefore our criticism of the equations of ref. [1]) receives further confirmation.

References

1) G. Chew and S. Mandelstam, UCRL-8728, April, 1959
2) W. Fraser and T. Fulco, UCRL-8806; Phys. Rev. **117** (1960) 1603
3) M. Cini and S. Fubini, CERN, preprint (1960)
4) J. Bowcock, W. N. Cottingham and D. Lurie, Nuovo Cim. **16** (1960) 918
5) M. Gourdin and A. Martin, Nuovo Cim. **16** (1960) 78
6) M. Gourdin and A. Martin, CERN, preprint
7) A. V. Efremov, V. A. Meshcheryakov and D. V. Shirkov, JETP **39** (1960) N2(8); see also JINR-preprint, D-503
8) H. Y. Tzu, JINR-preprint D-564
9) A. V. Efremov, V. A. Meshcheryakov and D. V. Shirkov, JINR-preprint E-545
10) Ho Tso-hsin, Hsien Ding-chang and W. Zollner, JINR-preprint D-547
11) G. Chew, M. Goldberger, F. Low and Y. Nambu, Phys. Rev. **106** (1957) 1337
12) K. Ishida, A. Takahashi and Y. Ueda, preprint
13) P. S. Isaev and M. Sewerynsky, JINR-preprint D-550
14) I. Wolf and W. Zollner, JINR-preprint D-562
15) G. F. Chew and S. Mandelstam, Preprint UCRL-9126

2.I

Nuclear Physics **22** (1961) 207—215; ©*North-Holland Publishing Co., Amsterdam*

Not to be reproduced by photoprint or microfilm without written permission from the publisher

PHOTODISINTEGRATION OF Al^{27}
(I) Photoneutron Cross Section

J. E. E. BAGLIN, M. N. THOMPSON and B. M. SPICER

Physics Department, University of Melbourne

Received 3 October 1960

Abstract: The $Al^{27}(\gamma, n)$ cross section has been observed up to 18.5 MeV with good resolution. It contains a plateau at 14 MeV and a hump at 16 MeV, and is consistent with recent high resolution measurements of the total absorption cross section.

1. Introduction

The photonuclear giant resonance in heavy non-spherical nuclei was observed to contain two peaks (see Fuller and Weiss [1]), Spicer *et al.* [2]), Parsons [3]), Thies and Spicer [4])). This splitting was initially interpreted in terms of the collective model as applied to deformed nuclei by Danos [5]) and Okamoto [6]).

It has, however, been pointed out by Litherland *et al.* [7]) and Bromley [8]) that a collective model can also be applied to nuclei as light as Al^{25} and Mg^{25}, and Spicer [9]) has applied this model to the photodisintegration of several light nuclei.

A search has been made for a similar resonance splitting in Al^{27} by observing the (γ, n) cross section. This nucleus was chosen because of its large positive deformation, and its availability as a 100 % pure isotope.

Prior to 1959, determinations of the (γ, n) and (γ, p) cross sections lacked the resolution required to test adequately the applicability of the Danos-Okamoto theory to the aluminium nucleus (Diven and Almy [10]), Katz and Cameron [11]), Montalbetti *et al.* [12]), Ferrero *et al.* [13]), Halpern and Mann [14])). The purpose of the present experiment was to determine the (γ, n) cross section with sufficient resolution to make this test.

2. Neutron Yield Determination

The aluminium target was spectroscopically pure (largest impurity 0.01 % Cu) and was in the form of a cylinder 3.85 cm in diameter, 13.5 cm long, and weighing 421 g.

Using the Melbourne 19 MeV synchrotron, the yield of photoneutrons from the target was determined for bremsstrahlung with peak energies ranging from 11.6 MeV to 18.6 MeV, the measurements being made at 0.25 MeV intervals.

The radiation dose was measured with a 25r Victoreen thimble used as a transmission ionization chamber. This chamber had been previously calibrated relative to the "lucite röntgen" (see Johns *et al.* [15])) in this laboratory.

Neutrons were detected with B^{10}-enriched BF_3 counters in a paraffin house similar to that described by Spicer *et al.* [2]). However, some modification of the counter-target separation was found to be necessary. Tests carried out using sources of neutrons of different energies indicated that a separation of target and counter centres of 10 cm rather than the previous 13 cm gave a detection efficiency more nearly insensitive to initial neutron energy.

Because of the relatively low yield of neutrons, and the accuracy required, every care was taken to reduce personal and random errors to a minimum. Counter efficiency was checked before and after each run, using a Ra-Be neutron source. The Victoreen thimble was periodically checked, and showed no detectable leakage. A chart record of transient fluctuations in the peak synchrotron magnetic field was used to apply an effective energy correction to each run. Measurements at each energy were performed several times, in order to reduce the effects of small variations in the machine energy, and statistical fluctuations. Each point was the result of from 12 to 18 measurements, involving a count from 4×10^4 to 10^6 neutrons.

3. Background Determination

The yield of background neutrons was determined in the same way as the total yield, but with the Al target removed, and at 16 MeV it amounted to 20 % of the total yield. This decreased to 0.7 % at 18 MeV, and increased to 50 % at 14 MeV.

At energies below the $Al^{27}(\gamma, n)$ threshold, the yield with the target in position was observed to be 30 % higher than the background yield with no target. This increase in yield was attributed to neutrons produced in the lead collimator and platinum target, which travelled down the beam hole and were scattered by the Al target.

To test this assumption the Al target was replaced by one of spectroscopically pure carbon, which was designed to have the same scattering characteristics for an incident evaporation spectrum of neutrons. With this target in position, the yield Y_c was determined. The photoneutron yield Y_{13} from the C^{13} present was calculated from the results of Cook [16]), and subtracted from Y_c, leaving a nett yield which was assumed to be the sum of the background with no target Y_{BG}, and the scattered yield Y_{sc}. Below the $Al^{27}(\gamma, n)$ threshold, Y_{sc} was found to be identical with the increment in background due to the presence of the aluminium target, and was proportional to Y_{BG} at all energies. This confirms the hypothesis that the increment in the case of aluminium was, in fact, also a scattering effect. The results are summarized in table 1, where $Y_{BG}+Y_{sc}$ is to be compared with $Y_{BG}\times1.31$.

Thus the effective background with the Al target in position could be derived, above or below threshold, by multiplying Y_{BG} by a constant factor (1.31 in this case).

TABLE 1

Background determination

Synchrotron energy (MeV)	Y_{BG}	Y_c	Y_{13}	$Y_{BG}+Y_{sc}=Y_c-Y_{13}$	Y_{sc}	$Y_{BG}\times 1.31$
17.35	147±3	255±4	66±2	189±6	42±5	193±4
15.35	97±2	182±6	53±2	139±6	43±6	133±3
13.35	49±3	92±1	35±2	57±5	8±4	64±4
12.35	29±6	60±4	27±2	33±4	4±4	38±1

To show in another way that the increase in yield below (γ, n) threshold was due to scattered neutrons, a 10 cm length of pure graphite was placed between the lead collimator and the paraffin counting block. This was sufficient to scatter all neutrons which would normally travel down the beam hole. With the graphite in position the yields below the $Al^{27}(\gamma, n)$ threshold, with and without the Al target in position were identical. Above the threshold the agreement between the yields, as determined, fully supported the constant background multiplying factor (1.31) referred to above.

4. Absolute Yield

The yield has been standardized relative to the yield from natural copper [17]). The photoneutron spectra from copper and aluminium are predominantly evaporation spectra, and both differ markedly from the spectrum of neutrons given by a radium-α—beryllium source. Therefore a comparison of aluminium photoneutron yield with that from copper was used to set an absolute yield scale, rather than a comparison with the Ra-Be source. This course of action has the further advantage that other laboratories follow this same procedure of standardization.

A target was constructed from discs of electrolytic copper. The total thickness of copper was calculated to have the same atomic absorption of γ-rays above 10 MeV, and the separation of the discs was such as to give the same total length as the Al target, thus ensuring identical conditions for neutron production and detection. The copper yield was measured at 17 MeV, 15 MeV, and 13 MeV, and normalized as above.

5. Cross Section

Yield points were derived by subtracting the modified background points from the total yield values, and allowing for counting geometry and atomic

absorption of the γ-rays in the aluminium. The yield points are plotted in fig. 1. The errors shown are standard errors, and not due only to counting statistics. They therefore include the effects of synchrotron energy variations.

The yield points shown in fig. 1 were analyzed in 0.5 MeV steps, using the method of Penfold and Leiss [18]). No smoothing of any kind was used. This gave two independent sets of cross section points interlaced at 0.25 MeV intervals, each point having its own standard error computed from the standard errors of the unsmoothed yield data.

The cross section points are shown in fig. 2, together with a smooth curve fitted by eye. A curve of best fit was also computed using Fourier synthesis up to the 11*th* order harmonics, and this agreed almost exactly with that drawn by eye.

To test the statistical validity of the cross section curve drawn, a Monte-Carlo technique was used, similar to that described by Thies [19]). A set of six cross section curves was synthesized by adding random statistical variations to each point on the cross section curve drawn through the experimental points. Each of these six exhibited the structure shown by the curve in fig. 2, and all were within the limits of error shown by the dotted lines.

Considering the experimental errors shown in fig. 2, and using the theory of Thies, the resolution was calculated to be $(0.7\ \text{MeV})^{-1}$. This indicates that the plateau region between 13.7 MeV and 14.7 MeV, the hump at 16.25 MeV, and the increasing cross section up to 18.5 MeV are all real.

The integrated cross section of the $Al^{27}(\gamma, n)$ reaction from threshold up to 18.5 MeV was found to be 28 MeV-mbarn.

6. Other Al^{27} Photodisintegration Experiments

Other measurements of the $Al^{27}(\gamma, n)$ cross section by direct neutron detection have been made by Montalbetti, Katz and Goldemberg [12]), Ferrero *et al.* [13]) and Gusakow [20]). To compare the resolutions of these experiments with the present one, some estimate of the standard errors in yield determination must be made. In the case of Montalbetti *et al.*, a standard error of $\pm 2\ \%$ was estimated from the distribution of the measured points about the smooth curve used in their analysis. Ferrero has indicated that the statistical errors in his yield determination ranged from 1 % to $1\frac{1}{2}$ %. According to Thies [19]) standard errors of this magnitude would allow peaks separated by 3 MeV or more to be resolved with 85 % assurance. However, this is insufficient resolution to observe the structure at 14 and 16 MeV.

The other cross section mentioned, is that determined by Gusakow. This reveals some structure near 17 MeV and shows evidence of the plateau region at about 14 MeV. It is difficult to assign an experimental resolution to this determination, since arbitrary yield curve smoothing was employed in the cross

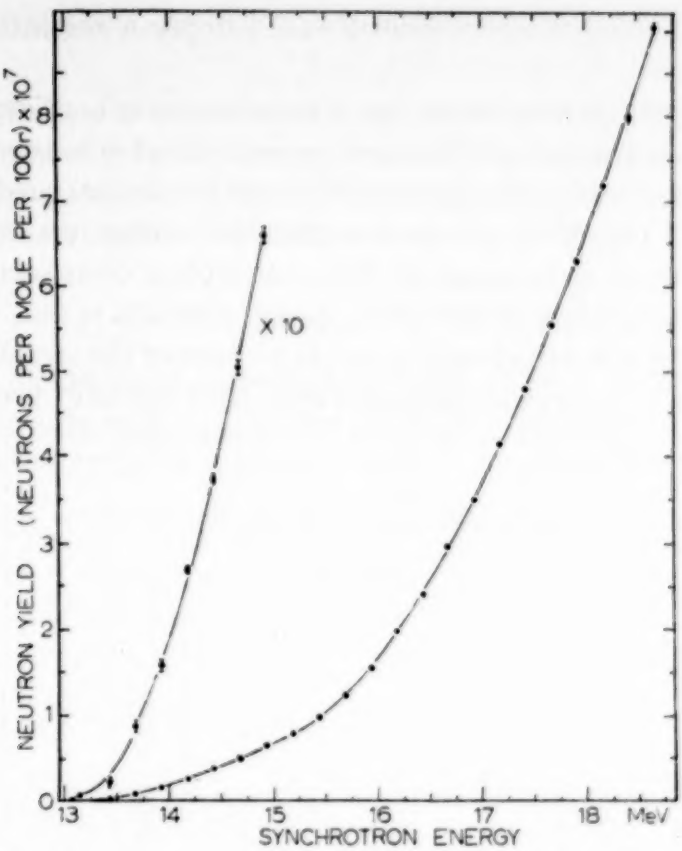

Fig. 1. Measured yield of photo-neutrons from aluminium, plotted as a function of synchrotron energy.

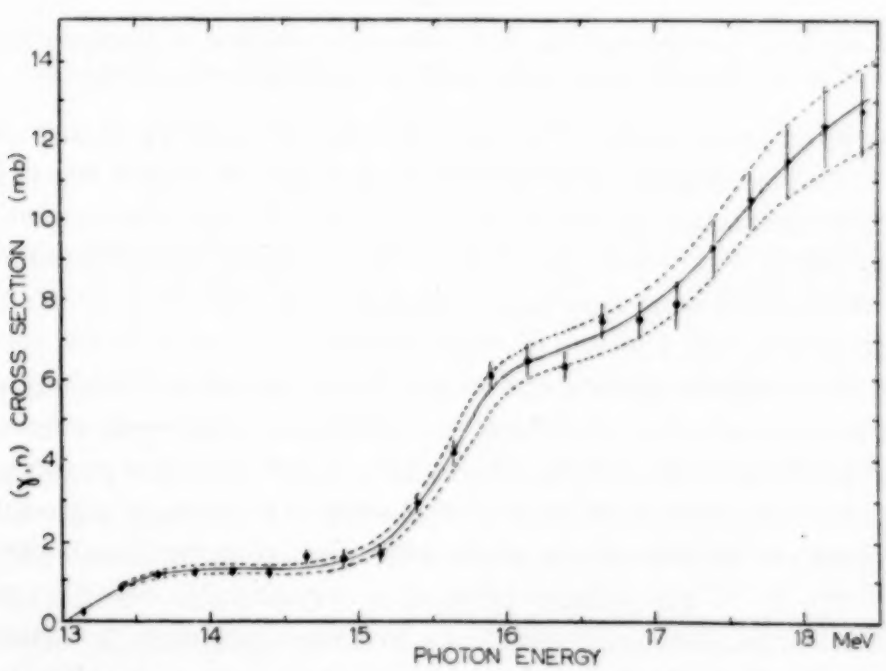

Fig. 2. Cross section for the $Al^{27}(\gamma, n)Al^{26}$ reaction plotted as a function of photon energy. The solid line is the curve of best fit consistent with the experimental points. The dotted lines define an estimated error band (see text).

section analysis. The structure drawn would imply a resolution better than (2.5 MeV)$^{-1}$.

In light nuclei the (γ, n) cross section does not necessarily reflect the behaviour of the total photo-absorption cross section, as it does for heavy nuclei. Thus to compare experimental results with the relevant theoretical predictions either a measurement of the $Al^{27}(\gamma, p)$ cross section (the other major photo-process for Al^{27}), or a direct determination of the absorption cross section is required.

The only determination of the $Al^{27}(\gamma, p)$ cross section is that of Halpern and Mann [14]), which is not sufficiently accurate to resolve the structure believed to be present. However, several measurements have recently been made of the

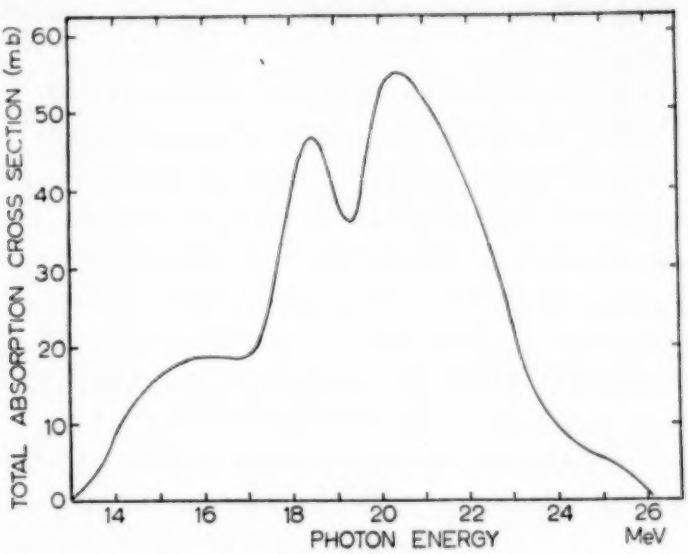

Fig. 3. Cross section for photo-absorption in aluminium obtained from an average of the determinations of Mihailovic and Ziegler weighted according to their resolutions.

total absorption cross section. The most detailed of these, by Mihailovic [21]), is estimated to have a resolution of (1 MeV)$^{-1}$, and that of Ziegler [22]), (3 MeV)$^{-1}$. The third determination by Kockum and Starfelt [23]) has poor resolution, but the experimental points are consistent with the other two determinations.

The peak absorption cross section indicated by Mihailovic is 80 mb and that by Ziegler 35 mb; yet the sum of experimental (γ, n) and (γ, p) peak cross sections is about 40 mb. Reconciliation can be brought about if it is remembered that the determination of the nuclear absorption cross section involves an allowance for atomic absorption. This is very large, and it is possible for the zero of the nuclear absorption cross section scale to be wrongly placed. For this reason the zero of Mihailovic's scale has been shifted up by 20 mb and that of Ziegler's down by 15 mb. When this is done a reasonable over-all agreement between the curves can be obtained. An average absorption cross section for Al^{27} is shown in fig. 3, this being the mean of determinations by Mihailovic and Ziegler, weighted according to the experimental resolution. The structure evident in this absorption cross section consists of peaks at 16 MeV, 18.3 MeV and

20.3 MeV, and it is more complex than that expected from the Danos-Okamoto theory.

There is a definite correspondence between the 16 MeV hump, and the rise up to 18 MeV occurring in this average cross section, and the same features in the (γ, n) cross section reported here. This (γ, n) cross section is also consistent with the recent absorption cross section results of Ziegler [24]).

7. The Ratio $\sigma(\gamma, p)/\sigma(\gamma, n)$

The plateau in the (γ, n) cross section about 14 MeV is not evident in the total absorption cross section. It is postulated that this is a result of suppression of neutron emission relative to proton emission just above the (γ, n) threshold.

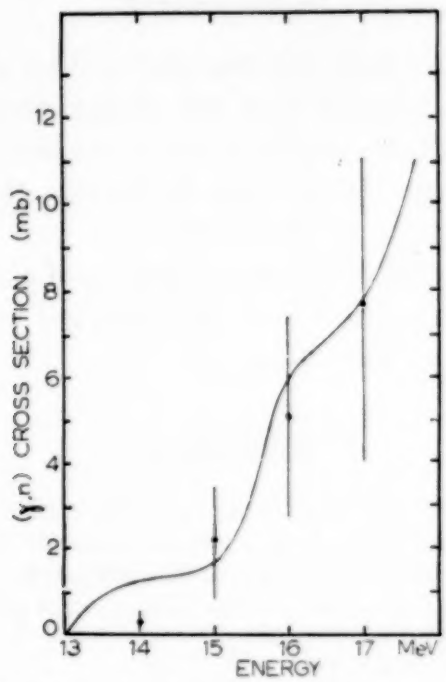

Fig. 4. Points show the $Al^{27}(\gamma, n)$ cross section deduced from the total absorption cross-section assuming neutrons to be emitted with $l = 3$ near threshold. The line indicates the observed photonuclear cross section.

This results from the low penetrability of the centrifugal barrier by the neutrons emitted with large orbital angular momentum.

The ground state of Al^{27} has spin and parity $\frac{5}{2}^+$. The fact that the known energy levels of Mg^{26} and Al^{26} below 6 MeV have even parity indicates that for electric dipole excitations of the Al^{27} nucleus up to 15 MeV the photo-nucleons must be emitted with odd orbital angular momentum.

The ratio of photoneutron to photoproton cross-sections was calculated taking into account penetration probabilities of the centrifugal barrier (see Blatt and Weisskopf [25])) for both particles, and of the Coulomb barrier for protons [26]).

Assuming that neutron and proton emission are the only decay modes of the photo-excited nucleus, a theoretical (γ, n) cross section was deduced from the experimental absorption cross section using the calculated ratio $\sigma(\gamma, p)/\sigma(\gamma, n)$,

$$\sigma(\gamma, n) = \sigma_{abs.} \left\{1 + \frac{\sigma(\gamma, p)}{\sigma(\gamma, n)}\right\}^{-1}.$$

The assumption that all nucleons were emitted with orbital angular momentum $l = 3$ gave the curve shown in fig. 4. The agreement with the measured (γ, n) cross section is good. No such agreement was obtained for any other value of l.

8. Summary

Both the present experiment and the total nuclear absorption cross-section obtained by Mihailovic indicate that the photon absorption cross-section of aluminium contains structure which is more complex than can be allowed on the Danos-Okamoto theory. It has been shown that the results of this experiment agree well with those of Mihailovic.

A general discussion of the photodisintegration of aluminium in terms of the model of single particle motion in a non-spherical potential is given in the accompanying paper (see page 216).

References

1) E. G. Fuller and M. S. Weiss, Phys. Rev. **112** (1958) 560
2) Spicer, Thies, Baglin and Allum, Aust. J. Phys. **11** (1958) 298
3) R. W. Parsons and L. Katz, Can. J. Phys. **37** (1959) 809
4) H. H. Thies and B. M. Spicer, Aust. J. Phys. (1960) (to be published)
5) M. Danos, Nuclear Physics **5** (1958) 23
6) K. Okamoto, Phys. Rev. **110** (1958) 143
7) Litherland, Paul, Bromley and Gove, Can. J. Phys. **36** (1958) 378
8) Bromley, Gove and Litherland, Can. J. Phys. **35** (1957) 1057
9) B. M. Spicer, Aust. J. Phys. **11** (1958) 490
10) B. C. Diven and G. M. Almy, Phys. Rev. **80** (1950) 407
11) L. Katz and A. G. W. Cameron, Phys. Rev. **84** (1951) 115
12) Montalbetti, Katz and Goldemberg, Phys. Rev. **91** (1953) 659
13) Ferrero, Malvano, Mendari and Terracini, Nuclear Physics **9** (1958–59) 32
14) J. Halpern and A. K. Mann, Phys. Rev. **83** (1951) 370
15) Johns, Katz, Douglas and Haslam, Phys. Rev. **80** (1950) 1062
16) B. C. Cook, Phys. Rev. **106** (1957) 300
17) King, Haslam and Parsons, Can. J. Phys. **38** (1960) 231
18) A. S. Penfold and J. E. Leiss, Analysis of Photo Cross Sections (University of Illinois, 1958)
19) H. H. Thies, Aust. J. Phys. (1960) (to e published)
20) M. Gusakow, Ph. D. Thesis, Faculty of Science, University of Paris (1958)
21) M. V. Mihailovic (1959), private communication;
see also: Dular, Kernel, Kregar, Mihailovic, Pregl, Rosina and Zupancic, Nuclear Physics **14** (1959) 131

22) B. Ziegler, Zeits. f. Phys. **152** (1958) 566
23) J. Kockum and N. Starfelt, Nuclear Instruments and Methods **5** (1959) 37
24) B. Ziegler, Nuclear Physics **17** (1960) 238
25) J. M. Blatt and V. F. Weisskopf, Theoretical Nuclear Physics, (J. Wiley and Sons, New York, 1952)
26) Feshbach, Shapiro and Weisskopf, Tables of penetrabilities for charged particle reactions, NYO-3077 (1953)

2.1

Nuclear Physics **22** (1961) 216—225; ©*North-Holland Publishing Co., Amsterdam*

Not to be reproduced by photoprint or microfilm without written permission from the publisher

PHOTODISINTEGRATION OF Al^{27}
(II) Theoretical

J. E. E. BAGLIN, M. N. THOMPSON and B. M. SPICER

Physics Department, University of Melbourne

Received 3 October 1960

Abstract: The intrinsic level scheme calculated for a deformed nucleus by Nilsson has been used in conjunction with a single particle excitation model to compute the photonuclear electric dipole absorption cross section for Al^{27}. The resultant curve contains peaks at 16, 18.5 and 21 MeV, in accord with the high resolution experimental results of Mihailovic. The calculated energy distribution of photoneutrons contains high energy direct emission groups, in agreement with experiment. Angular distributions computed also agree with experimental results. A new small cross section peak is predicted near 26 MeV.

1. Introduction

In terms of the hydrodynamic model proposed by Danos [1]) and Okamoto [2]), the photo-absorption giant resonance consists of two peaks, separated in energy by an amount depending on the nuclear deformation. Although this model will account for the absorption cross section as reported by Kockum and Starfelt [3]) and by Ziegler [4]), it fails to explain the more detailed structure observed by Mihailovic [5]).

In contrast with the above approach, Ferrero *et al.* [6]) have computed a (γ, n) cross section using the Wilkinson model of the nucear photoeffect, with the assumption of independent particle motion in a spherical potential well. This computed cross section is not consistent with the structure noted by Mihailovic. Thus it would appear that the Wilkinson model is also inadequate for the case of aluminium.

2. Proposed Model

The model proposed here refers to radiative transitions between single particle levels in a spheroidal potential well, and is similar to models used by Wilkinson [7]), Mottelson and Nilsson [8]), and later by Thies and Spicer [9]). However, because it differs from these in some respects, it is restated below.

(1). It is assumed that the intrinsic nucleon levels calculated by Nilsson [10]) apply to nuclei of all degrees of deformation. Nilsson has computed these level schemes using a Hamiltonian

$$H = H_0 + C\mathbf{l}\cdot\mathbf{s} + D\mathbf{l}^2,$$

which is the sum of a Hamiltonian for a single nucleon in a spheroidal oscillator

potential, and spin-orbit and l^2 terms, the latter effectively interpolating between an oscillator potential and a square well. The ratio $2D/C$ has been defined as a variable parameter μ. For a given value of δ, the nucleons fill the intrinsic levels according to the exclusion principle, until all nucleons are accommodated. Each neutron or proton state is twofold spin-degenerate, and it is assumed that the same levels and energy scales apply for both neutrons and protons. Unpaired nucleons are responsible for the ground state spin and parity of the nucleus.

Bishop [11]) has shown that if a non-zero value of the parameter μ is used for $N = 2$ levels in the Nilsson calculation, the unpaired proton in Al^{27} will appear in the $1d_{\frac{5}{2}}(\frac{5}{2})$ level. Thus the nucleus will have a ground state spin and parity of $\frac{5}{2}+$, agreeing with experimental measurements.

(2). Any nucleon can absorb the entire energy of an incident photon, and is thereby excited to a higher intrinsic level, with the rest of the nucleus in a ground or excited rotational state. Such a transition will naturally be subject to the selection rules for the multipole absorption under consideration. Transitions between collective vibrational states have not been taken into consideration.

(3). The probability $T_E(\lambda)$, for such an electric transition of multipole order λ and energy $\hbar\omega$ can be calculated from formulae given by Nilsson:

$$T_E(\lambda) = \frac{8\pi(\lambda+1)}{\lambda[(2\lambda+1)!!]^2} \frac{1}{\hbar}\left(\frac{\omega}{C}\right)^{2\lambda+1} B_E(\lambda),$$

where $B_E(\lambda)$ is the reduced transition probability.

The integrated cross section for the transition can be deduced from the relationship

$$\int \sigma dE = T_E(\lambda) \frac{(2\lambda+1)\pi^2\hbar^3C^2}{2(\hbar\omega)^2},$$

which has been derived from equations given by Blatt and Weisskopf [12]) in Chapter XII and Appendix B. Each absorption line was assumed to have a triangular profile. A width of 2 MeV was considered more appropriate than the value of 3 MeV used previously by Wilkinson [13]), since the Nilsson level scheme is obtained by elimination of one further degree of degeneracy in the level structure, and consequent removal of one source of line broadening suggested by Wilkinson. Some finite width is required, however, to allow in a crude way for the residual interactions neglected in this pure single particle model.

This calculation of transition strengths should be contrasted with the work of Thies and Spicer [9]) and Mottelson and Nilsson [8]), who assumed all the transitions allowed by asymptotic selection rules [14]) to have equal strengths.

(4). After excitation, the particular nucleon may interact with the other nucleons to form a compound nucleus, which will decay with photon or particle emission.

Particle emission can only occur from a level further than the threshold energy (E_{th}) above the topmost occupied level. If the original excitation leaves the nucleon in such a state, that nucleon is emitted directly, without the formation of a compound state; that is, the lifetime for direct emission is much less than that for decay to a compound nucleus state, provided that it is energetically possible.

However, it should be noted that transitions from the levels more strongly bound than the topmost occupied level may involve an excitation greater than E_{th} without the nucleon reaching a state from which the direct emission referred to above can occur. Under these conditions, emission can occur only after nucleon-nucleon interactions have brought about the concentration of the energy on one particular nucleon which is capable of being emitted. That is, a compound nucleus is formed.

3. Computation of Absorption Cross Section

The cross sections of all electric dipole transitions available to the nucleons in Al^{27} were calculated as indicated above. Each was given a width of 2 MeV, and their effects were summed to give the theoretical E1 absorption cross section.

The degree of deformation, which is here specified by δ (see Nilsson[10]), eq. (3)), has been deduced for Al^{27} from the observed spectroscopic quadrupole moment, using the concepts of Bohr and Mottelson [15]). This requires some estimate of the contribution to the observed moment made by the odd proton and by the stable Mg^{26} core, and an estimate of the strength of coupling between them. Okamoto suggests that strong coupling is appropriate for Al^{27}, but Bohr and Mottelson have also calculated an intermediate coupling factor. Taking the quadrupole moment of Al^{27} to be 0.153 barn (Koster[16]), Lew and Wessel [17])), the corresponding deformations are $\delta = 0.25$ for strong coupling, and $\delta = 0.14$ for intermediate coupling.

Using this data and the Danos-Okamoto theory, the ratio of the energies of the two component resonance peaks for Al^{27} is computed to be between 1.12 and 1.29, depending on the degree of coupling assumed.

Choice of a deformation parameter $\eta = 4$ (Nilsson[10]), eq. (12c)), corresponding to $\delta = 0.2$, and $\mu = 0.18$ for the $N = 3$ levels gave the computed cross section shown in fig. 1. No other choice of these parameters gave satisfactory agreement with the absorption cross sections found by Mihailovic and by Ziegler (see preceding paper, fig. 3, p. 212). The value $\mu = 0.18$ has also been used to derive ground state spins for nuclei whose last unpaired nucleon lies in an $N = 3$ level. The spins were found to be consistent with observed values supporting the particular value of μ which has been employed here.

The computed cross section exhibits three peaks at the relative positions

observed by Mihailovic. An increase in η would result in the lowest energy peak being shifted away from the other two, whilst an increase in μ would increase the separation between the lower pair and the third one.

The absolute energy scale obtained by Nilsson, using a static potential, would correspond to transition energies too low for the giant resonance energy to approach the experimental value. However, for the present computation, the modifications suggested by Frahn and Lemmer [18]) have been used. Their work,

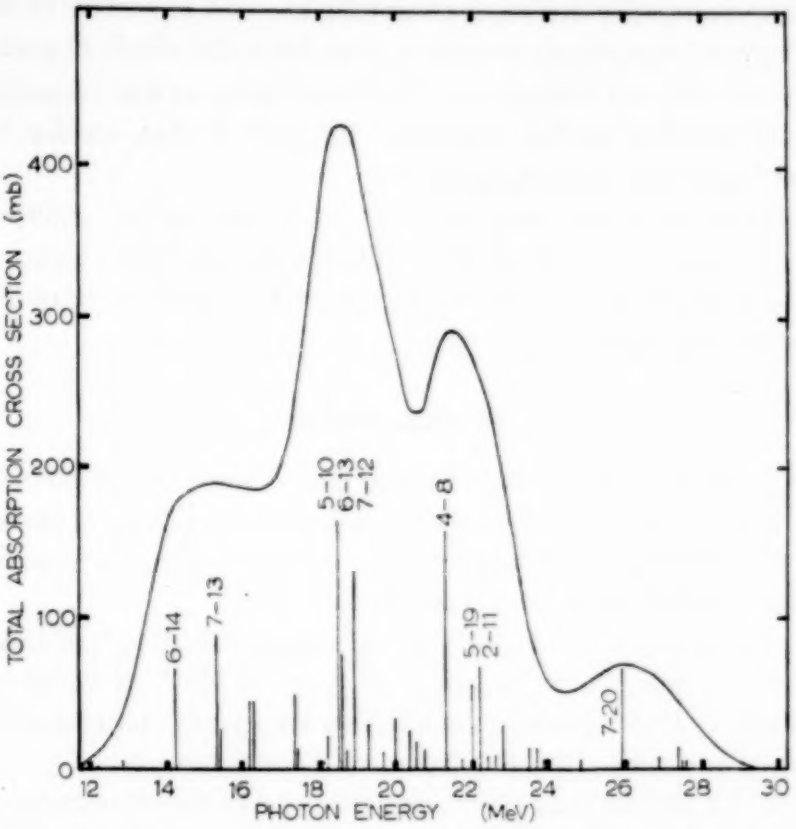

Fig. 1. Calculated absorption cross section for Al^{27}. Principal transition lines are labelled with numbers used by Nilsson to describe the initial and final levels in each case.

in effect, adapts the Nilsson eigenvalues to apply to the case of a velocity-dependent potential, using a "reduced nucleon mass" M at the centre of the nucleus, equal to half the free nucleon mass M_0. The resulting energy scale brings about the good agreement with experimental energies shown in fig. 1. Alternatively, it is possible, in principle, that a suitable energy scale could be produced by the mechanism suggested by Brown and Bolsterli [19]).

The assumptions listed below are fundamental to the model assumed, and their degree of validity will determine the accuracy of the computation referred to above.

First, a single-particle excitation has been assumed. The only allowance for interactions between the excited nucleon and the remaining individual nucleons is in the assignment of a natural width to each transition.

Next, the accuracy of the Nilsson level scheme is basic to the model. Experimental verifications of the level order in the region $A = 25$ to $A = 29$ have been obtained by Litherland *et al.* [20]) and Bromley *et al.* [21]), and the agreement between observed and predicted ground state spins indicates no major errors. Bishop has raised doubts as to the correct value of the parameter μ for light nuclei. However, modifications indicated by him will not greatly influence the predictions made here.

Finally, the transition strength estimates are not expected to be accurate, but should nevertheless be more informative than the result of assuming equal strengths for all allowed transitions. The inaccuracy of the transition strength formulae may account for the predicted integrated cross section being many times larger than the experimental value.

For transitions to levels with $N = 3$, no values of the eigenvectors were available for the case of $\mu = 0.18$. Thus Nilsson's quoted eigenvectors ($\mu = 0.35$) were used to compute the transition strengths. The error thereby introduced is expected to be less than 2 %.

4. Discussion

The cross section shown in fig. 1 displays evidence of the structures at 16, 18.5 and 21 MeV observed by Mihailovic. These could not be explained in terms of the Danos model. However, there seems to be a basic correlation between the single particle model used here and Danos' model.

Firstly, the area under the 16 MeV peak is approximately half that under the gross structure composed of the peaks at 18.5 and 21 MeV, as would be predicted by Danos. Further, the separation of the two structures changes with deformation in exactly the way expected from the Danos theory.

In addition, for all the transitions contributing to the structures at 18.5 and 21 MeV, the absorbed quantum has increased the oscillation energy in a plane perpendicular to the axis of symmetry. Conversely, for transitions contributing to the low energy resonance, the absorbed quantum has increased the oscillation energy along the axis of symmetry. As has been pointed out by Thies and Spicer [9]), this can be directly related to the Danos theory, where the lower resonance would be due to vibration of the "nuclear fluid" along the symmetry axis, and the higher peak would be due to vibration of the "fluid" in a plane perpendicular to this.

5. Energy Distribution of Photoneutrons

From the fourth postulate of the proposed model, the photoneutrons are expected to be of two types — those directly ejected, and those emitted after the formation of a compound nucleus. Of all the cross section contributions in Al^{27}, 58 % arise from excitation of levels of energy less than 13 MeV above the

topmost occupied level. Hence, in terms of this model, subsequent neutron emission can only occur via compound nucleus formation and decay, giving rise to a statistical neutron energy spectrum.

The remainder of the transitions leave the neutrons in states from which they can be directly emitted. The energy of these neutrons when emitted is the total excitation energy, less that required to raise the neutron to a state 13 MeV above the $1d_{\frac{5}{2}}(\frac{5}{2})$ level.

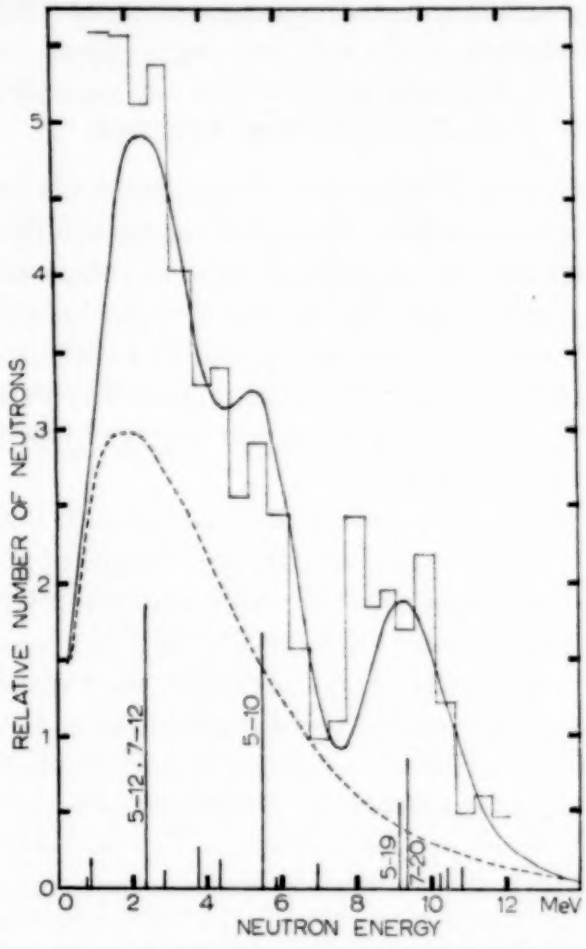

Fig. 2. Energy distribution of photoneutrons from Al^{27}. Solid line: calculated total distribution. Histogram: experimental results of Revzen and Sargent. Dotted line: evaporation spectrum which was added to groups arising from the transitions indicated by vertical lines.

Each group of neutrons has been assigned a width of 2 MeV, consistent with the natural width assigned to each level. On this basis, it is estimated that contributions to the neutron spectrum due to direct emission occur about equally at neutron energies of 2.4 MeV, 5.5 MeV and 9.4 MeV.

A theoretical energy distribution has been compounded from an evaporation spectrum and the direct emission spectrum discussed above. To calculate the evaporation spectrum, a constant nuclear temperature of 2 MeV was assumed for Al^{26}. This value was chosen by Revzen and Sargent [22]). The calculated

spectrum is shown in fig. 2, together with the experimental results of Revzen and Sargent [22]). Their results are consistent with an evaporation spectrum only for neutron energies up to 4 MeV. However, at 5.5 MeV and at about 9 MeV, the number of neutrons observed significantly exceeds the number expected from statistical theory. The theoretical energy distribution shown in fig. 2 agrees very well with the quoted experimental results.

The work of Cortini *et al.* [23]) using 30 MeV bremsstrahlung also supports the existence of a group of neutrons with energies of about 5.5 MeV superimposed on a statistical spectrum.

6. Fast Neutron Fraction

In a recent experiment, Ferrero *et al.* [6]) measured the cross section for the production of fast photoneutrons from Al^{27} using the Si^{28}(n, p) reaction as detector. They found that the fraction of photoneutrons with energies greater than 5.5 MeV increased rapidly for photon energies between 23 MeV and 26 MeV. This phenomenon could not be explained satisfactorily in terms of a purely statistical model, nor by the model proposed by Ferrero. However, the model proposed here accounts well for the energy dependence of the fast neutron fraction found by Ferrero.

The ratio of the photo cross section of neutrons with energies greater than 5.5 MeV, to the total neutron cross section was calculated at a number of γ-ray energies between 20 MeV and 30 MeV using the data of figs. 1 and 2. It is important to note that because a width of 2 MeV has been assigned to each transition any γ-ray will excite, to some degree, all transitions within 2 MeV of its energy. For transitions leading to compound nucleus formation the number of fast neutrons was deduced from a statistical energy spectrum corresponding to a constant nuclear temperature of 2 MeV in Al^{26}.

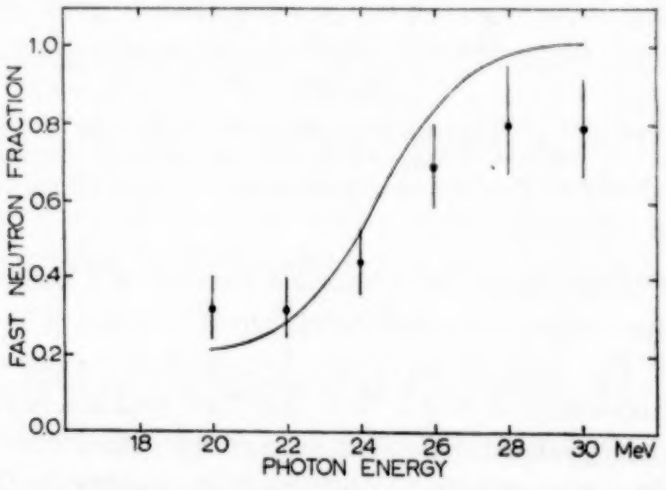

Fig. 3. Fraction of fast neutrons in the $Al^{27}(\gamma, n)$ cross section, plotted as a function of photon energy. The solid line is the result calculated using the model proposed in this paper, and the experimental results are those of Ferrero *et al.* [6]).

The calculated ratio as a function of photon energy is shown in fig. 3, together with the experimental results of Ferrero. Considering the errors involved in assigning the contributions of the various transitions, the agreement is good, particularly in the region between 23 MeV and 26 MeV where the rapid increase in fast neutrons has been observed.

7. Angular Distributions

Since the model proposed uniquely specifies the orbital angular momentum of the directly ejected particle, the possibility of interference terms contributing to the angular distribution has not been considered here.

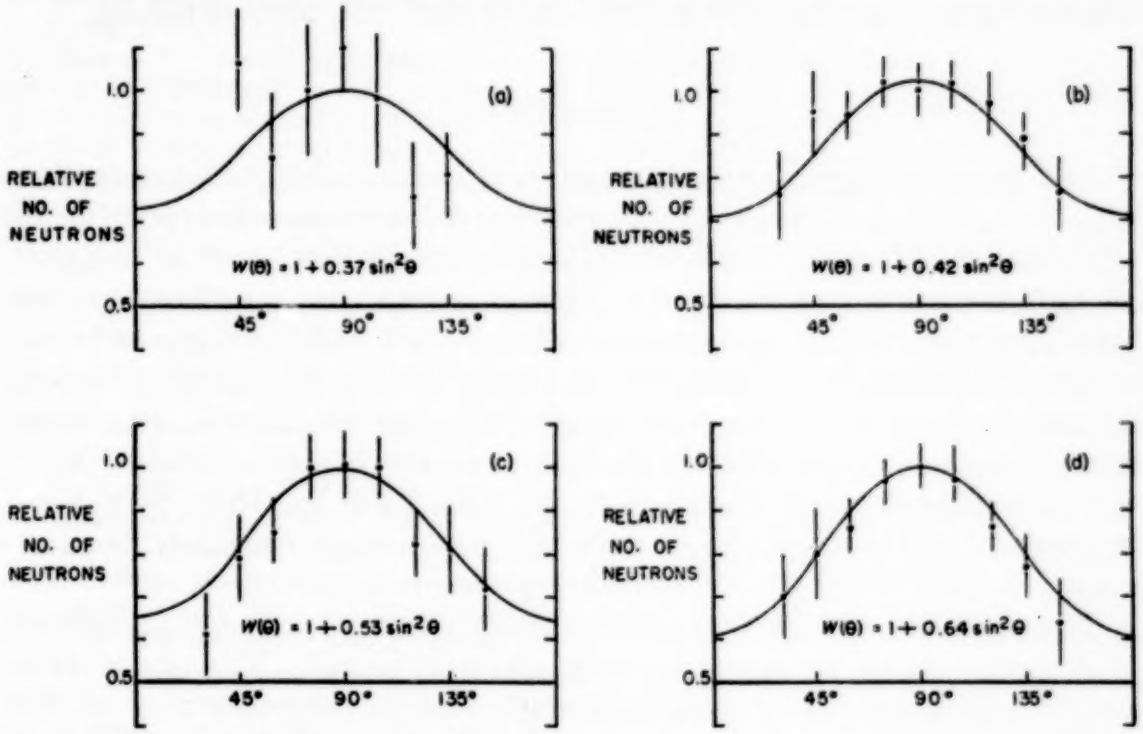

Fig. 4. Angular distribution of photoneutrons from Al^{27}. Solid lines are theoretical distributions for neutrons of energies above (a) 0 MeV, (b) 2.5 MeV, (c) 5 MeV, (d) 10 MeV. Points are experimental results of Dixon (a) and Johansson (b), (c), (d).

The angular distribution of nucleons from a light nucleus undergoing statistical decay is expected to be symmetric about 90°, and may be isotropic. In the following calculations, this distribution has been assumed to be isotropic. On the other hand, for directly emitted neutrons, Courant [24]) predicts an angular distribution given by

$$W(\theta) = 2l + (2+l)\sin^2\theta,$$

where the emission results from a transition of the neutron between initial and final states in which it has orbital angular momenta of l and $(l+1)$ respectively. θ is the angle at which the neutron is emitted relative to the direction of the incident photon.

In the case of Al^{27}, all the directly emitted neutrons result from transitions between the levels with $l = 2$ and $l = 3$, and an angular distribution of the form $(1+\sin^2\theta)$ is predicted. By considering the relative proportions of evaporation and direct neutrons indicated by the present cross section calculation, a theoretical angular distribution was calculated for neutrons of energies above 0 MeV, 2.5 MeV, 5 MeV and 10 MeV. These four results are shown in fig. 4, where they are compared with the experimental results of Dixon [25]) and Johansson [26]) who used threshold detectors. The agreement is in each case within the limits of experimental errors. However, it should be noted that the theoretical values will alter slightly, depending on the absolute energy scale decided upon, and that interference effects have not been considered.

8. Conclusions

The agreement between predicted and experimentally determined absorption cross sections and neutron energy and angular distributions indicates the validity of the model described above. The peak in the predicted cross section near 26 MeV is unusual and unexpected. There is no experimental evidence so far which definitely verifies its existence, although some evidence is present in the results of Mihailovic [5]), of Ziegler [27]), and in the fast neutron fraction observed by Ferrero [6]). However, it is interesting to note that Ferrero *et al.* [28]), during measurements of the fast neutron yield from a number of nuclei, found evidence for a second peak in the cross sections of Cr, As, I and Ta. These peaks were suggested at energies in the region of 26 MeV, which is approximately the same energy as that at which the predicted peak occurs in the case of Al^{27}.

The possibility of such a structure actually existing in the Al^{27} absorption cross section should be further investigated experimentally. This will be difficult in experiments using bremsstrahlung, owing to the presence of all the neutrons from the giant resonance. However, if the above theory is correct, the neutrons from this peak should all be directly emitted, having an energy of about 9 MeV, and a neutron detector insensitive to neutrons below this energy could be used.

The model put forward in this paper implies that approximately 50 % of the photoneutrons from Al^{27} arise from a direct emission process. This figure is higher than is usually estimated, and its study by more precise measurements of neutron energy and angular distributions would be desirable.

The application of this model to other light deformed nuclei is at present being carried out in this laboratory.

The authors wish to acknowledge the encouragement and interest of Professor Sir Leslie Martin and Acting Professor C.B.O. Mohr during the course of this work. Grateful acknowledgement is made by one of us (J. E. E. B.) of a Research

Fellowship from Imperial Chemical Industries of Australia and New Zealand Limited, and another (M. N. T.) of a Commonwealth Postgraduate Award, both held throughout this work.

References

1) M. Danos, Nuclear Physics **5** (1958) 23
2) K. Okamoto, Phys. Rev. **110** (1958) 143
3) J. Kockum and N. Starfelt, Nuclear Instruments and Methods **5** (1959) 37
4) B. Ziegler, Zeits. f. Phys. **152** (1958) 566
5) M. V. Mihailovic, private communication (1959);
see also: Dular, Kernel, Kregar, Mihailovic, Pregl, Rosina and Zupancic, Nuclear Physics **14** (1959) 131
6) Ferrero, Malvano, Menardi and Terracini, Nuclear Physics **9** (1958) 32
7) D. H. Wilkinson, Phil. Mag. **3** (1958) 567
8) B. R. Mottelson and S. G. Nilsson, Nuclear Physics **13** (1959) 281
9) H. H. Thies and B. M. Spicer, Aust. J. Phys. (1960) (to be published)
10) S. G. Nilsson, Mat. Fys. Medd. Dan. Vid. Selsk. **29**, no. 16 (1955)
11) G. R. Bishop, Nuclear Physics **14** (1960) 376
12) J. M. Blatt and V. F. Weisskopf, Theoretical Nuclear Physics (John Wiley and Sons, New York, 1952)
13) D. H. Wilkinson, Physica **22** (1956) 1039
14) G. Alaga, Nuclear Physics **4** (1957) 625
15) A. Bohr and B. R. Mottelson, Mat. Fys. Medd. Dan. Vid. Selsk. **27**, no. 16 (1953)
16) G. F. Koster, Phys. Rev. **86** (1952) 148
17) H. Lew and G. Wessel, Phys. Rev. **90** (1953) 1
18) W. E. Frahn and R. H. Lemmer, Nuovo Cim. **6** (1957) 664
19) G. E. Brown and M. Bolsterli, Phys. Rev. Letters **3** (1959) 472
20) Litherland, Paul, Bromley and Gove, Can. J. Phys. **36** (1958) 378
21) Bromley, Gove and Litherland, Can. J. Phys. **35** (1957) 1057
22) M. Revzen and B. W. Sargent, private communication (1959)
23) Cortini, Milone, Papa and Rinzivillo, Nuovo Cim. **14** (1959) 54
24) E. D. Courant, Phys. Rev. **82** (1951) 703
25) W. R. Dixon, Can. J. Phys. **33** (1955) 785
26) S. A. E. Johansson, Phys. Rev. **97** (1955) 434
27) B. Ziegler, Nuclear Physics **17** (1960) 238
28) Ferrero, Malvano and Tribuno, Nuovo Cim. **6** (1957) 385

8.A

Nuclear Physics **22** (1961) 226—244; © *North-Holland Publishing Co., Amsterdam*

Not to be reproduced by photoprint or microfilm without written permission from the publisher

ELASTIC SCATTERING OF NEGATIVE PIONS BY PROTONS AT 128 AND 162 MeV

Yu. A. BUDAGOV, S. WIKTOR, V. P. DZHELEPOV, P. F. YERMOLOV and V. I. MOSKALEV

Laboratory of Nuclear Problems, Joint Institute for Nuclear Research, Dubna, USSR

Received 13 July 1960

Abstract: The elastic scattering distribution of negative pions by protons has been measured with a hydrogen-filled diffusion cloud chamber in a magnetic field. In a set of exposures 344 and 941 elastic scattering events were recorded at angles θ(c.m.s.) $> 10°$. The total cross-sections for elastic scattering σ_{el} (128 MeV) $= (12.8 \pm 1.0)\ 10^{-27}$ cm^2 and σ_{el}(162 MeV) $= (21.4 \pm 1.2)\ 10^{-27}$ cm^2 were determined by calculating the total length of negative pion tracks in the chamber. The elastic $\pi^- -$p-scattering angular distributions were obtained in the form (the SP-analysis):

$$d\sigma/d\Omega(128\ \text{MeV}) = (1.00 \pm 0.08)[(0.55 \pm 0.07) + (0.34 \pm 0.12)\cos\theta + (1.30 \pm 0.24)\cos^2\theta]\ 10^{-27}\ \text{cm}^2/\text{sr},$$

$$d\sigma/d\Omega(162\ \text{MeV}) = (1.00 \pm 0.06)[(0.93 \pm 0.07) + (0.51 \pm 0.12)\cos\theta + (2.28 \pm 0.22)\cos^2\theta]10^{-27}\ \text{cm}^2/\text{sr}.$$

The differential forward scattering cross-sections are equal to $(2.20 \pm 0.32)\ 10^{-27}$ cm^2/sr and $(3.73 \pm 0.32)10^{-27}$ cm^2/sr respectively. The real parts of the forward scattering amplitude (in c.m.s.) have been calculated in units of $\hbar/m_\pi c$:

$$D_-^b(128\ \text{MeV}) = 0.261 \pm 0.031 \quad \text{and} \quad D_-^b(162\ \text{MeV}) = 0.216 \pm 0.038.$$

These quantities agree with those calculated from dispersion relations with the coupling constant $f^2 = 0.08$.

1. Introduction

Much attention has recently been paid to an experimental check of dispersion relations. These, first obtained by Goldberger, Miyazawa and Oehme [1]) for the scattering of charged pions by protons, connect the real parts of the forward scattering amplitudes, the S scattering lengths and the integral over the total cross-sections for $\pi^+ -$p and $\pi^- -$p-interactions throughout the energy range. In the integration region $0 \leqq \omega < \mu$ there is a contribution from the 'bound state', i.e., from a neutron as a possible intermediate state in scattering. This contribution may be expressed in terms of a renormalized coupling constant f^2, describing the pseudovector interaction. Basic to the derivation of dispersion relations are such general physical principles as the microscopic causality principle (the requirement that there should be no signals propagating with a velocity greater than that of light) and the hypothesis of the charge independ-

ence of nuclear forces. Comparison with experiment enables us to check the validity of these fundamental principles, and, on the other hand, independently to determine the coupling constant and the S scattering lengths.

The dispersion relations were first compared with experiment by Anderson, Davidon and Kruse [2]) and were shown to be in good agreement with it. In 1957, however, Puppi and Stranghellini [3]) noticed the fact that negative pions showed a discrepancy between experimental and theoretical data. Whereas the real parts of the forward scattering amplitude determined experimentally in the energy range to 400 MeV for positive pions were found in agreement with those calculated via dispersion relations with the coupling constant $f^2 = 0.09 \pm 0.01$, a better agreement was obtained for negative pions in the energy interval to 200 MeV if the coupling constant was assumed to be $f^2 = 0.04$. Simultaneously, Agodi, Cini and Vitale [4]) showed that the effects due to charge, electromagnetic corrections and the contribution from hyperons and K-mesons cannot account for the discrepancy observed. Yet, this discrepancy was, as can be seen from ref. [3]), substantiated by the results of merely one experiment: the measurements of elastic π^-—p-scattering performed by a group of the Carnegie Institute [5]) at energies of negative pions of 150 and 170 MeV, since the other experimental data in this energy range have a comparatively low accuracy. In this connection new experimental data on elastic π^-—p-scattering in the region from 100 to 200 MeV and comparison with the predictions of dispersion relations are certainly of interest.

The present paper offers the results of measurements with a hydrogen-filled diffusion cloud chamber of negative-pion elastic scattering by protons at energies of 128 and 162 MeV. The application of this technique has enabled us to avoid some specific difficulties involved in the use of electronic methods of measurement and made it possible to pass over to the region of smaller scattering angles, which proves highly essential for estimating the differential cross-section at 0^0.

2. Experimental Conditions and Apparatus

2.1. EXPERIMENTAL SET-UP

The experimental set-up is represented in fig. 1. A beryllium target (3) 40 mm thick was placed in an 670 MeV internal proton beam (2) of the synchrocyclotron of the Nuclear Problems Laboratory. Negative pions (4) generated in the target were extracted out of a vacuum chamber (1) by the magnetic field of an accelerator, and after passing through an additional concrete shielding (5), collimated by a collimator (6) (3.6 m long and an inside diameter of 50 mm) in the shielding wall (7). Then the beam of negative pions deflected by 40° with a clearing magnet (8), struck a diffusion chamber (11) inside an electromagnet (10). Placed before the chamber was an additional lead collimator (9) with a rectan-

gular aperture 350×50 mm^2. The beam of negative pions was traced by the usual current-carrying thread method. All in all about 90 000 stereophotographs were obtained. This material alongside elastic $\pi^- - p$-scattering enabled us to detect the β-decay of negative pions ($\pi^- \to e^- + \tilde{\nu}$) [6]) and to obtain some data on decays of neutral pions by the schemes $\pi^0 \to e^- + e^+ + \gamma$ [7]) and $\pi^0 \to 2e^- + 2e^+$ [8]).

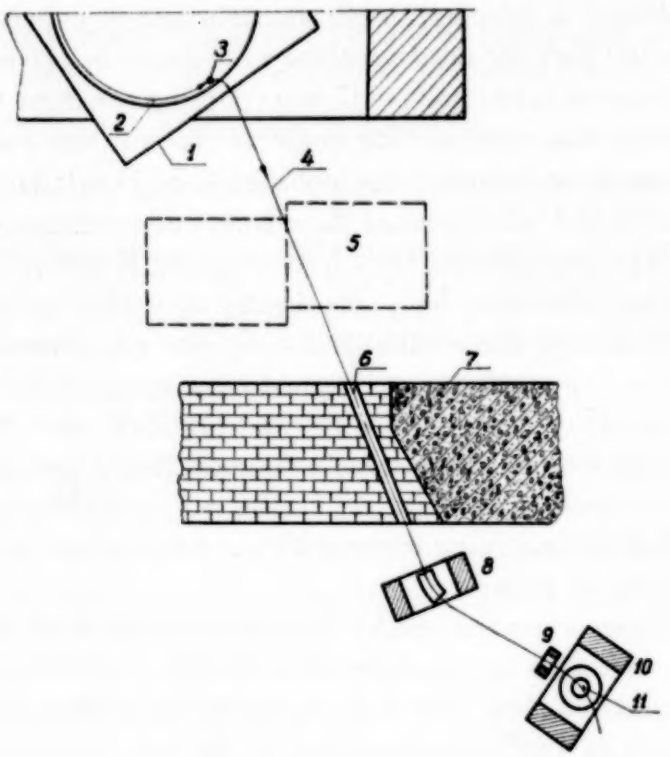

Fig. 1. The experimental arrangement.

2.2. DIFFUSION CLOUD CHAMBER

The diffusion cloud chamber was designed for work with light gases at pressures up to 25 atm [9]). The cloud chamber placed in a magnet is schematically represented in fig. 2. The chamber is a stainless steel reservoir consisting of three sections. In the lower, the main section, a required temperature gradient is maintained with a system of heaters and a copper coil through which colled acetone is pumped.

In the lower flange of the middle section there is a small tray for methyl alcohol used as the working liquid. At the temperature of the bottom $-70°$ and that of the tray $+10°$ an approximately linear temperature distribution with a gradient of 7° per cm is kept in the sensitive volume of the chamber, the height of the sensitive layer coming up to 6 or 7 cm. The temperature in various parts of the chamber is controlled and measured with copper constantan thermocouples.

The chamber was illuminated at an angle of 90° to the photographing axis through side windows of 30 mm thick plexiglass at the end of rectangular juts 150 mm long weld on the lower cylindrical part of the chamber. This increased the maximum working diameter of the chamber up to 380 mm, the diameter of the hole in the upper pole of the magnet being 460 mm.

The chamber was lighted by two IFP-500 xenon flash tubes through which capacities of 200 μF at a voltage of 2000 V were discharged at the moment of a

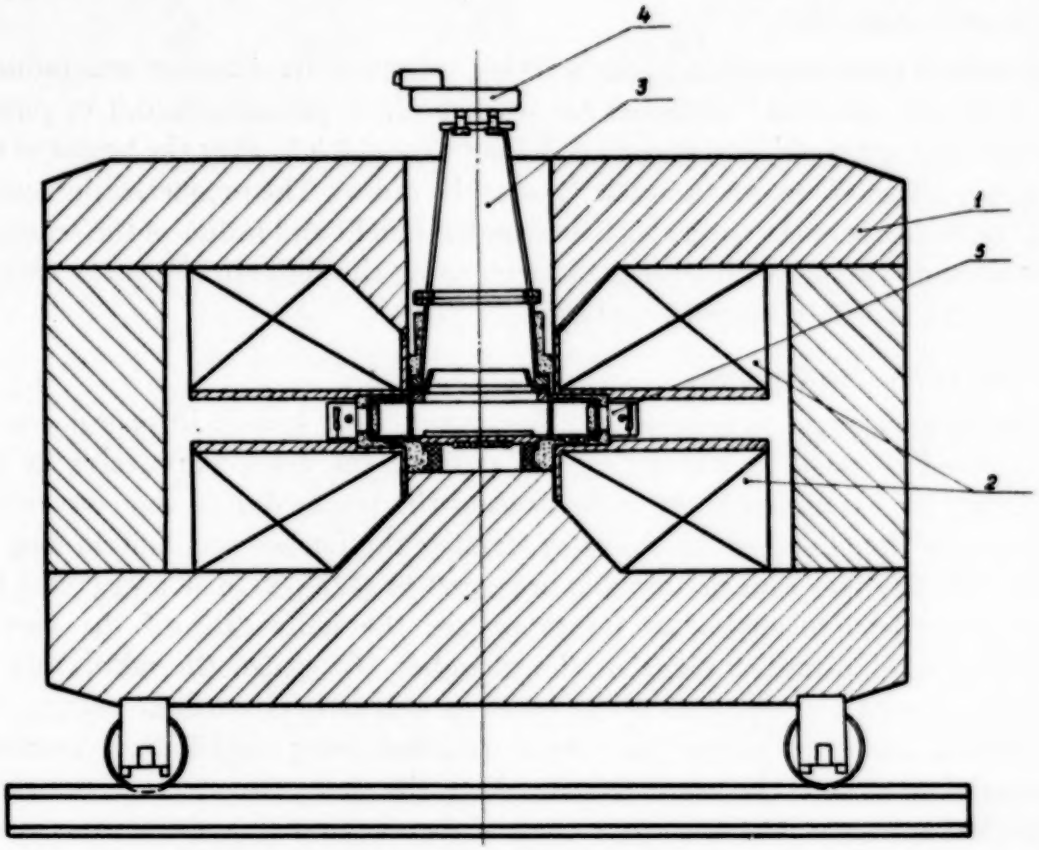

Fig. 2. A scheme of diffusion cloud chamber situated in the magnetsolenoid MC-4A. 1—an electromagnet yoke, 2—coils, 3—diffusion cloud chamber, 4—stereophotocamera, 5—illuminators.

flash. The light from each tube was formed into a parallel beam by two parabolic reflectors.

The photographs were taken by a stereocamera with two objectives Helios-37 ($f = 62$ mm) on Panchrom-X 35 mm film with a sensitivity of 1000 units GOST. The objectives were readjusted for the distortion due to photographing through the upper glass windows 25 mm thick. The resolution of the objectives was 50 lines/mm in the centre of the field of vision. The base of the stereocamera was equal to 120 mm, the object distance to 1 meter. The required depth of volume photographed was achieved at an aperture of 5.6.

The operation cycle of the chamber lasting 8 sec was controlled by an electronic circuit which a) switched on high-frequency voltage to the synchrocyclo-

tron dee for a definite number (usually 2 or 4) of acceleration cycles; b) started the flashes with a delay of 0.2 to 0.3 sec with respect to a particle pulse; c) switched on the camera film advance and d) switched on and off the electric clearing field. Required time delays between the operations were effected by one-shot multi-vibrator circuits. By regulating the number of acceleration cycles the intensity of the beam was kept such that some 30 negative pion tracks were on the average recorded in each picture.

2.3. ELECTROMAGNET

A 9000 G permanent field in the working volume of the chamber was induced by a MC-4A solenoid * designed for work both in permanent and in pulsed supply. The magnetic field variation did not exceed 3.5 % over the height of the chamber sensitive volume and 2.5 % over the radius. The magnetization curve and the decrease in the magnetic field over the height and radius of the sensitive volume were gauged with a magnetometer using the Hall effect ** and calibrated by the proton resonance method.

2.4. NEGATIVE PION BEAMS

The mean energy of mesons in a beam and their spread in energies were determined directly by measuring the radii of the track curvatures in the photographs. To diminish the distortions of the tracks due to the convention currents in the chamber the delay in starting the flashes was half as long as usual. The energies thus determined are equal to (128 ± 8) MeV and (162 ± 10) MeV where the uncertainties indicated are the halfwidths of the energy distribution of negative pions in the chamber. To gauge the admixture of negative muons and electrons in the beam as well as to control the energy, the absorption curves in copper have been obtained using scintillation counters. The mean energies of the beam determined by the above two methods coincided with good accuracy. The total admixture of negative muons and electrons in the beams was found to amount to (16 ± 2) %.

3. Scanning and Analysis

All photographs were scanned twice through stereoscopes by several scanners independently, and some of them were scanned for a third time especially thoroughly to estimate the efficiency of the previous double scanning which was found to be equal to 97 %. The investigation of the angular distribution of the missed events showed that this efficiency does not depend upon the specific form of a scattering event (the scattering angle or the azimuthal angle).

* MC-4A is a modification of MC-4. These solenoids were designed at the Electrophysical Apparatus Research Institute by N. S. Streltsov, A. V. Ugumov, N. N. Indyukov, Yu. P. Semenov, V. I. Sergeeva and A. G. Strukovskova.

** The authors are indebted to D. P. Vasilevskaya and Yu. N. Denisov for the permission to use the instrument.

As a result of double scanning 379 scattering events were detected at an energy of 128 MeV, and 1113 events at an energy of 162 MeV. These events were analyzed by the reprojection method. Both pictures of a stereopair were reprojected, through the same optical system with which they were taken, on a screen equipped with a scale for measuring the angles and mounted in gimbal rings fixed on a frame movable in two perpendicular directions (X and Y). The coordinates Z were measured by shifting the optical system vertically.

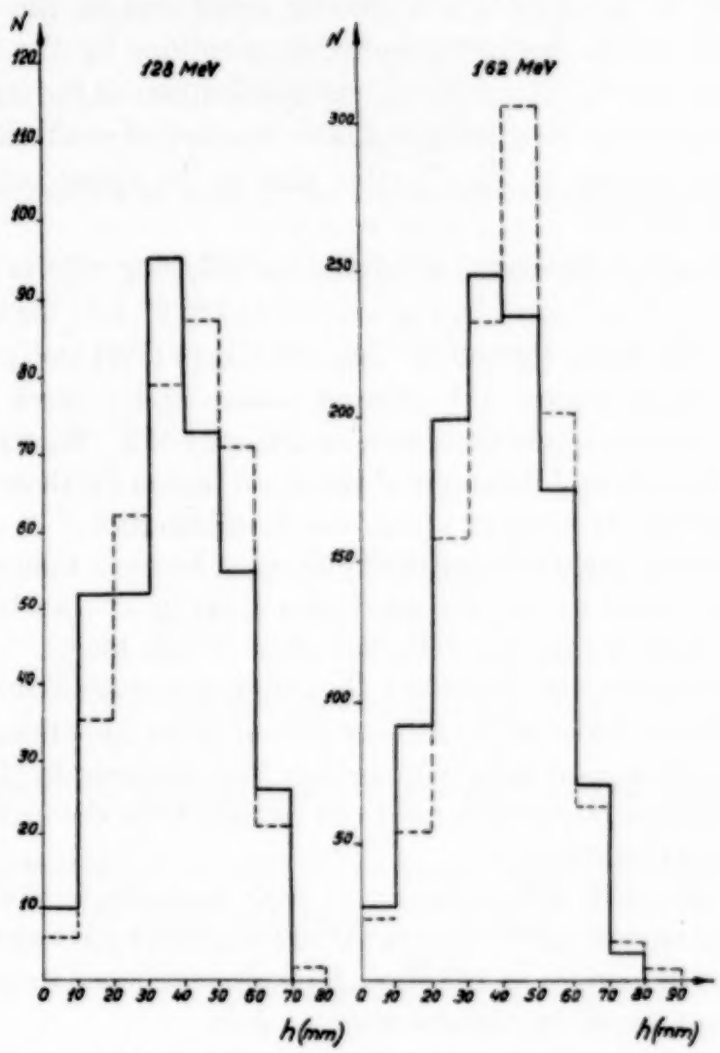

Fig. 3. Distributions with height of the sensitive layer of elastic scattering events (solid curve) and of the same number of negative pion accidental tracks (a dashed line).

The reprojector was similar to one described in ref. [10]). For each scattering event measurements were made of a) the coordinates of the interaction point (x, y, z) and the coordinate z_0 of the reference mark on the bottom of the chamber; b) the scattering angle of the meson θ_π and the recoil proton θ_p (with an accuracy of about 1°); c) the azimuthal angle φ of the scattering plane with an accuracy of about 2° ($\varphi = 0$ corresponds to the event with a horizontal scattering plane); d) the range of the recoil proton (whenever possible).

The correction for film shrinkage determined for each case as the ratio of the real distance between the bottom of the chamber and the objective main point to the measured one and usually found to be equal to 5—7 % was introduced into the values of the coordinates x, y, z. The effect of film shrinkage on the measurements of the angles ϑ and φ was very small and was therefore neglected.

The z-coordinate of an accidental negative pion track was measured simultaneously with the analysis of a scattering event and on the same picture. The comparison of the scattering event distributions by the height of the sensitive volume h with the corresponding distributions of the same number of accidental tracks shows that no appreciable number of scattering events was missed near the bottom of the chamber and at the upper boundary of the sensitive layer (fig. 3).

For further analysis the events satisfying the following criteria were selected:

1) The particle tracks must be coplanar to within 2°, i.e., the angle between any track and the plane formed by the two others must not exceed 2°.

2) The scattering angles of a negative meson and a recoil proton must satisfy the kinematic requirements with an accuracy of 2°; the track curvature, the ionization density and the range of the recoil proton (in those events which allow of measuring it) must also conform to kinematics.

3) The scattering angle of a negative pion must be more than 8° lab. system (10° c.m.s.), i.e., must exceed the maximum angle in $\pi^- - \mu^-$-decay.

4) None of three tracks must be less than 5 mm long.

5) The interaction point must not lie within a non-sensitive region more than 5 mm in size or darkened by an aggregate of drops more than 5 mm in size.

6) The interaction point must lie more than 1 cm off the walls of the chamber.

7) The incident negative pion must not deviate from the main direction of the beam by more than 5°.

8) The pictures with defects or a very high intensity were neglected.

The above-mentioned selection criteria were satisfied by 344 scattering events at 128 MeV and 941 events at 162 MeV. All undermentioned results on angular distributions are based on these statistical data.

4. Total Elastic Scattering Cross-Sections

The total elastic $\pi^- - p$-scattering cross-sections were determined by counting the total length of the negative pion tracks in the rectangular region S isolated in the central part of the chamber (fig. 4). All scattering events satisfying the above-mentioned selection criteria were counted in this region. The distributions with azimuthal angle φ, constructed for the above-mentioned cases (fig. 5), made it possible to determine the coefficients k, taking into account the inefficiency of recording the events with nearly vertical scattering plane.

The total number of tracks in the region S was determined by counting the tracks in all pictures whose number is a multiple of 25; the result was multiplied

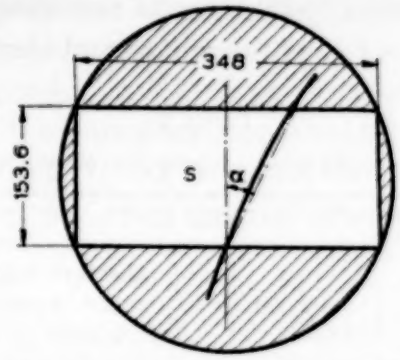

Fig. 4. The region S separated in the chamber for counting the total cross-section of elastic scattering.

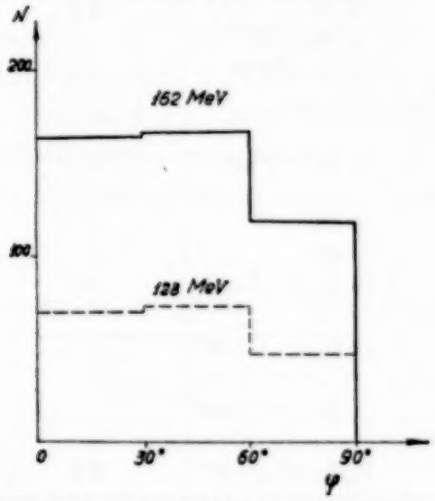

Fig. 5. Distribution with azimuthal angle φ of the scattering events situated in the region S.

by 25 and corrected for number of tracks at the end of each film. The total track length L was determined by the formula

$$L = 15.36 \frac{T\delta}{\cos \alpha_m} \text{ (cm)}, \tag{1}$$

where T is the total number of tracks, 15.36 cm the width of the region S, α_m the mean angle of tracks with respect to the edges of the region S (fig. 4), δ the coefficient taking into account the replacement of a length of the arc by a chord (in our case δ assumed to be equal to 1). The total track length was corrected for the gaps in the tracks, the length of these gaps being measured directly as the number of tracks was counted. This correction does not exceed 4 %. The total cross-sections were determined by the formula

$$\sigma_{exp} = \frac{N\beta}{Ln_{eff}(1-q)r}, \tag{2}$$

where N and L are the numbers of scattering events and the total length of tracks; n_{eff} is the effective number of hydrogen nuclei in 1 cm³; β is the coefficient taking into account the inefficiency of recording the events with φ close to 90°; q is the admixture of negative muons and electrons in a beam; and r is

TABLE 1

Determination of total cross-sections for elastic π^-—p-scattering

	128 MeV		162 MeV	
	Magnitude	Absolute root-mean square error (%)	Magnitude	Absolute root-mean square error (%)
The number N of scattering events in the region S	190	7.2	449	4.7
Correction for φ-inefficiency β	1.13	2.5	1.10	1.5
The total number of tracks T	0.991×10^6		1.446×10^6	
The total length of tracks L	15.3×10^6 cm	1	22.3×10^6 cm	1
The effective pressure in the chamber P_{eff}	22.5 atm		23.0 atm	
The number n_{eff} of nuclei in cm³ at the pressure of P_{eff}	1.22×10^{21} cm^{-3}	2	1.24×10^{21} cm^{-3}	2
The contamination of μ^--mesons and electrons in the beam q	0.16	2	0.16	2
The scanning efficiency r	0.97	1	0.97	1
The total cross-section σ_{exp}	14.2×10^{-27} cm²	8.2	22.2×10^{-27} cm²	5.8
The total cross-section for Coulomb scattering at the angles $\theta_{lab} > 8°$	1.6×10^{-27} cm²		1.1×10^{-27} cm²	
The correction for scattering in the angular interval $\theta_{lab} < 8°$	0.24×10^{-27} cm²		0.35×10^{-27} cm²	
The total cross-section σ_{el} for elastic scattering	12.8×10^{-27} cm²	8.2	21.4×10^{-27} cm²	5.8

TABLE 2

Total cross-sections for elastic π^-—p-scattering in the energy range 100—200 MeV

E(MeV)	$\sigma_{el}(10^{-27}$ cm²)	Ref.
98	6.15±0.22	[11])
118	9.6 ±2.0	[12])
120	11.3 ±1.6	[13])
128	12.8 ±1.0	this experiment
130	12.0	[14])
144	17.0 ±2.4	[13])
150	20.0 ±1.0	[5])
152	18.8	[14])
162	21.4 ±1.2	this experiment
165	22.5 ±1.5	[15])
169	21.2 ±2.0	[16])
170	23.5 ±1.0	[5])
187	22.5 ±1.3	[17])
189	23.0 ±1.4	[18])
194	26.4 ±2.7	[14])
210	28.7 ±3.1	[14])

the efficiency of film scanning. Table 1 lists the values used for calculating the total cross-sections, the root-mean-square errors being indicated as percentage. The total cross-sections for elastic π^-—p-scattering at energies of 128 and 162 MeV were obtained after subtracting the Coulomb corrections (for the method of calculating these see subsection 5.2) from the cross-sections calculated by eq. (2) and introducing the correction for scattering in the angle interval 0—8° (in lab. system) (table 1). As is seen from table 2, the cross-sections determined in the present paper, are in good agreement with other experimental data.

5. Angular Distribution of Elastic Scattering

The scattering angles of negative mesons were recounted in the centre-of-mass-system. Then all events were divided into eight angular intervals by 20° from $\theta = 10°$ up to $\theta = 170°$. The scattering events found in the interval $\Delta\theta = 0°$ to 10° (one event at 128 MeV and 9 events at 162 MeV) were neglected (see the selection criteria, sect. 3) due to an extremely low efficiency of observation since the recoil protons in meson scattering at the angles $\theta < 10°$ have a very small range and the scattering cases cannot be separated from $\pi^- - \mu^-$-

TABLE 3

Differential cross-sections for elastic π^-—p-scattering at 128 MeV

θ (c.m.s.)	ΔN	α	$\left(\frac{d\sigma}{d\Omega}\right)_{exp}$ (10^{-27} cm²/sr)	$\left(\frac{d\sigma}{d\Omega}\right)_{nucl}$ (10^{-27} cm²/sr)
20°	61	1.22±0.06	3.63±0.50	2.01±0.54
40°	78	1.14±0.05	2.31±0.28	2.07±0.28
60°	44	1.08±0.02	0.91±0.14	0.85±0.14
80°	37	1.08±0.02	0.68±0.11	0.66±0.11
100°	33	1.08±0.02	1.00±0.08 0.60±0.10	1.00±0.08 0.60±0.10
120°	33	1.08±0.02	0.69±0.12	0.70±0.12
140°	34	1.08±0.06	0.95±0.17	0.98±0.17
160°	23	1.25±0.10	1.40±0.31	1.43±0.31

TABLE 4

Differential cross-sections for elastic π^-—p-scattering at 162 MeV

θ (c.m.s.)	ΔN	α	$\left(\frac{d\sigma}{d\Omega}\right)_{exp}$ (10^{-27} cm²/sr)	$\left(\frac{d\sigma}{d\Omega}\right)_{nucl}$ (10^{-27} cm²/sr)
20°	139	1.20±0.04	4.76±0.43	3.60±0.46
40°	175	1.02±0.01	2.71±0.21	2.55±0.21
60°	159	1.09±0.01	1.96±0.16	1.91±0.16
80°	96	1.09±0.01	1.04±0.11	1.02±0.11
100°	86	1.09±0.01	1.00±0.06 0.93±0.10	1.00±0.06 0.92±0.10
120°	102	1.09±0.01	1.26±0.12	1.26±0.12
140°	124	1.12±0.03	2.11±0.20	2.13±0.20
160°	60	1.20±0.06	2.06±0.28	2.09±0.28

decays. Besides, the Coulomb scattering cross-section in this angular interval is very large. Nor was the interval $\Delta\theta = 170°—180°$ taken into account, also due to low efficiency (only one event $\theta = 173°$ was found with 3—5 being expected).

Columns 1 and 2 of tables 3 and 4 give the angles θ, corresponding to the midpoints of the angular intervals, as well as the numbers of scattering events ΔN in each interval. To obtain the differential cross-sections from these data it is necessary to take into account the inefficiency of recording the events with angles φ close to 90°, the Coulomb corrections and the corrections for the averaging over the angular interval.

5.1. CORRECTIONS FOR φ-INEFFICIENCY

The scattering events in nearly vertical planes ($\varphi \approx 90°$) may be missed in scanning with a higher probability than those in nearly horizontal planes; besides, the efficiency must, evidently, be lower for small and for very large scattering angles θ. Figs. 6 and 7 give the distributions of scattering events with azimuthal

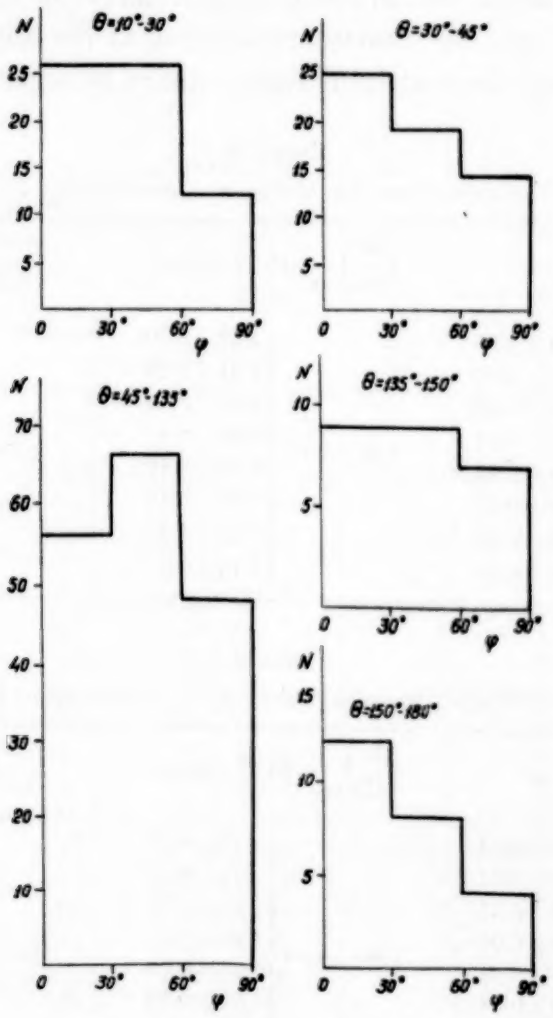

Fig. 6. Distributions with azimuthal angle φ of the scattering events at 128 MeV for different angular intervals $\Delta\vartheta$.

angle φ for different angular intervals $\Delta\theta$. The efficiency of recording the events in the interval $\Delta\theta = 45°—135°$ found from these distributions is 92—93 %, whereas for the angular intervals $\Delta\theta = 10°—30°$ and $\Delta\theta = 150°—170°$ it falls

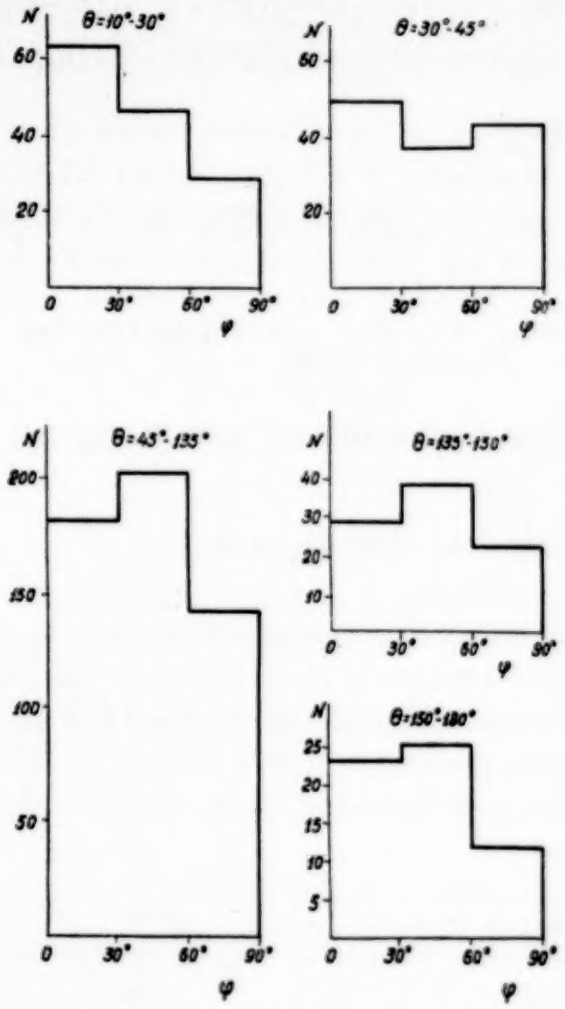

Fig. 7. Distributions with azimuthal angle φ of the scattering events at 162 MeV for different angular intervals $\Delta\theta$.

to 80—83 %. The coefficients α taking into account the correction for φ-inefficiency are given in columns 3 of tables 3 and 4.

5.2 COULOMB CORRECTIONS

These were calculated using the relativistic Coulomb scattering amplitudes obtained by Solmitz [19]). The differential scattering cross-section due to the Coulomb interaction may be written as

$$\left(\frac{d\sigma}{d\Omega}\right)_c = \frac{\Phi_1}{\sin^4 \frac{1}{2}\theta} + \frac{\Phi_2}{\sin^2 \frac{1}{2}\theta} + \Phi_3 + \Phi_4 \sin^2 \tfrac{1}{2}\theta, \qquad (3)$$

where θ is the scattering angle in the c.m.s. The first term of eq. (3) is the cross-

section for pure Coulomb scattering, while the others are due to the interference of the Coulomb and nuclear scattering. The coefficients Φ are calculated by the following formulas:

$$\Phi_1 = A^2(B+C)^2, \quad \Phi_2 = 4A^2D^2-4A^2C(B+C)+A(B+C)(E+F) \tag{4}$$
$$\Phi_3 = 4A^2(C^2-D^2)-2AC(E+F)-2AF(B+C)-4ADG, \quad \Phi_4 = 4A(CF+DG),$$

where

$$A = \frac{e^2}{2pc(\beta_\pi+\beta_p)}, \quad B = 1+\tfrac{1}{2}\beta_\pi\beta_p-\tfrac{1}{4}\beta_p^2(2\mu_p-1), \quad C = \tfrac{1}{2}\beta_\pi\beta_p+\tfrac{1}{4}\beta_p^2(2\mu_p-1),$$

$$D = \tfrac{1}{2}\mu_p\beta_\pi\beta_p+\tfrac{1}{4}\beta_p^2(2\mu_p-1), \quad E = \frac{1}{3k}(2\sin 2\alpha_1+\sin 2\alpha_3), \tag{5}$$

$$F = \frac{1}{3k}(2\sin 2\alpha_{11}+\sin 2\alpha_{31}+4\sin 2\alpha_{13}+2\sin 2\alpha_{33}),$$

$$G = \frac{1}{3k}(2\sin 2\alpha_{13}+\sin 2\alpha_{33}-2\sin 2\alpha_{11}-\sin 2\alpha_{31}).$$

In these formulas $p = \hbar k$ is the momentum in the c.m.s., β_π and β_p are the velocities of a pion and a proton in the c.m.s., μ_p is the magnetic moment of a proton in nuclear magnetons. The coefficients Φ for 128 and 162 MeV calculated by eqs. (4) and (5) are presented in table 5, the phases of meson-nucleon interaction obtained by Chiu and Lomon [20]) being used for calculating E, F and G.

TABLE 5

Coefficients Φ of eq. (3) for energies of 128 and 162 MeV (in 10^{-27} cm^2 /sr)

E (MeV)	Φ_1	Φ_2	Φ_3	Φ_4
128	2.18×10^{-4}	3.61×10^{-2}	-9.33×10^{-2}	3.21×10^{-2}
162	1.54×10^{-4}	2.57×10^{-2}	-7.26×10^{-2}	2.96×10^{-2}

The integration of eq. (3) within the limits $10° < \theta < 180°$ yields the corrections for the total elastic scattering cross-sections (see table 1):

$$\sigma_C = 2\pi\int_{10°}^{180°}\left(\frac{d\sigma}{d\Omega}\right)_C \sin\theta\, d\theta = \begin{cases} 1.6\times10^{-27}\text{ cm}^2 & \text{for } 128\text{ MeV}, \\ 1.1\times10^{-27}\text{ cm}^2 & \text{for } 162\text{ MeV}. \end{cases}$$

To obtain the differential cross-sections for purely nuclear scattering, the cross-sections $(d\sigma)_C = \int_{\Delta\theta}(d\sigma/d\Omega)_C\, 2\pi\sin\theta\, d\theta$ were subtracted from quantities $(d\sigma)_{exp}$ determined experimentally. The errors in the cross-sections $(d\sigma)_C$ were determined by varying the phase shifts in eqs. (5) within reasonable limits.

5.3 CORRECTION FOR AVERAGING OVER THE ANGULAR INTERVAL $\Delta\theta$

Since the value of the cross-section averaged over the final angular interval $\Delta\theta$ is assigned to the middle of the interval θ, the actual value of the cross-section for the angle θ will differ from the averaged one by the magnitude

$$\mathrm{d}(\theta) = -\frac{(\Delta\theta)^2}{24}\left[\frac{\mathrm{d}\sigma}{\mathrm{d}\Omega}(\theta)\right]'', \tag{6}$$

where $[\mathrm{d}\sigma/\mathrm{d}\Omega(\theta)]''$ is the second derivative of the differential cross-section. As a first approximation for calculating $\mathrm{d}(\theta)$ use was made of the dependence $\mathrm{d}\sigma/\mathrm{d}\Omega(\theta) = a'+b'\cos\theta+c'\cos^2\theta$ found by the least squares on the strength of the experimental differential cross-sections corrected for the Coulomb scattering. Then

$$\mathrm{d}(\theta) = \frac{(\Delta\theta)^2}{24}(b'\cos\theta+2c'\cos 2\theta). \tag{7}$$

The maximum value of the correction calculated by eq. (7) did not exceed 2.5 %.

5.4. DIFFERENTIAL ELASTIC SCATTERING CROSS-SECTIONS

The differential cross-sections $(\mathrm{d}\sigma/\mathrm{d}\Omega)_{\mathrm{exp}}$ (columns 4 of tables 3 and 4) were obtained from the angular distributions $\Delta N/\Delta\Omega$ by normalizing to the total cross-sections σ_{exp} (table 1) with taking account of the coefficients α. Columns 5 of table 3 and 4 list the differential cross-sections for elastic π^-—p-scattering due to purely nuclear interaction. These cross-sections are obtained by subtracting the Coulomb scattering cross-sections from $(\mathrm{d}\sigma/\mathrm{d}\Omega)_{\mathrm{exp}}$ and introducing the corrections for averaging over angular intervals. The errors indicated are the root-mean-square errors mainly due to statistical errors and small uncertainties from introducing the corrections. The common factor before the cross-sections is an error in the normalizing total cross-section.

A least squares fit of the form $\mathrm{d}\sigma/\mathrm{d}\Omega = a+b\cos\theta+c\cos^2\theta$ was made with respect to the differential cross-sections experimentally obtained. Table 6 lists the values of the coefficients a, b and c; $M = \sum_i(\varepsilon_i/\Delta\sigma_i)^2$ which is the sum of the squares of the deviations ε_i of the calculated cross-sections from the experimental points expressed in the units of the experimental errors $\Delta\sigma_i$; and, finally, the number of degrees of freedom $M_0 = n-m$ (n is the number of experimental points and m that of the parameters of the curve). The proximity of M to M_0 points to a good agreement between the curves in question and the experimental cross-sections.

The right-hand side of table 6 represents the matrices of the errors G_{ij}^{-1} calculated by the method set down in ref. [21]). The errors of the coefficients a, b and c are the square roots of the diagonal elements of the matrices. The off-diagonal elements are the product of the corresponding standard deviations multiplied by the correlation coefficient. For half of the matrices the correlation

coefficients between a, b and c (in %) are indicated instead of the off-diagonal elements. The curves obtained as well as the experimental points are presented in fig. 8. They are in agreement with the angular distributions for elastic π^-—p-

TABLE 6

The expansion coefficients $a+b\cos\theta+c\cos^2\theta$ and the errors matrices

Energy in MeV	Expansion coefficients $a+b\cos\theta+c\cos^2\theta$ (10^{-27} cm²/sr)	Error matrices μ $G_{ij}^{-1}\times 10^{-4}$ (10^{-27} cm²/sr)²		
128	1.00 ± 0.08 { $a = 0.55\pm0.07$; $b = 0.34\pm0.12$; $c = 1.30\pm0.24$ }	53.53	−3.73	−118.15
		−4.1%	153.65	86.48
		−66.3%	28.6%	593.87
	$M = 5.8$, $M_0 = 5$			
162	1.00 ± 0.06 { $a = 0.93\pm0.07$; $b = 0.51\pm0.12$; $c = 2.28\pm0.22$ }	49.78	0.76	−101.65
		0.9%	140.28	39.35
		−64.8%	14.9%	494.60
	$M = 5.2$, $M_0 = 5$			

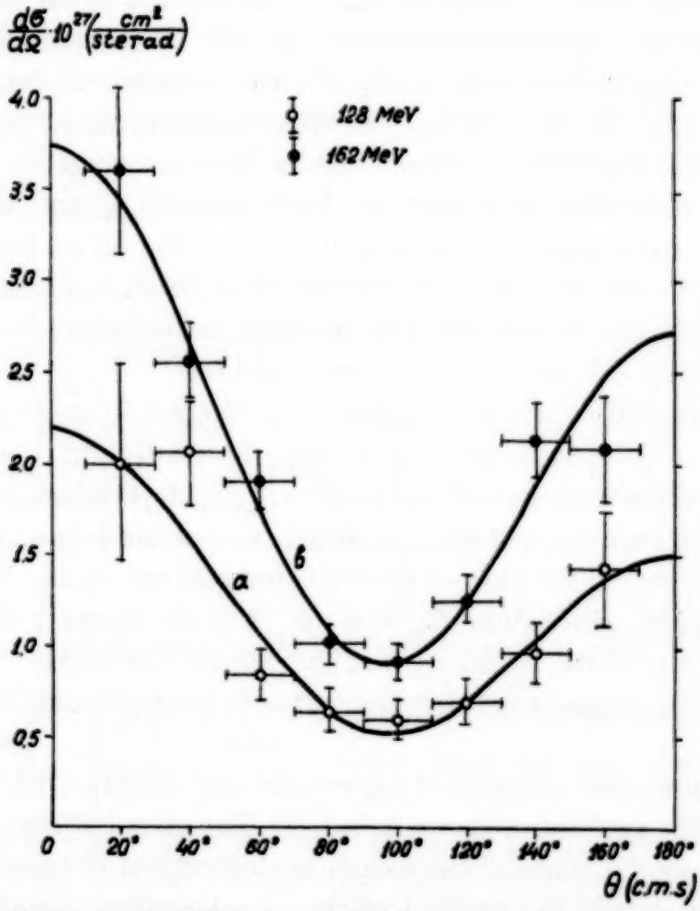

Fig. 8. Angular distributions of elastic π^-—p-scattering at 128 and 162 MeV. The curves a and b are obtained by least squares with account of the S- and P-waves only.

scattering measured by Ashkin *et al.* [5]) at 150 and 170 MeV, as well as with the results of Kruse and Arnold [14]) at the energies of negative pions 130 and 152 MeV.

5.5. DETERMINATION OF THE REAL PART OF THE FORWARD SCATTERING AMPLITUDE

The differential cross-sections for forward scattering at 128 and 162 MeV are equal to $(2.20\pm0.32)10^{-27}$ cm²/sr and $(3.73\pm0.32)10^{-27}$ cm²/sr respectively. Apart from the mean square deviations of the coefficients a, b and c, the indicated errors allow for the correlation between the coefficients (the off-diagonal elements of the error matrices). The magnitude of the real part of the forward scattering amplitude $\mathrm{Re}\,f(0,\omega)$ can be easily obtained by using the optical theorem

$$\mathrm{Im}\,f(0,\omega)=\frac{k}{4\pi}\sigma_t, \tag{8}$$

where σ_t is the total cross-section for π^-—p-interaction. Then

$$D_-{}^b=\mathrm{Re}\,f(0,\omega)=\sqrt{\frac{d\sigma}{d\Omega}(0)-\frac{k^2}{16\pi^2}\sigma_t{}^2}. \tag{9}$$

The quantities σ_t were taken from the energy dependence curve for total cross-sections obtained by Klepikov, Mescheryakov and Sokolov [22]) by analyzing all experimental data for the total cross-sections of π^+—p and π^-—p-interaction in a wide energy interval:

$$\sigma_t(128\ \mathrm{MeV})=(39.7\pm1.0)\times10^{-27}\ \mathrm{cm}^2,$$
$$\sigma_t(162\ \mathrm{MeV})=(63.3\pm1.0)\times10^{-27}\ \mathrm{cm}^2.$$

Then the real parts of the forward scattering amplitude in the centre-of-mass-system (in the units of $\hbar/m_\pi c$) are equal to

$$D_-{}^b(128\ \mathrm{MeV})=0.261\pm0.031,\quad D_-{}^b(162\ \mathrm{MeV})=0.216\pm0.038.$$

A larger relative error in the magnitude $D_-{}^b(162\ \mathrm{MeV})$ appears because the formula for calculating the error in $D_-{}^b$ contains the quantity $D_-{}^b$ in the denominator, and therefore a relative error infinitely increases as the energy approaches the resonance and $D_-{}^b\to0$.

6. Discussion

As the present experiment was in progress some new theoretical papers [23–31]) analyzed the possible causes of the discrepancy discovered by Puppi and Stanghellini. Zaidi and Lomon [23]) showed a close dependence of $D_-{}^b$ upon the slope of the curve describing the total cross-sections for π^-—p-interaction close

to the resonance. A detailed analysis of the errors arising when the dispersion relations are applied to $\pi^- - p$-scattering was made by Hamilton [29]) and Schnitzer and Salzman [30]). These authors showed that it is possible, by using the dependence of the total cross-sections upon the energy obtained by Anderson [32]) to reduce the discrepancy between the experimental and theoretical values of D_-^b to approximately one half. Besides, taking account of the normalization factor in the differential cross-sections and of the correlation between the coefficients a, b and c increases the errors in the experimental values of D_-^b at 150 and 170 MeV by a factor of about two compared with those indicated by

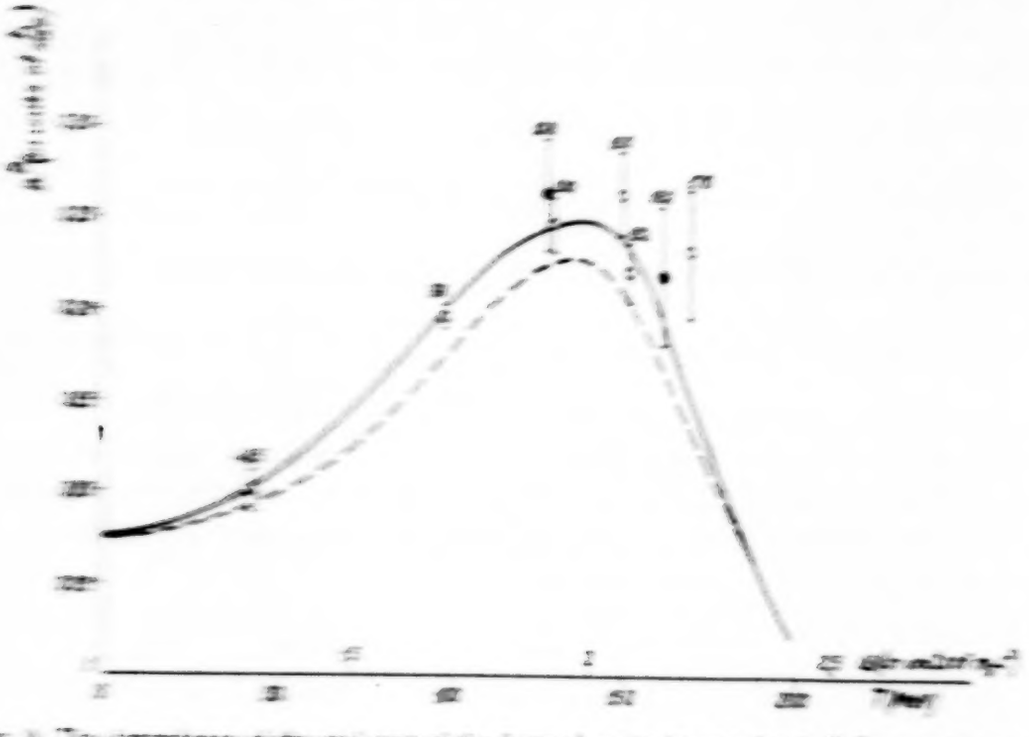

Fig. 9. The dependence of the real part of the forward scattering amplitude D_-^b upon the energy ω of the total energy of negative pions in the units $m_\pi c^2$. T is the kinetic energy of negative pions in MeV. The solid curve is that obtained by Klepikov *et al.* [33]) ($f^2 = 0.08$), the dashed line is that obtained by Schnitzer and Salzman [30]) ($f^2 = 0.08$).

Puppi and Stanghellini. Yet a certain discrepancy still remained. To account for it more exact data on the total cross-sections near the resonance were needed and new values of D_-^b had to be obtained [28–30]).

Quite recently Klepikov, Mescheryakov and Sokolov [33]) have calculated the curve $D_-^b(\omega)$ for $f^2 = 0.08$ using new data on the total cross-sections in the wide energy range including the results of the measurements $\sigma_t(\pi^- - p)$ performed with an accuracy of 2 to 3 %, by Zinov, Konin, Korenchenko and Pontecorvo [31]) in the negative pion energy range 160 to 330 MeV. In fig. 9 the curve obtained by Klepikov *et al.* is designated by a solid curve and that by Schnitzer and Salzman [30]) for $f^2 = 0.08$ by a dot-and-dash line. The quantities D_-^b obtained in the present paper are denoted by dots. Besides, the figure represents

the results of the latest papers by Barnes *et al.*[34]) (41.5 MeV), Edwards *et al.* [11]) (98 MeV) and Kruse and Arnold [14]) (130 and 152 MeV), as well as the values of D_-^b † at 150 and 170 MeV [3]), the errors for which were recalculated by Schnitzer and Salzman [28]). As is seen from fig. 9, our results and the data of all of the latest experimental papers on elastic π^-—p-scattering in the energy range up to the resonance are in good agreement with the new theoretical curve calculated with the coupling constant $f^2 = 0.08$.

Thus, we can assert at present that the experimental data on elastic scattering of negative pions by protons agree with the dispersion relations at $f^2 = 0.08$ which was established earlier for positive pion scattering.

The authors are grateful to L. I. Lapidus, S. N. Sokolov and V. A. Mescheryakov for stimulating discussions, L. I. Krasnoslobodzeva, T. S. Sazhneva and Yu. L. Saikina for assistance in scanning the photos, and A. A. Andrianova and G. D. Malysheva for calculating the error matrices.

† It will be noted that the quantities D_-^b at 150 and 170 MeV were calculated [3]) with somewhat underestimated cross-sections of ref. [5]), and the use of new data for $\sigma_t(\pi^- - p)$ is bound to lead to smaller values and thus to better agreement with the curve.

References

1) M. Goldenberger, H. Miyazawa and R. Oehme, Phys. Rev. **99** (1955) 986
2) H. Anderson, W. Davidon and U. Kruse, Phys. Rev. **100** (1955) 339
3) G. Puppi and A. Stanghellini, Nuovo Cim. **5** (1957) 1305
4) A. Agodi and M. Cini, Nuovo Cim. **5** (1957) 1256, **6** (1957) 686;
A. Agodi, M. Cini and B. Vitale, Phys. Rev. **107** (1957) 630
5) J. Ashkin, J. P. Blaser, F. Feiner and M. O. Stern, Phys. Rev. **101** (1956) 1149
6) Yu. A. Budagov, S. Wiktor, V. P. Dzhelepov, P. F. Yermolov and V. I. Moskalev, JETP **37** (1959) 878
7) Yu. A. Budagov, S. Wiktor, V. P. Dzhelepov, P. F. Yermolov and V. I. Moskalev, JETP **35** (1958) 1575; JETP **38** (1960) 1047
8) Yu. A. Budagov, S. Wiktor, V. P. Dzhelepov, P. F. Yermolov and V. I. Moskalev, JETP **36** (1959) 1080
9) Yu. A. Budagov, S. Wiktor, V. P. Dzhelepov, P. F. Yermolov and V. I. Moskalev, Proceedings of the Conference on Cloud-Chambers, Diffusion and Bubble Chambers (Joint Institute for Nuclear Research, Dubna, 1958)
10) A. T. Vasilenko, M. S. Kozodajev, R. M. Suliajev, A. I. Filippov, and Yu. A. Scherbakov, Pribory i tehnika eksperimenta N **6** (1957)
11) D. N. Edwards, S. G. F. Frank and J. R. Holt, Proc. Phys. Soc. **73** (1959) 856
12) J. Orear, Phys. Rev. **92** (1953) 156
13) H. Anderson, E. Fermi, R. Martin and D. Nagle, Phys. Rev. **91** (1953) 155
14) U. Kruse and R. Arnold, Proceedings of the Kiev Conference on High Energy Physics (July 1959), Pontecorvo's report
15) H. L. Anderson and M. Glicksman, Phys. Rev. **100** (1955) 268
16) E. Fermi, M. Glicksman, R. Martin and D. Nagle, Phys. Rev. **92** (1953) 161
17) M. Glicksman, Phys. Rev. **95** (1954) 1045
18) U. Kruse, H. L. Anderson, W. C. Davidon and M. Glicksman, Phys. Rev. **100** (1955) 279
19) F. T. Solmitz, Phys. Rev. **94** (1954) 1799
20) H. Y. Chiu and E. L. Lomon, Ann. of Phys. **6** (1959) 50
21) N. P. Klepikov and S. N. Sokolov, Analysis of experimental data by a maximum likelihood method (Joint Institute for Nuclear Research, Dubna, 1958)

22) N. P. Klepikov, V. A. Mescheryakov and S. N. Sokolov, Proceedings of the Kiev Conference on High Energy Physics, (July, 1959)
23) M. H. Zaidi and E. L. Lomon, Phys. Rev. **108** (1957) 1352
24) V. A. Mesheryakov, JETP **35** (1958) 290
25) J. Hamilton, Phys. Rev. **110** (1958) 1134
26) H. Y. Chiu, Phys. Rev. **110** (1958) 1140
27) L. Bertocchi and L. Lendinara, Nuovo Cim. **10** (1958) 734
28) H. J. Schnitzer and G. Salzman, Phys. Rev. **112** (1958) 1802
29) H. Y. Chiu and J. Hamilton, Phys. Rev. Lett. **1** (1958) 146
30) H. P. Noyes and D. N. Edwards, Bull. Am. Phys. Soc. **4** (1959) 50
31) H. J. Schnitzer and G. Salzman, Phys. Rev. **113** (1959) 1153
32) H. L. Anderson, Proc. of the Sixth Ann. Roch. Conf., (1956) p. 20
33) V. G. Zinov, A. D. Konin, S. M. Korenchenko and B. M. Pontecorvo, Proceedings of the Kiev Conference on High Energy Physics (July 1959), Pontecorvo's report
34) S. Barnes, B. Rose, G. Giacomelli, J. Ring and K. Miyake, Phys. Rev. (in press)

2.C

Nuclear Physics **22** (1961) 245—248; ©*North-Holland Publishing Co., Amsterdam*

Not to be reproduced by photoprint or microfilm without written permission from the publisher

RESONANCE ENERGIES AND HALF-WIDTHS FOR PROTON CAPTURE IN SODIUM AND PHOSPHORUS

S. L. ANDERSEN, O. DØRUM, E. GAUTVIK and T. HOLTEBEKK

Institute of Physics, University of Oslo, Blindern

Received 12 September 1960

Abstract: The gamma ray yield from proton induced reactions in sodium and phosphorus has been studied in the proton energy range between 0.7 and 1.5 MeV for sodium, and in the energy range between 0.8 and 1.6 MeV for phosphorus. One new resonance in ^{31}P at 1395.8 $\pm$ 0.7 keV is found. Relative determinations of the resonance energies are made with an accuracy of 0.05 – 0.1 %. For 13 of the resonances in sodium and one of the resonances in phosphorus the half widths are determined. For the rest of the resonances upper limits for the half-widths between 200 eV and 750 eV are determined.

1. Introduction

Several authors have previously reported resonances for proton capture in sodium [1–7]) and phosphorus [1,8–11]) in the energy region 700—1600 keV. With a few exceptions (Stelson and Preston [3]), Wagner and Heitzmann [7])), the widths measured are almost entirely due to finite thickness of targets and are of the order of 10 keV. Also the uncertainties in the energy determinations are of the same order of magnitude. By careful selection of target material and treatment of target during bombardment, we have been able to give more precise values for both resonance energies and widths.

2. Experimental Procedure

The experimental arrangement is almost the same as used previously [12]). The energy spread in the analyzed proton beam from the Van de Graaff generator is estimated to be between 250 and 500 eV, measured as interquartile range, depending on slit-widths of the electrostatic analyzer. The H^+ beam is used for all measurements.

The analyzer has been checked for a possible non-linearity in the energy region between 1000 and 1750 keV by comparing the values obtained by Bondelid and Kennedy for the (p, γ) resonances in ^{27}Al (992.4 $\pm$ 0.5 keV) and ^{13}C (1747.6 $\pm$ 0.9 keV) with our relative values for these two resonances. Including the relativistic correction, we get the value 1747.8 $\pm$ 0.5 keV for the ^{13}C resonance, when we use 992.4 keV for the ^{27}Al resonance. Thus the analyzer is linear in this energy region within the limits of error given.

Due to the weak resonances in Na we had to use targets containing as much as possible of this element. We therefore started with the same target technique as used for aluminium [12]). Targets of metallic sodium were prepared in site in the target chamber, and each spot on the target was bombarded for a very short time only. It was however, found that even in a vacuum better than 10^{-5} mm Hg the metallic surface of sodium was destroyed after some hours. The result was that the measured resonance widths increased with target age.

We therefore changed to a target system similar to that described by Butler and Gosset [13]) where the target is kept inside a tube cooled by liquid nitrogen. This system has proved to be very effective to avoid contamination on target. We have, as a test, bombarded a target with about 0.5 C/cm² of the H_2^+ beam without observing any change in the yield curve for a resonance.

The targets used in this chamber had to be prepared outside the vacuum-system, and were exposed to air for a short time. We therefore used more stable compounds for target material, namely, NaCl and NaBr, Zn_3P_2 and Cu_3P_2. The targets were usually between 10 and 50 keV thick. They were evaporated on tantalum backings.

3. Results

The energies of the resonances, are given in tables 1 and 2. The energy values are based upon the 990.8 keV [14]) value for the strong (p, γ) resonance in ^{27}Al. The limits of uncertainties given are due to analyzer calibration and to determination of the resonance point from the yield curve. For the weaker resonances, where large slit widths are to be used to obtain a sufficient number of counts, the latter error predominates.

The resonance widths given in tables 1 and 2 column 3, are obtained from the observed widths by correcting for energy spread in the proton beam, and

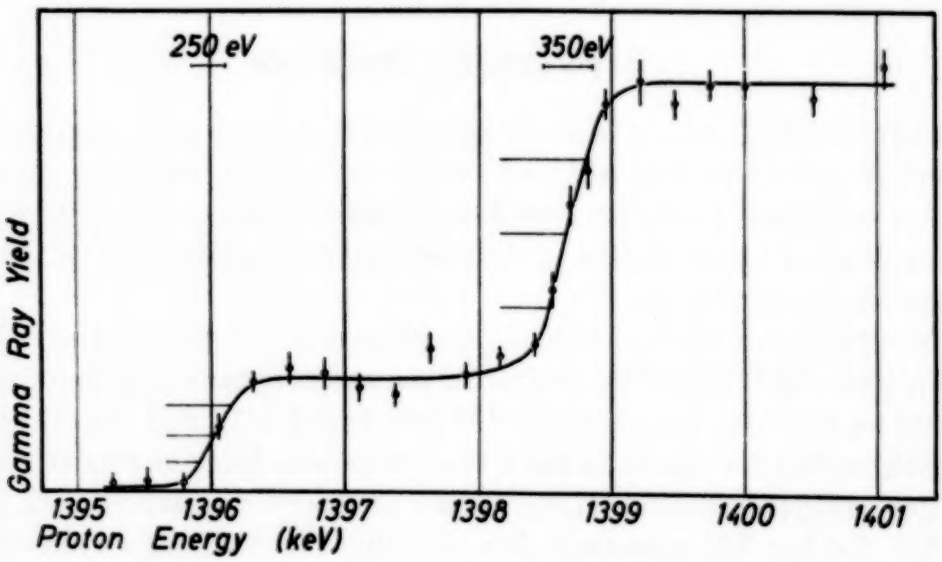

Fig. 1. The resonance doublet in phosphorus.

for the Doppler broadening due to thermal motion of the target atoms by the formula $\Gamma^2 = \Gamma_{obs}^2 - \sum \Gamma_i^2$, where Γ_{obs} is the observed interquartile range on the yield curve and Γ_i is the estimated interquartile range for the various energy-

TABLE 1

Energies and half widths of (p, γ) resonances in sodium (all values in keV)

No.	Resonance energy	Observed half width	$\sqrt{\Sigma\Gamma_i^2}$	Corrected half width	Γ from previous measurements
1	737.3±0.5	0.2 ±0.1	0.23	<0.2	≦0.09 [7]
2	743.2±0.5	0.4 ±0.2	0.23	<0.5	≦0.10 [7]
3	871.5±0.6	7.5 ±1.0	0.23	7.5 ±1.0	8 ±2 [2]
4	986.0±0.6	0.3 ±0.2	0.25	<0.4	≦1 [2]
5	1006.5±0.5	0.3 ±0.1	0.20	<0.35	≦0.5 [2, 3]
6	1008.0±1.0	0.5 ±0.3	0.20	<0.7	0.8 ±0.1 [3]
7	1019.0±0.6	5.0 ±1.0	0.60	5.0 ±1.0	6.6 ±0.5 [3]
8	1084.8±0.6	0.4 ±0.3	0.33	<0.55	1.1 ±0.5 [3]
9	1089.7±0.5	5.0 ±1.0	0.27	5.0 ±1.0	7.9 ±0.5 [3]
10	1161.0±1.0	1.2 ±0.2	0.14	1.2 ±0.2	1.2 ±0.1 [3]
11	1172.4±0.5	3.5 ±0.7	0.36	3.5 ±0.7	2.5 ±0.5 [2] 2.3 [3]
12	1201.8±1.0				≦0.3 ±0.1 [3]
13	1207.6±1.0	0.35±0.2	0.24	<0.45	0.4 ±0.1 [3]
14	1252.4±0.6	0.5 ±0.2	0.24	0.4 ±0.2	0.6 ±0.1 [3]
15	1281.0±1.0	5.2 ±0.4	0.25	5.2 ±0.4	7.1 ±0.2 [3]
16	1316.7±0.7	1.5 ±0.3	0.41	1.5 ±0.3	2.1 ±0.5 [3]
17	1326.2±1.0	2.8 ±0.6	0.33	2.8 ±0.6	3.5 ±0.2 [3]
18	1329.7±1.0	3.0 ±1.0	0.33	3.0 ±1.0	6.7 ±0.2 [3]
19	1360.8±0.7	0.9 ±0.4	0.42	0.8 ±0.4	1.2 ±0.2 [3]
20	1392.0±1.0	0.8 ±0.3	0.26	0.75±0.3	0.8 ±0.1 [3]
21	1415.1±0.8	0.2 ±0.1	0.19	<0.2	≦0.3 [3]
22	1456.3±0.8	8.5 ±1.0 [a]	0.90	7.5 ±1.0	9.8 ±0.2 [3]

[a]) Measured on 4 keV target

TABLE 2

Energies and half widths of resonances in phosphorus (all values in keV)

No.	Resonance energy	Observed half width	$\sqrt{\Sigma\Gamma_i^2}$	Corrected half width
1	811.8±0.5	0.35±0.20	0.25	<0.45
2	892.0±0.5	0.25±0.25	0.28	<0.35
3	1052.6±0.5	0.20±0.20	0.20	<0.30
4	1088.0±0.5	0.20±0.20	0.20	<0.30
5	1116.2±0.5	0.15±0.15	0.22	<0.15
6	1147.0±0.5	0.20±0.10	0.25	<0.16
7	1246.5±0.6	1.5 ±0.30	0.25	1.5 ±0.3
8	1396.0±0.7	0.25±0.15	0.25	<0.30
9	1398.7±0.7	0.30±0.15	0.30	<0.35
10	1436.3±0.7	0.20±0.10	0.30	<0.20
11	1468.6±0.7	0.25±0.15	0.30	<0.25
12	1553.9±0.8	0.35±0.15	0.30	<0.40
13	1581.5±0.8	0.50±0.20	0.40	<0.55

spreads. The main contribution to $\sum\Gamma_i$ is from the finite slit width settings on the analyzer. In cases where Γ_{obs} is nearly the same as or less than $\sum\Gamma_i$ we have calculated an upper limit Γ_{max} of Γ by the formula

$$\Gamma^2_{max} = \Gamma^2_{obs} - \sum\Gamma_i^2 - 2[(\Gamma_{obs}\Delta\Gamma_{obs})^2 + \sum(\Gamma_i\Delta\Gamma_i)^2]^{\frac{1}{2}}.$$

One new resonance doublet is found in phosphorus at 1398 keV (fig. 1). γ-ray spectra taken of both the resonances give significant results to ascribe them to proton capture in ^{31}P. The resonance in ^{31}P reported by Paul *et al.* [11]) at 825 keV seems to be too weak for any precise measurements. All other (p, γ) resonances in this energy region are included here.

The authors wish to express their thanks to Professor Roald Tangen for offering them the facilities to carry out this work, and for his valuable help with the discussion of the results.

This work was supported by The Royal Norwegian Council for Scientific and Industrial Research.

References

1) F. W. Inal and C. W. Strauss, Rev. Mod. Phys. **29** (1957) 663
2) Baumann, Presser, Rosa and Kuhn, Phys. Rev. **104** (1956) 376
3) F. H. Shilson and W. M. Preston, Phys. Rev. **95** (1954) 974
4) Deutsch, Snigurskiy and Kuhn, Phys. Rev. **93** (1954) 1035
5) J. O. Newton, Phys. Rev. **76** (1954) 541
6) Goldberg, Hansteen, Gallmann and Douglas, Phys. Rev. **93** (1954) 799
7) S. Wagner and M. Heinzmann, Z. Naturf. **15a** (1960) 74
8) D. R. Grove and J. M. Cooper, Phys. Rev. **82** (1951) 505
9) S. D. Kern and C. W. Cochran, Phys. Rev. **104** (1956) 711
10) Carter, Kington and Paul, Phys. Rev. **94** (1953) 654
11) Paul, Grove, Litherland and Bartholomew, Phys. Rev. **99** (1955) 1339
12) Andersen, Bø, Holtebekk, Lønsjø and Tangen, Nuclear Physics **9** (1958/59) 509
13) J. W. Butler and C. H. Johnson, Phys. Rev. **108** (1957) 1473
14) Bromiller, Staub and Weaver, Helv. Phys. Acta **29** (1956) 83
15) R. G. Bonanno and C. A. Kennedy, Phys. Rev. **115** (1959) 1601

7.A

Nuclear Physics **22** (1961) 249—261; © *North-Holland Publishing Co., Amsterdam*

Not to be reproduced by photoprint or microfilm without written permission from the publisher

ASYMPTOTIC BEHAVIOUR OF THE SCATTERING AMPLITUDE AT HIGH ENERGIES

V. N. GRIBOV

Leningrad Physical Technical Institute, Academy of Sciences of the U.S.S.R., Leningrad

Received 28 June 1960

Abstract: The asymptotic behaviour of the scattering amplitude is investigated at high energies. It is shown that at high energies the usual diffraction picture of scattering contradicts the unitarity conditions and analytic properties of the scattering amplitude formulated with the help of Mandelstam's representations. In terms of these conditions it is natural to expect that the cross section should decrease faster than $1/\ln E$.

1. Introduction

The asymptotic behaviour of scattering amplitudes in quantum field theory has been investigated in refs. [1–3]). In all cases, however, only rather general restrictions on possible asymptotics have been obtained. At present, mainly owing to Mandelstam [4]), it has become possible in studying asymptotic behaviours to make a more extensive use of unitary conditions and the dispersion relations for the momentum transfer. Since thus far we have been able to deal only with two-body states under unitarity conditions, we can hardly expect a complete solution of the problem. Nevertheless, some limited information can be obtained, as will be shown below.

The description of elastic scattering at high energies is based on the so-called diffraction picture. According to this picture, particles with an impact parameter ρ smaller than a certain R (of the order of $1/\mu$, μ being the meson mass) interact strongly with the scatterer and are discharged from the elastic channel, while particles with an essentially larger impact parameter are not scattered. This leads to a diffractional scattering with two main characteristics: both the total scattering cross-section σ_n and the differential cross-section for elastic scattering per unit interval of the square of the momentum transfer $d\sigma/dt$ are energy independent ($-t$ being the square of the momentum transfer).

The present paper investigates the consistency of this picture with the requirements of unitarity and analyticity for scattering amplitudes. It is shown that energy independence of σ_n and $d\sigma/dt$ cannot be reconciled with the conditions of unitarity and analyticity. In terms of these conditions it is natural to expect that σ_n and $d\sigma/dt$ decrease faster than logarithmically.

Investigating inelastic processes in the pole approximation, V. Berestetsky

and I. Pomeranchuk [5]) have arrived at a similar inconsistency of diffractional representations with the general properties of amplitudes in quantum field theory. Assuming that the elastic scattering cross-section remains constant, they concluded that the cross-section of inelastic processes tends to infinity. An assumption of a decrease of the scattering cross-section makes their results self-consistent.

2. General Properties of the Scattering Amplitude

For the sake of simplicity we shall first consider the scattering of two identical particles without spin (mesons) and shall assume that these particles are the lightest in the theory and are pseudoscalar.

The elastic scattering amplitude of these particles will be treated as a function of the two invariant variables: the square of the centre-of-mass energy S and the square of the momentum transfer $-t$. The quantity $A = A(S, t)$ is normalised in such a way that

$$A_1(S, 0) \equiv \operatorname{Im} A(S, 0) = \frac{S}{16\pi} \sigma_n \tag{1}$$

we shall assume that $A(S, t)$ possesses the analytic properties formulated by Mandelstam [4]) and shall use the Mandelstam plane (fig. 1).

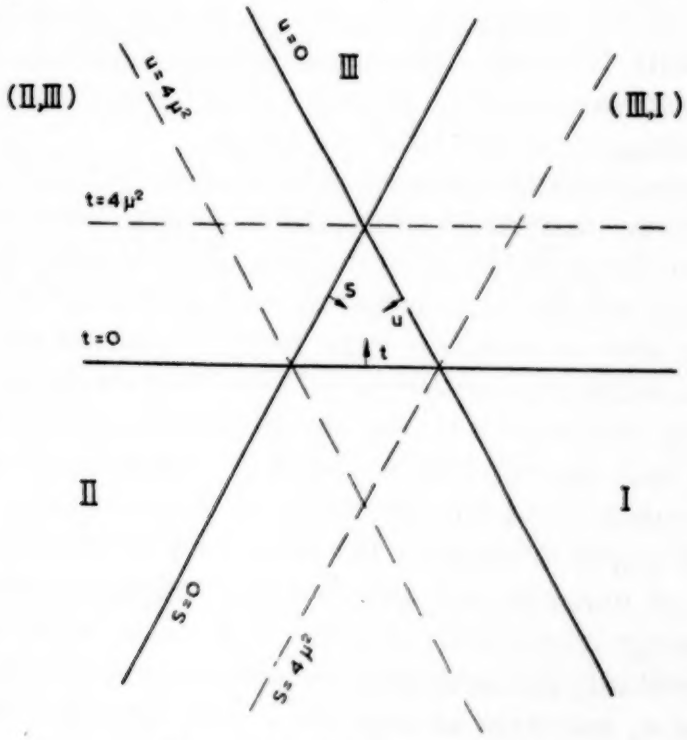

Fig. 1. The Mandelstam plane.

The functions $A(S,t)$ and $A_1(S,t)$ will interest us in the region I at $S \to \infty$, $-t \ll S$. In the $t < 4\mu^2$ region $A(S,t)$ and $A_1(S,t)$ can be represented as a series of Legendre polynomials. In particular, $A_1(S,t)$ can be written down in the form

$$A_1(S,t) = \sqrt{\frac{S}{S-4\mu^2}} \sum_{l=0}^{\infty} a_l(S)(2l+1)P_l\left(1+\frac{t}{2p^2}\right), \tag{2}$$

where $0 < a_l < 2$; $p = \frac{1}{2}\sqrt{S-4\mu^2}$ is the particle momentum in the centre-of-mass system.

If we use the dispersion relation for $A_1(S,t)$ as a function of "t"

$$A_1(S,t) = \frac{1}{\pi}\int_{t_1(S)}^{\infty} \frac{\operatorname{Im} A_1(S,t')\mathrm{d}t'}{t'-t} - \frac{1}{\pi}\int_{-\infty}^{t_2(S)} \frac{\operatorname{Im} A_1(S,t')\mathrm{d}t'}{t'-t}, \tag{3}$$

where

$$t_1(S) > 4\mu^2, \quad t_2(S) < -S,$$

then according to ref. [6]) we have

$$a_l(S) = \frac{4}{\pi\sqrt{S(S-4\mu^2)}}\int_{t_1(S)}^{\infty} Q_l\left(1+\frac{t'}{2p^2}\right)\operatorname{Im} A_1(S,t')\mathrm{d}t', \tag{4}$$

with

$$Q_l(z) = \frac{1}{2}\int \frac{P_l(z')}{z'-z}\,\mathrm{d}z'.$$

From this formula one can easily derive [6]) the asymptotic behaviour of $a_l(S)$ at $l \to \infty$. Since at $l \gg 1$ and $t'/2p^2 \ll 1$ we have

$$Q_l\left(1+\frac{t'}{2p^2}\right) = K_0(\rho\sqrt{t'}),$$

where $\rho = l/p$ is the impact parameter and $K_0(x)$ is the McDonald function, the quantity

$$a_l(S) \equiv a(\rho, S) = \frac{4}{\pi}\int_{4\mu^2}^{\infty} K_0(\rho\sqrt{t'})\operatorname{Im} A_1(S,t')\frac{1}{S}\mathrm{d}t', \quad \frac{S}{4\mu^2} \gg 1 \tag{5}$$

decreases exponentially at $\rho \gg 1/2\mu$ and any S, provided only that $\operatorname{Im} A_1(S,t')$ does not essentially change at $t-4\mu^2 \ll 4\mu^2$.

At this point the analytic properties of $A_1(S,t')$ are consistent with the diffraction picture. Exponential decrease of $a_l(S)$ at $l \gg p/2\mu$ means that the function $A_1(S,t)$ changes essentially only with a change of t by a value greater than or of the order of μ^2. This is a simple consequence of the uncertainty relation between l and scattering angle ϑ.

At $S \to \infty$ there are three possibilities:

$$a(\rho, S) \to a(\rho), \tag{6a}$$

$$a(\rho, S) \to 0, \tag{6b}$$

$a(\rho, S)$ oscillates around the mean value of $a(\rho)$ (6c). Passing from summation to integration in (2) and employing the relation (at $l \gg 1$ and $t/2p^2 \ll 1$)

$$P_l\left(1+\frac{t}{2p^2}\right) = J_0\left(\frac{l}{p}\sqrt{-t}\right) \equiv J_0(p\sqrt{-t}), \tag{7}$$

where $J_0(z)$ is the Bessel function, we shall obtain simple relations for $A_1(S, t)$ at $S \to \infty$ in each of these cases.

$$A_1(S,t) = \begin{cases} \frac{1}{4}S\int a(\rho, S)2\rho\, d\rho J_0(\rho\sqrt{-t}) & \text{at} \quad t<0, \\ \frac{1}{4}S\int a(\rho, S)2\rho\, d\rho I_0(\rho\sqrt{t}) & \text{at} \quad 0<t<4\mu^2, \end{cases} \tag{8}$$

where $I_0(z)$ is the Bessel function of imaginary argument.

In the first case

$$A_1(S,t) = Sf(t), \quad \sigma_n = 16\pi f(0) = \text{const.} \tag{9}$$

In the second case

$$A_1(S)/S \to 0, \quad \sigma_n \to 0. \tag{10}$$

In the third case

$$A_1(S,t) = Sf(S,t), \tag{11}$$

where $f(S, t)$, although it oscillates with S, as a function of t changes essentially only with changes in t of the order of μ^2.

Only the first case is completely consistent with the usual diffraction picture.

Note that, if in this case we assume (6a) to hold at any S, then, by virtue of (5), Im $A_1(S, t) = Sf(t)$, at least for $t-4\mu^2 \ll \mu^2$ (The author's attention to the fact that $A_1 = Sf(t)$ corresponds to the diffraction picture and that this expression must be fitted with the dispersion relation on t was drawn by I. Pomeranchuk.)

So far we have concerned ourselves only with analytic properties of $A_1(S, t)$ as a function of t and employed the unitarity condition in the physical region on a limited scale (the $0 < a_l < 2$ condition). However, as Mandelstam [4]) first showed, unitarity conditions in other physical regions also impose essential restrictions on amplitudes by virtue of the analytic property of $A(S, t)$ as a function of S.

Let us consider the unitarity condition in region (III) (fig. 1). At $4\mu^2 < t < 16\mu^2$, inelastic processes in channel t being forbidden, the unitarity condition

has a simple form:

$$A_3(S,t)=\frac{1}{4\pi}\sqrt{\frac{t-4\mu^2}{t}}\int\frac{dz_1\,dz_2}{\sqrt{1+2zz_1z_2-z_1^2-z_2^2-z^2}}A(S_1,t)A^*(S_2,t), \quad (12)$$

where $A_3(S,t)=\operatorname{Im}A(S,t)$ in region (III); $z=1+2S/(t-4\mu^2)$ is the cosine of scattering angle in the centre-of-mass system of channel (III):

$$z_{1,2}=1+2S_{1,2}/(t-4\mu^2).$$

This form of the unitarity condition differs from the usual one only by replacement of the variable φ_1 by z_2. Integration is performed over the region in which the radical is positive. It was shown by Mandelstam that this relation can be continued from region III ($z<1$) to regions I, III ($z>1$). In continuing (12) sufficiently far to regions I, III, expressions to the right and to the left become complex. Calculating their imaginary part and taking into account that $\operatorname{Im}A_1(S,t)=\operatorname{Im}A_3(S,t)=\rho(S,t)$ we shall obtain, according to Mandelstam,

$$\operatorname{Im}A_1(S,t)=\frac{1}{\pi}\sqrt{\frac{t-4\mu^2}{t}}\int\frac{dz_1\,dz_2}{\sqrt{z^2-2zz_1z_2+z_1^2+z_2^2-1}}A_1(S_1,t)A_1^*(S_2,t) \quad (13)$$

at $4\mu^2<t<16\mu^2$. Integration is performed over the domain

$$z_1z_2+\sqrt{(z_1^2-1)(z_2^2-1)}<z. \quad (14)$$

Note that this equation is valid irrespective of the asymptotic behaviour of $A_1(S,t)$ at $S\to\infty$.

3. Investigation of Behaviour of $A_1(S,t)$ for large S using the Unitarity Condition

Since $A_1=Sf(t)$ is the most natural expression for $A_1(S,t)$ obtained on the basis of diffraction picture, it is necessary first of all to substitute it into the unitarity condition and to check wheter it can be fulfilled.

This operation is simple enough since for such an asymptotic behaviour of A_1 and for $z\gg1$, an essential contribution to the integrand is made by $z_1\gg1$, $z_2\gg1$. Therefore it is possible to substitute $A_1(S_1,t)=S_1f(t)$ and $A_1^*(S_2,t)=S_2f^*(t)$ into the right-hand side of eq. (13). Then integrating we obtain

$$\operatorname{Im}A_1(S,t)=\frac{1}{6\pi}\sqrt{\frac{t-4\mu^2}{t}}(t-4\mu^2)S\ln S|f(t)|^2+SO(1). \quad (15)$$

Since the left-hand side must equal $S\operatorname{Im}f(t)$ under the assumption, then in

view of the presence of $\ln S$ in the right-hand side we come to the conclusion that $A_1(S,t) \neq Sf(t)$ for arbitrarily large S.

Since $A_1 = Sf(t)$ is impossible, it is necessary to find out what the character of a function satisfying eq. (13) can generally be. For this purpose we shall apply the Mellin transformation * to eq. (13), i.e. multiply the right and the left-hand sides by $z^{-(p+1)}$ and integrate over z. $A(S,t)$ does not have an essential singularity at $S \to \infty$, therefore $A_1(S,t)$ can be written in the form

$$A_1(S,t) = S^{\alpha(t)} B_t(S), \tag{16}$$

where $B_t(S)$ neither increases nor decreases as a power at $S \to \infty$. Thanks to this, the Mellin transformation makes sense at any $p > q$. At $z = 0$ there is no divergence as $A_1(S,t) = 0$ at $z < z_0$, $z_0 > 1$. Integrating over z we obtain

$$\int \operatorname{Im} A_1(S,t) z^{-(p+1)} \mathrm{d}z = \frac{1}{\pi}\sqrt{\frac{t-4\mu^2}{t}} \int \mathrm{d}z_1 (z_1^2-1)^{-(p+1)/2} A_1(S_1,t) \int \mathrm{d}z_2 (z_2^2-1)^{-(p+1)/2} A_1^*(S_2,t) c(\alpha), \tag{17}$$

where

$$\alpha = \frac{z_1 z_2}{\sqrt{(z_1^2-1)(z_2^2-1)}} \quad \text{and} \quad c(\alpha) = \int_1^\infty \frac{(x+\alpha)^{-(p+1)}}{\sqrt{x^2-1}} \mathrm{d}x.$$

Let us now consider this equation for p in the neighbourhood of q, $p = q+\delta$. In this case if $B_t(S)$ does not decrease at $S \to \infty$, then in the right hand side of (17) $z_1 \gg 1$ and $z_2 \gg 1$ become essential for $\delta \ll 1$. Under these conditions $\alpha \to 1$. Denoting

$$\psi(p) = \int z^{-(p+1)} A_1(S,t) \mathrm{d}z, \tag{18}$$

we then obtain

$$\operatorname{Im} \psi(p) = \frac{1}{\pi}\sqrt{\frac{t-4\mu^2}{t}} c(1) |\psi(p)|^2. \tag{19}$$

But since $|\operatorname{Im} \psi(p)| < |\psi(p)|$ it follows from (19) that

$$|\psi(p)| < \frac{\pi}{c(1)}\sqrt{\frac{t}{t-4\mu^2}} \tag{20}$$

at $\delta \ll 1$. This means that

$$\int z^{-\delta} z^{-q} A_1(S,t) \frac{\mathrm{d}z}{z} < \infty$$

for any $\delta \ll 1$, i.e.

$$\int^\infty B_t(S) \frac{\mathrm{d}S}{S} < \infty. \tag{21}$$

* The possibility of investigating eq. (13) with the help of the Mellin transformation was pointed out to the author by L.D. Landau.

The integral (21) can converge either due to the decrease of $B_t(S)$ or due to oscillations. It can be easily proved by direct substitution that a purely oscillatory solution does not satisfy eq. (13). Therefore we shall interpret the condition (21) as the condition that $B_t(S)$ decrease faster than $1/\ln S$. Since, apart from this, $B_t(S)$ by definition is not power dependent at $S \to \infty$, it is more convenient to regard $B_t(S)$ as a function of $\xi = \ln S$ and instead of (16) to write down

$$A_1(S, t) = S^q B_t(\xi), \quad \int B_t(\xi) \mathrm{d}\xi < \infty. \tag{16a}$$

Thus we find that in order to make eq. (13) valid it is necessary for $A_1(S, t)$ to have the form of (16a) at $4\mu^2 < t < 16\mu^2$.

In this section we have so far been concerned with the behaviour of $A_1(S, t)$ as a function of S. Now let us see what can be deduced from (16a) on the behaviour of $A_1(S, t)$ as a function of t. If the order of the power in (16a) is a function of t, then $A_1(S, t)$ will change essentially with the change in t not by the order μ^2 but by the order $\mu^2/\ln S$, i.e., arbitrarily fast for sufficiently great S. Such a behaviour of $A_1(S, t)$ can hardly be considered possible, because firstly, for this behaviour of $A_1(S, t)$ the amplitudes $a_l(S)$ calculated by (5) would not, generally speaking, decrease exponentially for $l \gg p/2\mu$, and secondly, it seems extremely unlikely that a function, which in the region $t < 4\mu^2$ changes essentially only with a change of t of the order of μ^2 would begin to change arbitrarily fast when analytically continued beyond the branch point into the region $t > 4\mu^2$. In any case it seems reasonable to postopone the treatment of such rapidly changing functions until a more detailed investigation is carried out and to assume that q is independent of t and is equal to unity. Assuming that $B_t(\xi)$ also changes essentially only with a change of t of the order μ^2 we shall come to the conclusion that the third case (6), (11) is impossible too and that

$$A_1(S, t)/S \to 0 \quad \text{at} \quad S \to \infty. \tag{22}$$

So far we have shown only that the decrease of $B_t(\xi)$ is a necessary condition of $A_1(S, t)$ satisfying eq. (13). It is easy to show that there exists a solution of such a structure. We shall assume that $B_t(\xi)$ is a power-type function of ξ, i.e. it possesses the property that $B_t(\xi_1+\xi_2) = B_t(\xi_1)$ if $\xi_1 \gg \xi_2$, and we shall put for simplicity $q = 1$ (the same result is easily arrived at in case of arbitrary q).

Contrary to (15), in the case of the asymptotic behaviour of (16a) regions $z_1 \gg 1$, $z_2 \sim 1$; $z_1 \sim 1$, $z_2 \gg 1$ prove to be essential for the integrand in the right-hand side of (13) at $z \gg 1$. Therefore an asymptotic expression for $A_1(S, t)$ cannot be directly substituted into it.

We shall write down (13) in the following way

$$\operatorname{Im} A_1(S, t) = \frac{1}{\pi} \sqrt{\frac{t-4\mu^2}{t}} \int_{z_0^2}^{u_m(z)} \mathrm{d}u \int_{z_0}^{u/z_0} \frac{\mathrm{d}z_1}{z_1} \frac{A_1(z_1) A_1^*(u/z_1)}{\sqrt{z^2-2zu+u^2/z_1^2+z_1^2-1}}, \tag{23}$$

where

$$u = z_1 z_2, \quad A_1(z) \equiv A_1(S,t) \quad \text{with} \quad A_1 = 0 \quad \text{at} \quad z < z_0.$$

The main contribution to the integral over u is made by $u \approx z$. Therefore, the integral over z_1 can be broken into two parts from z_0 to λ and from λ to u/z_0 and λ can be chosen in such a way that

$$z_0 \ll \lambda \ll u/z_0.$$

In the integral from z_0 to λ, $u/z_1 \gg 1$ and therefore we may substitute for $A_1^*(u/z_1)$ the asymptotic expression

$$\frac{u}{z_1} B_t^* \left(\ln \frac{u}{z_1}\right) \tfrac{1}{2}(t-4\mu^2) \approx \tfrac{1}{2}(t-4\mu^2) \frac{u}{z_1} B_t(\ln u).$$

Then we obtain

$$\tfrac{1}{2}(t-4\mu^2)u \int_{z_0}^{\lambda} \frac{dz_1}{z_1} \frac{A_1(z_1)}{z_1\sqrt{z^2-2zu+u^2/z_1^2+z_1^2-1}} B_t^*(\ln u).$$

Since $\int A_1(z)dz_1/z_1^2$ converges according to the assumption, the main contribution to the integral from z_0 to λ is made by $z_1 \approx 1$ and therefore one can neglect $z_1^2 - 1$ as compared with the remaining terms and integrate not up to λ but up to the zero of the radical.

In the same way we may treat the integral from λ to u/z_0. It will yield the complex conjugate expression. Transforming to the original variables, (22) can be written in the form

$$\operatorname{Im} A_1(S,t) = \frac{1}{\pi}\sqrt{\frac{t-4\mu^2}{t}} \int \frac{dz_1\, dz_2}{\sqrt{z^2-2zz_1z_2+z_2^2}} A_1(S_1,t) B_t^*(\ln S_2) S_2$$

$$+ \frac{1}{\pi}\sqrt{\frac{t-4\mu^2}{t}} \int \frac{dz_1\, dz_2}{\sqrt{z^2-2zz_1z_2+z_1^2}} S_1 B_t(\ln S_1) A_1^*(S_2,t), \quad (24)$$

where integration is performed respectively over the regions:

$$z_2(z_1+\sqrt{z_1^2-1}) \leqq z, \quad z_1(z_2+\sqrt{z_2^2-1}) \leqq z.$$

After this transformation the first integral is easily integrated over z_2 and the second-over z (certainly asymptotically at $S \to \infty$).

As a result we obtain

$$\operatorname{Im} A_1(S,t) = SB_t(\xi)\varphi^*(t) + SB_t^*(\xi)\varphi(t), \quad (25)$$

where

$$\varphi(t) = \frac{1}{2\pi}\sqrt{\frac{t-4\mu^2}{t}} \int_{z_0}^{\infty} dz' A_1(S',t) \left[z' \ln \frac{z'+1}{z'-1} - 2\right]$$

$$= \frac{1}{2\pi}\sqrt{\frac{t-4\mu^2}{t}} \int_{-1}^{1} z dz \int_{z_0}^{\infty} \frac{A_1(S,t)}{z'-z} dz'. \quad (26)$$

The integral (26) converges provided eq. (16a) is fulfilled. Eq. (25) shows that (13) is really satisfied if $A_1(S, t)$ has the form of (16a). Simultaneously an equation for $B_t(\xi)$ emerges as a function of t. This equation holds only at $4\mu^2 < t < 16\mu^2$ but if we assume it to be valid for any t we obtain immediately

$$B_t(\xi) = B(\xi) \exp\left[(t-4\mu^2)\int_{4\mu^2}^{\infty} \frac{\delta(t')}{t'-t}\,\frac{\mathrm{d}t'}{t'-4\mu^2}\right], \tag{27}$$

where $\exp[2i\delta(t)] = (1-2i\varphi(t))(1+2i\varphi^*(t))^{-1}$, and it is assumed that $\delta(t)$ does not decrease at $t \to \infty$. Thus, in the physical region $A_1(S, t) = SB(\xi)f(t)$ we have

$$\sigma_n = B(\xi)16\pi f(0) < \frac{c}{\xi} \quad \text{at} \quad S \to \infty, \tag{28}$$

while $\mathrm{d}\sigma/\sigma_n \mathrm{d}t$ is independent of S.

If from the outset we had proceeded from the assumption that $A_1(S, t) = \phi(S)f(t)$, then without making any further assumptions we would have arrived at the fact that $\phi(S) = SB(\xi)$ and that $f(t)$ satisfies the equation

$$\operatorname{Im} f(t) = f(t)\varphi^*(t) + f^*(t)\varphi(t). \tag{29}$$

It is noteworthy that the value $\varphi(t)$ (26) is in a certain way related to the scattering phase shifts at centre-of-mass system energy $\sqrt{t}$. Indeed, the scattering amplitude in region (III) can be written as

$$A(z, t) = \frac{1}{\pi}\int_{z_0}^{\infty} \frac{A_1(z', t)}{z'-z}\,\mathrm{d}z' - \frac{1}{\pi}\int_{-\infty}^{-z_0} \frac{\operatorname{Im} A(z', t)}{z'-z}\,\mathrm{d}z', \tag{30}$$

where z is the cosine of the scattering angle in the centre-of-mass system. If we now wanted to evaluate the p-wave amplitude by multiplying $A(z, t)$ by z and integrating over z we would obtain zero by virtue of the symmetry of $A(,z\,t)$. However, if we take only the first term in (30), multiply it by z and carry out the integration, we obtain $\varphi(t)$ with an accuracy up to the factor.

4. On the Energy Value at which the Cross-Section Decrease may prove to be essential

It is very difficult to make a definite estimate of energies at which the cross-section decrease may prove to be essential since we can use the unitary condition only in the interval $4\mu^2 < t < 16\mu^2$, which contains no contribution from the inelastic processes in the third channel.

However, one may attempt to make a rough estimate of the critical energy. It is rather interesting that such an estimate involves a numerical parameter which renders this energy very great.

In order to make this estimate we shall assume that starting with $S = A$ the

cross-section becomes constant and $A_1 = Sf(t)$. Substituting $A_1 = Sf(t)$ into the unitarity condition (13) we arrive at eq. (15). To estimate up to what energy $A_1 \approx Sf(t)$, it is necessary to determine up to what energy the first term in (15) containing $\ln S$ remains small as compared with the entire $\operatorname{Im} A_1$. We shall see then that the cross-section may remain constant up to energies at which

$$\frac{1}{6\pi}\sqrt{\frac{t-4\mu^2}{t}}\,(t-4\mu^2)|f|^2 \ln\frac{S_0}{A} \ll \operatorname{Im} f(t). \tag{31}$$

If we now put $\operatorname{Im} f \approx f$, neglect the fact that $f(t)$ increases with t in the interval from 0 to $4\mu^2$ and substitute $\sigma_n/16\pi$ for $f(t)$, then instead of (31) we obtain

$$\frac{1}{96}\sqrt{\frac{t-4\mu^2}{t}}\,\frac{(t-4\mu^2)\sigma_n}{\pi^2}\ln\frac{S_0}{A} \ll 1. \tag{32}$$

Eq. (32) makes sense up to $t = 16\mu^2$, and therefore if $\sigma_n \approx 1/\mu^2$, eq. (32) means roughly that

$$\ln (S_0/A) \ll 100. \tag{33}$$

In spite of the fact that the value S_0 proves to be very large and that the cross-section possibly tends to zero only at unattainably high energies, the first term in (15) may result in a 10 % change of the cross-section already with a change of energy from 10^9 eV to 10^{13} eV.

5. Pion-Pion Scattering at High Energies

So far we have considered scattering of neutral particles without spins. In this section we shall show that the same reasoning can easily be applied to the case of pion-pion scattering.

In a following paper it will be shown that the same holds for pion-nucleon and nucleon-nucleon scattering. The scattering amplitude describing scattering of π-mesons with momentum p_1 in isobaric state α by π-mesons with momentum p_2 and isobaric state β into π-mesons with momenta $-p_3$, $-p_4$ and isobaric states γ, δ can be written in the form

$$T_{\alpha\beta,\gamma\delta} = \delta_{\alpha\beta}\delta_{\gamma\delta}A(S_{12}, S_{13}, S_{23}) + \delta_{\alpha\gamma}\delta_{\beta\delta}A(S_{13}, S_{12}, S_{23}) + \delta_{\alpha\delta}\delta_{\beta\gamma}A(S_{23}, S_{12}, S_{13}). \tag{34}$$

In virtue of the crossing symmetry we have

$$A(x; y, z) = A(x; z, y). \tag{35}$$

We shall consider at first the behaviour of $T_{\alpha\beta\gamma\delta}$ as $S_{12} \to \infty$ and $S_{13} \approx -\mu^2$

and shall proceed from the assumption that

$$\begin{aligned} A(S_{12}; S_{13}, S_{23}) &\to S_{12}F_3(S_{13}), \\ A(S_{13}; S_{23}, S_{12}) &\to S_{12}F_2(S_{13}), \\ A(S_{23}; S_{12}, S_{13}) &\to S_{12}F_1(S_{13}). \end{aligned} \tag{36}$$

It is well known that the Feynman amplitude $A(S_{12}; S_{13}, S_{23})$ is not an analytic function of S_{12} in the upper half plane. (The functions corresponding to the retarded commutators are analytic in the upper half plane.)Therefore if we pass through the upper half plane from S_{12} to $-S_{12}$ we shall obtain not $A(-S_{12}; S_{13}, 4\mu^2+S_{12}-S_{13})$ but $A^*(-S_{12}; S_{13}, 4\mu^2+S_{12}-S_{13})$. However $A^*(-S_{12}; S_{13}, 4\mu^2+S_{12}-S_{13}) \to S_{12}F_1^*(S_{13})$ as $S_{12} \to \infty$. Hence, in view of the fact that $S_{12}F_3(S_{13})$ as $S_{12} \to -S_{12}$ transforms into $-S_{12}F_3(S_{13})$ we obtain

$$F_1^*(S_{13}) = -F_3(S_{13}), \tag{37}$$

and in a similar way we shall obtain for $A(S_{11}; S_{12}, S_{23})$

$$F_2(S_{13}) = -F_2^*(S_{13}). \tag{38}$$

If both functions $F_1(S_{13})$ and $F_2(S_{13})$ were non-zero it would follow from (34) firstly that the backward scattering is of the same order as the forward for any α, β and secondly that the cross-section of the forward charge exchange is of the same order as elastic scattering. The second is evident; to make the first evident it is sufficient to consider $T_{\alpha\beta,\gamma\delta}$ as $S_{12} \to \infty$ and $S_{23} \approx -\mu^2$ and to put $\alpha = \gamma$, $\beta = \delta$. As $S_{12} \to \infty$ and $S_{23} \approx -\mu^2$ we shall have from (34)

$$T_{\alpha\beta,\alpha\beta} = S_{12}\{F_1(S_{23}) + \delta_{\alpha\beta}F_3(S_{23}) + \delta_{\alpha\beta}F_2(S_{23})\}. \tag{39}$$

It follows from (39) that in order to prevent particles of different charges from backward scattering with the same amplitude as for forward scattering it is necessary that $F_1(S_{23}) = 0$. Then it will follow from (37) that $F_3(S_{13}) = 0$. In this case we obtain as $S_{12} \to \infty$, $S_{13} \to -\mu^2$

$$T_{\alpha\beta,\gamma\delta} = \delta_{\alpha\gamma}\delta_{\beta\delta}S_{12}F_2(S_{13}), \tag{40}$$

i.e. only scattering without charge-exchange occurs in the forward direction. Thus if we assume that backward scattering of particles with different charges is comparatively small we come to the conclusion that pion-pion scattering is characterized at high energies by a single scaler function $A(S_{13}; S_{23}, S_{12})$ symmetrical with respect to S_{12} and S_{23} in exactly the same way as for neutral particles without spins.

The unitarity condition for the channel in which S_{13} is the energy (area III in fig. 1) is written in a way analogous to (12) for each of the three amplitudes

corresponding to definite isobaric spins 0, 1 and 2.

$$\begin{aligned} T_0 &= 3A(S_{13}; S_{23}, S_{12}) + A(S_{12}; S_{13}, S_{23}) + A(S_{23}; S_{12}; S_{13}), \\ T_1 &= A(S_{12}; S_{13}, S_{23}) - A(S_{23}; S_{12}, S_{13}), \\ T_2 &= A(S_{12}; S_{13}, S_{23}) + A(S_{23}; S_{12}, S_{13}). \end{aligned} \tag{41}$$

Each of these relations can be continued into region $|z| > 1$. However, for $z \gg 1$, since $A(S_{12}; S_{23}, S_{13})$ and $A(S_{23}; S_{12}, S_{13})$ make a small contribution to scattering at high energy, it is sufficient to consider only the relation for T_0 which is identical with (13) and will lead to the same results as for neutral particles.

Another interesting consequence of these results is noteworthy. Under the same assumption as in section 3 we find that

$$A_1(S_{13}; S_{12}, S_{23}) = SB(\xi)f(t), \tag{42}$$

with $S = S_{12}$ and $t = S_{13}$.

If there were no $B(\xi)$ it would follow from (38) that

$$A = iSf(t), \tag{43}$$

i.e., the scattering amplitude is imaginary (the real part could be of the order of $1/S$ as compared with the imaginary).

In the presence of $B(\xi)$ the situation changes drastically. With the substitution of S for $-S$, $B(\xi)$ will be replaced by $B(\xi+i\pi)$. It is easy to show that in this case the correct expression for the whole amplitude instead of (43) will have the form

$$A(S, t) = iSB[\ln(-iS)]f(t). \tag{44}$$

The function $A(S, t)$ in this case cannot be imaginary. If $B(\xi) \approx q/\xi$ as $S \to \infty$, then

$$B[\ln(-iS)] \sim \frac{1}{\xi^q}\left[1+q\,\frac{i\pi}{2\xi}\right]. \tag{45}$$

Thus, the real part of $A(S, t)$ is small only logarithmically as compared with the imaginary part.

The main results obtained in the work can be summarized in the following way:

1) It is shown that the representation of the scattering amplitude at high energies in the form $Sf(t)$ which holds if the scattering is of diffractional character contradicts the untarity condition.

2) It follows from the conditions of unitarity and analyticity under natural assumptions that the total cross-section for the scattering decreases at high energies.

The treatment does not claim to be mathematically rigorous, but in our opinion it is convincing enough from the physical standpoint to encourage further investigation.

In conclusion the author wishes to express his profound gratitude to L. D. Landau and I. J. Pomeranchuk for their exceptional interest to the work, numerous discussions and valuable remarks without which the work could hardly have been be carried out. The author is also thankful to K. A. Ter-Martirosian, V. B. Berestetsky, I. M. Shmushkevich and I. T. Diatlov for helpful discussions.

References

1) K. Symanzik, Nuovo Cim. **5** (1957) 659
2) Arnowitt and Feldman, Phys. Rev. **108** (1957) 144
3) S. Aramaki, Progr. of Theor. Phys. **22** (1959) 485
4) S. Mandelstam, Phys. Rev. **112** (1958) 1344
5) V. B. Berestetsky and I. J. Pomeranchuk, JETP **39** (1960) 4
6) A. D. Galanin, A. F. Grashin, B. L. Ioffe and I. J. Pomeranchuk, JETP **37** (1959) 1663

8.B

Nuclear Physics **22** (1961) 262—282; ©*North-Holland Publishing Co., Amsterdam*

Not to be reproduced by photoprint or microfilm without written permission from the publisher

A NEW MAJORANA FIELD THEORY

H. UMEZAWA† and A. VISCONTI

Faculté des Sciences de Marseille, France

Received 16 June 1960

Abstract: After a short introduction, we review in sect. 2 the various isospin schemes for strong and weak interactions and we show that they can be reduced to a common scheme by writing down an invariant of a set of 2×2 matrices, whose elements are linear combinations of the particle wave functions. Various properties and difficulties of those schemes are discussed.

In sect. 3, we propose a scheme where each set of a particle and its antiparticle is described by a quaternion. Several interesting properties of that scheme are pointed out: the rule for constructing quaternions leads directly to charge conservation; the strangeness conservation for strong interactions and the rule $|\Delta S| = 1$ for the weak interactions are direct consequences of this theory, furthermore all the unwanted electromagnetic interactions are naturally excluded.

1. Introduction

The weak interactions present several important and characteristic features First of all, the rule $|\Delta \mathbf{I}| = \frac{1}{2}$ which is a generalization of the rule $|\Delta I_3| = \frac{1}{2}$ (or in terms of the hypercharge: $|\Delta U| = 1$) seems to be consistent with all the known weak interactions, except for the decay $K^+ \to \pi^+ + \pi^0$. Then, the mixture of vector (V) and axial vector interactions (A) seems to fit the known experiments and finally there are, for the time being, no phenomena violating the PC invariance.

Furthermore, the V and A interactions belong to the 2nd kind of interaction, whose coupling constants have the dimensions $(L)^\eta$ with $\eta \geqq 0$ in contradistinction to the first kind of interaction where $\eta \leqq 0$. The distinction between these two classes could be traced to their renormalizability properties, since it is generally believed that no interactions of the 2nd kind can be renormalized††. It is also known that the coupling constants for weak interactions are about $(10^{-17})^2$ cm^2 for fermion-fermion interactions and 10^{-20} cm for fermion-boson interactions. In other words, the weak interactions imply extremely small lengths, much smaller than the Compton wave length of the particles known so far. Therefore, one may reasonably suppose that in the theory of elementary particles, one has to consider [3, 4]) a fundamental length l. However, it must be noted that this assumption does not necessarily mean the nonlocal character of the interactions. Consider, for instance, the low energy phenomena which

† On leave from the Physics Dept. University of Tokyo (Japan).

†† See ref. [1, 2]) for the details of this classification.

involve particles whose wave lengths are well above l; these interactions, which we will call the strong interactions are independent of l, correspond thus to $l = 0$ and belong to the first kind of interactions. The effects involving the fundamental length l are extremely small, when they appear among the former low energy phenomena. They are consequences of weak interactions and belong to the 2nd kind of interactions.

The strong interactions are then scalar (S) or pseudo scalar (PS) (both theories are renormalizable), while the weak fermion-boson interactions are of the types V or A.

Finally, there is another remarkable feature of the weak interactions: in contradistinction to the stronger ones, they are usually defined by violations of laws which express the conservation of some quantum numbers (strangeness or hypercharge, for instance!) in the case of the strong interactions. But, from our point of view, the definition of the weak interactions has its ground essentially in the consideration of the fundamental length l. It should be therefore desirable to try to understand their systematics by means of only conservation laws.

We are thus faced with the following problems:

1) How to substitute for the rule $|\Delta \mathbf{I}| = \frac{1}{2}$ an invariance law?

2) Why do we have the conservation of the hypercharge in strong interactions but not in the weak ones?

3) How the PC invariance in strong interactions leads to the P invariance?

On the other hand, the answer to these questions must not bring any change in the experimentally well established mass spectra of the particles. In particular, the strong interactions have to be charge independent (in the ordinary meaning of the word), and the theory must allow all the mass differences between particles in different sets of charge multiplets (e.g. between the Ξ, N, Λ, Σ multiplets) †.

Our aim in the present paper is to investigate the former problems along the lines we just mentioned: after an extensive study of several isospin schemes (sect. 2) we shall introduce in sect. 3 a new scheme (the scheme of new Majorana fields), where by association of particles and antiparticles we shall build up real quaternions. Therefore, to each particle antiparticle set will correspond a quaternion and the investigation of the symmetry properties of the interaction hamiltonian will show several important and interesting features of this theory.

† The problem of the charge independence of the strong K interactions needs some comment: there are not enough experimental data which would compel one to conclude that they are (although the cross section of K^- capture by the deuteron agrees with the charge independence hypothesis). However, it seems reasonable to expect that if these interactions were not charge independent, there would have been a quite big mass difference between, say, proton and neutron. This is a reason to assume — as we shall do in this paper — the charge independence of the strong K interactions.

It is, however, worth while to note that we shall not deal with the problems of K^+ decay ($K^+ \to \pi^+ + \pi^0$): this problem will be discussed in a forthcoming paper.

2. Isospin Schemes and the 2×2 Matrix Scheme

Let us call "conventional or scheme (I)" the isospin scheme where the nucleon, the Ξ and the K particles build up isodoublets while the Σ, π particles build up isotriplets (or isovectors) and the Λ an isoscalar. The $|\Delta \mathbf{I}| = \frac{1}{2}$ rule for weak interactions has been deduced from this scheme. It has been noticed several times, however, that the charge independence of strong interactions does not necessarily lead to the former scheme uniquely.

For instance, the charge independent strong π-interactions can be described either in terms of [5]) the former scheme (I) as:

$$\mathfrak{N} = \begin{pmatrix} \mathrm{p} \\ \mathrm{n} \end{pmatrix}, \quad \xi = \begin{pmatrix} \Xi^0 \\ \Xi^- \end{pmatrix}, \quad k = \begin{pmatrix} \mathrm{K}^+ \\ \mathrm{K}^0 \end{pmatrix}, \quad \bar{k} = \begin{pmatrix} -\mathrm{K}^{0*} \\ \mathrm{K}^{+*} \end{pmatrix},$$

$$\boldsymbol{\Sigma} = \begin{pmatrix} \dfrac{\Sigma^+ + \Sigma^-}{\sqrt{2}} \\ \dfrac{\Sigma^- - \Sigma^+}{i\sqrt{2}} \\ \Sigma^0 \end{pmatrix}, \quad \boldsymbol{\pi} = \begin{pmatrix} \dfrac{\pi^+ + \pi^-}{\sqrt{2}} \\ \dfrac{\pi^- - \pi^+}{i\sqrt{2}} \\ \pi^0 \end{pmatrix}, \quad \Lambda, \tag{1}$$

or in terms of [6,7]) the baryon doublet scheme (II):

$$\mathfrak{N},\ \xi,\ k,\ \boldsymbol{\pi},\ \mathrm{X} = \begin{pmatrix} \Sigma^+ \\ \mathrm{Y}_0 \end{pmatrix}, \quad \mathrm{Z} = \begin{pmatrix} \mathrm{Z}^0 \\ \Sigma^- \end{pmatrix}, \tag{2}$$

with

$$\mathrm{Y}_0 = \frac{b\Lambda^0 - \Sigma^0}{\sqrt{2}}, \quad Z^0 = \frac{b\Lambda^0 + \Sigma^0}{\sqrt{2}}, \quad b \text{ a real constant.}$$

Furthermore, the same interaction can also be written in terms of the triplet-singlet scheme (III):

$$\mathbf{N} = \begin{pmatrix} \dfrac{\mathrm{p} + a\Xi^-}{\sqrt{2}} \\ -\dfrac{\mathrm{p} - a\Xi^-}{i\sqrt{2}} \\ -\dfrac{\mathrm{n} - a\Xi^0}{\sqrt{2}} \end{pmatrix}, \quad \mathrm{N}_0 = \frac{\mathrm{n} + a\Xi^0}{i\sqrt{2}}, \ \boldsymbol{\Sigma},\ \Lambda,\ \boldsymbol{\pi}, \tag{3}$$

where a is a real constant. In the same way, we shall assign to the K-meson the following set built up by an isovector and an isoscalar:

$$\mathbf{K} = \begin{pmatrix} \dfrac{K^+ + K^{+*}}{\sqrt{2}} \\ -\dfrac{K^+ - K^{+*}}{i\sqrt{2}} \\ -\dfrac{K^0 + K^{0*}}{\sqrt{2}} \end{pmatrix}, \quad K_0 = \frac{K^0 - K^{0*}}{i\sqrt{2}}. \tag{4}$$

To each scheme belongs an isospace which is well defined: let us call a theory charge independent in a given scheme when it is invariant with respect to the rotations in the isospace belonging to that scheme †. When $a = 1$, d'Espagnat, Prentki and Salam [8]) showed that the scheme (III) leads to a hamiltonian charge independent in both schemes (III) and (I).

Now, the charge independence in scheme (I), on one hand, does not lead to any mass differences between the particles belonging to each charge multiplet set $\mathfrak{N}$, ξ, Σ, π, $\mathbf{K}$ and is, on the other hand, compatible with the experimental evidence that the nucleons, pions, Ξ, Σ, π particles have different masses, therefore each of the hamiltonians has to be charge independent in scheme (I). One must notice, too, that a free lagrangian charge independent in scheme (II) (in (III)) is charge independent in scheme (I), only when $b = 1$ ($a = 1$) and when the bare masses of Σ, Λ (nucleon and Ξ) are equal ††.

In order to have an insight into the connection between these schemes, let us consider the strong interactions with π mesons, i.e. $NN\pi$, $\Xi\Xi\pi$, $\Sigma\Sigma\pi$, $\Sigma\Lambda\pi$ in the schemes (I), (II) and (III). They are obtained by building up all the possible isoscalars by means of field quantities. Since we assumed the strong interactions to be of first kind, we get in scheme (I) the following interaction hamiltonian:

$$H_\pi^{(I)} = g_1 \mathfrak{N}^* O\tau \cdot \mathfrak{N}\pi + g_2 \xi^* O\tau \cdot \xi\pi - ig_3 \Sigma^* \wedge O\Sigma \cdot \pi + g_4 \Sigma^* O \wedge \pi + g_4 \Lambda^* O\Sigma \cdot \pi, \tag{5a}$$

where O is:

$$O = \begin{cases} \gamma_4 \\ i\gamma_4\gamma_5 \end{cases}, \tag{5b}$$

while one gets

$$H_\pi^{(II)} = g_1 \mathfrak{N}^* O\tau \cdot \mathfrak{N}\pi + g_2 \xi^* O\tau \cdot \xi\pi + g_3 X^* O\tau \cdot X\pi + g_3 Z^* O\tau \cdot Z\pi \tag{6a}$$

† Note that in the three schemes, we shall normalize the field quantities p, n, Ξ^0, $\Sigma^{\pm,0}$, Λ^0, $\pi^{\pm,0}$, in such a way that they satisfy the canonical commutation relations.

†† One may introduce a modified scheme (II′) by replacing k and $\bar{k}$ by the isovector $\mathbf{K}$ and the isoscalar K^0, as given by (4). But for $b = 1$, the process $K^- + p \to \Sigma^+ + \pi^-$ is forbidden and therefore the scheme (II′) disagrees with the expriments. For $b \neq 1$, the free lagrangian is no longer charge independent in scheme (II′).

in scheme (II), and

$$H_\pi^{(III)} = -ig_1\{\mathbf{N}^* \wedge O\mathbf{N} \cdot \boldsymbol{\pi} + \mathrm{N}_0^* O\mathbf{N} \cdot \boldsymbol{\pi} - \mathbf{N}^* \cdot O\mathrm{N}_0 \boldsymbol{\pi}\}$$
$$-ig_3 \boldsymbol{\Sigma} \wedge O\boldsymbol{\Sigma} \cdot \boldsymbol{\pi} + g_4 \boldsymbol{\Sigma}^* \cdot O\Lambda\boldsymbol{\pi} + g_4 \Lambda^* O\boldsymbol{\Sigma} \cdot \boldsymbol{\pi} \quad (6b)$$

in scheme (III).

By taking the real coupling constants $g_2 = a^2 g_1$, $g_4 = b g_3$, one finds $H_\pi^{(I)} = H_\pi^{(II)} = H_\pi^{(III)}$.

In other words, one may obtain the same interaction hamiltonian which is charge independent in the three schemes, but, as said before, the free lagrangian is charge independent neither in (II) nor in (III), when the constants a, b are different from 1 and the masses of Σ, Λ (N and Ξ) different. The interaction hamiltonian for charge independent K interactions can be written as follows:

$$H_K^{(I)} = g'_1 \mathfrak{N}^* O\boldsymbol{\tau} \cdot k\boldsymbol{\Sigma} + g'_2 \xi^* O\boldsymbol{\tau} \cdot k\boldsymbol{\Sigma} + g'_3 \mathfrak{N}^* Ok\Lambda + g'_4 \xi^* Ok\Lambda + \text{h.c.} \quad (7a)$$

in scheme (I), and

$$H_K^{(II)} = ig'_1\{\mathbf{N}^* \wedge O\mathbf{K} \cdot \boldsymbol{\Sigma} + \mathrm{N}_0^* O\mathbf{K} \cdot \boldsymbol{\Sigma} - \mathbf{N}^* O\mathrm{K}_0 \cdot \boldsymbol{\Sigma}\}$$
$$-g'_3\{\mathbf{N}^* \cdot O\mathbf{K}\Lambda + \mathrm{N}_0^* O\mathrm{K}_0 \Lambda\} + \text{h.c.} \quad (7b)$$

in scheme (III).

By taking the real coupling constants $g'_2 = ag'_1$, $g'_3 = bg'_1$ and $g_4 = abg'_1$, one obtains, as before, the same hamiltonian in the above two schemes.

The strong K interactions are not charge independent in scheme (II): there is indeed no way to construct an isoscalar by means of an odd number of doublets. In this theory of global symmetry, Gell-Mann [6]) assumed that the strong K interactions are charge independent only in scheme (I) (but not in (II)). However, recent experiments show that the cross-section $\sigma(\mathrm{K}+\mathrm{N} \to \mathrm{K}+\mathrm{N})$ has about the same value as that of the pion-nucleon scattering: it seems, therefore, reasonable to believe that these interactions are not weaker than the π-interactions and that the symmetry properties are about the same in both the interactions.

The schemes (II) and (III) have a great advantage: even the weak interactions between baryons and bosons are charge independent. But there is an important drawback too. If the total hamiltonian without (the electromagnetic interaction) is charge independent in scheme (III), there is no way to account for the mass difference between the nucleon and Ξ. On the other hand, the weak interactions, which are charge independent in (II), disagree with experiments: the Σ^- decay is forbidden as discussed later on.

One may explain in another way the existence of the former three charge independent schemes, and the method we are going to develop here, will introduce some of the mathematical concepts, which will be used extensively later on.

Suppose that we are considering the vectorial space built up by all 2×2

matrices; I, e_1, e_2, e_3 build up a system of generators of this space. Furthermore, we have:

$$e_i e_j = -ie_k, \quad [e_i, e_j] = -2\delta_{ij}, \tag{8}$$

and i, j, k are a cyclic permutation of the numbers 1, 2, 3. The standard representation of this basis is

$$e_1 = i\sigma_1 = \begin{pmatrix} 0 & i \\ i & 0 \end{pmatrix}, \quad e_2 = i\sigma_2 = \begin{pmatrix} 0 & 1 \\ -1 & 0 \end{pmatrix}, \quad e_3 = i\sigma_3 = \begin{pmatrix} i & 0 \\ 0 & -i \end{pmatrix}, \tag{9}$$

and if A is any 2×2 matrix, we may write

$$A = \frac{1}{\sqrt{2}}\,(a + \mathbf{a}\cdot\mathbf{e}), \tag{10}$$

where in terms of the former representation

$$a_1 = \frac{A_{12}+A_{21}}{i\sqrt{2}}, \quad a_2 = \frac{A_{12}-A_{21}}{\sqrt{2}}, \quad a_3 = \frac{A_{11}-A_{22}}{i\sqrt{2}}, \quad a = \frac{1}{\sqrt{2}}\,\mathrm{Tr}\,A. \tag{11}$$

It is also worth while noting the following formula which may be of use:

$$\mathrm{Tr}\,\{ABC\} = \frac{1}{\sqrt{2}}\,(abc - \mathbf{a}\cdot\mathbf{b}c - \mathbf{a}\cdot b\mathbf{c} - a\mathbf{b}\cdot\mathbf{c} + \mathbf{a}\wedge\mathbf{b}\cdot\mathbf{c}). \tag{12}$$

Now, let us define the two matrices

$$\hat{A} = \mathrm{Tr}\,A - A = \begin{pmatrix} A_{22} & -A_{12} \\ -A_{21} & A_{11} \end{pmatrix}, \tag{13}$$

$$A^\dagger = \hat{A}^* = \begin{pmatrix} A_{22}^* & -A_{21}^* \\ -A_{12}^* & A_{11}^* \end{pmatrix}. \tag{14}$$

We shall call the matrix $\hat{A}$ the "associated matrix" † of A. A matrix is self associated (antiassociated) if $\hat{A} = A$ $(\hat{A} = -A)$, and to any given matrix corresponds a self associated part $\frac{1}{2}(A+\hat{A})$ and an antiassociated part $\frac{1}{2}(A-\hat{A})$:

$$A = \tfrac{1}{2}(A+\hat{A}) + \tfrac{1}{2}(A-\hat{A}).$$

One has for instance

$$\mathbf{e}^\dagger = \mathbf{e}, \quad \mathbf{e}^* = -\mathbf{e}, \quad \hat{\mathbf{e}} = -\mathbf{e}. \tag{15}$$

A matrix A is called a real quaternion if $A = A^\dagger$, and imaginary one if $A^\dagger = -A$. If $\mathbf{q}$ is a vector of the tridimensional space, the 2×2 matrix

$$Q = \exp\left(-\tfrac{1}{2}\theta\mathbf{e}\cdot\frac{\mathbf{q}}{|\mathbf{q}|}\right) \tag{16}$$

is on one hand a real quaternion and a unitary matrix (since the e_j are antihermitian) and on the other hand, as well known, Q is the operator describing

† Note that $\widehat{AB} = \hat{B}\hat{A}$, $(AB)^\dagger = A^\dagger B^\dagger$.

the rotation of angle θ around the unit axis $\mathbf{q}/|\mathbf{q}|$. It is also known that the three generators e_1, e_2, e_3 behave like vectors under the rotation (i.e. $e_j \to Q^* e_j Q = e'_j$ where e'_j is the vector obtained by rotating the e_j vector around the axis $\mathbf{q}/|\mathbf{q}|$ by the angle θ).

This remark shows therefore that the quantities a_0 and $\mathbf{a}$ which describe the matrix A in (10) behave respectively as an isoscalar and an isovector † in the transformation $A \to QAQ^*$:

$$A \to A' = QAQ^* = Q\{a+a_k e_k\}Q^* = a+a_k \alpha_{ik} e_i = a+a'_i e_i, \qquad (17)$$

where the matrix α represents the rotation and $a'_i = \alpha_{ik} a_k$. We can further prove that any unitary and real quaternion with c-number elements can be written in the form of (16). The transformation (17) has therefore a clear cut geometrical meaning (we shall call it the "both sides transformation") and it can be shown that the self associated (antiassociated) part of a matrix behaves like an isoscalar (isovector) under the both sides transformation (see (15)). Now let us consider the "right hand side transformation" defined as follows:

$$A \to A' = AQ^*. \qquad (18)$$

Since Q is a real quaternion ($\hat{Q} = Q^*$), we have

$$A' = AQ^* = A\hat{Q} = \widehat{(QA)} \qquad (19)$$

and the transformation (18) is equivalent to $\hat{A}' = Q\hat{A}$, which can be written in terms of matrix as follows:

$$\begin{pmatrix} A'_{22} & -A'_{12} \\ -A'_{21} & A'_{11} \end{pmatrix} = Q \begin{pmatrix} A_{22} & -A_{12} \\ -A_{21} & A_{11} \end{pmatrix}. \qquad (20)$$

We may therefore say that the right hand side transformation (18) is completely equivalent to the "left hand transformation" of the isodoublets,

$$\begin{pmatrix} A'_{22} \\ -A'_{21} \end{pmatrix} = Q \begin{pmatrix} A_{22} \\ -A_{21} \end{pmatrix} = Q\mathfrak{A}_1, \quad \begin{pmatrix} -A'_{12} \\ A'_{11} \end{pmatrix} = Q \begin{pmatrix} -A_{12} \\ A_{11} \end{pmatrix} = Q\mathfrak{A}_2.$$

We thus see that the matrix A behaves like a set of an isovector and an isoscalar under the both sides transformation (17) while it is transformed as a set of two isodoublets under the right hand side transformation (18),

$$\mathfrak{A}_1 = \begin{pmatrix} -A_{12} \\ A_{11} \end{pmatrix}, \quad \mathfrak{A}_2 = \begin{pmatrix} A_{22} \\ -A_{21} \end{pmatrix}. \qquad (21)$$

In this way the baryon doublet scheme (II) and the triplet-singlet scheme (III) may be viewed as two schemes obtained by the transformations (17) and (18)

† We have indeed $e'_j = \alpha_{jk} e_k = Q^{-1} e_i Q$, and since $\alpha^T = \alpha^{-1}$ it follows that $Q e_k Q^* = \alpha_{mk} e_m$.

applied to a single scheme, where all the particles will be represented by 2×2 matrices build up in the following way †:

$$\mathrm{N} = i\begin{pmatrix} -\mathrm{n} & \mathrm{p} \\ a\Xi^- & -a\Xi^0 \end{pmatrix} = \frac{1}{\sqrt{2}}(\mathrm{N}_0 + \mathbf{N}\cdot\mathbf{e}), \tag{22}$$

$$\Sigma = i\begin{pmatrix} -\dfrac{b\Lambda^0-\Sigma^0}{\sqrt{2}} & \Sigma^+ \\ \Sigma^- & -\dfrac{b\Lambda^0+\Sigma^0}{\sqrt{2}} \end{pmatrix} = \frac{1}{\sqrt{2}}(b\Lambda^0 + \boldsymbol{\Sigma}\cdot\mathbf{e}), \tag{23}$$

$$\pi = i\begin{pmatrix} \dfrac{\pi^0}{\sqrt{2}} & \pi^+ \\ \pi^- & \dfrac{-\pi^0}{\sqrt{2}} \end{pmatrix} = \frac{1}{\sqrt{2}}\boldsymbol{\pi}\cdot\mathbf{e}, \tag{24}$$

$$\mathrm{K} = \begin{pmatrix} -\mathrm{K}^0 & \mathrm{K}^+ \\ \mathrm{K}^{+*} & \mathrm{K}^{0*} \end{pmatrix} = \frac{-i}{\sqrt{2}}(\mathrm{K}_0 + \mathbf{K}\cdot\mathbf{e}). \tag{25}$$

All the former matrices have been expressed in terms of the isovectors and isoscalars as defined in scheme (III) by means of the formula (10). Remembering the relations

$$\boldsymbol{\pi}^* = \boldsymbol{\pi}, \quad \mathbf{K}^* = \mathbf{K}, \quad \mathrm{K}_0{}^* = \mathrm{K}_0, \tag{26a}$$

one obtains

$$\pi^\dagger = \hat{\pi}^* = \pi, \quad \mathrm{K}^\dagger = \hat{\mathrm{K}}^* = -\mathrm{K}, \quad \hat{\pi} = -\pi, \quad \pi^* = -\pi. \tag{26b}$$

We may, therefore, characterize the π and K matrices as real and imaginary quaternions. On the other hand the doublets $\mathfrak{A}_1$ and $\mathfrak{A}_2$ given by the formula (21) are

$$\mathfrak{A}_1 = -i\mathfrak{N} = -i\begin{pmatrix} \mathrm{p} \\ \mathrm{n} \end{pmatrix}, \quad \mathfrak{A}_2 = -ia\xi = -ia\begin{pmatrix} \Xi^0 \\ \Xi^- \end{pmatrix}, \tag{27a}$$

for the matrix N, and

$$\mathfrak{A}_1 = -i\mathrm{X} = \begin{pmatrix} \Sigma^+ \\ \mathrm{Y}^0 \end{pmatrix}, \quad \mathfrak{A}_2 = -i\mathrm{Z} = \begin{pmatrix} \mathrm{Z}^0 \\ \Sigma^- \end{pmatrix}, \tag{27b}$$

for the matrix Σ (see (24) and (25)).

Consider now the hamiltonians H_π and H_K defined as follows:

$$H_\pi = i\sqrt{2}O_{\alpha\beta}\,\mathrm{Tr}\,\{g_1\mathrm{N}_\alpha{}^*\mathrm{N}_\beta\pi + g_3\Sigma_\alpha{}^*\Sigma_\beta\pi\}, \tag{28a}$$

$$H_\mathrm{K} = -\sqrt{2}g'_1O_{\alpha\beta}\,\mathrm{Tr}\,\{\mathrm{N}_\alpha{}^*\mathrm{K}\Sigma_\beta + \mathrm{h.c.}\}, \tag{28b}$$

† It should be noted that K_0 is not the particle K^0 but the isoscalar attached to the isovector **K** in scheme (III).

where O is given by (5b) and the trace operation is to be performed on the isospins indices. As well known, a canonical transformation generated by the unitary operator Q in isospace leaves the trace invariant, hence the formula (28) may be as well put into the form

$$H_\pi = i\sqrt{2}O_{\alpha\beta}\,\mathrm{Tr}\,\{g_1 Q\mathrm{N}_\alpha^* Q^* Q\mathrm{N}_\beta Q^* Q\pi Q^* + g_3 Q\Sigma_\alpha^* Q^* Q\Sigma_\beta Q^* Q\pi Q^*\}, \quad (29a)$$

$$H_\mathrm{K} = -\sqrt{2}g'_1 O_{\alpha\beta}\,\mathrm{Tr}\,\{Q\mathrm{N}_\alpha^* Q^* Q\mathrm{K}Q^* Q\Sigma_\beta Q^* + \mathrm{h.c.}\}. \quad (29b)$$

They can be interpreted in three ways:

a) One may consider this canonical transformation as just the both sides transformation (17),

$$\mathrm{N}_\alpha \to Q\mathrm{N}_\alpha Q^*, \quad \Sigma_\alpha \to Q\Sigma_\alpha Q^*, \quad \pi \to Q\pi Q^*, \quad \mathrm{K} \to Q\mathrm{K}Q^*. \quad (30)$$

Taking into account the text before formula (17), we are thus led directly to the triplet singlet scheme (III). Indeed a straightforward calculation taking (12) into account shows that the hamiltonians (29a) and (29b) are equal to (6b) and (7b) represtively.

b) One may consider the hamiltonian (29a) as resulting from the transformation

$$\mathrm{N}_\alpha \to \mathrm{N}_\alpha Q^*, \quad \Sigma_\alpha \to \Sigma_\alpha Q^*, \quad \pi \to Q\pi Q^*, \quad (31)$$

applied to (28a) and this leads to the doublet scheme (II), if we take into account the formula (27). We may remark that (29b) cannot be deduced from (28b) by the former transformation (31) together with: $\mathrm{K} \to \mathrm{K}Q^*$, i.e. H_K is not charge independent in schema (II).

c) One may consider finally the transformations

$$\mathrm{N}_\alpha \to \mathrm{N}_\alpha Q^*, \quad \Sigma_\alpha \to Q\Sigma_\alpha Q^*, \quad \mathrm{K} \to \mathrm{K}Q^*, \quad \pi \to Q\pi Q^*, \quad (32)$$

of the hamiltonians (29) and this leads, as easily seen, to the scheme (I): the hamiltonians H_π and H_K are both charge independent in scheme (I).

Let us now consider the weak π baryon interactions. It can be shown that the following hamiltonian is invariant under the transformation (31):

$$i(f\gamma_4\gamma_\mu + f'\gamma_4\gamma_\mu\gamma_5)_{\alpha\beta}\,\mathrm{Tr}\,\{\mathrm{N}_\alpha^*\Sigma_\beta\partial_\mu\pi\} + \mathrm{h.c.} \quad (33)$$

Therefore it is charge independent in scheme (II). On the other hand it is not invariant under the transformation (32), but it leads us to the rule $|\Delta\mathbf{I}| = \frac{1}{2}$. Indeed, if one looks at the transformation of the product $\Sigma_\alpha\pi$ by the formula (32),

$$\Sigma_\alpha\pi \to Q\Sigma_\alpha\pi Q^*,$$

one sees that $\Sigma_\alpha\pi$ behaves as a set of isovector and isoscalar, while N_α behaves as two doublets, one may then conclude that $\mathrm{Tr}\,\{\mathrm{N}_\alpha^*\Sigma_\beta\pi\}$ satisfies the rule mentioned above. One can show that (33) is equivalent to an interaction propos-

ed by Takeda [7]). A perturbation treatment in its lowest order shows that the Σ^- decay is forbidden and therefore this decay may be explained only by an extremely large π mesonic correction. One of the authors (H. U.) [9]) and independently d'Espagnat and Prentki [10]) proposed once consideration of the following hamiltonian for the weak baryon-pion interactions †:

$$
\begin{aligned}
&H(\Sigma N\pi)\\
&= if[\tfrac{1}{2}n^*\gamma_4\gamma_\mu\gamma(1+\rho\gamma_5)\Sigma^0\partial_\mu\pi^0+\tfrac{1}{2}p^*\gamma_4\gamma_\mu\gamma(1-\rho\gamma_5)\Sigma_0\partial_\mu\pi^+ \qquad (34a)\\
&-\frac{1}{\sqrt{2}}p^*\gamma_4\gamma_\mu\gamma(1-\rho\gamma_5)\Sigma^+\partial_\mu\pi^0+n^*\gamma_4\gamma_\mu\Sigma^-\partial_\mu\pi^++\rho n^*\gamma_4\gamma_\mu\gamma\gamma_5\Sigma^+\partial_\mu\pi^-+\text{h.c.}],
\end{aligned}
$$

$$
H(\Lambda N\pi) = -\frac{i}{\sqrt{2}}f'\left[p^*\gamma_4\gamma_\mu\gamma(1+\gamma_5)\Lambda\partial_\mu\pi^+-\frac{1}{\sqrt{2}}n^*\gamma_4\gamma_\mu\gamma(1+\gamma_5)\Lambda\partial_\mu\pi^0+\text{h.c.}\right], \qquad (34b)
$$

where

$$
\rho = \pm 1, \quad \gamma = 1 \quad \text{or} \quad \gamma_5.
$$

It has been proved by d'Espagnat and Prentki [10]) that (29) and (30) together with $\Xi-\pi$ weak interactions can be charge independent in scheme III when we assume $\rho = 1$. This can be seen from the following relation:

$$
\begin{aligned}
&-\frac{1}{\sqrt{2}}f\{(\gamma_4\gamma_\mu\gamma)_{\alpha\beta}\,\mathrm{Tr}[N_\alpha^*\partial_\mu\pi\Sigma_\beta]-(\gamma_4\gamma_\mu\gamma_5\gamma)_{\alpha\beta}\,\mathrm{Tr}\{N_\alpha^*\Sigma_\beta\partial_\mu\pi\}\}\\
&\quad = H(\Sigma N\pi)+H(\Lambda N\pi)-if\Big\{\frac{1}{\sqrt{2}}\Xi^{-*}\gamma_4\gamma_\mu\gamma(1-\gamma_5)\Sigma^-\partial_\mu\pi^0\\
&\quad -\frac{1}{\sqrt{2}}\Xi^{-*}\gamma_4\gamma_\mu\gamma(1-\gamma_5)\Sigma^0\partial_\mu\pi^-+\tfrac{1}{2}\Xi^{0*}\gamma_4\gamma_\mu\gamma(1+\gamma_5)\Sigma^0\partial_\mu\pi^0 \qquad (35)\\
&\quad +\Xi^{0*}\gamma_4\gamma_\mu\gamma_5\gamma\Sigma^-\partial_\mu\pi^++\Xi^{0*}\gamma_4\gamma_\mu\gamma\Sigma^+\partial_\mu\pi^-\\
&\quad +\frac{b}{\sqrt{2}}\Xi^{-*}\gamma_4\gamma_\mu\gamma(1+\gamma_5)\Lambda\partial_\mu\pi^-+\frac{b}{\sqrt{2}}\Xi^{0*}\gamma_4\gamma_\mu\gamma(1+\gamma_5)\Lambda\partial_\mu\pi^0+\text{h.c.}\Big\},
\end{aligned}
$$

with $f' = bf$, $\rho = 1$.

† The lowest order perturbation applied to (34) is in agreement with the following experimental results:

$$
\begin{aligned}
&\frac{\sigma(\Lambda^0\to p+\pi^-)}{\sigma(\Lambda^0\to n+\pi^0)} = 2, \qquad \alpha(\Lambda^0\to p+\pi^-) < -0.67\pm 0.13,\\
&\sigma(\Sigma^+\to p+\pi^0)\approx\sigma(\Sigma^+\to n+\pi^+)\approx\sigma(\Sigma^-\to n+\pi^-),\\
&|\alpha(\Sigma^+\to p+\pi^0)| > 0.70\pm 0.30, \qquad \alpha(\Sigma^+\to n+\pi^+)\approx\alpha(\Sigma^-\to n+\pi^-)\approx 0,
\end{aligned}
$$

where α is the asymmetry factor. Note that one may conclude from experiments for the Σ^- decay that $P_\alpha\approx 0$, where P is the polarization of the Σ^-. We assumed here that $\alpha\approx 0$ (instead of $P\approx 0$) in the Σ^- decay.

3. New Majorana Field Formalism

As we have seen, all the known schemes in isospace can be formulated in terms of 2×2 matrices. We have gone even further and tried to pave the way to a theory where all the interactions — including the weak ones — must be governed by invariance laws only. But, by associating particles of different masses (e.g. nucleon and Ξ) in our fundamental matrices, we were forced to violate some of the invariance laws in order to explain the mass differences (cf. text just before the formula (7)). Therefore, we have to construct our basic 2×2 matrices by means of particles of same mass (electromagnetic mass differences are here disregarded.) This is only possible if we construct, say, the nucleon basic matrix by means of nucleons and antinucleons. In order to do this, we shall be led to use in an extensive way the formalism of the quaternion algebra.

In sect. 2, we defined the real (imaginary) quarternion as a matrix A, whose elements are c-numbers, and which satisfies the relations

$$A = A^\dagger \equiv \hat{A}^* \quad (A = -A^\dagger).$$

One can extend without difficulty this definition to commuting fields; we shall define the $B^\dagger$ corresponding to a Bose field as follows:

$$B^\dagger = \hat{B}^*, \tag{36}$$

where the hermitic conjugation * is to be worked out both in Hilbert space and in isospace, and the operation $\widehat{\ }$ in isospace only.

Let us now consider a fermion field F with components F_α and define $\bar{F} = F^*\gamma_4$. Since the hermitic conjugation for a boson field is equivalent to the charge conjugation, we are led to define $F^\dagger$ as follows:

$$F_\alpha{}^\dagger = \widehat{(C\bar{F})}_\alpha, \tag{36a}$$

where C is the well known charge conjugation matrix $(C^{-1}\gamma_\mu C = -\gamma_\mu{}^{\mathrm{T}})$. If j and l are isospin indices running from 1 to 2,

$$(F_\alpha{}^\dagger)_{jl} = (C\gamma_4{}^{\mathrm{T}})_{\alpha\rho}\widehat{(F_\rho{}^*)}_{jl}, \tag{36b}$$

where the * operation is to be worked out both in Hilbert space and isospace. A fermion field will be called a real or an imaginary quaternion if we have

$$F^\dagger = F \quad \text{or} \quad F^\dagger = -F.$$

On the other hand,

$$\widehat{C\bar{F}} = \frac{1}{\sqrt{2}}\,(C\bar{F}_0{}^{\mathrm{T}} + C\overline{\mathbf{F}}^{\mathrm{T}}\hat{\mathbf{e}}^*). \tag{37}$$

Therefore if the quaternion F is real, we obtain

$$C\bar{F}_0{}^{\mathrm{T}} = F_0, \quad C\overline{\mathbf{F}}^{\mathrm{T}} = \mathbf{F}$$

and if it is imaginary,

$$C\bar{F}_0^{\mathrm{T}} = -F_0, \quad C\bar{\mathbf{F}}^{\mathrm{T}} = -\mathbf{F}^{\mathrm{T}}.$$

One may conclude that the decomposition of a real or an imaginary quaternion into an isoscalar F_0 and an isovector $\mathbf{F}$ defined two Majorana fields F_0 and $\mathbf{F}$. As well known, there is no conservation law for the fermion number in Majorana's theory. In order to avoid this drawback, we shall assign to the particles F_0 and $\mathbf{F}$ a definite handedness. We may first remark that by means of the well known handedness projection operators

$$h_\pm = \tfrac{1}{2}(I \pm \gamma_5), \tag{38}$$

one may prove that the field

$$F_1 = \frac{1}{\sqrt{2}}(h_+ F + h_- F'), \tag{39}$$

(with $F' = C\bar{F}^{\mathrm{T}}$) is again a Majorana field. We have indeed for the field $h_+ F$, for instance †

$$\overline{C(h_+ F)}^{\mathrm{T}} = C\gamma_4^{\mathrm{T}} h_+^{\mathrm{T}} \bar{F}^{\mathrm{T}} = h_- F'. \tag{40}$$

Since the particle and its antiparticle are of opposite handedness, we can define the fermion number as shown later.

Let us, then, define the basic quaternions by associating, in a same matrix, particles and antiparticles, each of them having a definite handedness. We define first the following four 2×2 matrices in isospace:

$$\mathrm{N}_+ = \begin{pmatrix} -h_+\mathrm{n} & h_+\mathrm{p} \\ h_-\mathrm{p}' & h_-\mathrm{n}' \end{pmatrix}, \qquad \xi_+ = \begin{pmatrix} h_-\Xi^{0\prime} & h_-\Xi^{-\prime} \\ h_+\Xi^- & -h_+\Xi^0 \end{pmatrix},$$

$$\Sigma_+ = i\begin{pmatrix} \dfrac{1}{\sqrt{2}}(h_+\Sigma^0 + h_-\Sigma^{0\prime}) & h_+\Sigma^+ + h_-\Sigma^{-\prime} \\ h_+\Sigma^- + h_-\Sigma^{+\prime} & -\dfrac{1}{\sqrt{2}}(h_+\Sigma^0 + h_-\Sigma^{0\prime}) \end{pmatrix}, \tag{41}$$

$$\Lambda_+ = \frac{1}{\sqrt{2}}(h_+\Lambda^0 + h_-\Lambda^{0\prime})\begin{pmatrix} 1 & 0 \\ 0 & 1 \end{pmatrix},$$

and the four matrices:

$$\mathrm{N}_-, \ \xi_-, \ \Sigma_-, \ \Lambda_-, \tag{42}$$

which are deduced from the matrices (41) by exchanging h_+ for h_- and vice versa. The π and K matrices are given by (24) and (25) and in all the above definitions the prime denotes the antiparticle.

We note further that $\Sigma_\pm$, $\Lambda_\pm$, π, are real quaternions and $\mathrm{N}_\pm$, $\xi_\pm$, K, are imaginary quaternions. We assign, therefore, to each field a real or an imaginary

† Another formula which will be of use later on is $\psi'^* O\psi' = \varphi^* O\psi$, where O is γ_4 or $i\gamma_4\gamma_5$.

quaternion as follows: to fields of hypercharge† 0, i.e. to Σ, Λ and π particles we will assign real quaternions, to fields of hypercharge different from 0 we will assign imaginary quaternions. Let us note further that $\hat{\pi} = -\pi$, $\hat{\Sigma} = -\Sigma$, $\hat{\Lambda} = \Lambda$.

Following (10), isoscalars and isovectors corresponding to the above quaternions are given by

$$\mathrm{N}_+ = \frac{1}{\sqrt{2}} (\mathrm{N}_{+0} + \mathbf{N}_+ \cdot \mathbf{e}) \ldots \text{etc.}, \tag{43}$$

where

$$\begin{aligned} \mathrm{N}_{+1} &= \frac{h_+ \mathrm{p} + h_- \mathrm{p}'}{\sqrt{2}}, \qquad \mathrm{N}_{+2} = -\frac{h_+ \mathrm{p} - h_- \mathrm{p}'}{i\sqrt{2}} \\ \mathrm{N}_{+3} &= -\frac{h_+ \mathrm{n} + h_- \mathrm{n}'}{\sqrt{2}}, \quad \mathrm{N}_{+0} = \frac{h_+ \mathrm{n} - h_- \mathrm{n}'}{i\sqrt{2}}, \ldots \text{etc.} \end{aligned} \tag{44}$$

It is remarkable that all the components of the isoscalars and isovectors are Majorana fields. Let us now consider the structure of the interaction hamiltonian. To obtain conservation of the baryon number, we shall introduce a generalized gauge transformation

$$F_+ \to L(h_+, h_-) F_+ L(h_+, h_-) = h_+ \mathrm{e}^{i\varphi} + h_- \mathrm{e}^{-i\varphi}, \tag{45}$$

where φ is a real c-number. If the quaternion F_+ is real (imaginary), the transformation (45) keeps its real (imaginary) character. The transformation for F_- has to be

$$F_- \to L(h_-, h_+) F_-, \tag{46}$$

because F_- is obtained by exchanging h_+ and h_- in F_+. Our generalized gauge transformation is built up of two transformations (45), (46). On the other hand, it is easy to verify the following formulas:

$$L^*(h_+, h_-) L(h_+, h_-) = L^*(h_-, h_+) L(h_-, h_+) = 1, \tag{47}$$

$$L(h_+, h_-)\gamma_4 = \gamma_4 L(h_-, h_+), \qquad L(h_+, h_-)\gamma_4\gamma_5 = \gamma_4\gamma_5 L(h_-, h_+), \tag{48}$$

and that $L(h_+, h_-)$ commutes with the matrices $\gamma_4\gamma_\mu$, $\gamma_4\gamma_\mu\gamma_5$.

Since we assumed in sect. 1 that the strong interactions are of the γ_4 or $\gamma_4\gamma_5$ type (first kind interactions) and the weak interactions are of the $\gamma_4\gamma_\mu$ or $\gamma_4\gamma_\mu\gamma_5$ the (second kind interactions), the generalized gauge invariance together with the formulas (48) shows that in strong interactions, the two bary ons must be F_+ and G_- respectively, while in weak interactions, the two baryons are F_+ and G_+ respectively, or F_- and G_-. It is also worth while noting that the following baryon products are identically zero:

† The hypercharge of a field is twice the average value of the charges of the fields which build up the charge multiplet of the given field in scheme (I).

$$\begin{aligned}&\xi_-{}^*\gamma_4 \mathrm{N}_+ = \xi_+{}^*\gamma_4 \mathrm{N}_- = \xi_-{}^*\gamma_4\gamma_5 \mathrm{N}_+ = \xi_+{}^*\gamma_4\gamma_5 \mathrm{N}_- = 0,\\ &\xi_+{}^*\gamma_4\gamma_\mu \mathrm{N}_+ = \xi_-{}^*\gamma_4\gamma_\mu \mathrm{N}_- = \xi_+{}^*\gamma_4\gamma_\mu\gamma_5 \mathrm{N}_+ = \xi_-{}^*\gamma_4\gamma_\mu\gamma_5 \mathrm{N}_- = 0.\end{aligned} \tag{49}$$

We shall now give four theorems which will lead us to selection rules for the choice of hamiltonians: let us consider two fermion fields F and G and a boson field B and, as previously, define the matrices

$$O = \begin{matrix}\gamma_\mu \\ i\gamma_4\gamma_5\end{matrix}, \quad O_\mu = i\gamma_4\gamma_\mu.$$

The trace operation in the following theorems is to be taken in isospace.

THEOREM I

The operators $O_{\alpha\beta}\,\mathrm{Tr}\{F_\alpha{}^* G_\beta B\}$ and $O_{\alpha\beta}\,\mathrm{Tr}\{F_\alpha{}^* B G_\beta\}$, are hermitic when there is an even of zero number of imaginary quaternions among the three quaternions F, G and B.

THEOREM II

The equation

$$O_{\alpha\beta}\,\mathrm{Tr}\{F_\alpha{}^* G_\beta B + \mathrm{h.c.}\} = O_{\alpha\beta}\,\mathrm{Tr}\{F_\alpha{}^* B G_\beta + \mathrm{h.c.}\} = 0$$

holds when there is an odd number of imaginary quaternions among the three quaternions F, G and B.

THEOREM III

The operators $O_{\mu\alpha\beta}\,\mathrm{Tr}\{F_\alpha{}^* G_\beta B\}$ and $O_{\mu\alpha\beta}\,\mathrm{Tr}\{F_\alpha{}^* B G_\beta\}$ are hemitic when there is an odd number of imaginary quaternions F, G and B.

THEOREM IV

The equation

$$O_{\mu\alpha\beta}\,\mathrm{Tr}\{F_\alpha{}^* G_\beta B + \mathrm{h.c.}\} = O_{\mu\alpha\beta}\,\mathrm{Tr}\{F_\alpha{}^* B G_\beta + \mathrm{h.c.}\} = 0$$

holds when there is an even number of imaginary quaternions among F, G and B.

The reader may find the proof of these theorems in the appendix. In the following we shall assume that the Dirac matrices in the interactions are hermitic and that coupling constants are real.

Then, the theorem II excludes the following combinations among the strong interactions:

$$\begin{aligned}&(\mathrm{N}, \Sigma, \pi), \quad (\mathrm{N}, \Lambda, \pi), \quad (\xi, \Sigma, \pi), \quad (\xi, \Lambda, \pi), \quad (\mathrm{N}, \mathrm{N}, \mathrm{K}),\\ &(\xi, \xi, \mathrm{K}), \quad (\mathrm{N}, \xi, \mathrm{K}), \quad (\Sigma, \Sigma, \mathrm{K}), \quad (\Sigma, \Lambda, \mathrm{K}), \quad (\Lambda, \Lambda, \mathrm{K}).\end{aligned} \tag{50}$$

These results added to the ones obtained in (49) show an extremely remarkable property of our scheme: almost all the strong interactions which violate the hypercharge conservation (or the strangeness conservation) are excluded. There

are two exceptions,

$$O_{\alpha\beta}\,\mathrm{Tr}\,\{\xi_{-\alpha}^{*}\pi \mathrm{N}_{+\beta}\} \quad \text{and} \quad O_{\alpha\beta}\,\mathrm{Tr}\,\{\xi_{+\alpha}\pi \mathrm{N}_{-\beta}\}, \tag{51}$$

and both are characterized by the fact that the pion quaternion appears between the two baryons field quantities. But, as we shall see later, there is a reason to exclude these interactions. Let us now consider the weak interactions: we shall exclude later the case $O_\mu = i\gamma_4\gamma_\mu\gamma_5$ by means of a space reflection invariance. We are therefore left with $O_\mu = i\gamma_4\gamma_\mu$, and then the theorem IV excludes the following combinations for weak interactions:

$$\begin{aligned}&(\mathrm{N},\mathrm{N},\pi),\quad (\mathrm{N},\xi,\pi),\quad (\xi,\xi,\pi),\quad (\Sigma,\Sigma,\pi),\quad (\Sigma,\Lambda,\pi),\\ &(\Lambda,\Lambda,\pi),\quad (\mathrm{N},\Sigma,\mathrm{K}),\quad (\mathrm{N},\Lambda,\mathrm{K}),\quad (\xi,\Lambda,\mathrm{K}),\quad (\xi,\Sigma,\mathrm{K}).\end{aligned} \tag{52}$$

This remark gives the well known hypercharge rule for weak interactions: $|\Delta U| = 1$ (or $|\Delta S| = 1$ for strangeness). To discuss the problem of the space reflection, we shall briefly discuss the free field equations of the quaternions. From their definitions (41) and (42) it is easy to see that they satisfy

$$\gamma_\lambda \partial_\lambda F_+ = -m_F F_-, \quad \gamma_\lambda \partial_\lambda F_- = -m_F F_+, \tag{53}$$

where F is one of the baryons and m_F its mass. These equations are invariant under the following space inversion †:

$$\mathbf{x} \to -\mathbf{x}, \quad t \to t, \quad F_\pm \to \rho_s \gamma_4 F_\pm, \tag{54a}$$

with $\rho_s = \pm 1, \pm i$. We shall choose $\rho_s = 1$ for all the baryons. One further assumes that the boson quaternions transform as

$$\pi(x) \to \pi(x') \quad \text{and} \quad \mathrm{K}(x) \to \mathrm{K}(x'), \tag{54b}$$

under the space reflection and that the interactions are invariant under this space reflection. Then we are led to choice $O = \gamma_4$ for the strong interactions and $O_\mu = i\gamma_4\gamma_\mu$ for the weak ones.

Collecting the strong π interactions, we may write

$$\begin{aligned}H_\pi &= g_1\gamma_{4\alpha\beta}\,\mathrm{Tr}\,\{\mathrm{N}^{*}_{+\alpha}\mathrm{N}_{-\beta}\pi\} + g_2\gamma_{4\alpha\beta}\,\mathrm{Tr}\,\{\xi^{*}_{+\alpha}\xi_{-\beta}\pi\} + g_3\gamma_{4\alpha\beta}\,\mathrm{Tr}\{\Sigma^{*}_{+\alpha}\Sigma_{-\beta}\pi\}\\ &\qquad + g_4\gamma_{4\alpha\beta}\,\mathrm{Tr}\,\{\Lambda^{*}_{-\alpha}\Sigma_{+\beta}\pi + \varepsilon\Lambda^{*}_{+\alpha}\Sigma_{-\beta}\pi\}\\ &= \frac{ig_1}{\sqrt{2}}\,\mathfrak{N}^{*}\boldsymbol{\tau}\cdot\gamma_4\gamma_5\mathfrak{N}\boldsymbol{\pi} + \frac{ig_2}{\sqrt{2}}\,\xi\boldsymbol{\tau}\cdot\gamma_4\gamma_5\xi\boldsymbol{\pi}\\ &\qquad + \frac{g_3}{\sqrt{2}}\,\boldsymbol{\Sigma}^{*}\wedge\gamma_4\gamma_5\boldsymbol{\Sigma}\cdot\boldsymbol{\pi} - \frac{g_4}{\sqrt{2}}\left\{\Lambda^{0*}\gamma_4\gamma\boldsymbol{\Sigma}\cdot\boldsymbol{\pi} + \mathrm{h.c.}\right\},\end{aligned} \tag{55}$$

† The equations in (53) are invariant under the following space-inversion too:

$$F_\pm \to \rho_s\gamma_4 F_\mp,\ \mathbf{x} \to -\mathbf{x},\ t \to t\ (\rho_s = \pm 1, \pm i).$$

This corresponds to the well known P-transformation. We do not however, assume that the theory is invariant under this kind of space reflection.

where the particles $\mathfrak{N}$, ξ, Σ, Λ^0 and π^0 have been defined in scheme (I). ε is equal to ± 1 and

$$\gamma = \tfrac{1}{2}(1+\varepsilon)+\tfrac{1}{2}(1-\varepsilon)\gamma_5. \tag{56}$$

The hamiltonian (55) is the most general hamiltonian under the following assumptions: (a) the invariance of the interaction under space reflection (54a) and (54b), (b) the Dirac matrix O is hermitic and the coupling constants g_1 are real, and (c) the quaternion π never appears between two baryon quaternions.

The (55) shows evidently that H_π is charge independent in scheme (I). This can be seen also from the fact that (55) is invariant under the right hand side transformation for N, ξ and K (which are equivalent to isodoublets) and under the both sides transformations for Λ, Σ and π (which are equivalent to isoscalars and isovectors):

$$\mathrm{N} \to \mathrm{N}Q^*,\ \xi \to \xi Q^*,\ \mathrm{K} \to \mathrm{K}Q^*,\ \Sigma \to Q\Sigma Q^*,\ \pi \to Q\pi Q^*,\ \Lambda \to Q\Lambda Q^*. \tag{75}$$

Note that this invariance is entirely due to the assumption (c). However, this transformation does not leave invariant the real or imaginary character of the quaternions; only the "both sides transformation" preserves this invariance. Since we assume that the real or imaginary character of the quaternions is intrinsic, we require only that the interactions must be invariant under the "both sides transformation" $A \to QAQ^*$, where A is one of the quaternions N, $\xi, \ldots$ and Q is a unitary real quaternion. One may see from (55) that the π-nucleon, $\pi-\Xi$ and $\pi-\Sigma$ interactions naturally appear to be P-invariant †. On the other hand, the $\Lambda\Sigma\pi$ can be P-invariant only when $\varepsilon = \pm 1$ since we have then $\gamma = 1$ or γ_5. The space reflection (54) does not lead to these values of ε as a direct consequence. The value $\varepsilon = \pm 1$ is then to be considered as a supplementary hypothesis. Moreover, it is a remarkable result that the nucleon-pion interaction appears to be pseudoscalar in (55).

As is shown in (55), the type of the $\Lambda\Sigma\pi$ interaction depends on the constant ε i.e. (scalar for $\varepsilon = 1$ and pseudoscalar for $\varepsilon = -1$).

Consider now the K strong interactions, making use of the assumptions (a) and (b) used for the π strong interactions and replacing (c) by (c'); "the quaternion K never appears between two baryon quaternions", we may write down the following hamiltonian:

$$\begin{aligned} H_{\mathrm{K}} = {} & g'_1 O_{\alpha\beta}\,\mathrm{Tr}(\mathrm{N}^*_{+\alpha}\mathrm{K}\Sigma_{-\beta}+\varepsilon_1(+\leftrightarrow-)) \quad +g'_2 O_{\alpha\beta}\,\mathrm{Tr}(\mathrm{N}^*_{-\alpha}\mathrm{K}\Lambda_{+\beta}+\varepsilon_2(+\leftrightarrow-)) \\ & +g'_3 O_{\alpha\beta}\,\mathrm{Tr}(\xi^*_{+\alpha}\mathrm{K}\Sigma_{-\beta}+\varepsilon_3(+\leftrightarrow-)) + g'_4 O_{\alpha\beta}\,\mathrm{Tr}(\xi^*_{-\alpha}\mathrm{K}\Lambda_{+\beta}+\varepsilon_4(+\leftrightarrow-)) \\ = {} & +\frac{i}{\sqrt{2}} g'_1 \mathfrak{N}^* O\gamma^{(1)}\boldsymbol{\tau}\cdot k\Sigma - \frac{1}{\sqrt{2}} g'_2 \mathfrak{N}^* O\gamma^{(2)} k\Lambda \\ & + \frac{i}{\sqrt{2}} g'_3 \xi^* O\gamma^{(3)}\boldsymbol{\tau}\cdot k\Sigma - \frac{1}{\sqrt{2}} g'_4 \xi^* O\gamma^{(4)} k\Lambda + \mathrm{h.c.}, \end{aligned} \tag{58}$$

† This P-invariance is due to the following relation:

$$O_{\alpha\beta}\,\mathrm{Tr}\{\mathrm{N}^*_{+\alpha}\mathrm{N}_{-\beta}\pi\} = -O_{\alpha\beta}\,\mathrm{Tr}\{\mathrm{N}^*_{-\alpha}\mathrm{N}_{+\beta}\pi\}, \text{ etc.}$$

where k and $\hat{k}$ have been defined in (1) and

$$\gamma^{(i)} = \begin{cases} 1 \\ \gamma_5 \end{cases} \quad \text{for} \quad \varepsilon_i = \begin{cases} 1 \\ -1 \end{cases} \tag{59}$$

and the symbol $(+ \leftrightarrow -)$ means the replacement of $\mathrm{N}_+, \xi_+, \ldots$ by $\mathrm{N}_-, \xi_-, \ldots$.

This interaction is charge independent in the ordinary scheme (I). This fact is due to the assumption (c'). (58) is also invariant under the both sides transformation. It is P-invariant only when $|\varepsilon_i| = 1$.

Let us now discuss the weak interactions. It can be proved that

$$H(\Sigma \mathrm{N}\pi) = if_1(\gamma_4\gamma_\mu)_{\alpha\beta}\,\mathrm{Tr}[\{\mathrm{N}^*_{+\alpha}(\partial_\mu\pi\Sigma_{+\beta} + \rho\Sigma_{+\beta}\partial_\mu\pi\} + \varepsilon\mathrm{N}^*_{-\alpha}\{\partial_\mu\pi\Sigma_{-\beta} - \rho\Sigma_{-\beta}\partial_\mu\pi\}], \tag{60}$$

$$H(\Lambda \mathrm{N}\pi) = if_2(\gamma_4\gamma_\mu)_{\alpha\beta}\,\mathrm{Tr}\,[\mathrm{N}^*_{+\alpha}\{\partial_\mu\pi\Lambda_{+\rho} + \Lambda_{+\beta}\partial_\mu\pi\} + \varepsilon\mathrm{N}^*_{-\alpha}\{\partial_\mu\pi\Lambda_{+\rho} - \Lambda_{+\beta}\partial_\mu\pi\}] = 2if_2(\gamma_4\gamma_\mu)_{\alpha\beta}\,\mathrm{Tr}[\mathrm{N}^*_{+\alpha}\Lambda_{+\beta}\partial_\mu\pi]. \tag{61}$$

Here $H(\Sigma \mathrm{N}\pi)$ and $H(\Lambda \mathrm{N}\pi)$ are defined by (34a) and (34b), where now γ corresponds to ε as follows:

$$\gamma = \begin{cases} 1 \\ 5 \end{cases} \quad \text{for} \quad \varepsilon = \begin{cases} 1 \\ -1 \end{cases}. \tag{62}$$

These interactions are invariant under the both sides transformation as one may easily check.

We now come to the electromagnetic interactions. We introduced at the beginning of sect. 2 the associated part and the antiassociated part of a matrix A by writing

$$A_1 = \tfrac{1}{2}(A + \hat{A}), \quad A_2 = \tfrac{1}{2}(A - \hat{A}), \quad A = A_1 + A_2. \tag{63}$$

Under the transformation $A \to QAQ^*$, one has

$$\hat{A} \to \widehat{QAQ^*} = Q\hat{A}Q^*, \tag{64}$$

since from $Q^\dagger = Q$ one deduces $Q^* = \hat{Q}$. Therefore, A_1 and A_2 are transformed as A under the both sides transformation: the separation of A in A_1 and A_2 is an invariant one. One may prove also that if A is real (imaginary), A_1 and A_2 are real (imaginary). We define the electromagnetic quaternion corresponding to the four-potentiel A_μ, as follows:

$$\mathfrak{A}_\mu = \tfrac{1}{2}\begin{pmatrix} A_\mu & 0 \\ 0 & -A_\mu \end{pmatrix} = -\tfrac{1}{2}iA_\mu e_3. \tag{65}$$

One has

$$\mathfrak{A}_\mu{}^+ = -\mathfrak{A}_\mu, \quad \hat{\mathfrak{A}}_\mu = -\mathfrak{A}_\mu. \tag{66}$$

To A_μ corresponds therefore a fixed direction (e_3) in isospace.

We shall assume that only the antiassociated part A_2 interacts with the electromagnetic field †. Further, let us not the following relations:

$$i(\gamma_4\gamma_\mu)_{\alpha\beta}\,\mathrm{Tr}[\mathrm{N}^*_{+2\alpha}\xi_{+2\beta}\mathfrak{A}_\mu] = i(\gamma_4\gamma_\mu)_{\alpha\beta}\,\mathrm{Tr}\,[\mathrm{N}^*_{+2\alpha}\mathfrak{A}_\mu\xi_{+2\beta}]$$
$$= i(\gamma_4\gamma_\mu)_{\alpha\beta}\,\mathrm{Tr}\,[\mathrm{N}^*_{-2\alpha}\xi_{-2\beta}\mathfrak{A}_\mu] = i(\gamma_4\gamma_\mu)_{\alpha\beta}\,\mathrm{Tr}\,[\mathrm{N}^*_{-2\alpha}\mathfrak{A}_\mu\xi_{-2\beta}] = 0. \quad (67)$$

Taking into account the theorem IV, we are left with the following combinations for the electromagnetic interactions:

$$(\mathrm{N}_2, \mathrm{N}_2, \mathfrak{A}_\mu),\quad (\xi_2, \xi_2, \mathfrak{A}_\mu),\quad (\Sigma, \Sigma, \mathfrak{A}_\mu),\quad (\pi, \pi, \mathfrak{A}_\mu),\quad (\mathrm{K}_2, \mathrm{K}_2, \mathfrak{A}_\mu). \quad (68)$$

It must be noted that $\pi_1 = 0$, $\pi_2 = \pi$, $\Sigma_1 = 0$, $\Sigma_2 = \Sigma$, $\Lambda_1 = \Lambda$, and $\Lambda_2 = 0$.

The position of $\mathfrak{A}_\mu$ is of no importance because we have

$$\mathrm{Tr}\,(A_2B_2\mathfrak{A}_\mu) = \mathrm{Tr}\,(\hat{A}_2\hat{B}_2\hat{\mathfrak{A}}_\mu) = -c\,\mathrm{Tr}\,(\mathfrak{A}_\mu B_2A_2) = -\mathrm{Tr}(A_2\mathfrak{A}_\mu B_2), \quad (69)$$

where A_2 and B_2 are given anti-adjoint quaternions and c is $+1$ (or -1) when A_2 and B_2 are bosons (or fermions) respectively. Thus, we are left with the following electromagnetic interaction hamiltonian:

$$ie(\gamma_4\gamma_\mu)_{\alpha\beta}\,\mathrm{Tr}\,[\mathrm{N}_2{}^{+*}\mathrm{N}_2{}^{+}\mathfrak{A}_\mu + (+\leftrightarrow -)] = -e\not{p}^*O_\mu \mathrm{p}A_\mu,$$
$$ie(\gamma_4\gamma_\mu)_{\alpha\beta}\,\mathrm{Tr}\,[\xi_2{}^{+*}\xi_2{}^{+}\mathfrak{A}_\mu + (+\leftrightarrow -)] = e\Xi^{-*}O_\mu\Xi^-A_\mu,$$
$$ie(\gamma_4\gamma_\mu)_{\alpha\beta}\,\mathrm{Tr}\,[\Sigma^{+*}\Sigma\mathfrak{A}_\mu + (+\leftrightarrow -) = -e(\Sigma^{+*}O_\mu\Sigma^+ - \Sigma^{-*}O_\mu\Sigma^-A_\mu, \quad (70)$$
$$ie\,\mathrm{Tr}\,[\pi\partial_\mu\pi\mathfrak{A}_\mu] = -\tfrac{1}{2}ie(\pi^+\partial_\mu\pi^- - \pi^-\partial_\mu\pi^+)A_\mu,$$
$$ie\,\mathrm{Tr}\,(K_2\partial_\mu K_2\mathfrak{A}_\mu) = -\tfrac{1}{2}ie(K^{+*}\partial_\mu K^+ - K^-\partial_\mu K^-)A_\mu.$$

It is remarkable that the theory automatically leads us to the right combinations for the electromagnetic interactions. Let us note that $H(\Sigma\mathrm{N}\pi)$ and $H(\Lambda\mathrm{N}\pi)$ (eqs. (60), (61)) can be written in terms of $\mathrm{N}_{\pm1}$ and $\mathrm{N}_{\pm2}$ as follows:

$$H(\Sigma\mathrm{N}\pi) = 2if_1(\gamma_4\gamma_\mu)_{\alpha\beta}\,\mathrm{Tr}[\mathrm{N}^*_{+1\alpha}\Sigma_{+\beta}\partial_\mu\pi_- \varepsilon\mathrm{N}^*_{-2\alpha}\Sigma_{-\beta}\partial_\mu\pi], \quad \text{for } \rho = 1, \quad (71)$$

or

$$H(\Sigma\mathrm{N}\pi) = 2i\varepsilon f_1(\gamma_4\gamma_\mu)_{\alpha\beta}\,\mathrm{Tr}\,[\mathrm{N}^*_{-1\alpha}\Sigma_{-\beta}\partial_\mu\pi_- \varepsilon\mathrm{N}^*_{+2\alpha}\Sigma_{+\beta}\partial_\mu\pi], \text{ for } \rho = 1, \quad (72)$$

and

$$H(\Lambda\mathrm{N}\pi) = 2if_2(\gamma_4\gamma_\mu)_{\alpha\beta}\,\mathrm{Tr}\,[\mathrm{N}^*_{+2\alpha}\Lambda_{+\beta}\partial_\mu\pi]. \quad (73)$$

We shall close this section by the study of the charge conservation law. The reader may have noticed that we always used the following rule called the charge rule in constructing the quaternions: for any quaternion A, $a_{12}\Phi_0$ and

† This assumption excludes the $\Sigma^0 - \Lambda^0 - \gamma$ interaction as a direct one; the decay $\Sigma^0 \to \Lambda^0 + \gamma$ can appear through several steps involving strong and electromagnetic interactions.

$a_{21}\Phi_0$ describe a positive and negative charge state, respectively, and $a_{11}\Phi_0$ and $a_{22}\Phi_0$, neutral states only in the representation (2). Here Φ_0 is the vacuum state. We shall now prove that the charge conservation law is based on this rule. Indeed making a product $C = AB$ out of two quaternions A, B, we may see that C satisfies the charge rule when A and B do: $C_{11}\Phi_0$ a neutral state, etc. ... Therefore, when A, B, ... are constructed according to the charge rule, the state

$$\mathrm{Tr}\,[AB\ldots]\Phi_0$$

is neutral and this property corresponds to the conservation of charge.

4. Concluding Remarks

In the last section, we have formulated a new Majorana theory under the fundamental assumptions that any field must be described by a real or imaginary quaternion and that the theory is invariant under the both sides transformation. The Σ, Λ and π have been assumed to be real and N, ξ and K imaginary and the basic quaternions have been constructed according to the charge rule. We have further assumed the invariance of the theory under the space reflection (54). Taking the coupling constants and Dirac matrices to be real and hermitic respectively, we are then naturally led to the conservation of charge, the conservation of hypercharge, (there are two exceptions (51)) the P-invariance of the nucleon-pion, $\xi-\pi$, $\Sigma-\pi$ interactions and the pseudoscalar character of latter interactions. Assuming that the electromagnetic field is represented by an imaginary quaternion and that it interacts only with the antiassociated parts of all fields, all the unwanted electromagnetic interactions appear to be zero. The invariance under the both sides transformation governs all the interactions including the electromagnetic interactions. The strong interactions appear to be charge independent in the scheme (I) when we assume a) that π never appears between two baryon quaternions and b) that K stands between them. This assumption holds only in the case of strong interactions and excludes the unwanted interactions (51). The weak baryon-pion interactions lead us to the $|\Delta \mathbf{I}| = \frac{1}{2}$ rule in scheme (I) and will explain the known interactions. In many cases, we have found terms of the form $\varepsilon(+ \leftrightarrow -)$. Nothing has been said, in this article about the four fermion weak interactions: this will be discussed in a separate paper. As was shown in sect. 2, the invariance under both sides transformations leads us to an isoscalar and isovector scheme. It is furthermore, important to remark that the Lorentz space is not, in the formalism of the new Majorana fields theory, independent of the isospace. Some of the components of the quaternions are left handed states, and some are right handed ones. This seems to be very characteristic of this theory.

The authors would like to acknowledge extremely helpful discussions with Professors D. Kastler and J. M. Souriau who introduced them to the quaternion algebra and who took a continuous interest in this work in all its stages.

One of us (H. U.), would like togratefully acknowledge a fellowship of invited Professor at the University of Marseille.

Appendix

Consider two fermion fields F_1, F_2 and a boson field B and suppose that

$$F_1^\dagger = \rho_1 F_1, \quad F_2^\dagger = \rho_2 F_2, \quad B^\dagger = \rho B, \tag{A.1}$$

where ρ_1, ρ_2 and ρ are c-numbers. We want to show that if $O = \gamma_5$ or $i\gamma_4\gamma_5$, then

$$O_{\alpha\beta}\,\mathrm{Tr}\,\{F^*_{1\alpha} F_{2\beta} B\} = (\rho_1\rho_2\rho)^{-1} O_{\beta\alpha}\,\mathrm{Tr}\{B^* F^*_{2\beta} F_{1\alpha}\}. \tag{A.2}$$

One may first show that

$$F'^*_{1\alpha} O_{\alpha\beta} F'_{2\beta} = F^*_{2\alpha} O_{\alpha\beta} F_{1\beta},$$

where $F'_{r\alpha} = C_{\alpha\lambda} F_{r\lambda}$ and taking into account the anticommutation properties of the Fermi fields.

Then by using (A.1) one may write the left hand side of (A.2) as follows:

$$\begin{aligned} O_{\alpha\beta}\,\mathrm{Tr}\{F^*_{1\alpha} F^*_{2\beta} B\} &= O_{\alpha\beta}(\rho_1\rho_2\rho)^{-1}\,\mathrm{Tr}\,\{F^{*\dagger}_{1\alpha} F_{2\alpha}{}^\dagger B^\dagger\} \\ &= -O_{\alpha\beta}(\rho_1\rho_2\rho)^{-1}\,\mathrm{Tr}\,\{\overbrace{B^*(C\bar{F}_2)_\beta (C\bar{F}_1)_\alpha{}^*}\} \\ &= -O_{\alpha\beta}(\rho_1\rho_2\rho)^{-1}\,\mathrm{Tr}\,\{B^*(C\bar{F}_2)_\beta (\bar{F}_1{}^* C^{-1})_\alpha\}, \end{aligned}$$

since the association operation does not change the trace of a given matrix.

Finally, if one notes that $-C^{-1}\gamma_4 O\gamma_4 C = O^{\mathrm{t}}$, where "t" means the transpose in spinspace, a few algebraical steps are enough to prove (A.2).

In a similar way we can prove that

$$i\gamma_4\gamma_{\mu\alpha\beta}\,\mathrm{Tr}\,\{F^*_{1\alpha} F_{2\beta}\partial_\mu B\} = -(\rho_1\rho_2\rho)^{-1} i\gamma_4\gamma_{\mu\alpha\beta}\,\mathrm{Tr}\,\{B^* F^*_{2\beta} F_{1\alpha}\}.$$

To prove this, use is made of the following relation:

$$iF'^*_1\gamma_4\gamma_\mu F'_2 = -iF_2{}^*\gamma_4\gamma_\mu F_1.$$

The formulae (A.2) and (A.3) are at the basis of the four theorems of sect. 3.

References

1) W. Heisenberg, Solvay Berichte report (1939)
2) S. Sakata, H. Umezawa and S. Kamefuchi, Prog. Theor. Phys. **17** (1952) 377
3) H. Umezawa, Prog. Theor. Phys. Suppl. **17** (1959) 67
4) H. Umezawa, M. Konuma and K. Nakagawa, Nuclear Physics **7** (1958) 169

5) M. Gell-Mann, Phys. Rev. **92** (1953) 833;
K. Nishijima, Prog. Theor. Phys. **13** (1955) 285;
K. Nishijima and T. Nakano, Prog. Theor. Phys. **10** (1953) 581
6) M. Gell-Mann, Phys. Rev. **106** (1957) 1296
7) G. Takeda, Prog. Theor. Phys. **19** (1958) 63
8) B. d'Espagnat, J. Prentki and A. Salam, Nuclear Physics **5** (1958) 447
9) H. Umezawa and K. Nakagawa, Nuovo Cimento (to be published)
10) B. d'Espagnat and J. Prentki, Nuclear Physics

1.C:
1.E.6

Nuclear Physics **22** (1961) 283—300; © *North-Holland Publishing Co., Amsterdam*
Not to be reproduced by photoprint or microfilm without written permission from the publisher

THE MOMENT OF INERTIA OF LARGE SUPERFLUID FERMION SYSTEMS

RICHARD E. PRANGE †
Institute for Theoretical Physics, University of Copenhagen, Denmark

Received 31 August 1960

Abstract: The moment of inertia of a superfluid system is calculated according to the Bardeen-Cooper-Schrieffer-Bogoliubov model. In order to obtain sensible results, it is necessary to include not only the independent pair excitations, but also the phonon excitations. A method of calculating the effects of these excitations is developed, which exhibits the fact that many of the excitations cannot be easily produced, since there is an "energy gap" against their formation. Other excitations are, however, easily produced. These excitations are characteristic of a macroscopic irrotational flow, and may be described loosely as a centre-of-mass motion of the "bound" pairs of the Bardeen-Cooper-Schrieffer-Bogoliubov theory. Thus the irrotational flow moment of inertia is predicted. This result does not apply to finite systems in which the shell spacing is significantly large. Corrections to the formula of Belyaev for finite nuclei are suggested. Finally, some remarks are made on the origin of the cranking model.

1. Introduction

The calculation of the moment of inertia of quantum-mechanical many-body systems is a subject which has been very often discussed in the recent literature [1]). The investigation of the well-known rotational spectra of finite nuclei has excited much interest, but recent advances in the microscopic theory of superfluidity, particularly of superconductors, has led to the possibility that the mechanical properties of such systems might be studied in some detail. This theory, which was first presented in its elementary form by Bardeen, Cooper and Schrieffer (BCS) [2]) and by Bogoliubov [3]), was called a theory of superfluid systems because the most primitive calculations predict a complete superfluidity. By a complete superfluidity we mean that the fluid has no inertia of any kind. This cannot be strictly correct, of course, but it does indicate that the systems described by the microscopic theory might well have superfluid properties.

One of the main purposes of the present work is to provide a detailed prediction of the accepted microscopic theory. The chief difficulty is the usual one, which up to now has prevented the solution of the problem. This difficulty is that the many-body system has been successfully described only in a "momentum" space representation in which the states of individual particles are speci-

† National Science Foundation Postdoctoral Fellow. Present address: Institute for Advanced Study, Princeton, N.J.

fied, whereas the simple mechanical properties are easily considered in a coordinate space representation, in terms of hydrodynamical flows, for instance. Even the simplest problems, such as that of a system of non-interacting particles, become very cumbersome for this reason [4,5]).

The prediction which is obtained in this work is that superfluids should exhibit the irrotational flow moment of inertia. It would be of even greater interest to obtain a complete hydrodynamics, but this has not been done, nor has the theory been applied at finite temperatures so far. It is not hard to guess at the result, which would be that the "superfluid component" would be governed by an irrotational flow hydrodynamics. Such speculations are familiar from the theory of Bose superfluids; however, it is interesting to note that this "irrotationality" has so far not been deduced from any of the microscopic theories of the Bose system [6]). It is hoped that the present result will shed some light on the Bose superfluid.

It ought to be emphasized that we have not, strictly speaking, obtained the exact prediction of the accepted microscopic theory. Our argument can be regarded almost as a justification of Landau's original remark [7]). Landau's idea was that the elementary excitations of the system (in his case the phonons in helium) arranged themselves into a current flowing according to a curlfree velocity field. We find that the forces set up by the rotation of the box or potential containing the system excite phonons, and other excitations. The interactions responsible for the superfluidity inhibit the formation of nearly all the excitations by creating an "energy gap" against their formation. There is no such inhibition against those phonon excitations characteristic of irrotational flow, however. We assume that these irrotational "phonons" are the only such special group of excitations. We have been unable to construct other special groups of uninhibited excitations, nor can we find any general reasons for their existence. However, the equations are so complicated that their study alone does not enable us to rule out the possibility that other types of excitations may be uninhibited by the interaction. That the irrotational flow is not disturbed by the effect of interparticle interaction follows from the fact that the velocity potential generating the flow is a function of the coordinates only, therefore commuting with the interaction potential. Thus, the interaction has no effect on this type of excitation.

The rest of this paper will essentially detail these remarks. First, however, we shall discuss briefly some of the possible applications to realistic physical systems. There are three observable fermion systems which are, or may be, superfluid. These are the electrons in a superconductor, liquid He^3, and finite nuclei. The theory exposed below is believed to apply quite well to the electrons, except for the modifications imposed by the solid state physics. However, the electrons follow the motion of the ions. If they did not, a current would be set up by the ion motion, producing magnetic fields inside the sample, which is

excluded by the Meissner effect [8]). Liquid He^3, in addition to offering formidable experimental difficulties (it shows no signs of becoming superfluid down to temperatures considerably less than 0.1 degree), gives rise to special theoretical problems also. According to some of the latest ideas on the subject [9]), the present theory of superfluidity has to be modified there in rather drastic ways. Thus that system must be further examined.

Most of the main results of the theory presented below do not apply to finite nuclei. In addition to the customary difficulties associated with the choice and treatment of the "residual" interactions of the nucleons, and the self-consistency requirements for the potential, it also turns out that ordinary nuclei are much too small for the theory to apply. Our main equations are presumably applicable to finite systems, but to solve them, in addition to treating the number of particles as large, we must utilize the relation

$$\frac{\hbar v_F}{\Delta} \ll R. \tag{1}$$

This relation insists that the correlation length, given by the Fermi velocity over the energy gap, be much shorter than the dimension of the system. Alternatively, (1) may be rewritten

$$\frac{1}{m}\frac{\hbar}{R} p_F \ll \Delta, \tag{1a}$$

which requires that the energy gap be much larger than the normal level spacing at the Fermi surface. Conditions (1) are far from satisfied in actual nuclei: in fact, the "correlation length" is about ten times the size of the nucleus.

In spite of this, the theory developed in the sequel is not without interest in the case of finite nuclei. The elementary theory of superconductivity has already been applied there [10, 11]), and has been evaluated numerically by a number of workers [11, 12]). These evaluations agree rather well with one another and with experiment, although it is difficult to assess the precision which one may hope to attain. Even so, there remains some difficulty with the theoretical formulation. In view of the notorious failures of intuition which have plagued the theorist in the past, it is all the more important to understand these difficulties, even though the good agreement with experiment leads us to believe that the standard formulation is correct, in the main.

The difficulty with superfluid systems, which manifests itself in several ways, comes from the truncation of the Hamiltonian implicit or explicit in all of the simpler formulations of the BCS theory. This truncation, it may be remembered, ignores all of the interaction except for that part scattering particles in paired single-particle states from one paired state into another. A state is paired with its time-reversed state. The truncation introduces

violent velocity dependences, leading to a breakdown of gauge invariance, for instance, and also resulting in an effectively infinite non-locality of the interaction. This in turn results in some completely wrong properties in the infinite limit. For instance, if one "pushes" [4]) the external potential, in order to compute the mass, the non-locality of the interaction permits particles scattering on one side of the box to reappear on the other, without at the same carrying any momentum. Thus, a very small mass is predicted by the calculation. In the finite case, the non-locality is less important, but it still results in a mass less than the true mass. Similarly, a truncated potential predicts zero moment of inertia for very large numbers of particles. This cannot be the case, of course. Hence, we must take into account all of the interaction, and not just the pairing part.

What is more, the truncation procedure itself is not unique. In fact, two different formulations of the theory have led to somewhat different results. As long as the Hamiltonian is time reversal invariant, there will exist "pairs" of states, and a unique prescription is possible. The imposition of rotation introduces the additional Coriolis force which changes sign under inversion of the time. One may, as seems natural from the point of view of the BCS form of the theory, first truncate the Hamiltonian and, then, add the Coriolis force [10]). Alternatively, as another extreme, one could add the Coriolis force, compute the new single-particle states which are slightly perturbed from the original ones, and "pair" those states connected adiabatically with the original paired states. This prescription is distinct from the first one. There are an infinite number of prescriptions leading to different results. Migdal, working from the Green's function formulation, exhibited a class of possible prescriptions [11]).

For these reasons, it is important to carry the theory beyond the state in which only the reduced Hamiltonian is considered. Fortunately, students of the Meissner effect in the theory of superconductivity, and others, have developed methods for carrying out this programme [3, 13]). We could merely apply these methods to the present problem. This has, in fact, already been done by Rockmore [14]), for a special case, namely that of particles confined in a cube with periodic boundary conditions. We generalize his analysis to the general situation. This, in itself, is no great feat, although it turns out to be essential. Periodic boundary conditions are exceptional for this problem, unexpectedly enough. They have universally been used up to now, because of additional simplifications introduced in the labelling of the single-particle states.

Unfortunately, the equations obtained, essentially the equations of motion for the elementary excitations, are so complicated in the general case that it is difficult to gain much insight from them. Accordingly, we present a new derivation of these equations which has the merit of providing some insight into certain aspects of the equations, although it obscures other facets of the problem. These equations have the virtue that they give the correct answers in

those cases in which the correct answer is already known. They provide corrections to the simplest formulas which are essential for very large systems, but which may be of importance even for finite systems. The ambiguities resulting from the truncation of the potential are avoided also.

In an appendix we make some remarks on the cranking model formulation.

2. Fundamental Equations

We start from the Hamiltonian

$$H = \sum_{i=1}^{A} \left[-\frac{1}{2M} \nabla_i^2 + U(x_i) \right] + \sum_{i<j} v(x_i, x_j). \tag{2}$$

Here, $U(x)$ is the single-particle potential, while $v(x, y)$ is the interaction between two particles. We insist that U and v are functions only of the coordinates of the particles, and not of their momenta. Some explanation ought to be made in justification of this assumption, since it is seldom in practice. We shall, however, postpone the discussion until the appendix when it will be better motivated.

We regard the potential U as an external box which can be cranked with an angular frequency ω small compared with any other frequency appearing. Application of the usual "cranking" model formalism allows us to write the Hamiltonian in the rotating system as

$$H' = H - \omega L_z, \tag{3}$$

where the added term represents the Coriolis force. It is usual to treat this term in second order perturbation theory, whence the formula for the moment of inertia is obtained

$$\mathcal{I} = 2 \sum_n \frac{\langle 0|L_z|n\rangle\langle n|L_z|0\rangle}{E_n - E_0}. \tag{4}$$

The evaluation of formula (4) has formed the subject of much research. It is not at all trivial to evaluate since the states appearing are the true eigenstates of the many-particle system. We shall only discuss the approximations which have been made when the system is supposed to be superfluid. For this purpose, to fix the notation, let us recall that it is customary to make the Bogoliubov transformation [10])

$$\alpha_r = U_r a_r + V_r a_{-r}^\dagger, \tag{5}$$

where we consider operators $a_r^\dagger$, a_r which create or destroy a particle in the state labelled by r. The wave functions of these states are given by

$$\left[-\frac{1}{2M} \nabla^2 + U(x) \right] \psi_r(x) = \varepsilon_r \psi_r(x) \tag{6}$$

and we denote the time-reversal conjugate state of r by $-r$. The U_r and V_r satisfy

$$U_r^2+V_r^2=1, \quad U_{-r}=U_r, V_{-r}=-V_r, \tag{7}$$

in order that (5) be a canonical transformation. After making the transformation, the Hamiltonian becomes

$$H=\sum E_r\alpha_r^\dagger\alpha_r+H_1, \tag{8}$$

when written in field theoretic language. Here we need to define †

$$\begin{aligned} E_r &= [(\tilde{\varepsilon}_r-\varepsilon_F)^2+\Delta_r^2]^{\frac{1}{2}}, \\ \tilde{\varepsilon}_r &= \varepsilon_r+\sum_s(\langle rs|v|sr\rangle-\langle rs|v|rs\rangle)V_s^2, \\ V_r^2 &= \tfrac{1}{2}\left(1-\frac{\tilde{\varepsilon}_r-\varepsilon_F}{E_r}\right), \\ \Delta_r &= \sum_s\langle r-r|v|-ss\rangle U_sV_s. \end{aligned} \tag{9}$$

The quasi-particle interaction term H_I contains products of four of the quasi-particle operators α_r, and will not be exhibited explicitly. In order to achieve the form (8) in a simple way, some special assumptions are needed about the potentials [10]). These assumptions are not interesting in what follows, so we write (8) for the sake of clarity. In fact, the arguments of the rest of this paper are independent of special forms of the interactions and external potential, within the limitations already described, and under the assumption that the general approximations inherent in the theory of superconductivity are valid. However, as will be seen, even this theory enters only at one point, so that it may be speculated that the result we shall obtain is quite independent of the detailed validity of the theory.

In Belyaev's evaluation of (4), he considered those states which result upon the neglect of the term H_I in (8). In other words, he approximated the ground state by the quasi-particle vacuum, and the excited states by states containing two quasi-particles. In this approximation, he obtained

$$\mathscr{I}=2\sum_{rs}\frac{|(L_z)_{rs}|^2}{E_r+E_s}(U_rV_s-U_sV_r)^2, \tag{10}$$

which is the formula that has been compared with experiment. It may very well be an excellent approximation for finite nuclei, but it certainly fails in the infinite limit, since both it and its "pushing" equivalent predict a vanishingly small moment of inertia or mass. It gives a much smaller moment than in the "normal" case because the energy denominators do not become small, and there is no compensating increase in the matrix elements. As we pointed out in

† Note that r labels both the particle and quasi-particle states. Unless otherwise indicated, matrix elements are defined in terms of particle states.

the introduction, an almost identical problem has already been solved. The problem to which we refer is that of the gauge invariance of the Meissner effect. There one studies a formula, like (4), in which ωL_z is replaced by $\mathbf{j}_p \cdot \mathbf{A}$, where $\mathbf{j}_p$ is the paramagnetic current operator, and $\mathbf{A}$ the vector potential. One then has an exact sum rule which requires the paramagnetic energy shift to have a definite large value for a longitudinal potential $\mathbf{A}$. In order to satisfy this sum rule, and to maintain the gauge invariance, it was found necessary to include the phonon-like excitations in the intermediate states of (4). These excitations are entirely responsible for the energy shift, since the contribution of the free quasi-particles is negligible. The phonon excitations become so important, first, because they have small excitation energies, and secondly, because they are excited very readily by the perturbation, i.e. the matrix elements are large. We could try to attack the formula (4) directly, as has been done for the Meissner effect, by computing the explicit wave functions, matrix elements, and excitation energies, but this is a very difficult procedure, and what is more, not a very general one. For only one case, that of periodic boundary conditions, might it be feasible, since there it is possible to label the excitations by their momenta. This affords a considerable simplification. One might think that for large systems it would be good enough to construct approximate eigenstates with given momenta, since their lifetimes would be very long, given by the collisions with the walls. However, great care is needed, because it is exactly the interaction with the rotating walls that sets up these excitations in the first place. Thus, we shall avoid the restriction to periodic boundary conditions.

Instead, our procedure will be to set up an approximate sum rule, which takes the effect of the "phonons" and other simple elementary excitations into account implicitly, without the necessity of describing them in detail. The device is a simple one. We imagine transforming (3) by a canonical transformation $\exp i\omega S$. The transformation is chosen to eliminate, approximately, the first order terms in ω. It is easy to construct, formally, the operator which does this, but that leads back to (4). Instead, we rephrase the requirement, and demand

$$[S, H] = iL_z. \tag{11}$$

Inserting (11) into (4), we obtain for the moment of inertia

$$\mathcal{I} = \langle 0|[iL_z, S]|0\rangle = \langle 0|2[S, [H, S]] - [iL_z, S]|0\rangle, \tag{12}$$

where we have recorded the second expression because it happens to be variationally correct.

It is a bothersome point that $\exp i\omega S$ may not admit an expansion in ω. We can think of S as $\mathcal{I}\theta$, where θ is a collective angular variable, which must appear only in periodic functions. We must imagine, therefore, that the external

potential is such that θ is small, in which case the expansion would be valid, and the periodicity requirements unimportant [15]). (See appendix 2).

We can find a formal expression which satisfies (11), but which leads back to the cranking formula. Instead, we wish to satisfy (11) approximately. To accomplish this we make two approximations. First, we assume that S is a single-particle operator, that is, in the language of field theory, we suppose that S may be written

$$S = \sum_{rs} S_{rs} a_r^\dagger a_s. \tag{13}$$

This approximation is based on the assumption that the important collective excitations can be described in terms of two single-particle states. It is fundamental to the present theory of superfluidity, where one assumes that the effect arises from the "binding" of pairs of particles. It neglects the possibility of "bound" complexes which must be described in terms of four particles at a time, for instance. The second approximation, which is not independent of the first, is to require only certain matrix elements of (11) to hold. Thus, we require

$$(rs|[S, H]|0) = (rs|iL_z|0), \tag{14}$$

where the state $|0)$ is construed to the quasi-particle vacuum, and $|rs)$ is any two quasi-particle state. If the value of S obtained from (13) and (14) is inserted into (12), exactly the same equation is obtained as has been previously found by the now standard methods developed in the theory of superconductivity. Thus, it is much better to use simple approximations to the states in determining S, than it is to use the same approximations directly in (4).

We wish to emphasize again that these approximations give the same results as the standard procedures in which products of operators, $\alpha_r \alpha_s$ for instance, are regarded as entities. Equations of motion are then obtained for these operator pairs. Some future generalizations suggest themselves immediately. We might, for instance, try to improve the description of the states, $|0)$ and $|rs)$. One improvement would be to incorporate the two particle correlations after the fashion of the Brueckner theory. It should be noted that doing this would not simply replace the potential v by the reaction matrix K everywhere. In particular, the potential operator in the Hamiltonian is not replaced by the reaction matrix. The importance of this will become evident below.

One might also note that this formulation is enough to ensure that the correct mass is obtained in the "pushing" model, since (11) is satisfied exactly by $S = z_{op}$ (when L_z is replaced by P_z). Also, we have so far made no assumptions concerning the size of the system. Thus, the equation should represent an improvement in the case of finite nuclei, even though the corrections to equation (10) which it predicts may be relatively small. This correction should be checked by numerical methods.

3. Solution of the Equations

We now proceed to the solution of eqs. (12) to (14). It is a trivial matter, in principle, to insert the expression (13) into (14) and perform the required contractions. Since the resulting equations have been obtained before [13,14]), and since only certain features of their structure are of interest to us here, we will not exhibit the calculation beyond making a few remarks. In order to present the result in a reasonably simple form, we have utilized largely the time reversal properties of the Hamiltonian, which can be written

$$\langle rs|v|s'r'\rangle = \langle -r'-s'|v|-s-r\rangle, \quad S_{rs} = S_{-s-r}, \quad (L_z)_{rs} = -(L_z)_{-s-r}. \tag{15}$$

It follows from (11) that S ought to be an even operator under time reversal, since L_z is odd. We have also pretended that the interaction matrix elements satisfy the selection rule

$$\langle r-r'|v|-ss\rangle = \delta_{rr'}\langle r-r|v|-ss\rangle, \tag{16}$$

for instance [10]). Eq. (16) is seldom satisfied in practice, but it leads to terms correcting the final equation which are of order $1/A$, where A is the total number of particles under consideration. These terms, although not negligible, as will be pointed out below, only complicate the expression unnecessarily. The relations (9) are also employed.

We first record the result in its standard form, generalized to an arbitrary potential. This is obtained by separating the Hamiltonian according to (8). Then, one finds

$$(\mathscr{T}+\mathscr{V})F = \mathscr{L}, \tag{17}$$

where

$$(\mathscr{T}F)_{rs} = (E_r+E_s)F_{rs}, \tag{17a}$$

$$(\mathscr{V}F)_{rs} = \sum_{r's'} \mathscr{V}_{rsr's'}F_{r's'}, \tag{17b}$$

$$\mathscr{V}_{rs,r's'} = \langle rs'|v|sr'\rangle[(U_rU_s+V_rV_s)(U_{r'}U_{s'}+V_{r'}V_{s'}) - (U_rV_s-U_sV_r)(U_{r'}V_{s'}-U_{s'}V_{r'})],$$

$$(\mathscr{L})_{rs} = (iL_z)_{rs}(U_rV_s-U_sV_r), \tag{17c}$$

and F is related to S by

$$F_{rs} = (U_rV_s+U_sV_r)S_{rs}. \tag{17d}$$

For the sake of symmetry we have multiplied through by the non-vanishing factor $U_rV_s+U_sV_r$ so that the expression for the moment becomes

$$\mathscr{I} = \sum_{rs} F_{rs}^*(iL_z)_{rs}(U_rV_s-U_sV_r). \tag{18}$$

Neglect of the integral term $\mathscr{V}$, which is equivalent to the neglect of the quasi-particle interaction H_1 in (8), leads at once to the Belyaev formula (10). We

have already argued that this is not correct in the infinite limit. In terms of the integral equation the incorrectness of the approximation can be seen as follows: The operator L_z (or almost any operator one is likely to consider in its place) is a very smooth one, that is to say, it can only induce transitions between single-particle states lying very close together. Hence, it can only cause a transition from one state into three or four states lying nearest to the original one, whereas, macroscopically, a very large number of states are practically indistinguishable from one another. Thus, we need to consider eq. (17) only for values of r, s extremely close together and, what is more, these values must lie in the neighbourhood of the "Fermi surface", otherwise the r.h.s. will vanish, and the equation will have vanishing solutions.

For such values of r, s, the replacement of the operator $\mathscr{T}+\mathscr{V}$ by $\mathscr{T}$ alone is wrong, because $\mathscr{T}$ is much too large. That is, $\mathscr{T}^{-1}\mathscr{L}$ is much too small and leads to a negligible moment of inertia. Since we know, on physical grounds, that the moment cannot be so small, it must be that, for the correct solution of the equation, $\mathscr{T}+\mathscr{V}$ is much smaller (by a factor $1/A^{\frac{1}{3}}$) than $\mathscr{T}$ alone; in other words, $\mathscr{T}$ and $\mathscr{V}$ must almost cancel. For this reason, the eq. (17) is very difficult to solve.

One might despair of solving (17) and, indeed, to prove that one has obtained the solution is extremely difficult. However, the problem is typical of much of the theory of superconductivity. One guesses at the solution of the equation on physical grounds, one then shows that the proposed solution has special features which make it mathematically plausible, and finally one hopes that the factors one has ignored do not change the essential features of the solution.

It is to be emphasized that these considerations do not apply in the finite case. In that case, we might very well expect that the quasi-particle interaction term can be treated by iteration. For, in a finite nucleus, the residual attractive forces are believed to be so weak that they barely "bind" particles in time-reversed paired states $(r, -r)$. The forces between particles in states not quite paired, $(r, -r')$ say, are considerably weaker, and probably do not succeed in binding the pair. Thus, for these states, it is probably legitimate to use perturbation theory, and hence to treat the quasi-particle interaction term $\mathscr{V}$ by iteration.

Returning to the infinite case, we wish to rewrite (14) in such a way that the full symmetry properties of the Hamiltonian can be utilized. To do this, we write the equation so that the parts coming from the kinetic energy and potential energy terms are explicitly separated. The result may be written

$$KS+PS=L, \tag{19}$$

where KS is the matrix element of $[T, S]$ and PS is the matrix element of $[v, S]$. The explicit forms of these operators are given by

$$(KS)_{rs}=(\varepsilon_r-\varepsilon_s)(V_s^2-V_r^2)S_{rs}, \tag{19a}$$

$$(PS)_{rs}$$

$$= (\Delta_r+\Delta_s)(U_sV_s+U_rV_r)S_{rs}+(\tilde{\varepsilon}_r-\varepsilon_r-\tilde{\varepsilon}_s+\varepsilon_s)(V_s^2-V_r^2)S_{rs} \tag{19b}$$

$$+\sum_{r's'}\langle rs'|v|sr'\rangle[(U_sV_s+U_rV_r)(U_{s'}V_{s'}+U_{r'}V_{r'})-(V_s^2-V_r^2)(V_{s'}^2-V_{r'}^2)]S_{r's'},$$

$$(L)_{rs} = (iL_z)_{rs}(V_s^2-V_r^2). \tag{19c}$$

The moment of inertia becomes

$$\mathscr{I} = \sum S_{rs}^*(iL_z)_{rs}(V_s^2-V_r^2) \equiv (L, S) = \sum S_{rs}^* L_{rs}. \tag{20}$$

Eq. (19) can of course be obtained directly from (17) by applying the identities (9) judiciously.

As we have already pointed out, after eq. (18), we need only consider the case in which the states r, s are very "close together". Then, the operator K will be a small one, whereas, in general, the operator P will be large, i.e. $(\Delta_r+\Delta_s)(U_rV_r+U_sV_s) \gg (\varepsilon_r-\varepsilon_s)(V_s^2-V_r^2)$. Only exceptionally will the integral terms in P manage to cancel the terms "$\Delta_r+\Delta_s$" exactly. If this cancellation is not nearly exact, then P will be much larger than K, by a factor $A^{\frac{1}{3}}$, and K could be neglected. This suggests that we expand the solution S, in terms of eigenvalues of P. (P is a hermitean operator in some Hilbert space, S is a vector in it.) Thus, we expand

$$S = \sum c_i\pi_i, \tag{21}$$

where the vectors π satisfy

$$P\pi_i = p_i\pi_i. \tag{22}$$

As a general rule, the eigenvalues p_i are large. It is convenient to write (19) in the representation defined by the π_i. We obtain

$$\sum_j K_{ij}c_j+p_ic_i = L_i \quad \text{(every } i\text{)}. \tag{23}$$

In general then, the numbers p_i will be much larger than the matrix elements K_{ij}, so that for these values of i we obtain

$$c_i \approx L_i/p_i$$

and the contribution of this part of S to the moment of inertia is

$$\approx \sum_i |L_i|^2/p_i, \quad (i \text{ with large } p_i),$$

which can be neglected. Furthermore, we can neglect these terms in the summation over j in (23). Thus, if we restrict ourselves to a subspace of the original Hilbert space, spanned by those π_k whose eigenvalues are small, we can determine the coefficients c_k independently of the exact value of the remaining coefficients. We have thus split the problem of the solution of (19) into two independent parts. One part of the solution is of little interest to us, since it does not contribute to the moment of inertia, even though we need it to satisfy (19). The other part contains all that is of interest to us.

We now turn our attention to the problem of separating the π's in the way which we have just indicated. We first note that any (single-particle) operator ϑ, which exactly commutes with the potential energy operator, will lead to a vector in the Hilbert space, with components

$$\vartheta_{\nu\mu} = \int d^3x \psi_\nu^*(x) (\vartheta_{op} \psi_\mu)(x) = \int d^3x \, d^3y \psi_\nu^*(x) \vartheta(x, y) \psi_\mu(y). \tag{24}$$

This vector will be an eigenvector of P with eigenvalue zero. It may be, because of the special restriction on the matrix elements indicated in (14), that there are additional classes of operators, not actually commuting with the potential, which have vanishing eigenvalues. It is also possible that there are operators, not commuting with the potential, which have small eigenvalues, not necessarily zero. Since we have no physical insight into what kind of operators to consider, and since the direct study of (19) has proved fruitless in this respect, we make the assumption that all the vectors π_k with small eigenvalues come from single-particle operators commuting with the potential.

If we suppose that the interaction potential is some function of the distance between the interacting particles, then the single-particle operators commuting with the potential are the total momentum operator, the total angular momentum operator, and any operator which is a function of the coordinates only.

The momentum operators are ruled out, because they have the wrong time inversion properties. Thus we restrict ourselves to a subspace of the Hilbert space generated by operator functions of the coordinates only (coordinate operators), that is, to operators ϑ whose kernel, as defined in (24), is diagonal, $\vartheta(x, y) = \vartheta(x)\delta(x-y)$. There are some tricky mathematical difficulties associated with this assumption since, for instance, no such operator is actually in the Hilbert space, but is represented by an unnormalizable vector. Making the assumption, for the present, we can proceed to solve the equations.

Before doing that, let us note that we have hardly used at all the detailed structure of (19b). We have only observed that, for a general operator S, the important matrix elements of the commutator $[v, S]$ are much larger * than the matrix elements of the commutator $[T, S]$. It might be expected that this property will be preserved in future improvements of the theory, since it gives a gauge invariant Meissner effect, for instance. Thus the theory of superfluidity seems to provide an "energy gap" against all those excitations not generated by a canonical transformation which is a function of the coordinates only. Once we admit that the effect of the interaction is to inhibit the formation of excitations not of this type, the irrotational flow moment of inertia follows in the well-known way. We emphasize that we have not assumed irrotational flow from the start, but have been led to it on the basis of the microscopic theory of superfluidity.

* Note that this is not the case if the interaction leads to a "normal" state. The matrix elements of $[v, S]$ between "normal" states are *not* much larger than those of $[T, S]$.

From the point of view of the canonical transformation, we have been led to consider the wave function

$$\psi'(x_1 \ldots x_A) = \mathrm{e}^{iM\omega \sum_{i=1}^{A} \vartheta(x_i)} \psi(x_1 \ldots x_A),$$

where we have reverted to the Schroedinger notation, and also introduced an explicit factor M for dimensional convenience. One finds for the current at the point x,

$$j(x) = \rho(x)\nabla\omega\vartheta(x),$$

where $\rho(x)$ is the mass density of particles at the point in question. Thus $\omega\vartheta(x)$ is a velocity potential, and the velocity field obtained from it is necessarily irrotational, since we must assume $\vartheta(x)$ to be single-valued. For the sake of completeness, we shall explicitly verify that the irrotational current is obtained. We have to solve then the matrix equation

$$\sum_i K_{ij} c_j = L_i \tag{25}$$

(ϑ_i, ϑ_j are coordinate operators). We can cast this into the form of a variational principle by demanding that

$$\mathscr{I} = 2(L, \vartheta) - (\vartheta, K\vartheta) = \left(L \frac{1}{K} L\right) - \left(L - K\vartheta, \frac{1}{K}(L - K\vartheta)\right) \tag{26}$$

be stationary with respect to variations of ϑ among the operator functions of the coordinates. Writing out (26) in detail, we find

$$-2M \sum_r V_r^2 [\sum_s (iL_z)_{rs}\vartheta_{sr} - \vartheta_{rs}(iL_z)_{sr} + M\vartheta_{rs}(\varepsilon_r - \varepsilon_s)\vartheta_{sr}]. \tag{27}$$

Inserting the matrix elements explicitly, eq. (24), and using the completeness of the sums on s, we obtain

$$\mathscr{I} = 2 \sum_r V_r^2 M \tfrac{1}{2} \int \psi_r^* \left[\vartheta(\mathbf{x})(-\nabla^2\vartheta(\mathbf{x}) - 2\nabla\vartheta(\mathbf{x})\nabla) - \left(x\frac{\partial}{\partial y} - y\frac{\partial}{\partial x}\right)\vartheta(\mathbf{x})\right] \psi_r \mathrm{d}^3x. \tag{28}$$

An integration by parts, and identification of the mass density

$$\rho(\mathbf{x}) = M \sum_r V_r^2 |\psi_r(\mathbf{x})|^2,$$

lead to

$$\mathscr{I} = -2 \int \rho(\mathbf{x}) \left[\left(x\frac{\partial}{\partial y} - y\frac{\partial}{\partial x}\right)\vartheta(\mathbf{x}) + \tfrac{1}{2}(\nabla\vartheta)^2\right] \mathrm{d}^3x. \tag{29}$$

Variation of this expression with respect to ϑ yields the condition

$$\nabla \cdot \rho(\mathbf{x})\nabla\vartheta(\mathbf{x}) + \left(x\frac{\partial}{\partial y} - y\frac{\partial}{\partial x}\right)\rho(\mathbf{x}) = 0, \tag{30}$$

which is the continuity equation, the second term being the total time derivative of the density in the rotating system of coordinates.

We still need to make a few remarks for mathematical completeness. In order to obtain a mathematically rigorous solution to (14), we need to know the spectrum of the operator P. In keeping only the coordinate operators, we have, in the preceding arguments, pretended that the eigenvalue, $p_i=0$, is discrete and that all other eigenvalues are large. The fact that the eigenvectors, ϑ_i, are not normalizable leads one to believe that this is not the case, but that there is a continuum of eigenvalues in the neighbourhood of zero. However, the coordinate operators may still be shown to be a solution of the equation, provided the continuous spectrum of eigenvalues comes to zero steeply enough. To be more precise, let λ be the eigenvalue with eigenvector $\pi(\lambda)$, and let $L(\lambda)$ be the inner product $(\pi(\lambda), L)$. Then, if $L(\lambda)$ is practically constant for finite values of λ, less than $A^{\frac{1}{3}}$, say, it can be shown that only the coordinate operators contribute to the moment of inertia. This is probably the case, since it can be made plausible that $L(\lambda)$ is an ordinary function of $\lambda/A^{\frac{1}{3}}$.

One may also observe that the periodic boundary condition seems to be an exceptional case, since L_z does not couple to an irrotational current. For periodic boundary conditions, the only irrotational currents are those flowing in one side of the box, and out the other. The physical meaning of periodic boundary conditions is obscure in this case, but it is surprising that these conditions should be exceptional.

The author takes great pleasure in thanking Professor Niels Bohr for the hospitality extended to him at the Institute for Theoretical Physics. Stimulating discussions with A. Bohr, B. Mottelson, S. Kahana, B. Bayman, R. Amado, and many others are gratefully acknowledged.

Appendix

A.1. THE CRANKING MODEL

In this appendix we discuss the cranking model. For systems actually confined to an external box, the cranking formulation is clearly good, except that perturbation theory might not be adequate to reach rotational frequencies of experimental interest. One need not rely upon the primitive estimate demanding the level shifts to be small in comparison with their spacing, however. One needs only that the expansion of $H' = \exp(-iwS)H \exp(iwS)$ terminate after the ω^2 term. If the solution proposed in the body of the paper is correct, this will be true almost exactly, thus indicating that the cranking prediction may be valid at relatively high frequencies.

In the case of finite nuclei, the procedure is more delicate, because good approximations to the wave functions are not readily available. One can set up

variational principles for the wave function [16]) by demanding that

$$(\Psi_0, \mathrm{e}^{-iS\omega}[H-\omega L_z-E]\mathrm{e}^{iS\omega}\Psi_0)$$

be stationary. If we choose Ψ_0 to be an approximate wave function, and choose the best single-particle operator for S, we obtain the conditions

$$\begin{aligned}&(\Psi_0, [a_r^\dagger a_s, i[H, S]-L_z]\Psi_0) = 0 \qquad (\text{all } r, s),\\ &\left(\Psi_0 \frac{1}{i}[L_z, S]\Psi_0\right)=\mathscr{I},\end{aligned} \tag{A.1}$$

defining S. These are identical with (14) if Ψ_0 is chosen to be the BCS wave function in an external potential.

Some insight may perhaps be gained if we realize that the wave function usually chosen by means of a model Hamiltonian with a distorted external potential is not meant to be an approximation to the actual eigenfunction of the exact Hamiltonian. Rather it is supposed to be a useful linear combination of exact eigenfunctions. Restricting ourselves to a two-dimensional case for simplicity, we have the expansion, for the model wave function,

$$\Psi_0 = \sum_{m,i} a_{m,i}\Psi_{m,i}.$$

Here, m labels the angular momentum, and i the rotational band. The ideal is to choose the wave function Ψ_0 in such a way that only one rotational band, $i = 0$, appears. If this could be done, the projection procedure advocated by Peierls and Yoccoz [17]) would be exact, since the exact wave functions would be obtained. Unfortunately, significant amounts of higher rotational bands are probably mixed in, so the simple projection technique is not satisfactory. It breaks down because, by comparing the energies of the projected states, one finds

$$E_0^m - E_0^0 = \frac{\sum_i \varepsilon_{m,i}|a_{m\ i}|^2}{\sum_j |a_{m,i}|^2} - \frac{\sum_i \varepsilon_{0,i}|a_{0,i}|^2}{\sum_j |a_{0,j}|^2}.$$

This difference is not equal to $m^2/2\mathscr{I}$, even if the exact eigenvalues have the form $\varepsilon_{m,i} = m^2/2\mathscr{I}+\varepsilon_{0,i}$, since the coefficients $a_{m,i}$ can be expected to vary with m. If, given Ψ_0, one could construct Ψ_k according to

$$\Psi_k = \sum_{m,i} a_{m,i}\Psi_{m+k,i}$$

with the same coefficients $a_{m,i}$ it would be possible to improve greatly the computation of the moment of inertia. Then, one could compare the energies

$$E_m^m - E_0^0 = (\sum_i \varepsilon_{m,i}|a_{0,i}|^2 - \sum_i \varepsilon_{0,i}|a_{0,i}|^2)/\sum_j |a_{0,j}|^2,$$

which no longer depends on m through the coefficients. Moreover, one does not

even need the projection, as long as the spectrum has the rotational form and the admixture of higher bands is not too large.

The construction of Ψ_k, given Ψ_0, would be easy, if we had a canonical transformation exp iwS available which sent $\Psi_{m,i}$ into $\Psi_{m+k,i}$. This requires a series of conditions on the commutator of the form

$$(\Psi_{m,i}, [S, [H, S]-iL_z]|\Psi_{m,i}) = 0.$$

Instead of these conditions, we can demand only the average condition

$$(\Psi_0, [S, [H, S]-iL_z]\Psi_0) = 0,$$

which leads to (14). The point we wish to make here is that, in these formulations, the commutator with the true Hamiltonian appears, and not the commutator with the model Hamiltonian [15]). Thus velocity dependences, effective masses, etc., appear only through the wave functions, and not through the Hamiltonian.

A.2. CONDITIONS FOR THE EXPANSION OF U

In this appendix we discuss the conditions under which an expansion of $U = \exp i\omega S$ may be useful. The motivation for this discussion is that S is usually regarded as an angular variable which should appear only in periodic functions. If S is not a proper operator, many of the steps taken in the body of this paper must be viewed with suspicion. We shall show here that S is, under rather general conditions, a proper operator, at least for those cases in which the system is enclosed in an external potential. Unfortunately, in order to discuss the matter properly, we must resort to the formal mathematics at the foundations of quantum mechanics [18]).

Let us first note that for any hermitean operator S, the operator U is defined *everywhere* on the Hilbert space of wave functions. This is in contrast to the domain $\mathscr{D}$ of the Hamiltonian H, which in general is *not* the whole space, but only some dense subset of the space. For example, if the Hilbert space is that of all functions square integrable over a cube, the domain $\mathscr{D}$ may be all functions periodic over this region, or all functions vanishing at the boundary.

The unitary transformation U will only be useful, in general, if it preserves the domain of H, that is, if the domain of $U^{-1}HU$ is also the domain of H. For arbitrary ω, this will be true only if S also has this property. In fact, the commutator $[H, S]$ will not be defined unless $S\mathscr{D} \subset \mathscr{D}$. Of course, the domain of S must include $\mathscr{D}$.

We then wish to consider the operator $H-\omega L_z$. We suppose that H has discrete eigenvalues E_N and that the eigenfunctions of H are in the domain of $H-L_z$. Actually, we can restrict our considerations to the ground state of H. We are also only interested in the effect of S on the ground state of H. What we can prove is: if (1) L_z is defined on the ground state of H, and (2) L_z has vanishing matrix elements connecting the ground state with any state of the same

energy, an S exists which preserves the domain of H, and whose commutator with H is L_z, when acting on the ground state. We really only need to consider S as it acts on the ground state, and can define its action on other states as convenience dictates.

The proof is trivial. Under the stated conditions, we can formally construct the operator S to be

$$S = \sum_N \frac{|N\rangle\langle N|L_z|0\rangle\langle 0|}{E_N - E_0} + \text{h.c.},$$

where $|N\rangle$ are the states of H, with $|0\rangle$ the ground state. We may choose the energy of this state to be zero. We must now verify that $S|0\rangle$ exists, and also that $HS|0\rangle$ exists. We exhibit only the latter. The condition for this may be written

$$\sum_N \langle 0|L_z|N\rangle \frac{E_N^2}{(E_N - E_0)^2} \langle N|L_z|0\rangle < \infty.$$

But this is satisfied, since this condition is also the condition that L_z is defined on the ground state.

It is apparent that the conditions of the theorem are almost always satisfied when we are dealing with an external potential. For if L_z had a non-vanishing ground state expectation, the energy shift would depend on the direction of rotation.

References

1) A. Bohr and B. R. Mottelson, Kongel. Norske Vid. Selsk. Forh. **31** (1958) 12;
B. R. Mottelson, Cours de l'école d'été de physique théorique des Houches (Dunod, Paris 1959) p. **383**;
H. J. Lipkin and S. Goldstein, Nuclear Physics **5** (1958) 202;
H. J. Lipkin and S. Goldstein, Nuclear Physics **7** (1958) 184;
R. F. Nataf, Nuclear Physics **2** (1957) 497;
S. Hayakawa and T. Marumori, Progr. Theoret. Phys. **17** (1957) 43;
F. Villars, Nuclear Physics **3** (1957) 240;
Marumori, Suekane and Yamamoto, Progr. Theoret. Phys. **16** (1956) 320;
A. S. Davydov and G. F. Filipov, Physica **22** (1956) 1167;
T. Tamura, Nuovo Cim. **4** (1956) 713;
T. Miyazima and T. Tamura, Progr. Theoret. Phys. **15** (1956) 255;
T. Marumori, Progr. Theor. Phys. **14** (1955) 608;
T. Marumori and E. Yamada, Progr. Theoret. Phys. **13** (1956) 557;
Marumori, Yakawa and Tanaka, Progr. Theoret. Phys. **13** (1956) 442
R. Nataf, Compt. Rend. **240** (1954) 2510; **241** (1955) 31;
F. Coester, Phys. Rev. **99** (1955) 170;
S. Tomonaga, Prog. Theoret. Phys. **13** (1955) 467;
H. A. Tolhoek, Physica **21** (1955) 1;
G. Suessman, Z. Physik, **139** (1954) 543;
A. Bohr, Rotational states in atomic nuclei (Ejnar Munksgaard, Copenhagen 1954);
A. Bohr and B. R. Mottelson, Mat. Fys. Medd. Dan. Vid. Selsk. **30**, No. 1 (1955);
D. R. Inglis, Phys. Rev. **96** (1954) 1059

2) Bardeen, Cooper and Schrieffer, Phys. Rev. **108** (1957) 1175
3) N. N. Bogoliubov, Doklady Akad. SSSR **119** (1958) 244 (Trans.: Sovjet Phys. Doklady **3** (1958) 292; see
Bogoliubov, Tomachov and Shirkov, A new method in the theory of superconductivity (Consultants Bureau, New York 1959)
4) R. Amado and K. A. Brueckner, Phys. Rev. **115** (1959) 778
5) R. Rockmore, Phys. Rev. **116** (1959) 469
6) C. S. Lin, Report at the International Congress on many-particle problems, Utrecht, June 1960
7) L. D. Landau, J. Phys. (USSR) **5** (1941) 71
8) F. London, Superfluids (Wiley, New York 1950) Vol. I, p. 78
9) Brueckner, Soda, Anderson and Morel, Phys. Rev. **118** (1960) 1442;
V. S. Emery and A. M. Sessler, Phys. Rev. **119** (1960) 43
10) S. T. Belyaev, Mat. Fys. Medd. Dan. Vid. Selsk. **31**, No. 11 (1959)
11) A. B. Migdal, Nuclear Physics **13** (1959) 655
12) J. J. Griffin and M. Rich, Phys. Rev. **118** (1960) 850;
S. G. Nilsson and O. Prior, Mat. Fys. Medd. Dan. Vid. Selsk. **32**, no. **16** (1960)
13) P. W. Anderson, Phys. Rev. **112** (1958) 1900;
G. Rickhayzen, Phys. Rev. **115** (1959) 795;
J. M. Blatt and T. Matsubara, Prog. Theoret. Phys. (Kyoto) **20** (1958) 781;
K. Yosida, Prog. Theoret. Phys. (Kyoto) **21** (1959) 745;
Y. Nambu, Phys. Rev. **117** (1960) 648;
K. Sawada, Phys. Rev. **106** (1957) 372;
G. Wentzel, Phys. Rev. **108** (1957) 1593;
14) R. M. Rockmore, Phys. Rev. **118** (1960) 1645
15) Lipkin, De Shalit and Talmi, Phys. Rev. **103** (1956) 1773;
M. Jean and J. Touchard, Compt. Rend. **245** (1957) 1001;
A. Bohr and B. R. Mottelson, Kongel. Norske Vid. Selsk. Forh. **31** (1958) 12
16) E. P. Gross, Nuclear Physics **14** (1959) 389;
D. S. Thouless, Nuclear Physics **21** (1960) 225
17) E. L. Hill and J. A. Wheeler, Phys. Rev. **89** (1953) 1102;
F. Coester, Nuovo Cim. **4** (1956) 1307;
R. E. Peierls and J. Yoccoz, Proc. Phys. Soc. A **70** (1957) 381;
T. H. R. Skyrme, Proc. Roy. Soc. A **239** (1957) 399;
J. Yoccoz, Proc. Phys. Soc. A **70** (1957) 398;
T. H. R. Skyrme, Proc. Phys. Soc. A **70** (1957) 433
18) J. von Neumann, Mathematical foundations of quantum mechanics (Dover, New York 1945)

1.E.2

Nuclear Physics **22** (1961) 301—305; ©*North-Holland Publishing Co., Amsterdam*

Not to be reproduced by photoprint or microfilm without written permission from the publisher

CORRECTIONS TO NUCLEAR *Q* VALUES RESULTING FROM ATOMIC BINDING AND EXCITATION

ROBERT F. CHRISTY

W. K. Kellogg Radiation Laboratory, California Institute of Technology, Pasadena, California †

Received 26 September 1960

Abstract: Corrections to the measured energies of nuclear reactions associated with the binding and excitation of atomic electrons are calculated.

1. Introduction

Nuclear Q values, and hence atomic masses, are commonly measured under conditions of resolution such that the losses of energy associated with atomic excitation are unresolved. It then becomes necessary to estimate these excitations and correct the Q measurement accordingly. In addition we may ask how we should correct for atomic binding effects in order to arrive at a Q value, defined as the difference in the energies of the atoms in their lowest states. We may distinguish three distinct effects to examine: the first is associated with the recoil of the nucleus in the reaction; the second involves the change of nuclear charge (if any) as it affects atomic binding and excitation; the third involves the excitation effects associated with the passage of charged particles through the electron shells. The first, "Nuclear Recoil" would be present even for reactions involving neutrons and nuclei. The last would be present even if no change in nuclear charge occurred as in the scattering of charged particles by nuclei. In what follows, these corrections will be estimated with the object of retaining corrections that may amount to even a hundred volts but not attempting to calculate 10 eV corrections.

2. The Nuclear Recoil

We think here of a reaction involving neutral bombarding and final particles and a target atom initially at rest. The energy and direction of the incident beam is known and the energy and direction of the emergent particles are being measured. From this information the Q value is to be calculated. In fact, if the reaction particles could be observed with high resolution and in the absence of Doppler broadening, a number of reaction energies would be observed corre-

† Work supported in part by the joint program of the Office of Naval Research and the U. S. Atomic Energy Commission.

sponding to different possible final atomic states. We suppose here that the actual resolution is insufficient to resolve these so that the observed mean Q corresponds to an average over final atomic energies. Clearly what we observe is Q plus the mean excitation energy of the atom, which must then be corrected for; at the same time we must calculate correctly the recoil energy of the (excited) atom.

We can calculate the expectation value of H (the energy) at any time since it is independent of time; this is simplest immediately after the reaction, which we suppose to take place in a time short compared to atomic periods, when we still know the atomic wave function; alternately we can resolve into stationary atomic states and then average the energy. In the first case, if the final nuclear mass is M_F, we note that giving the nucleus a recoil velocity $\mathbf{v}_R$ corresponds to multiplying its wave function by exp $(iM_F\mathbf{v}_R \cdot \mathbf{r}/\hbar)$. The appropriate part of the H operator is $\frac{1}{2}p_F^2/M$. If the initial nuclear velocity (thermal or otherwise) is randomly directed, the expectation value of the change in energy associated with recoil is $\frac{1}{2}M_F v_R^2$. Alternatively, if we calculate the energy by resolving into atomic states we find a kinetic energy of $\frac{1}{2}M_F^2 v_R^2/M_{atom}$ since the recoil momentum $M_F v_R$ is now shared by the atom, in addition, in the system of coordinates in which the atom is moving, the electrons find themselves with an initial velocity v_R opposed to the recoil. If we calculate the expectation value of $\frac{1}{2}p^2/m$ summed over all electrons for a state which is the ground state times exp $(i\sum_i m\mathbf{v}_R \cdot \mathbf{r}_i/\hbar)$ we get $\sum_i \frac{1}{2}mv_R^2$. If we now add this to the kinetic recoil energy of the atom we get just $\frac{1}{2}M_F v_R^2$ as before. The conclusion is that if a nuclear reaction imparts a momentum p to the atomic nucleus of mass M_F, the total energy imparted (kinetic and excitation) is on the average just $\frac{1}{2}p^2/M_F$.

3. The "Monopole" Charge Effects

Serber and Snyder [1]) have discussed the energy left in the atomic excitation associated with the change $(Z_F - Z_I)$ of the nuclear charge. If we assume the collision is fast compared to atomic periods, the change in energy of the electron system is just $e(Z_F - Z_I)\phi(Z_I)$, where $e\phi(Z_I) \approx -36.7\ Z_I^{\frac{4}{3}}$ eV is the potential at the nucleus due to the initial electron cloud. However, the ground state binding energy of the electrons, $E(Z) \approx -15.7\ Z^{\frac{7}{3}}$ eV also changes during the collision and this is included in the atomic mass which is used in the definition of Q. The excitation energy remaining is just the difference of the above values, i.e.

$$\Delta E \approx 24.5(Z_F - Z_I)^2 Z_I^{\frac{4}{3}} \text{ eV}$$

for a Thomas Fermi atom.

Actually, such corrections become significant only for Z large or E small, in which circumstance the electrical interaction with the atomic electrons is fast for the outer electrons but adiabatic with respect to the inner electrons, provid-

ed we are dealing with heavy particle interactions. We can approximately evaluate the atomic excitation by considering the excitation of the atom associated with the passage of the charged particles through those outside regions of the atom where they are faster than the atomic electrons. We have determined this region by the relation

$$\tfrac{1}{2}mv_1^2 = -e\phi(r),$$

where v_1 is the velocity of the particle, m the electron mass, and $\phi(r)$ is the potential in the atom at r which is determined to satisfy this equation. The required excitation energy is just the second order correction to the atomic energy due to the presence of a charge Z_1 at r. This was evaluated by a perturbation procedure on the Thomas-Fermi atom.

For the passage of a single charged particle of mass M_1, energy E_1, charge Z_1, through the atom we calculate an excitation energy

$$\Delta E = 34 \frac{Z_1^2}{Z_1^{\frac{1}{3}}} \left(\frac{E_1(\text{MeV})}{A_1}\right)^{\frac{1}{2}} \text{eV},$$

provided it is less than that given by the Serber-Snyder formula $\Delta E \approx 24.5\ Z_1^2 Z_1^{\frac{1}{3}}$ eV.

4. The "Dipole" Charge Effects

In addition to the excitation energy above, calculated as though the particles penetrated the atom as spherical waves, we have higher multipole effects since the bombarding and emerging particles are actually able to transfer momentum as well. The "dipole" part (i.e. that which corresponds to an average momentum transfer) of this effect is readily calculated. This energy loss problem is unique in that the particles causing it do not have the usual distribution of impact parameters but are, essentially, directed at the nucleus and execute straight line paths to and away from the nucleus. The (vector) momentum imparted to each atomic electron on the entry of the bombarding particle into the nucleus is just given by the change in momentum of the bombarding particle as it enters the corresponding electron shell with potential $e\phi_i(Z_1)$. This change is just an energy change of $eZ_1\phi_i(Z_1)$ and a momentum change of $eZ_1\phi_i(Z_1)/v_1$ directed opposite to v_1 the velocity of the bombarding particle of (positive) charge Z_1. This momentum transfer must be added vectorially to the momentum transfer associated with the emerging particle with v_2 and Z_2 and directed parallel to v_2. The appropriate energy transfer to each electron with momentum transfer Δp_i calculated above will depend on whether Δp_i occurs fast or slow compared to the electron period. We must include only those passages for which the v_1 or v_2 is larger than v_{electron}. The total energy transfer to the atomic electrons is then $\sum_i \frac{1}{2}(\Delta p_i)^2/m$ summed over those electrons satisfying the above condition.

An additional effect is that the bombarding particle gains momentum (and energy) from the interaction with the electrons. As a result, the recoil energy of the nucleus will be augmented. This can be computed by augmenting the energy E_1 of the bombarding particle by $-eZ_1\phi_i(Z)$ summed over all electrons for which the passage of particle 1 is fast compared to $v_{\text{electron}} \approx (2\,\text{Ionization Potential}/m)^{\frac{1}{2}}$ and augmenting the energy E_2 of the final particle by $-eZ_2\phi_i(Z)$ summed again over the appropriate electrons. These corrected energies $E_1-eZ_1\sum_i'\phi_i(Z_1)$ and $E_2-eZ_2\sum_i'\phi_i(Z_F)$ should then be used in the recoil energy calculation.

A calculation of $\sum'_i \frac{1}{2}(\Delta p_i)^2/m$ summed over only the appropriate electrons, determined as given above for the Thomas-Fermi atom gives an expression for the excitation energy ΔE associated with this effect when a particle of velocity v_1 and charge Z_1 enters a nucleus of charge Z_1:

$$\Delta E \approx 5.4\, Z_1^{\frac{2}{3}} Z_1^{\frac{1}{3}}\ \text{eV},$$

which may be comparable with the monopole excitation energy.

5. Corrections for Electrons Bound to Bombarding or Emergent Particles

Until now we have assumed that these particles 1 and 2 were bare nuclei and have presumed that the appropriate nuclear (not atomic) mass would be used in the calculations of recoil etc. In fact, these particles, particularly α-particles, may have bound electrons as they enter and leave the target. In the stripping of a bound electron, the nuclear velocity is preserved except for the electric interaction between the nucleus and the electron which will diminish the nuclear energy by $-eZ_1\phi(Z_1)$ the electrostatic potential energy of the original nucleus and electron. Thus, the nuclear energy in the reaction will be $\frac{1}{2}M_1v_1^2+eZ_1\phi(Z_1)$, where M_1 is the nuclear mass and v_1 the original velocity. Conversely if the emergent particle picks up an electron before it is observed with velocity v_2 the nuclear energy as it emerges from the reaction would be $\frac{1}{2}M_2v_2^2+eZ_2\phi(Z_2)$, where M_2 is the final nuclear mass and v_2 the velocity as observed with the bound electron(s) which contribute the potential $\phi(Z_2)$.

6. Conclusion

The effects discussed above result in the following (non-relativistic) expression for the energy balance in the reaction

$$\tfrac{1}{2}M_1v_1^2+Q_a = \tfrac{1}{2}M_2v_2^2+\Delta E_{\text{monopole}}+\Delta E_{\text{recoil}},$$

where $\Delta E_{\text{monopole}}$ includes effects in the (light) bombarding particles calculated on the Serber-Snyder formula as well as effects on the (heavy) target and residual atoms. ΔE_{recoil} includes the dipole charge effects and the nuclear recoil effect as discussed above.

The principal effect of the above calculations is to show that all these corrections are negligible at the present level of precision in nuclear reaction measurements. However, if effects of the order of 100 eV or less become relevant they can be estimated by the means discussed above.

Reference

1) R. Serber and H. Snyder, Phys. Rev. **87** (1952) 152

3.A; 3.B

Nuclear Physics **22** (1961) 306—315; © *North-Holland Publishing Co., Amsterdam*

Not to be reproduced by photoprint or microfilm without written permission from the publisher

ANGULAR DISTRIBUTIONS OF PHOTOELECTRONS EJECTED FROM URANIUM BY 1.118 MeV GAMMA RAYS

SÖLVE HULTBERG †, TOM O'CONNOR and JOSEPH H. HAMILTON

Physics Department, Vanderbilt University, Nashville, Tennessee ††

Received 12 September 1960

Abstract: At a gamma-ray energy of 1118 keV, we have studied longitudinal angular distributions of photoelectrons ejected from the K-, L-, and M+N+ . . .-shells of uranium. The application of these angular functions to the calculation of the photoelectric correction factor f is discussed. It is important to obtain f at an energy such as 1.118 MeV to increase the accuracy, around 1 MeV, in the curve of f versus energy. A smooth-curve relationship, in a log-log diagram, has been found between the gamma-ray energy $h\nu$ and the angle θ_m of maximum photoelectric cross-section. It is pointed out that the Swedish computer BESK now undertakes calculations of f at four gamma-ray energies: 412, 662, 1118 and 1332 keV (assuming rectangular symmetry and taking source size into account). This new calculation increases the accuracy of f values such that the overall accuracy in f between 400 and 1400 keV is now considered to be of the order of 1 %.

1. Introduction

An extended knowledge of photoelectric angular distributions has proved to be of particular importance for the determination of absolute values of internal conversion coefficients according to the internal-external conversion method of Hultberg and Stockendal [1]). Investigations of such angular functions is also of interest from a theoretical point of view since in this way detailed information is obtained about the nature of the photoeffect. For instance, it is important to establish as accurately as possible the ratio τ_a/τ_K between the integrated photoelectric cross-section of the whole atom (τ_a) and that of the K-shell (τ_K) [1]). This ratio makes possible an accurate comparison of the theoretical τ_K and the τ_K as derived from absorption measurements which give τ_a as the primary information.

In the deduction of gamma-ray intensities from an analysis of photolines the so-called photoelectric correction factor f has been introduced [1]). A study of the behavior of f as a function of energy reveals that, in many cases, f will go through a maximum at an energy in the neighborhood of 1 MeV. To increase the accuracy of the interpolation around 1 MeV of the curve of f versus energy we studied the photoelectric angular distributions of the uranium K-, L-, and

† On leave from the Nobel Institute of Physics, Stockholm, Sweden.

†† Work supported in part by a grant from the National Science Foundation.

M+N+ . . .-shells at a gamma-ray energy of 1.118 MeV. The gamma-rays were obtained from the decay of Sc^{46}.

2. Experimental Arrangements and Results

This work was carried out with the Vanderbilt iron-free, double-focusing spectrometer [3]). A side window, continuous flow, G. M. counter was used as the detector. Special lead shielding was used to minimize the background in the counter from direct radiation.

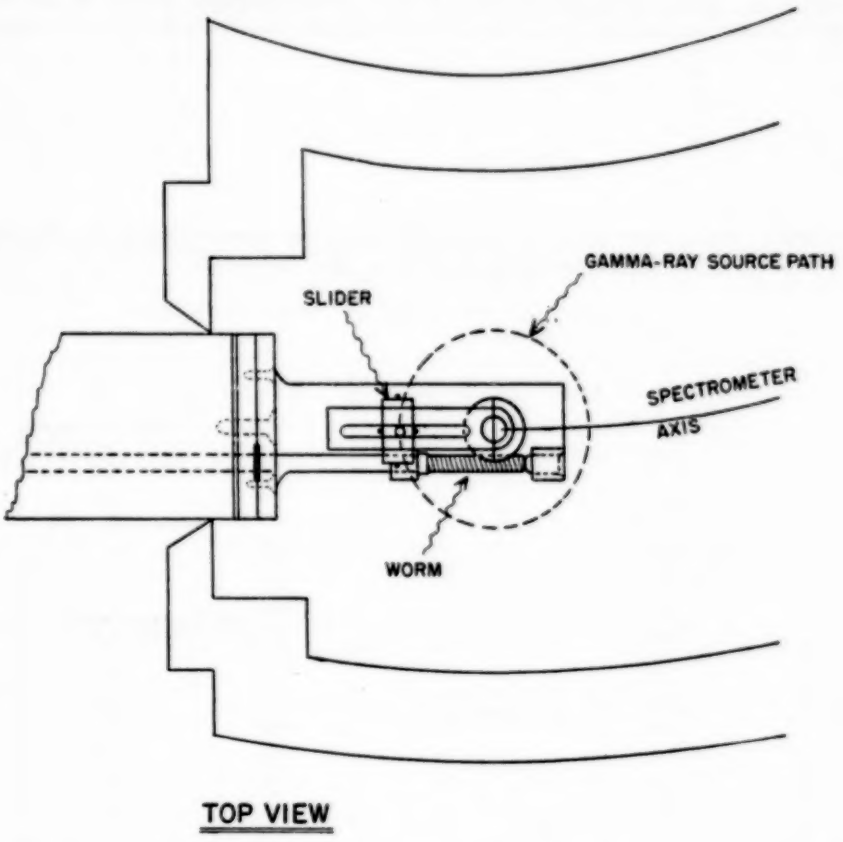

Fig. 1. Experimental arrangement inside iron-free double-focusing spectrometer for the study of photoelectric angular distributions. By turning a dial outside the spectrometer, the gamma-ray source can be rotated around the converter.

The experimental arrangement used with the spectrometer is shown in figs. 1 and 2.

The gamma-ray source consisted of 25 mg of Sc_2O_3, packed into a 2×2 mm cylindrical cavity of an aluminium container and irradiated for two days with a neutron flux of 2×10^{14} neutrons cm^{-2} sec^{-1} at Oak Ridge National Laboratory. The source activity was about 230 mc. The distance a between the source and the converter was 25 mm. By means of a dial (see fig. 2) outside the spectro-

meter, the source could be rotated around the converter which remained fixed. The position of the gamma-ray source with respect to the converter is defined by the angle θ, according to the schematic diagram of fig. 3.

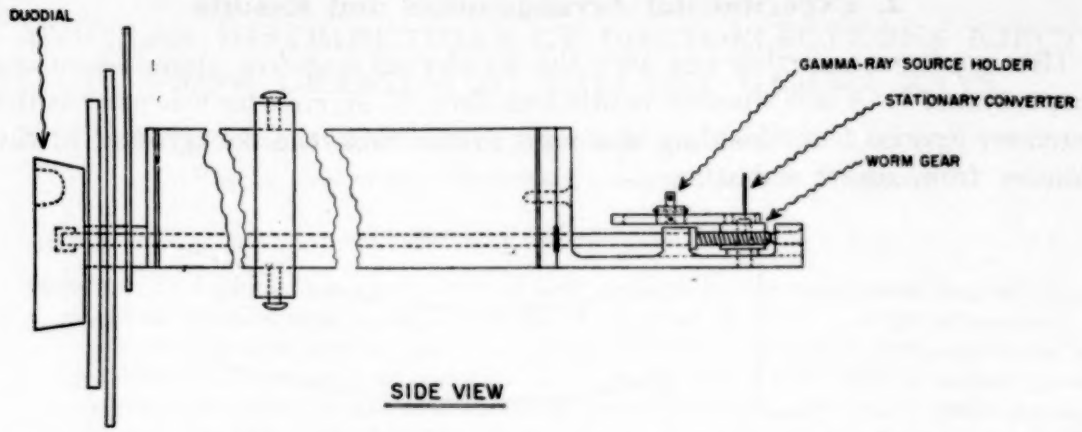

Fig. 2. Side view of source rod which is removable from the spectrometer. The Duodial, source converter and worm gear are indicated.

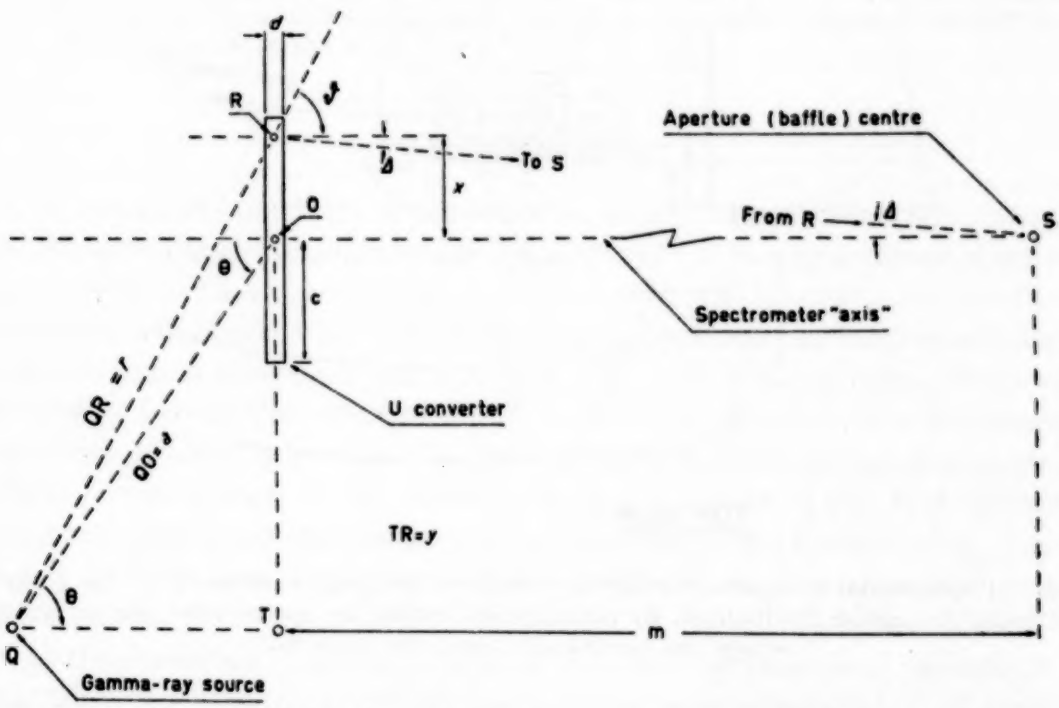

Fig. 3. Schematic diagram, defining the position of the gamma-ray source with respect to the normal through the centre of the converter. The normal is defined as $\theta = 0$.

The gear arrangement shown in fig. 1 was such that θ changed by 360° when the dial was rotated through exactly 40 turns, each of which thus corresponded to a variation in θ of 9°. The circumference of the dial had 100 subdivisions so that θ could easily be set with an accuracy of 0.09° which is far

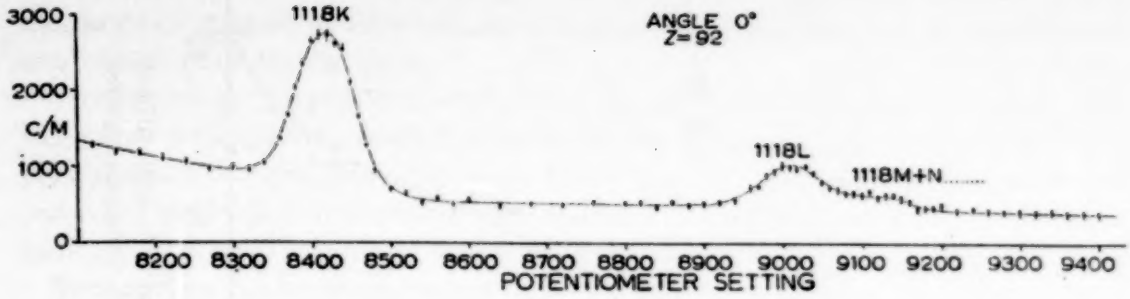

Fig. 4. Photoline spectrum, as recorded at $\theta = 0$. The gamma-ray energy is $h\nu = 1118$ keV. A circular uranium converter was used (diameter 14.0 mm). Resolution about 1 %.

TABLE 1

Numerical values of the photoelectric angular functions, per unit solid angle, of photoelectrons ejected from the uranium K-, L-, and M+N+ . . .-shells at $h\nu = 1118$ keV. Uncorrected experimental functions J_e are given (cf. Discussion)

$\theta°$	K-shell	L-shell	M+N+ . . .-shell
0	740	181	62
3	738	181	62
6	735	178	61
9	720	173	61
12	700	164	60
15	665	154	58
18	620	140	56
21	570	125	53
24	515	110	48
27	460	95	42
30	405	82	36
33	345	70	30
36	290	59	23
39	240	49	18
42	205	39	13
45	170	32	10
48	140	25	7
51	120	20	5
55	95	15	3
60	68	9	1
65	50	5	0
70	35	1	
75	22	0	
80	14		
85	6		
90	2		
100	0		

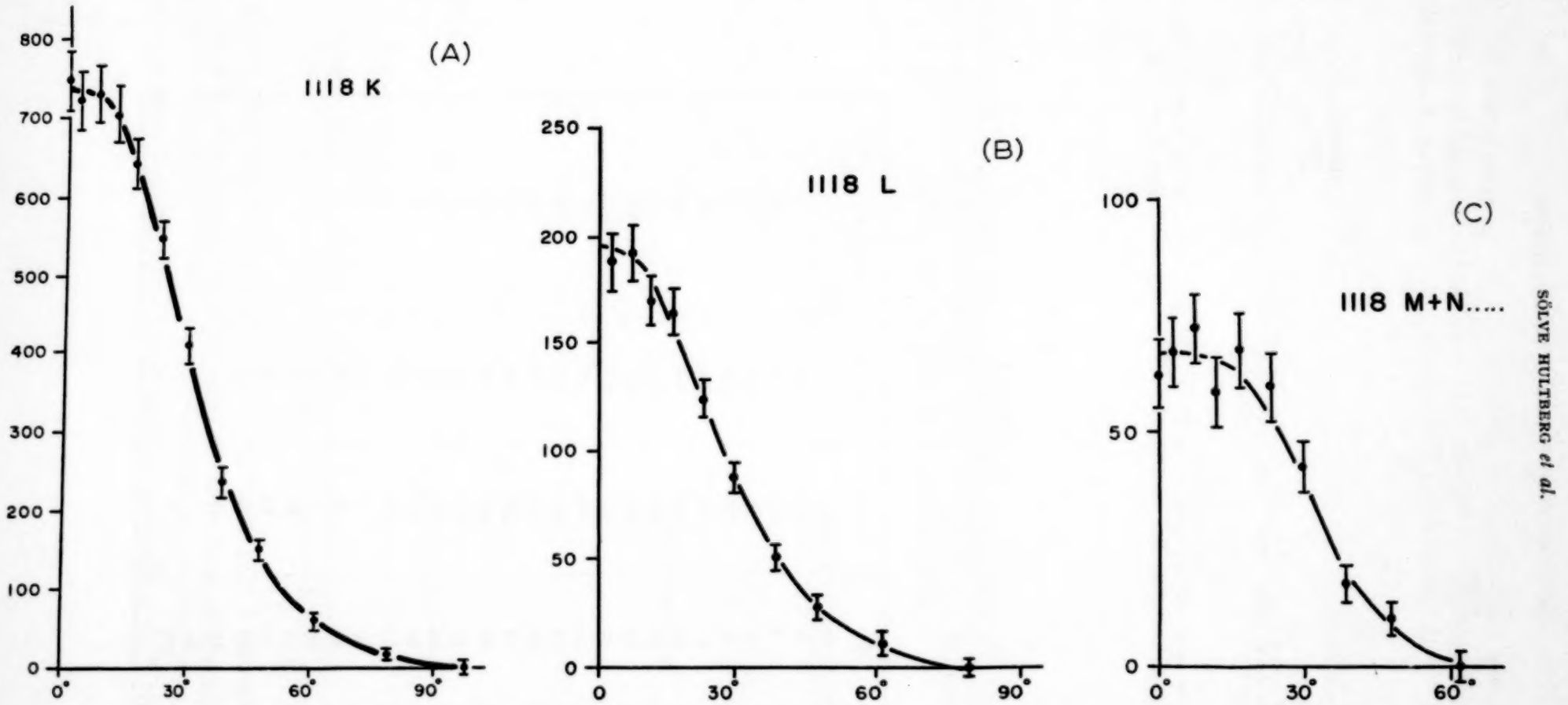

Fig. 5. Uncorrected experimental angular distributions J_e of photoelectrons ejected at $h\nu = 1118$ keV. (A) from the uranium K-shell, (B) from the L-shell, and (C) from the M+N+ . . .-shells. Estimated uncertainties in the individual measurements are indicated. Ordinates represent intensities per unit solid angle (fixed setting of spectrometer aperture).

better than required for these experiments. During the measurements the dial was always rotated in only one direction to avoid possible uncertainties from any small play in the gear.

The experiments were carried out in a manner similar to previous works [1, 2]). For every setting of the angle θ, a complete spectrum of K-, L-, and M+N+ . . . photolines was recorded. The L- and M+N+ . . . photolines were no longer recorded after their intensities were found to be indistinguishable from background. A typical spectrum is shown in fig. 4 for $\theta = 0°$.

We used a circular uranium converter (diameter 14.0 mm) with a thickness of 3.9 mg/cm^2. The continuum around the peaks was carefully recorded to allow an accurate interpolation of the background under the peaks. Because of the relatively poor resolution (about 1 %), the L and M+N+ . . . lines were not completely resolved. With the help of the peak heights which could be reasonably well estimated, it was possible, however, to obtain the L and M+N+ . . . contributions separately.

By plotting the photoline areas (per unit momentum interval) versus θ, photoelectric angular distributions were obtained for the uranium K-, L-, and M+N+ . . .-shells, as given in fig. 5.

In fig. 5 we have indicated errors that represent estimated uncertainties in the photoline areas (5 % and up).

The angular functions $J_e(\theta)$ of fig. 5 represent intensities per unit solid angle (spectrometer aperture fixed) and they are presented numerically in table 1.

It should be observed that the K, L, and M+N+ . . . functions of table 1 are mutually correct on a relative scale so that K/L, K/(M+N+ . . .), etc. ratios of photolines and of total absorptions in the different shells can be formed. The latter ratios (τ_1/τ_2) are given by eq. (3) and the former ratios can be written (ref. [1])):

$$\frac{(A_\gamma)_1}{(A_\gamma)_2} = \frac{\tau_1 f_1}{\tau_2 f_2}, \tag{1}$$

where A is the photoline intensity and the subscripts 1, 2 refer to specific shells (K, L or M+N . . .).

3. Discussion

In fig. 5 we have obtained certain angular functions by plotting the intensities of three groups of photolines versus the angle θ which we use in the sense of fig. 3 to describe the emission direction of a photoelectron with regard to the incidence direction of the gamma ray. We have already introduced the notation $J_e(\theta)$ for these angular functions where the subscript e serves to stress the experimental nature. Theoretically, it is possible to calculate angular functions $J(\theta)$ which represent the probability per unit solid angle that a photoelectron

be emitted in the direction θ, if we define the incidence direction of the gamma ray as $\theta = 0$. We then pose the following question. What is the relation between the functions $J_e(\theta)$ and $J(\theta)$? From fig. 3 it is clearly understood that J_e and J cannot be identical. This follows from the fact that obviously our converter has to have a certain lateral extension (i.e. a finite radius) and likewise a finite thickness. Both these facts mean that we cannot, in our experiments, define the relative angle θ sharply. The converter radius introduces a "geometric" distortion [1]) since our measurements only give a type of mean value of $J(\theta)$ inside an angular interval $(\theta-\Delta_1\theta, \theta+\Delta_2\theta)$ where $\Delta_1\theta$, $\Delta_2\theta$ are given by the maximum displacements from the converter centre O of the interaction point R (cf. fig. 3). Obviously, this kind of diffuseness in θ has a maximum at $\theta = 0$ and a minimum at $\theta = 90°$. The thickness of the converter manifests itself by scattering of the photoelectrons so that they will emerge from the converter surface in directions that will differ in general from the initial directions. This introduces a further confusion of angles and we may define it as the "scattering" distortion [1]). Both the geometric and the scattering distortions tend to smooth out (rapid) variations in the angular functions so that differences between minima and maxima will be less pronounced in $J_e(\theta)$ than in $J(\theta)$. The degree of this smoothing-out effect will be strongly dependent on the particular choice of the parameters c and d (cf. fig. 3) and quite naturally we will have $J_e \to J$ as c and d tend toward zero. To infer $J(\theta)$ from $J_e(\theta)$ we might then undertake special experiments where the behavior of $J_e(\theta)$ is studied as a function of c and d which would then permit an extrapolation to $c = d = 0$ [1]). Such a procedure is necessary for carrying out a detailed comparison with theory.

In the present case, however, we did not undertake such "extrapolation" experiments for the following reasons. No theoretical predictions are yet available for heavy elements. It turns out that the correction factor f [1]) is very insensitive (to within about 1 % in most cases; see also ref. [4])) to the exact values of c and d that characterize a particular angular distribution. This means that we can compute the desired f factors to a satisfactory accuracy without having to find the angular distribution that would correspond to $c = 0$ and to the particular d value used in the experiment.

Let us assume that the converter is thin enough so that no photoelectrons are absorbed inside the converter material. Such an assumption is justified here since no appreciable broadening of the measured photolines was observed. Then we can write, according to ref. [1]):

$$\int_0^\pi J_e(\theta) \sin\theta \, d\theta = K \int_0^\pi J(\theta) \sin\theta \, d\theta, \tag{2}$$

where K is a constant during the measurements. Essentially, eq. (2) states that our measured function J_e is merely a redistribution (distortion) of J, apart from the constant K. Using the definition of the integrated photoelectric

cross-section τ of a specific shell, we obtain for the ratio τ_1/τ_2 of such cross-sections of shells 1 and 2 [1]):

$$\frac{\tau_1}{\tau_2} = \frac{[\int_0^\pi J_e(\theta) \sin\theta \, d\theta]_1}{[\int_0^\pi J_e(\theta) \sin\theta \, d\theta]_2}. \tag{3}$$

Evaluating (3) from table 1, we obtain at $h\nu = 1118$ keV:

$$\frac{\tau_K}{\tau_L} = 5.3 \pm 0.3; \quad \frac{\tau_K}{\tau_{M+N+\ldots}} = 14.0 \pm 0.9; \quad \frac{\tau_L}{\tau_{M+N+\ldots}} = 2.7 \pm 0.2; \quad \frac{\tau_a}{\tau_K} = 1.26 \pm 0.01.$$

These values are in good agreement with those found earlier at three other energies [1]). It is interesting to notice that, at high energies, Pratt [5]) finds theoretically $\tau_K/\tau_L = 5.3$ and $\tau_L/\tau_{M+N+\ldots} = 2.7$ for uranium. This confirms that the photoelectric absorption ratios are remarkably independent of energy.

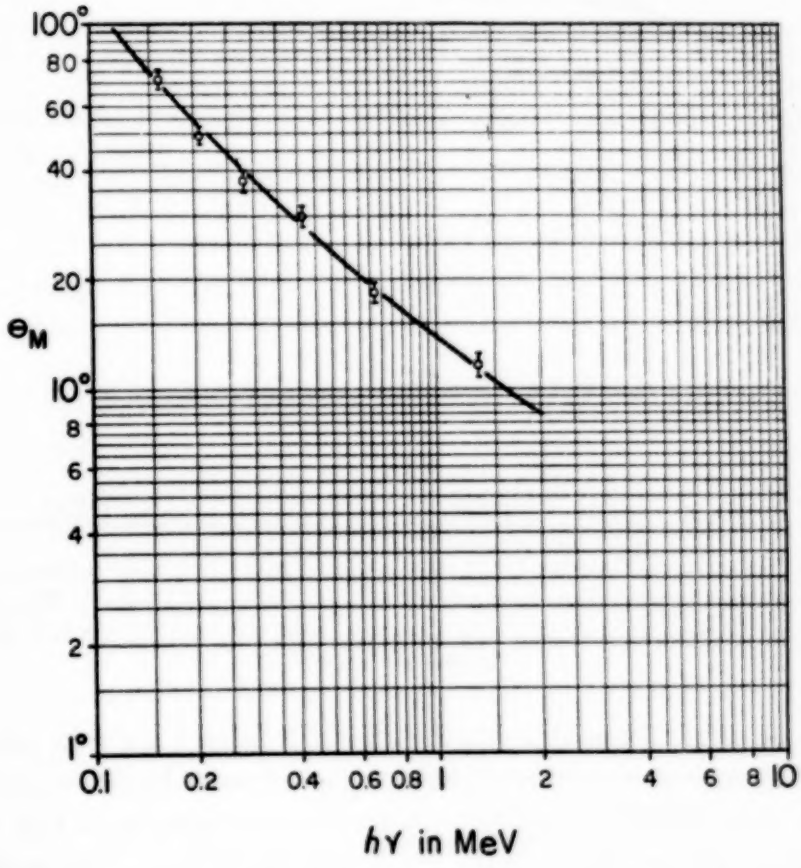

Fig. 6. The angle θ_m of maximum K-shell photoelectric emission from uranium, plotted as function of the energy $h\nu$ of the incident photons. The points are experimental and are taken from refs. [1, 6, 7]).

From the $J_e(\theta)$ functions of fig. 5, we cannot easily determine the angle θ_m of maximum photoelectric emission. We can, however, infer $\theta_m(1118)$ from fig. 6 which shows θ_m as a function of the gamma-ray energy in a log-log dia-

gram. These data in fig. 6 are fitted nicely by the smooth curve shown. This curve makes accurate predictions at other energies rather easy. This simple relationship between θ_m and $h\nu$ has not been demonstrated before.

The experimental information for fig. 6 has been obtained from refs. [1,6,7]). At the threshold energy Nagel [8]) finds for the K shell that $\theta_m = 97°$. This is seen to be consistent with an extrapolation of the curve of fig. 6 which yields $\theta_m = 97° \pm 3°$ at $h\nu = 116$ keV (the K-shell threshold of uranium). From the latter diagram we obtain $\theta_m(1118) = 12.7°$.

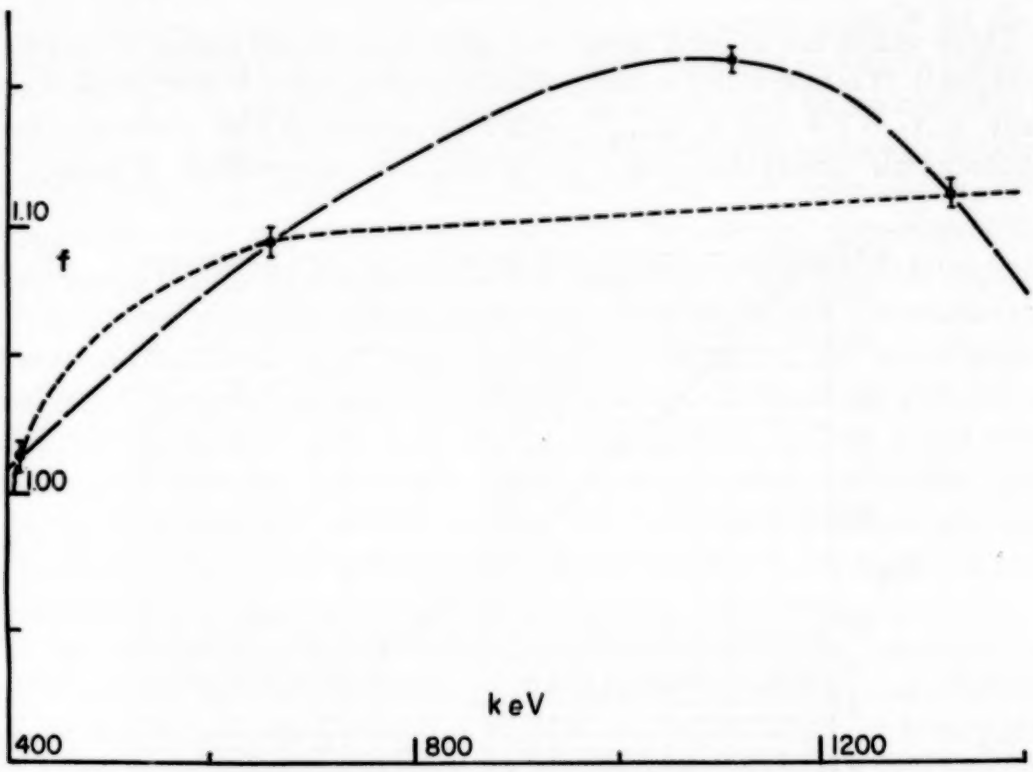

Fig. 7. Typical f values calculated for 3×16 mm² source with a 5×21 mm² converter which were used in the Vanderbilt spectrometer in the study of conversion coefficients [9]). The small dashed curve is a possible extrapolation of the f values made without the point at 1118 keV obtained from the present work.

It should be pointed out that the functions of table 1 are now available for f-factor calculations at the Swedish electronic computer BESK [2]) so that f can be obtained from BESK at the four gamma-ray energies $h\nu = 412$, 662, 1118 and 1332 keV and for three shells (K, L and M+N+ . . .) at each energy. The calculations at 1118 keV help to increase the general accuracy in the curve of f versus energy, as can be appreciated from fig. 7 which illustrates a particular case. The overall accuracy in f may be taken to be of the order of 1 % in the energy region 400—1400 keV. It should be emphasized, however, that to obtain this accuracy each of the parameters entering the calculation of f must be carefully determined from the experimental set-up.

In the near future $f_{159\ K,\ L,\ L_I+L_{II},\ L_{III}}$ and $f_{208\ K}$ will be available[6]) (subscripts indicate energy in keV and shells). All this applies to uranium as converter material. However, the Z dependence of f is probably very weak, at least above $Z = 78$[10]). Application forms for f calculations can be obtained from the Nobel Institute of Physics, *Stockholm* 50, Sweden.

References

1) S. Hultberg and R. Stockendal, Arkiv för fysik **14** (1959) 565;
   S. Hultberg, Arkiv för fysik **15** (1959) 307
2) S. Hultberg and Z. Sujkowski, Phys. Rev. Letters **3** (1959) 227
3) Q. L. Baird, Ph. D. Thesis, Vanderbilt University (1958);
   J. C. Nall, Ph. D. Thesis, Vanderbilt University (1958);
   J. C. Nall, Q. L. Baird and S. K. Haynes, Phys. Rev. **118** (1960) 1278
4) R. Stockendal, Arkiv för fysik **17** (1960) 579
5) R. H. Pratt, Phys. Rev. **119** (1960) 1619
6) J. H. Hamilton, S. F. Frey and S. Hultberg, Nuclear Physics (to be published)
7) Z. Sujkowski (private communication)
8) B. Nagel, Arkiv för fysik **18** (1960) 29
9) W. F. Frey, J. H. Hamilton and S. Hultberg, Nuclear Physics (to be published)
10) C. de Vries, Ph. D. Thesis, Amsterdam (1960); parts are published in Nuclear Physics **18** (1960) 428, 446, 454

2.H

Nuclear Physics **22** (1961) 316—317; © *North-Holland Publishing Co., Amsterdam*

Not to be reproduced by photoprint or microfilm without written permission from the publisher

INELASTIC SCATTERING FROM Th^{232} AND U^{238}

E. Z. SKURNIK, B. ELBEK and M. C. OLESEN

Institute for Theoretical Physics, University of Copenhagen, Copenhagen, Denmark

Received 7 October 1960

Abstract: The reduced electric quadrupole transition probabilities and excitation energies of the first excited states in Th^{232} and U^{238} have been determined from inelastic scattering measurements with protons and deuterons.

The work reported here is a continuation of similar measurements done earlier [1–6]) at this Institute. In these experiments, the Coulomb excitation of low-lying states of deformed nuclei have been investigated by studying the scattered projectiles in a magnetic spectrograph utilizing photographic recording of the particles. In the present investigation, Th^{232} and U^{238} targets have been bombarded with protons and deuterons of energies between 3.5 and 4.5 MeV. The scattering angle was 145°. The nuclei investigated are strongly deformed and the first excited state is therefore a $2+$ rotational state which can be reached from the ground state by an E2 Coulomb excitation.

The experimental procedure was the same as in the previous measurements and will not be described in detail. The targets were prepared by vacuum evaporation in the electron bombardment device described earlier [5]). Thorium nitrate and natural metallic uranium were used, respectively, as charging material for the small carbon crucible of the evaporation apparatus. In addition to these targets we also used targets prepared in an electromagnetic isotope separator by the sputtering method described in ref. [4]). Thin aluminium coated formvar foils were used as backings for the evaporated targets, whereas the separated targets were prepared on thin carbon foils.

The cross sections for Coulomb excitation of the levels in question were determined from the ratio between the inelastic and the elastic yields, assuming the validity of the Rutherford scattering law under the present conditions. In order to obtain the Coulomb excitation cross section per unit solid angle in the centre-of-mass system, the measured ratio was multiplied with the Rutherford cross section per unit solid angle evaluated in the centre-of-mass system. From the measured cross section for inelastic scattering the reduced electric quadrupole transition probability was determined by means of the formula for the differential cross section of E2 excitation. To this purpose, we used the semiclassical function $\mathrm{d}f_{\mathrm{E2}}(\xi, \vartheta)$ which, for the case considered here, is well justified [6, 7]).

The results obtained from 8 exposures of Th^{232} and 12 exposures of U^{238} showed no systematic variation in the $B(E2)$ values computed from measurements performed at different bombarding energies or with different particles.

TABLE 1

Excitation energies and reduced transition probabilities for excitation of the first 2+ levels in Th^{232} and U^{238}. The errors quoted for our $B(E2)$-values represent the standard deviations of the individual measurements. The errors in the excitation energies are estimated to be less than 1 keV.

Nucleus	Excitation energy (keV)	$B(E2)$ ($e^2 \times 10^{-48}$ cm^4)	Q_0 (10^{-24} cm^2)	β	$B(E2)$ from other measurements
$_{90}Th^{232}$	49.6	9.8±0.6	9.93±0.30	0.257	8.50±0.37 [9] 11.5 ±1.7 [10]
$_{92}U^{238}$	44.5	12.7±0.7	11.30±0.30	0.280	11.05±0.98 [9] 13.2 ±2.0 [10]

The results for both of the nuclei investigated are given in table 1. In addition to the excitation energies and the reduced transition probabilities $B(E2; 0 \rightarrow 2)$, the intrinsic nuclear quadrupole moments Q_0 and the deformation parameters β are given; these are calculated using the formulae V.10 and V.12 of ref. [8]), assuming a nuclear radius of $R = 1.2\, A^{\frac{1}{3}}\, 10^{-13}$ cm for calculation of the deformation parameter. The table also contains the $B(E2)$ values resulting from the lifetime measurements reported by Bell *et al.* [9]) and from the conversion electron measurements reported by Rester *et al.* [10]). Our values are seen to be in between the two other sets of measurements. The differences between the $B(E2)$ values derived from the lifetime measurements and our values are 14 % for both of the nuclei investigated, and could possibly indicate the presence of a systematic error in the theoretical conversion coefficients.

The authors are indebted to Mr. G. Sidenius and Mr. O. Skilbreid for the targets prepared in the isotope separator. We also wish to thank Mrs. R. Hansen and Miss G. Bertram-Hansen who scanned many of the photographic plates.

One of us (E. Z. S.) gratefully acknowledges a Ford Foundation fellowship.

References

1) V. Ramšak, M. C. Olesen and B. Elbek, Nuclear Physics **6** (1958) 451
2) B. Elbek, K. O. Nielsen and M. C. Olesen, Phys. Rev. **108** (1957) 406
3) B. Elbek, M. C. Olesen and O. Skilbreid, Nuclear Physics **10** (1959) 294
4) B. Elbek, M. C. Olesen and O. Skilbreid (to be published)
5) M. C. Olesen and B. Elbek, Nuclear Physics **15** (1960) 134
6) E. M. Bernstein and E. Z. Skurnik (to be published)
7) J. Bang, Mat. Fys. Medd. Dan. Vid. Selsk. **32**, no. 5 (1960)
8) K. Alder, A. Bohr, T. Huus, B. Mottelson and A. Winther, Revs. Mod. Phys. **28** (1956) 432
9) R. E. Bell, S. Bjørnholm and J. C. Severiens, Mat. Fys. Medd. Dan. Vid. Selsk. **32**, no. 12 (1960)
10) D. H. Rester, M. S. Moore, Frank Durham and C. M. Class (to be published)

1.C:2.E

Nuclear Physics **22** (1961) 318—335; ©*North-Holland Publishing Co., Amsterdam*

Not to be reproduced by photoprint or microfilm without written permission from the publisher

THE HIGH ENERGY OPTICAL MODEL AND NUCLEAR FORCES

J. DĄBROWSKI

Department of Physics, University of Washington, Seattle, Washington

and

Institute for Nuclear Research, Warsaw, Poland

and

J. SAWICKI

Department of Physics, University of California, Berkeley, California †

Received 9 September 1960

Abstract: An iteration procedure is discussed for the integral equation relating the t-matrix for two-nucleons in the medium to the free nucleon-nucleon t-matrix. The real and imaginary parts of the medium and high energy optical model potential are discussed from the point of view of this procedure. Numerical results are obtained for the Gammel-Thaler and Signell-Marshak potentials.

1. Introduction

A great many papers have been published on the presently classical problem of relating the information from the two-nucleon scattering data to the properties of the complex potential describing the scattering of nucleons from nuclei. In particular, Watson's multiple scattering theory has been successful in explaining the optical potential in the asymptotic region of high energy scattering where some of the effects of self-consistency and the identity of particles are of little importance. The set of basic equations of that theory was reviewed e.g. in ref. [1]) (further referred to as "I").

The object of the present paper is two-fold. First we want to propose certain approximate procedures introducing corrections to Watson's theory leading to an extension of its validity to medium energy range. Secondly we present numerical results for the case of infinite nucleus based on both the recent phenemonological nucleon-nucleon potentials of Gammel, Christian and Thaler, Gammel and Thaler, and Signell and Marshak, and on some results of the Brueckner theory of nuclear structure. However, the rearrangement energy part of the optical potential will not be discussed in the present paper. It is believed that this quantity is small in the energy region of the incoming particle above about 20 MeV [2]).

The basic quantity of the Watson theory is the effective scattering operator,

† Part of this work was performed during the summer 1959 when the author was a visitor of the Department of Physics, University of Washington, Seattle, Washington.

the t-matrix. The expression for the optical potential in the case of nuclear matter involves in lowest order the forward scattering on the energy shell part of the t-matrix. In the high energy region this t-matrix has been replaced by its "phase shift approximation" i.e. by the corresponding free nucleon-nucleon scattering amplitude. This is the well-known theory of Riesenfeld and Watson [3]).

On the other hand, no realistic approximation of the t-matrix involving the exclusion principle and the self-consistency requirements and still corresponding to realistic two-body forces has been proposed so far (except for the approach of ref. [22])). The only case for which the t-matrix can be easily calculated exactly with such requirements is the case of the separable nucleon-nucleon potential. The optical potential for this case was computed by Verlet and Gavoret [4]), and in I.

Galitskii [5]) indicated an equation relating the t-matrix t_Q of a pair of interacting fermions embedded in a sea of identical particles to the "free" t-matrix of these two particles. The effect of the medium, i.e. of the presence of the other particles is taken into account only by the exclusion principle operator Q acting in intermediate states. This equation can be written symbolically as

$$t_Q = t_0 + t_0 \frac{Q-1}{a} t_Q \tag{1}$$

where a is the "free" energy denominator; i.e.

$$a = \frac{\hbar^2 k^2}{M} - \frac{\hbar^2 k''^2}{M} + i\eta$$

where k is the initial and k'' is the intermediate state relative momentum of the interacting pair. Eq. (1) can easily be generalized to the case of the "self-consistent" energy denominator e of the Brueckner type theory involving the self-consistent single particle energies. This generalized equation can be written in symbolic form

$$t = t_0 + t_0 \left(\frac{Q}{e} - \frac{1}{a} \right) t \tag{2}$$

or, more explicitly

$$\langle \mathbf{k}|t|\mathbf{k}'\rangle_K = \langle \mathbf{k}|t_0|\mathbf{k}'\rangle + \int d\mathbf{k}'' \langle \mathbf{k}|t_0|\mathbf{k}''\rangle \left\{ \frac{Q(\frac{1}{2}\mathbf{K} \pm \mathbf{k}'')}{E - E'' + i\eta} - \frac{M}{\hbar^2} \frac{1}{k^2 - k''^2 + i\eta} \right\} \langle \mathbf{k}''|t|\mathbf{k}'\rangle_K \tag{3}$$

Let $\mathbf{k}_0$ be the incoming particle momentum, and $\varkappa$ the struck target particle momentum; $\mathbf{k} = \frac{1}{2}(\mathbf{k}_0 - \varkappa)$ is the relative momentum of the pair, $\mathbf{K} = \mathbf{k}_0 + \varkappa$ is the centre of mass momentum; $E = \hbar^2 k^2/M + \mathscr{V}(k, K)$ and $E'' = \hbar^2 k''^2/M + \mathscr{V}(k'', K)$ are the effective energies of the relative motion of the pair, and

$E-E''=E_0-E_1$, where $E_0=\hbar^2k_0^2/2M+V(k_0)+\hbar^2\kappa^2/2M+V(\kappa)$ is the sum of the total single particle energies of the incoming particle 0 and the struck target particle 1, initially †; $V(k_0)$ is the self-consistent single particle potential being the optical potential in our case. In the following we shall make use of the smallness of the imaginary part of the optical potential V and we shall replace V by its real part (the validity of this approximation may be questionable at high energies; however, at very high energies $t\approx t_0$, anyway).

In the following we shall present a discussion of the iteration procedure for eq. (3) leading to successive approximations of the t-matrix. Generally, the knowledge of the off-energy-shell propagation of t_0 is needed. This information is available only in the low energy limit for the effective range theory (compare e.g. Fulton and Schwed [6]), Gel'fand and Levitan [7]). However, we shall see in the following that for the case of nuclear matter in the high energy range the main part of the optical potential can be calculated without the knowledge of the off-energy-shell components of t_0.

Ohnuma [8]), and Saperstein and Feldman [9]) have applied the Gammel and Thaler [10]), and Signell and Marshak [11]) nucleon-nucleon phase-shifts to the theory of the optical potential given by Riesenfeld and Watson [3]). We shall present the corresponding results based on a more accurate theory and, in particular, with the averaging of the momentum of the target particle over the Fermi sea, and with the exclusion principle taken into account. Our results are then compared with the results of refs. [8]), [9]) and [3]), the latter corresponding to the Feshbach and Lomon [12]) phase shifts, and with the results of the classical theory of the imaginary potential given by Clementel and Villi [13]), and Lane and Wandel [14]).

2. Approximation Procedure for the t-Matrix

Let us concentrate on eqs. (2), (3). Forgetting the spin and isobaric spin dependence of t_0 for the moment let us rewrite eq. (2) as

$$t=t_0+t_0\left(\frac{Q}{e}-\frac{1}{a}\right)t_0+t_0\left(\frac{Q}{e}-\frac{1}{a}\right)t_0\left(\frac{Q}{e}-\frac{1}{a}\right)t_0+\ldots. \tag{4}$$

The leading first two terms of this series are

$$\langle\mathbf{k}|t_1|\mathbf{k}'\rangle_K=\langle\mathbf{k}|t_0|\mathbf{k}'\rangle + \int d\mathbf{k}''\langle\mathbf{k}|t_0|\mathbf{k}''\rangle\left[\frac{Q}{e}(\mathbf{k},\mathbf{k}'',\mathbf{K})-\frac{1}{a}(\mathbf{k},\mathbf{k}'')\right]\langle\mathbf{k}''|t_0|\mathbf{k}'\rangle. \tag{5}$$

For the case of the Fermi gas model of nuclear matter we can use eq. (26) of I for the optical potential. The part of this potential corresponding to t_1 can be

† E_1 is the corresponding quantity in the intermediate state: $E_1=\hbar^2k_0''^2/2M+V(k_0'')+\hbar^2\kappa''^2/2M+V(\kappa'')$.

written as

$$V_1(k_0) = 4\int^{<k_p} \mathrm{d}\varkappa \langle \mathbf{k}|t_1|\mathbf{k}\rangle_K . \tag{6}$$

We proceed to evaluate t_1 keeping in mind the fact that t_0 is complex and nonhermitian. Let us introduce formally the momentum dependent "effective mass" $M^*(k, k''; K)$ as

$$(E-E'')^{-1} \equiv \frac{M^*(k, k''; K)}{k^2-k''^2} \tag{7}$$

and the notation

$$F_Q(\mathbf{k}, \mathbf{k}''; \mathbf{K}) \equiv Q(\tfrac{1}{2}\mathbf{K}\pm\mathbf{k}'')\frac{M^*(k, k''; K)}{M} - 1. \tag{7a}$$

We can now rewrite t_1 of eq. (5) in the form

$$\begin{aligned}\langle \mathbf{k}|t_1|\mathbf{k}\rangle_K = \langle \mathbf{k}|t_0|\mathbf{k}\rangle &- \frac{i\pi kM}{2\hbar^2}\int \mathrm{d}\Omega_{\mathbf{k}''} F_Q\left(\mathbf{k}, k\frac{\mathbf{k}''}{k''}; \mathbf{K}\right) \\ &\times \left[\left|\left\langle \mathbf{k}|t_0|k\frac{\mathbf{k}''}{k''}\right\rangle\right|^2 + \left\langle \mathbf{k}|t_0|k\frac{\mathbf{k}''}{k''}\right\rangle\left\{\left\langle k\frac{\mathbf{k}''}{k''}|t_0|\mathbf{k}\right\rangle - \left\langle \mathbf{k}|t_0|k\frac{\mathbf{k}''}{k''}\right\rangle^*\right\}\right] \\ &+ \frac{M}{\hbar^2}\mathrm{P}\int \frac{\mathrm{d}\mathbf{k}''}{k^2-k''^2} F_Q(\mathbf{k}, \mathbf{k}''; \mathbf{K})\langle \mathbf{k}|t_0|\mathbf{k}''\rangle\langle \mathbf{k}''|t_0|\mathbf{k}\rangle\end{aligned} \tag{8}$$

where the symbol "P" stands for the principal value. First we shall use the "optical theorem"

$$\mathrm{Im}\,\langle \mathbf{k}|t_0|\mathbf{k}\rangle = -\frac{\pi kM}{2\hbar^2}\int \mathrm{d}\Omega_{\mathbf{k}''}\left|\left\langle \mathbf{k}|t_0|k\frac{\mathbf{k}''}{k''}\right\rangle\right|^2 . \tag{9}$$

A similar equation obtains for the general case involving spin and iso-spin dependent t_0.

Next we shall employ for the antihermitian part of t_0 i.e. for $t_0 - t_0^* = t_0 - t_0^\dagger$ the following expression:

$$\begin{aligned}\left\langle k\frac{\mathbf{k}''}{k''}|t_0|\mathbf{k}\right\rangle - \left\langle \mathbf{k}|t_0|k\frac{\mathbf{k}''}{k''}\right\rangle^* &= \frac{M}{\hbar^2}\int \mathrm{d}\mathbf{q}\left\langle \mathbf{q}|t_0|k\frac{\mathbf{k}''}{k''}\right\rangle^*\langle \mathbf{q}|t_0|\mathbf{k}\rangle\left[\frac{1}{q^2-k^2+i\eta} - \frac{1}{q^2-k^2-i\eta}\right] \\ &= -i\pi k\frac{M}{\hbar^2}\int \mathrm{d}\Omega_q\left\langle k\frac{\mathbf{q}}{q}|t_0|k\frac{\mathbf{k}''}{k''}\right\rangle^*\left\langle k\frac{\mathbf{q}}{q}|t_0|\mathbf{k}\right\rangle .\end{aligned} \tag{10}$$

This antihermitian correction to t was neglected in eqs. (66)—(73)of I. These equations are a good approximation only if the imaginary part of t_0 is small

(e.g. if $t_0 \approx V_{01}$). If one sets $t_0 \approx V_{01}$ in eqs. (66)—(68) of I, the numerical change in the calculated Im $V_{(\mathrm{in})}$ of I is very small indeed.

Eq. (10) is a special case of eq. (II) of ref. [5]) being a consequence of the unitarity of the Möller ("wave") matrix Ω_0 related to t_0 by $t_0 = V_{01}\Omega_0$, where V_{01} is the nucleon-nucleon potential. We also observe that the "optical theorem" of eq. (9) is again a special case of eq. (10). We can now simplify eq. (8) in the form

$$\langle \mathbf{k}|t_1|\mathbf{k}\rangle_K = \mathrm{Re}\langle \mathbf{k}|t_0|\mathbf{k}\rangle - \frac{i\pi kM}{2\hbar^2}\int \mathrm{d}\Omega_{\mathbf{k}''} Q\left(\tfrac{1}{2}\mathbf{K}\pm k\frac{\mathbf{k}''}{k''}\right)\frac{M^*(k,k'';K)}{M}\left|\left\langle \mathbf{k}|t_0|k\frac{\mathbf{k}''}{k''}\right\rangle\right|^2 + \langle \mathbf{k}|\Delta_{\mathrm{a}}|\mathbf{k}\rangle_K + \langle \mathbf{k}|\Delta_{\mathrm{b}}|\mathbf{k}\rangle_K, \tag{11}$$

where

$$\langle \mathbf{k}|\Delta_{\mathrm{a}}|\mathbf{k}\rangle_K = -\frac{\pi^2k^2M^2}{2\hbar^4}\int \mathrm{d}\Omega_{K''} F_Q\left(\mathbf{k},\, k\frac{\mathbf{k}''}{k''};\, \mathbf{K}\right)\left\langle \mathbf{k}|t_0|k\frac{\mathbf{k}''}{k''}\right\rangle \times \int \mathrm{d}\Omega_{\mathbf{q}}\left\langle k\frac{\mathbf{q}}{q}|t_0|k\frac{\mathbf{k}''}{k''}\right\rangle^*\left\langle k\frac{\mathbf{q}}{q}|t_0|\mathbf{k}\right\rangle \tag{12}$$

and

$$\langle \mathbf{k}|\Delta_{\mathrm{b}}|\mathbf{k}\rangle_K = \frac{M}{\hbar^2}\mathrm{P}\int \frac{\mathrm{d}\mathbf{k}''}{k^2-k''^2} F_Q(\mathbf{k},\mathbf{k}'';\mathbf{K})\langle \mathbf{k}|t_0|\mathbf{k}''\rangle\langle \mathbf{k}''|t_0|\mathbf{k}\rangle. \tag{13}$$

The first term of eq. (11) is the leading term for the real part of t_1. If one replaces now Q by Q^{F}, appropriate to the Fermi gas, which is the operator excluding the states with $|\frac{1}{2}\mathbf{K}\pm\mathbf{k}''| < k_{\mathrm{F}}$ then the next term of eq. (12) goes over into the well-known "frivolous" model in the limit $M^*(k,k'';K) \to M$. The terms Δ_{a} and Im Δ_{b} are the consequence of the nonhermiticity of t_0. The procedure leading to eq. (11) was introduced in order to establish the correspondence to the "frivolous model." The contributions of $\mathrm{Im}(\Delta_{\mathrm{a}}+\Delta_{\mathrm{b}})$ to Im $V_1(k_0)$ are rather difficult to estimate, in general. In particular, Im Δ_{b} can be estimated only for particular simple models. In section 5 the effect of Im Δ_{a} is studied for a realistic case, and the effect of $\mathrm{Im}(\Delta_{\mathrm{a}}+\Delta_{\mathrm{b}})$ only for a rather unrealistic numerical example of the Yamaguchi separable potential.

3. Calculations in the "Frivolous Model" of the Imaginary Potential

3.1. THE AVERAGE t-MATRIX

The actual t-matrix to be used in our calculations has to be properly averaged over spin and isobaric spin states. We can write the averaged t-matrix as

$$\langle \mathbf{k}|t|\mathbf{k}\rangle_{\mathrm{av}} = \tfrac{1}{4}\,\mathrm{Tr}\,\tfrac{1}{2}[\langle \mathbf{k}|t|\mathbf{k}\rangle_{\mathrm{n\text{-}p}} + \langle \mathbf{k}|t|\mathbf{k}\rangle_{\mathrm{n\text{-}n}}] \tag{14}$$

where n-p (n-n) corresponds to the interacting pair of particles being a neutron-proton (neutron-neutron) system; "Tr" is the trace operator for the σ_0-, σ_1-spin

states. Eq. (14) can be rewritten more conveniently in the form

$$\langle \mathbf{k}|t|\mathbf{k}\rangle_{\mathrm{av}} = \tfrac{1}{4}\mathrm{Tr}[\tfrac{3}{4}\langle \mathbf{k}|t|\mathbf{k}\rangle_{T=1} + \tfrac{1}{4}\langle \mathbf{k}|t|\mathbf{k}\rangle_{T=0}] \tag{15}$$

where $T = 0$, 1 are the isobaric spin singlet and triplet states. Defining a quantity J for abbreviation, we can write similarly

$$\begin{aligned} J \equiv \left|\left\langle \mathbf{k}|t_0|k\frac{\mathbf{k}''}{k''}\right\rangle\right|^2 = \tfrac{1}{4}\mathrm{Tr}\Bigg[\tfrac{3}{4}\left\langle \mathbf{k}|t_0|k\frac{\mathbf{k}''}{k''}\right\rangle_{T=1}\left\langle \mathbf{k}|t_0^{\dagger}|k\frac{\mathbf{k}''}{k''}\right\rangle_{T=1} \\ + \tfrac{1}{4}\left\langle \mathbf{k}|t_0|k\frac{\mathbf{k}''}{k''}\right\rangle_{T=0}\left\langle \mathbf{k}|t_0^{\dagger}|k\frac{\mathbf{k}''}{k''}\right\rangle_{T=0}\Bigg]. \end{aligned} \tag{16}$$

It should be remarked that this quantity is not exactly proportional to

$$\tfrac{1}{2}[\sigma_{\mathrm{nn}}(\theta) + \sigma_{\mathrm{n\text{-}p}}(\theta)] = \tfrac{1}{2}[|2f(\theta)_{T=1}|^2 + |f(\theta)_{T=1} + f(\theta)_{T=0}|^2]$$

in the usual notation for the partial scattering amplitudes in the isospin states $T = 0$, 1.

The quantity J can be expressed in terms of the nucleon-nucleon phase shifts and tensor coupling parameters ε_j and the angle ϑ between $\mathbf{k}$ and $\mathbf{k}''$. Using the well-known techniques of Blatt and Biedenharn we can write

$$J = \sum_L A_L P_L(\cos\vartheta).$$

The leading term A_0 is fairly simple. In fact

$$\begin{aligned} A_0 &= \left(\frac{\hbar^2}{2\pi^2 M}\right)^2 \frac{1}{8k^2}\{[\sum_{l\,\mathrm{odd}} + 3\sum_{l\,\mathrm{even}}](2l+1)\sin^2\delta_l \\ &+ [\sum_{l\,\mathrm{even}} + 3\sum_{l\,\mathrm{odd}}][(2l+1)\sin^2\eta_l + (2l+3)(\sin^2\eta_{l+1,\alpha} + \sin^2\eta_{l+1,\beta})] + 3\sin^2\eta_0\} \\ &\equiv \left(\frac{\hbar^2}{2\pi^2 M}\right)^2 \frac{\tilde{f}(k)}{8k^2} \end{aligned} \tag{17}$$

where the δ_l are the singlet states phase shifts; η_l, $\eta_{l+1,\alpha}$ and $\eta_{l+1\,\beta}$ are the uncoupled ($j = l$) and coupled Blatt and Biedenharn triplet states phase shifts, and η_0 is the $^3P_0$-phase shift. The corresponding expression for the real part of t_0 is given in Riesenfeld and Watson [3]). Explicit expressions for the coefficients A_L with $L = 1, 2, 3, 4$ can be easily obtained from eqs. (48b, c) and (52b, c) of Feshbach and Lomon [12]) by properly averaging over the isospin states (e.g. with the phase shifts of Gammel, Christian and Thaler [15]) $A_2/A_0 \approx 0.09$ at the laboratory energy $E_{\mathrm{L}} = 40$ MeV in the nucleon-nucleon scattering).

3.2. THE EXCLUSION PRINCIPLE OPERATOR AND THE "MODIFIED FRIVOLOUS MODEL"

The exclusion principle requires that the momenta of both the particles of the interacting pair in the intermediate states be above the Fermi sea. These

restrictions set limits on the relative momentum k'' and on the angle θ between $\mathbf{K}, \mathbf{k}''$. It is easy to derive the following set of conditions: A) if $K \geqq 2k_F$ then $\frac{1}{2}K - k_F \leqq k'' \leqq \frac{1}{2}K + k_F$, and B) if $K \leqq 2k_F$ then $\sqrt{k_F^2 - \frac{1}{4}K^2} \leqq k'' \leqq \frac{1}{2}K + k_F$. Also in both the cases A) and B)

$$-\alpha_0 \leqq \cos\theta = \frac{\mathbf{K}\cdot\mathbf{k}''}{Kk''} \leqq \alpha_0 = \frac{\frac{1}{4}K^2 + k''^2 - k_F^2}{Kk''},$$

such that

$$\int d\Omega_{k''} Q^F\left(\tfrac{1}{2}\mathbf{K} \pm k\frac{\mathbf{k}''}{k''}\right) = \begin{cases} 4\pi\alpha_0 \text{ for } k'' = k \text{ satisfying A) or B),} \\ 0 \quad \text{otherwise.} \end{cases}$$

The "Modified Frivolous Model" part of $\mathrm{Im}\,\langle \mathbf{k}|t_1|\mathbf{k}\rangle_K$ of eq. (14) can be rewritten as

$$t_{\mathrm{MFM}} \equiv \begin{cases} -\dfrac{\pi k M}{2\hbar^2}\displaystyle\int_0^{2\pi} d\varphi \int_{-\alpha_0}^{\alpha_0} d(\cos\theta)\, \frac{M^*(k,k;K)}{M} J(k^2, \cos\vartheta) \text{ for} \\ \qquad\qquad\qquad\qquad\qquad\qquad k'' = k \text{ satisfying A) or B),} \\ 0 \quad \text{otherwise.} \end{cases} \tag{18}$$

However,

$$P_L(\cos\vartheta) = \frac{4\pi}{2L+1}\sum_m Y^*_{Lm}(\theta,\varphi) Y_{Lm}(\Omega_\psi),$$

where Ω_ψ is the angle between $\mathbf{k}$ and $\mathbf{K}$. Consequently we have

$$t_{\mathrm{MFM}} = \begin{cases} -\dfrac{\pi^2 k M}{\hbar^2}\displaystyle\sum_L A_L P_L\left(\frac{\mathbf{K}\cdot\mathbf{k}}{Kk}\right)\frac{M^*(k,k;K)}{M}\int_{-\alpha_0}^{\alpha_0} P_L(\cos\theta)(\cos\theta) \text{ for} \\ \qquad\qquad\qquad\qquad\qquad\qquad k'' = k \text{ satisfying A) or B),} \\ 0 \quad \text{othersise.} \end{cases} \tag{19}$$

The anisotropy correction terms with odd L vanish and the correction of the A_2 term was computed by Verlet and Gavoret [4]) and found to be small. In the following we shall confine ourselves to the approximation

$$t_{\mathrm{MFM}} \begin{cases} \approx -\dfrac{\pi^2 k M}{\hbar^2} A_0(k) 2\alpha_0 \dfrac{M^*(k,k'';K)}{M} \text{ if } k = k'' \text{ satisfies A) or B)} \\ = 0 \text{ otherwise.} \end{cases} \tag{20}$$

Using eq. (17) we can rewrite this equation as

$$t_{\mathrm{MFM}} \begin{cases} \approx -\dfrac{\hbar^2}{2\pi^2 M}\dfrac{1}{8k}\tilde{f}(k)\alpha_0 \dfrac{M^*(k,k;K)}{M} \text{ for } A) \text{ or B),} \\ = 0 \text{ otherwise.} \end{cases} \tag{21}$$

Schematically eqs. (20), (21) correspond to the relationship:

$$\mathrm{Im}\, t_0(\vartheta = 0)_{\mathrm{av}} = k \frac{2\pi^2 M}{\hbar^2} |t_0|^2_{\mathrm{av}},$$

a special simplified form of the optical theorem.

The corresponding imaginary potential can be written as

$$\mathrm{Im}\, V_{\mathrm{MFM}}(k_0) = 4 \int^{<k_F} \mathrm{d}\varkappa t_{\mathrm{MFM}}(k, K). \tag{22}$$

In analogy to Verlet and Gavoret [4]) we introduce the variables $u = \frac{1}{2}K$ and k in the latter integral. It is then easy to show that

$$\mathrm{Im}\, V_{\mathrm{MFM}}(k_0) \tag{23}$$
$$= -\frac{4\hbar^2}{2\pi^2 M} \frac{16\pi}{8k_0} \int_{\frac{1}{2}(k_0-k_F)}^{\frac{1}{2}(k_0+k_F)} \mathrm{d}k\, \tilde{f}(k) \int_{\max\{\sqrt{k_F^2-k^2},\, k_0-k\}} \frac{M^*(k, k; 2u)}{M} \frac{u^2+k^2-k_F^2}{2ku} u\, \mathrm{d}u.$$

The approximations of our theory apply to the high energy range, and so we can restrict ourselves to the case $k_0 > \sqrt{2}\, k_F$ for which $k_0 - k > \sqrt{k_F^2 - k^2}$; consequently, we can replace the lower limit of the u-integration by $k_0 - k$. Introducing now the dimensionless variables $x = k/k_F$ and $y = u/k_F$ we have

$$\mathrm{Im}\, V_{\mathrm{MFM}}(k_0) = -\frac{2}{\pi} \frac{\hbar^2 k_F^2}{M} \frac{1}{\nu} \int_{\frac{1}{2}(\nu-1)}^{\frac{1}{2}(\nu+1)} \frac{\mathrm{d}x}{x} \tilde{f}(x) \int_{\nu-x}^{[\frac{1}{2}(\nu^2+1)-x^2]^{\frac{1}{2}}} \mathrm{d}y\, \mu(x, y)(x^2+y^2-1) \tag{24}$$

where $\nu = k_0/k_F$ and $\mu(x, y) = M^*(k, k; 2u)/M$.

In the following section we shall present various different forms of $\tilde{f}(x)$ corresponding to different assumptions and nucleon-nucleon potentials. In fact $\tilde{f}(x)$ is a slowly varying function of x. For the special case of the simplifying assumption $\tilde{f}(x) \approx \tilde{f}_{\mathrm{av}} \approx \tilde{f}(\frac{1}{2}\nu)$ and $\mu(x, y) \approx \bar{\mu}(\nu)$, i.e. the case of a constant effective mass being in general a function of ν, the integral involved can be conveniently performed in the form

$$\int_{\theta_{\min}}^{\theta_{\max}} \frac{\mathrm{d}\theta}{\cos\theta} \int_{\nu\,(\sin\theta+\cos\theta)^{-1}}^{\sqrt{\frac{1}{2}(\nu^2+1)}} (r^2 - 1)\mathrm{d}r,$$

where

$$\theta_{\max} = \arccos \frac{\frac{1}{2}(\nu-1)}{\sqrt{\frac{1}{2}(\nu^2+1)}} \text{ and } \theta_{\min} = \arccos \frac{\frac{1}{2}(\nu+1)}{\sqrt{\frac{1}{2}(\nu^2+1)}}.$$

It follows that our imaginary potential takes on the approximate form

$$\mathrm{Im}\, V_{\mathrm{MFM}}(k_0) = -\frac{2}{\pi} \frac{\hbar^2 k_F}{M} \frac{\bar{\mu}(\nu)}{\nu} \tilde{f}(\tfrac{1}{2}\nu) G \tag{25}$$

where

$$G = \frac{v^2-5}{6}\sqrt{\tfrac{1}{2}(v^2+1)}\ln\left|\frac{(v+1)\left(1+\dfrac{\frac{1}{2}(v+1)}{\sqrt{\frac{1}{2}(v^2+1)}}\right)}{(v-1)\left(1+\dfrac{\frac{1}{2}(v-1)}{\sqrt{\frac{1}{2}(v^2+1)}}\right)}\right| + \tfrac{1}{3}v^2 + v(1-\tfrac{1}{3}v^2)\ln\frac{v+1}{v-1}. \tag{26}$$

3.3. THE EFFECTIVE MASS OF WADA AND BEY

In their recent paper on the nuclear saturation problem Wada and Bey [16]) presented a 3-parameter single particle self-consistent potential corresponding to S-state interactions of the Brueckner pairs. This single particle potential is

$$V(k_i) = \tfrac{1}{2}\frac{ck_i^2-b}{1+ak_i^2} \tag{27}$$

where the parameters a, b and c, were determined for several nuclear densities (k_F) and several radii of the hard core repulsive interactions combined with the S-state square well attractive potentials.

The expression $MF_Q(k, k''; K)/\hbar^2(k^2-k''^2)$ of sect. 2 corresponds now to the form

$$\frac{Q}{\dfrac{\hbar^2k^2}{M}-\dfrac{\hbar^2k''^2}{M}+\dfrac{c'k^2-b'}{1+a'k^2}-\dfrac{c'k''^2-b'}{1+a'k''^2}} - \frac{1}{\dfrac{\hbar^2}{M}(k^2-k''^2)} \tag{28}$$

if one introduces the relative and the centre of mass momenta, where

$$a' = \frac{2a}{(1+\frac{1}{2}aK^2)}, \quad b' = \frac{b-\frac{1}{4}(c-ab)K^2}{1+\frac{1}{2}aK^2} \text{ and } c' = \frac{c-ab}{(1+\frac{1}{2}aK^2)}.$$

It then follows that

$$\frac{M^*(k, k''; K)}{M} = \frac{(1+a'k^2)(1+a'k''^2)}{(1+a'k^2)(1+a'k''^2)+M(a'b'+c')} \tag{29}$$

In the particular case $k'' = k$ (on the energy shell) and in the dimensionless notation of the previous section we have

$$\mu(x, y) = \frac{[1+2ak_F^2(x^2+y^2)]^2}{[1+2ak_F^2(x^2+y^2)]^2+M(ab+c)}. \tag{30}$$

The most realistic solution of Wada and Bey [16]) is presented in their fig. 2a and corresponds to the binding energy per nucleon $E_B = -13.6$ MeV and the following set of parameters: $k_F \approx 1.25\,f^{-1}$, the hard core radius $r_c = 0.35\,f$, $a = 0.0903\,\mu^{-2}$, $b = 1.18\,\mu$, $c = 0.0576\,\mu^{-1}$, where $\mu = 0.714\,f^{-1}$ (140 MeV) is the pion mass parameter.

The question of the relationship of the nuclear potential $V(k_i)$ of eq. (27) to the real part of our optical potential computed in the phase shift approximation is considered in sect. 6. It should be pointed out that at the energies corresponding to $\nu \gtrsim 2$ the rearrangement energy omitted in both the cases is expected to be small [2]) and the near equality of the two potentials to hold.

4. Numerical Results for the "Modified Frivolous Model"

We have considered the cases of the sets of phase shifts corresponding to the potentials given by Gammel, Christian and Thaler [15]) (GCT), Gammel and Thaler [10]) (GT) and Signell and Marshak [11]) (SM). The function $\tilde{f}(x)$ for these cases is plotted in fig. 1. The respective values of Im $V_{\mathrm{MFM}}(k_0)$ were computed

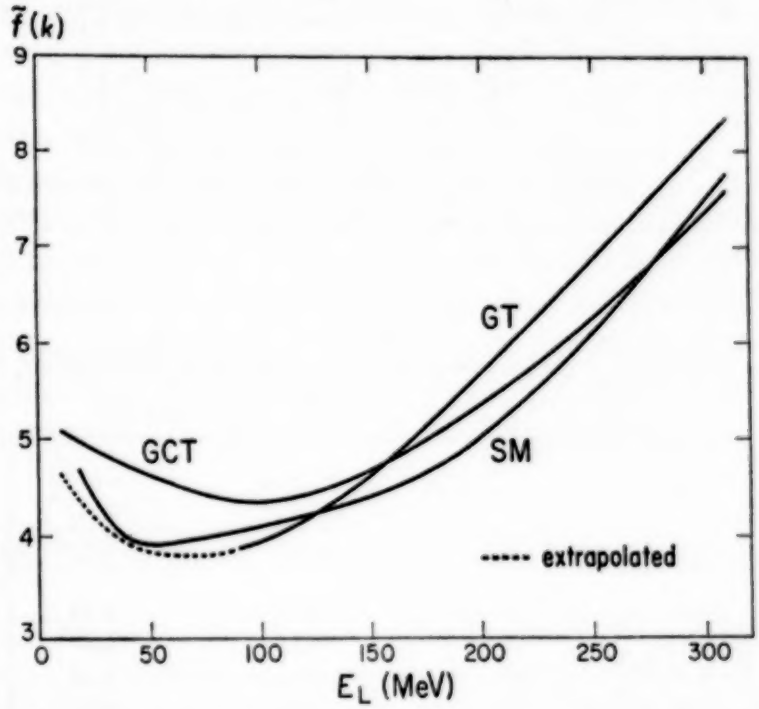

Fig. 1. The quantity $\tilde{f}(k)$ of eq. (17) as a function of the nucleon aboratory energy E_L for the Gammel-Christian-Thaler, Gammel-Thaler, and Signell-Marshak potentials. In the nonrelativistic approximation $E_L = 2\hbar^2 k^2/M$.

using the effective mass function $\mu(x, y)$ of eq. (30) with the constant parameters of Wada and Bey listed in the previous section and $\tilde{f}_{\mathrm{av}} \approx f(\frac{1}{2}r)$. The results are presented in table 1.

The incoming neutron laboratory energies E_0 in table 1 being equal to the energies in the medium were computed with the use of the single particle potential of Wada and Bey as

$$E_0 = \frac{\hbar^2 k_0^2}{2M} + V(k_0) = \frac{\hbar^2 k_0^2}{2M} + \tfrac{1}{2}\frac{ck_0^2 - b}{(1+ak_0^2)}. \tag{31}$$

In order to realize the effect of the effective mass function $\mu(x, y)$, Im $V_{\mathrm{MFM}}(k)$ was computed also for the case $\mu \equiv 1$. The results for the GCT potential are listed in table 2. By comparison with table 1 we observe that Im $V_{\mathrm{MFM}}(k_0)$ for $\mu \equiv 1$ is deeper and varies much less with energy. However, it still increases monotonically with increasing E_0.

TABLE 1

Im $V_{\mathrm{MFM}}(k_0)$ as a function of the incoming neutron energy E_0 for the nucleon-nucleon potentials of Gammel-Christian-Thaler [15]), Gammel-Thaler [10]) and Signell-Marshak [11])

ν	E_0(MeV)	Im $V_{\mathrm{MFM}}(k_0)$ (MeV)		
		GCT	GT	SM
1.5	41	−10.7	−9.2	−9.6
1.75	78	−13.9	−12.6	−13.1
2.0	118	−15.8	−15.6	−15.1
2.5	202(−15)	−19.5	−20.7	−19.1
3.0	291(−15)	−25.1	−27.7	−25.4

The (−15) for $\nu = 2.5$ and 3 in the second column correspond to the fact that for these energies the potential of Wada and Bey is a poor approximation; we take $E_0 = \hbar^2 k_0^2/2M - 15$ MeV, as the average separation energy is −15 MeV.

TABLE 2

Im $V_{\mathrm{MFM}}(k_0)$ as a function of the incoming neutron energy as computed from the GCT phase shifts for $\mu \equiv 1$ and its ratio to Im $V^{nx}_{\mathrm{MFM}}(k_0)$

ν	$E_0 = \frac{\hbar^2 k_0^2}{2M} - 15$ (MeV)	Im $V_{\mathrm{MFM}}(k_0)$ (MeV)	$\frac{\mathrm{Im}V_{\mathrm{MFM}}(k_0)}{\mathrm{Im}V^{nk}_{\mathrm{MFM}}(k_0)}$
1.5	25	−14.6	0.38
1.75	52	−17.6	0.52
2.0	82	−19.3	0.62
2.5	155	−22.4	0.76
3.0	244	−27.3	0.83

In order to check the goodness of the $\tilde{f}_{\mathrm{av}} \approx \tilde{f}(\frac{1}{2}\nu)$ approximation we used a graphical interpolation curve fitting $\tilde{f}(x)$ for the GCT case of fig. 1. For the typical point $\nu = 2$ we obtain in this case Im $V_{\mathrm{MFM}}(k_0 = 2k_{\mathrm{F}}) \approx -16.2$ MeV as compared with −15.8 MeV in the $\tilde{f}_{\mathrm{av}} \approx \tilde{f}(\frac{1}{2}\nu)$ approximation.

Let us now compare our results with the "classical" results of Clementel and Villi [13]) based on the method of Goldberger [17]). The main qualitative difference between the V_1 of these authors and our Im $V_{\mathrm{MFM}}(k_0)$ is that their V_1 increases with E_0 only up to about 80 MeV and at about 100 MeV it starts decreasing while our Im $V_{\mathrm{MFM}}(k_0)$ increases monotonically with increasing E_0 even for $\mu \equiv 1$ at least up to $E_0 \approx 300$ MeV. The main reason for this is that (in our

notation) the assumption of these authors can be written as

$$\tilde{f}_{\mathrm{CV}}(x) \approx \frac{6.63x^2}{0.00834+x^2} \approx 6.63. \tag{32}$$

In other words their $\tilde{f}(x)$ is a constant while all the functions $\tilde{f}(x)$ for the cases GCT, GT and SM increase monotonically with increasing x for large x. A function $\tilde{f}(x)$ similar to $\tilde{f}_{\mathrm{CV}}(x)$ is also considered by Lane and Wandel [14]). It should be mentioned that also V_{CI} of Riesenfeld and Watson [3]) is a function increasing monotonically with energy.

Even if Im $V_{\mathrm{MFM}}(k_0)$ were a fair approximation to the imaginary potential no conclusive evidence for or against any of the considered cases could be presently available. There is only a few data available for light and some medium heavy nuclei (compare the review article by Glassgold [18])) while only data on very heavy nuclei are relevant here. As we shall show below, unfortunately, Im $V_{\mathrm{MFM}}(k_0)$ can be hardly expected to be a fair approximation to the imaginary potential, anyway.

In conclusion we display the effect of the exclusion principle alone on Im $V_{\mathrm{MFM}}(k_0)$ on the typical example $\mu \approx$ const, $\tilde{f}_{\mathrm{av}} \approx \tilde{f}(\frac{1}{2}v)$. The ratios of Im $V_{\mathrm{MFM}}(k_0)$ to Im $V^{nx}_{\mathrm{MFM}}(k_0)$ differing from the former only by removing the exclusion principle operator Q from the integrations are presented in column 4 of table 2. We can readily see that the Q operator is of fundamental importance for Im $V_{\mathrm{MFM}}(k_0)$ except for the highest energies. The results of column 4 are in essential agreement with the results of Verlet and Gavoret [4]).

5. Effects of the Nonhermicity of t_0 on Im $V_1(k_0)$

In section 2 we have presented the contribution to Im $V_1(k_0)$ of the "nonhermicity of t_0 "corrections Δ_a and Δ_b to the first iteration matrix $\langle \mathbf{k}|t_1|\mathbf{k}\rangle_K$. Unfortunately, in the case of the realistic two-body forces of section 4 we cannot evaluate $\langle \mathbf{k}|\Delta_b|\mathbf{k}\rangle_K$ because the off-energy-shell elements of t_0 have not been available until now. One could try to perform some estimates by using certain rather arbitrary form-factors to imitate the extension of $\langle \mathbf{k}|t_0|\mathbf{k}\rangle$ to $\langle \mathbf{k}''|t_0|\mathbf{k}(k \neq k'')\rangle$ as certain extrapolations, or else employ the $\langle \mathbf{k}''|t_0|\mathbf{k}(k=k'')\rangle$-matrix of Gel'fand and Levitan [7]) which was discussed by Fulton and Schwed [6]) in their theory of the neutron-deuteron scattering. Unfortunately, the latter t_0 matrix applies only to low energies and is not relevant to our high energy problem except for only rough qualitative estimates.

We shall now discuss the quantity Im $(V_{\mathrm{MFM}}+V_a)$ which corresponds to $\langle \mathbf{k}|t_{\mathrm{MFM}}+\Delta_a|\mathbf{k}\rangle_K$. Since we find that it is not practical here to use the optical theorem and to calculate t_{MFM} and Δ_a separately, we go back to our original eq. (5). The imaginary part of this equation after the Δ_b part has been omitted

takes the form

$$\operatorname{Im}\langle \mathbf{k}|t_{\mathrm{MFM}}+\Delta_{\mathrm{a}}|\mathbf{k}\rangle_K = \operatorname{Im}\langle \mathbf{k}|t_0|\mathbf{k}\rangle - \frac{\pi M k}{2\hbar^2}\int \mathrm{d}\Omega_{\mathbf{k}''} F_Q(\mathbf{k}, k\mathbf{k}''/k''; \mathbf{K}) \times \operatorname{Re}\{\langle \mathbf{k}|t_0|k\mathbf{k}''/k''\rangle\langle k\mathbf{k}''/k''|t_0|\mathbf{k}\rangle\}. \tag{33}$$

Let us now introduce the notation

$$J' = \operatorname{Re}\{\langle \mathbf{k}|t_0|k\mathbf{k}''/k''\rangle\langle k\mathbf{k}''/k''|t_0|\mathbf{k}\rangle\}_{\mathrm{av}}, \tag{34}$$

where the subscript "av" denotes the proper avarage over spin and isobaric spin states. In eqs. (33) and (5) the spin and isobaric spin dependence of the t-matrices has been dropped for the sake of simplicity. The calculation of J' follows closely our earlier calculation of the analogical quantity J in section 3. We write J' in the form $J' = \sum_L A'_L P_L(\cos\vartheta)$, and similarly as in section 3 we drop higher L terms since they involve higher phase shifts and generally smaller interference terms. That means we approximate J' by

$$J' \approx A'_0 = (\hbar^2/2\pi^2 M)^2 \tilde{f}'(k)/8k^2, \tag{35}$$

where we have introduced the quantity $\tilde{f}'$ analogical to the quantity $\tilde{f}$ of eq. (17). Similarly as in section 3 we express A'_0 in terms of the nucleon-nucleon phase shifts. The expression obtained for A'_0 differs from the expression (17) for A_0 only in that each of the $\sin^2\delta(\eta)$ of eq. (17) must be multiplied by the corresponding $\cos 2\delta(2\eta)$.

Now using the procedure, technique and notation of section 3 we can write the final expression for the corresponding part of the optical potential $\operatorname{Im}(V_{\mathrm{MFM}}+V_{\mathrm{a}})$ for $\nu \geqq \sqrt{2}$ as:

$$\operatorname{Im}(V_{\mathrm{MFM}}+V_{\mathrm{a}}) \approx -\frac{2}{\pi\nu}\frac{\hbar^2 k_{\mathrm{F}}^2}{M}\left\{2\int_{\frac{1}{2}(\nu-1)}^{\frac{1}{2}(\nu+1)} \mathrm{d}x \tilde{f}(x)\left(\frac{1-\nu^2}{4}+\nu x-x^2\right) - \int_{\frac{1}{2}(\nu-1)}^{\frac{1}{2}(\nu+1)}\frac{\mathrm{d}x}{x}\tilde{f}'(x)\int_{\nu-x}^{\sqrt{\frac{1}{2}(1+\nu^2)-x^2}} \mathrm{d}y\mu(x,y)\left[x^2+y^2-1-\frac{2xy}{\mu(x,y)}\right]\right., \tag{36}$$

or:

$$\operatorname{Im}(V_{\mathrm{MFM}}+V_{\mathrm{a}}) = -\frac{2}{\pi\nu}\frac{\hbar^2 k_{\mathrm{F}}^2}{M}\left\{2\int_{\frac{1}{2}(\nu-1)}^{\frac{1}{2}(\nu+1)} \mathrm{d}x[\tilde{f}(x)-\tilde{f}'(x)]\left(\frac{1-\nu^2}{4}+\nu x-x^2\right) + \int_{\frac{1}{2}(\nu-1)}^{\frac{1}{2}(\nu+1)}\frac{\mathrm{d}x}{x}\tilde{f}'(x)\int_{\nu-x}^{\sqrt{\frac{1}{2}(1+\nu^2)-x^2}} \mathrm{d}y\mu(x,y)(x^2+y^2-1)\right\}. \tag{37}$$

In the region of ν where $\tilde{f}(x)$ and $\tilde{f}'(x)$ are slowly varying functions of x and can be approximately replaced by their average values in the x-interval $[\frac{1}{2}(\nu-1), \frac{1}{2}(\nu+1)]$, equal to $\tilde{f}_{\mathrm{av}}$ and $\tilde{f}'_{\mathrm{av}}$, respectively, and also if $\mu(x, y) \approx \bar{\mu}(\nu)$,

we can write:

$$\mathrm{Im}(V_{\mathrm{MFM}}+V_{\mathrm{a}}) \approx -\frac{2}{\pi\nu}\frac{\hbar^2 k_{\mathrm{F}}^2}{M}\{\tfrac{1}{3}(\tilde{f}_{\mathrm{av}}-\tilde{f}'_{\mathrm{av}})+\tilde{f}'_{\mathrm{av}}\bar{\mu}(\nu)G\}, \tag{38}$$

where G is given by eq. (26). A calculation of this type was performed using the SM phase shifts. In the rather rough approximation of eq. (38) we obtain: Im $(V_{\mathrm{MFM}}+V_{\mathrm{a}}) \approx -17.5$ MeV for $\nu = 2$ and ≈ -30 MeV for $\nu = 3$. If we compare these numbers with the respective numbers of table 1, i.e., -15.1 MeV for $\nu = 2$ and -24.4 MeV for $\nu = 3$, we see that Im V_{a} is important even at energies as high as 280 MeV, where Im V_{MFM} may be still a poor approximation unless Im V_{b} is of opposite sign to Im V_{a} and cancels most of the effect of Im V_{a}.

Let us in turn consider a model example. The separable nucleon-nucleon interaction enables us to calculate the t_0-matrix exactly and to go around the difficulty of the off-energy-propagation. Im $V_1(k_0)$ can be now calculated with no approximation and compared with the exact Im $V(k_0)$ as obtaind in ref. [4]). The Yamaguchi potential of ref. [4]) was used and $M^* = M$. The explicit analytical expressions for the imaginary potential Im V_{a} and Im V_{b} (corresponding to Δ_{a} and Δ_{b}) are given in the appendix. The final numerical results obtained indicate that at least for this particular model the total contribution of Im $(V_{\mathrm{a}}+V_{\mathrm{b}})$ is large except for high energies ($\nu \gtrsim 3$). In fact, this contribution even largely excedes the magnitude of Im V_{MFM} at low and medium energies. Both Im V_{a} and Im V_{b} are of the same sign and the same order of magnitude. They increase the imaginary well depth too much which indicates that the convergence of our iteration procedure is poor except for high energies. On the other hand, the Yamaguchi potential greatly underestimates Im V_{MFM} which is known from ref. [4]). For $\nu = 3$ it is found that Im $V_{\mathrm{MFM}} = -2.8$ MeV, while Im V_1 = Im $(V_{\mathrm{MFM}}+V_{\mathrm{a}}+V_{\mathrm{b}}) = -(2.8+0.46+0.34)$ MeV $= -3.6$ MeV. On the other hand, the exact imaginary potential in this case is Im $V = -3.1$ MeV which is closer to Im $(V_{\mathrm{MFM}}+V_{\mathrm{a}})$ than to Im V_{MFM}. However, Im V_1 overestimates Im V by about 16 %.

It seems to be obvious from the above discussions that the convergence of the series of eq. (4) is very poor at low energies and rather good at high energies. In the medium energy region one should consider at least the second iteration correction term following from eq. (4):

$$\langle \mathbf{k}|\Delta_2 t|\mathbf{k}\rangle_K = \int \mathrm{d}\mathbf{k}'''\langle \mathbf{k}|t_0|\mathbf{k}'''\rangle\left[\frac{Q}{e}(\mathbf{k},\mathbf{k}''';\mathbf{K})-\frac{1}{a}(\mathbf{k},\mathbf{k}''')\right]$$
$$\times\int \mathrm{d}\mathbf{k}''\langle \mathbf{k}'''|t_0|\mathbf{k}''\rangle\left[\frac{Q}{e}(\mathbf{k}'',\mathbf{k}''';\mathbf{K})-\frac{1}{a}(k'',k''')\right]\langle \mathbf{k}''|t_0|\mathbf{k}\rangle. \tag{39}$$

In order to compute even the imaginary part of this operator one has to know the off-energy-shell matrix elements of t_0. The only very rough estimate of Im $\langle \mathbf{k}|\Delta_2 t|\mathbf{k}\rangle_K$ was obtained for the case $K \approx 0$, $k = 1.1\, k_{\mathrm{F}}$ (the low energy

limit). The S-state phase shifts only, and the effective mass of Wada and Bey [16]) were used. The off-energy-shell behaviour of t_0 was imitated by weighting form factors of the Yamaguchi type. In this particular case the ratio $[\mathrm{Im}\langle \mathbf{k}|\Delta_2 t|\mathbf{k}\rangle_{K\approx 0}/\mathrm{Im}\langle \mathbf{k}|t_{\mathrm{MFM}}|\mathbf{k}\rangle_{K\approx 0}] \approx -8\,\%$. This, of course, does not mean that the total contribution of $\Delta_2 t$ to the optical potential must be small, and the problem remains open until the knowledge of $\langle \mathbf{k}|t_0|\mathbf{k}''(k''\neq k)\rangle_K$ is gained.

Except for the high energies it is perhaps more practical to employ the knowledge of the Brueckner reaction matrix for the GT potential [19, 20]) by using the well known integral equation relating the t matrix to the reaction matrix [21]). This procedure has already been applied by Shaw [22]).

6. The Real Part of the Optical Potential

Using eq. (11) we can write the real part of the t matrix to first order of our iteration procedure:

$$\mathrm{Re}\,\langle \mathbf{k}|t_1|\mathbf{k}\rangle_K = \mathrm{Re}\langle \mathbf{k}|t_0|\mathbf{k}\rangle + \mathrm{Re}\langle \mathbf{k}|\Delta_a+\Delta_b|\mathbf{k}\rangle_K. \tag{40}$$

Since the first order corrections of the exclusion principle and the self-consistency, i.e., Δ_a and Δ_b, are not expected to be large percentagewise particularly at higher energies (though they are certainly an open problem), we have only calculated the zero order potential

$$\mathrm{Re}\,V_0(k_0) = 4\int^{<k_F} \mathrm{d}\varkappa\ \mathrm{Re}\langle \mathbf{k}|t_0|\mathbf{k}\rangle. \tag{41}$$

Riesenfeld and Watson [3]) give the explicit expression for the weighted average of $\mathrm{Re}\,\langle \mathbf{k}|t_0|\mathbf{k}\rangle$ over the spin and isobaric spin states. However, in the approximation of these authors, one does not perform the $\varkappa$-integration, but rather one replaces the right hand side of eq. (41) by its high energy limit asymptotic value equal to $(2\pi)^3\rho_0\ \mathrm{Re}\,\langle \frac{1}{2}\mathbf{k}_0|t_0|\frac{1}{2}\mathbf{k}_0\rangle$, ρ_0 being the normal nuclear density. The expression analogous to that for t_{MFM} of eq. (21) is:

$$\{\mathrm{Re}\langle \mathbf{k}|t_0|\mathbf{k}\rangle\}_{\mathrm{av}} = -(\hbar^2/2\pi M)\bar{d}(k)/16k, \tag{42}$$

where $\bar{d}(k)$ is exactly of the form of the curly bracket factor of eq. (17) for A_0 with $\sin^2\delta(\eta)$ replaced everywhere by $\sin 2\delta(2\eta)$. In our previous notation the final result is of the form

$$\mathrm{Re}\,V_0(k_0) = -\frac{2}{\pi v}\frac{\hbar^2 k_F^2}{M}\int_{\frac{1}{2}(v-1)}^{\frac{1}{2}(v+1)} \mathrm{d}x\bar{d}(x)\left(\frac{1-v^2}{4}+vx-x^2\right). \tag{43}$$

This quantity was computed for the three potentials: GCT, GT and SM as a function of the incoming nucleon energy. The density parameter was used the same as in section 4. The results are shown in fig. 2. The curves for the GT and SM cases are similar to those given by Ohnuma [8]) for the C^{12} target nucleus

from the Riesenfeld and Watson [3]) formula for the real part of the optical potential. Our well depths are higher than Ohnuma's, one reason for that being a factor ≈ 1.24 arising from the difference in the nuclear density assumed. It is well known that usually the higher the density (k_F) the deeper and steeper the real nuclear potential (compare, e.g., Wada and Bey [16])). In fact, one of the reasons for our Re $V_0(k_0)$'s being too "flat" may be that our density is too small. Usually the real potential is expected to fall off to zero at energies E_0 not far above 300 MeV.

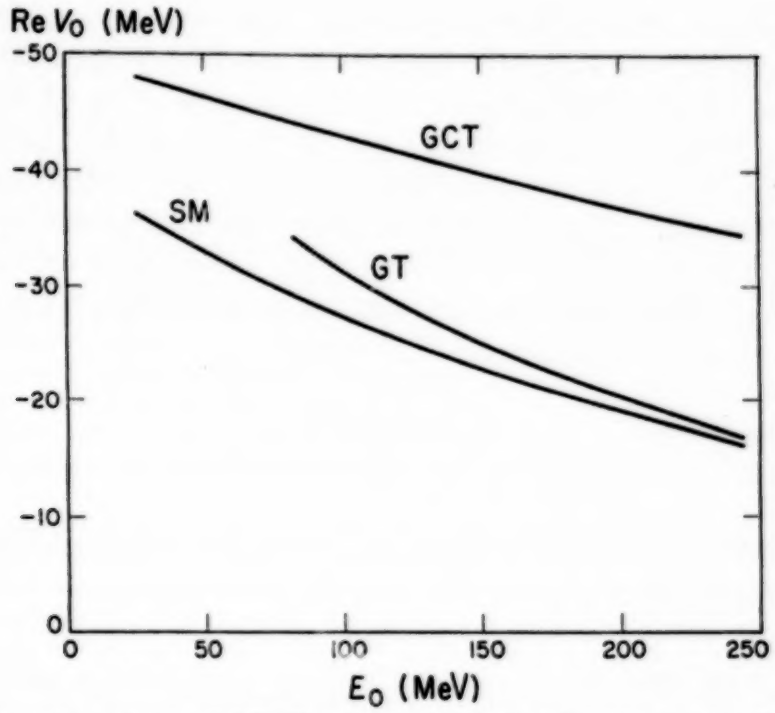

Fig. 2. The zero order real potential Re V_0 as a function of the laboratory energy E_0 of the scatter ing nucleon for the Gammel-Christian-Thaler, Gammel-Thaler, and Signell-Marshak potentials. Here we have set $E_0 = E_L$.

Our curves for the GT and SM cases are very similar and the GCT curve being the least realistic case is definitely too "flat" and lies too high. The real potential well corresponding to the unrealistic Feshbach and Lomon [12]) phase shifts was computed as a function of energy by Riesenfeld and Watson [3]). Their well depth seems to be unusually small (compare their fig. 3).

The self-consistency effect considered in section 4 was based on the assumption that our computed real potential would be rather close to the single particle potential of Wada and Bey [16]) shown in their fig. 2a. In fact our Re $V_0(k_0)$ for the GT and SM cases is close to Wada and Bey's "V" only at low energies. However, in any case, the uncertainty in the function $\mu(x, y)$ is of no fundamental importance for the imaginary potential Im $V_{MFM}(k_0)$.

Our Re $V_0(k_0)$ differs significantly from the real nuclear potential obtained for the GT case by Brueckner and Gammel [19]) who have taken into account the

effect of the identity of particles (compare their fig. 4). It is not clear, however, how much of the discrepancy is due to our approximate treatment of the identity of particles and self-consistency effects on one hand, and to other approximations such as the neglect of the difference between the t-matrix and the reaction matrix, or taking into account only S and D phase shifts — in ref. [19]) — on the other hand. In addition, the density used in ref. [19]) is considerably higher than ours. It is also possible that some of this discrepancy may be blamed on the effect of $\Delta_a+\Delta_b$ and of higher order terms of the expansion (4).

The authors feel greatly indebted to Dr. D. Kunz for his numerical computation of the quantity Im V_b for the Yamaguchi potential on the IBM 650 electronic computer of the University of Washington. One of us (J. D.) is greatly indebted to Professor R. Peierls for his comments on the optical theorem. One of us (J. S.) wishes to acknowledge private communications from Drs. P. Mittelstaedt and G. Shaw, and discussions with Professor K. A. Brueckner and Professor S. A. Moszkowski. The authors express their sincere thanks to Professor J. S. Blair and the members of his Department for their warm hospitality at the University of Washington.

Appendix

CALCULATION OF IM V_a AND V_b FOR THE SEPARABLE TWO-BODY POTENTIAL AND $M^* = M$

The separable potential considered here corresponds to S-state interactions. We can use the notation: $\langle \mathbf{k}|t_0|\mathbf{k}\rangle = t_0(k)$. Consequently we have:

$$\operatorname{Im} V_a = -\frac{(4\pi)^5 M^2}{2\hbar^4 k_0}\int_{\frac{1}{2}(k_0-k_F)}^{\frac{1}{2}(k_0+k_F)} \mathrm{d}k'' k''^3 \operatorname{Im} t_0(k'')|t_0(k'')|^2 \int_{k_0-k''}^{\sqrt{\frac{1}{4}(k_0^2+k_F^2)-k''^2}} \mathrm{d}u\, u(\alpha_0-1). \tag{A.1}$$

The symbol α_0 is defined in subsection 3.2 of the present paper. Let us introduce the dimensionless notation of sections 3—6 in which $t_0(x) = -\tilde{\lambda}(\hbar^2/Mk_F)[A(x)+iB(x)]$, where $A(x)$ and $B(x)$ are dimensionless and $\tilde{\lambda} = \lambda/k_F^3$, where λ is the Yamaguchi parameter [4]). The potential is $\langle \mathbf{k}'|v|\mathbf{k}\rangle = -\lambda(\hbar^2/M)g(k')g(k)$, where $g(k) = (k^2+\beta^2)^{-1}$. Using the method and notation of section 3 one arrives at the final result valid for $\nu \geqq \sqrt{2}$:

$$\operatorname{Im} V_a = 8(2\pi)^5\tilde{\lambda}^3\frac{\hbar^2 k_F^2}{M}\frac{1}{\nu}\int_{\frac{1}{2}(\nu-1)}^{\frac{1}{2}(\nu+1)} \mathrm{d}x x^2 B(x)[A(x)^2+B(x)^2]\{\sqrt{\tfrac{1}{2}(1+\nu^2)-x^2} \times [\tfrac{1}{6}(\nu^2-5)+\tfrac{2}{3}x^2]+\nu(1-\tfrac{1}{3}\nu^2)+\tfrac{3}{2}x(\nu^2-1)-4\nu x^2+\tfrac{10}{3}x^3\}. \tag{A.2}$$

A similar calculation yields the following result for Im V_b: a) for $\nu \geqq 3$:

$$\operatorname{Im} V_b = \frac{\hat{c}}{\nu}\int_{\nu(\nu-1)}^{\frac{1}{2}(\nu+1)} \mathrm{d}x x \int_{\nu-x}^{\sqrt{\frac{1}{2}(\nu^2+1)-x^2}} \mathrm{d}y \int_{y-1}^{y+1} \mathrm{d}z \frac{z}{x^2-z^2}[(y-z)^2-1] \times [A(x)B(z)+A(z)B(x)], \tag{A.3}$$

b) for $\nu \leqq 3$

$$\operatorname{Im} V_{\mathrm{b}} = \frac{\hat{c}}{\nu}\left\{\left[\int_{\frac{1}{2}(\nu-1)}^{\frac{1}{2}(\nu+1)} \mathrm{d}x x \int_{\nu-x}^{\sqrt{\frac{1}{2}(1+\nu^2)-x^2}} \mathrm{d}y \int_{y-1}^{y+1} \mathrm{d}z + \int_{\nu-1}^{\frac{1}{2}(\nu+1)} \mathrm{d}x x \int_{1}^{\sqrt{\frac{1}{2}(1+\nu^2)-x^2}} \mathrm{d}y \int_{y-1}^{y+1} \mathrm{d}z \right.\right.$$
$$\left.\left. + \int_{\nu-1}^{\frac{1}{2}(\nu+1)} \mathrm{d}x x \int_{\nu-x}^{1} \mathrm{d}y \int_{\sqrt{1-y^2}}^{y+1} \mathrm{d}z\right] [(y-z)^2-1] - 2\int_{\nu-1}^{\frac{1}{2}(\nu+1)} \mathrm{d}x x \int_{\nu-x}^{1} \mathrm{d}y y \int_{0}^{\sqrt{1-y^2}} \mathrm{d}z z\right\}$$
$$\times \frac{z}{x^2-z^2}[A(x)B(z)+A(z)B(x)], \qquad \text{(A4)}$$

where $\hat{c} = (16\pi)^2 \tilde{\lambda}^2 \hbar^2 k_{\mathrm{F}}^2/2M$.

References

1) J. Dąbrowski and J. Sawicki, Nuclear Physics **13** (1959) 621
2) P. Mittelstaedt, Nuclear Physics **17** (1960) 499, see also Proc. International Conference on the Nuclear Optical Model, Tallahassee, 1959
3) W. B. Riesenfeld and K. M. Watson, Phys. Rev. **102** (1956) 1157
4) L. Verlet and J. Gavoret, Nuovo Cim. **10** (1958) 505
5) V. M. Galitskii, JETP (USSR) **34** (1958) 151
6) T. Fulton and P. Schwed, Phys. Rev. **115** (1959) 973
7) I. M. Gel'fand and B. M. Levitan, Doklady Akad. Nauk S.S.S.R. **77** (1951) 557
8) S. Ohnuma, Phys. Rev. **111** (1958) 1173
9) A. M. Saperstein and D. Feldman, Nuovo Cim. **14** (1959) 457
10) J. L. Gammel and R. M. Thaler, Phys. Rev. **107** (1957) 1337
11) P. S. Signell and R. E. Marshak, Phys. Rev. **109** (1958) 1229
12) H. Feshbach and E. Lomon, Phys. Rev. **102** (1956) 891
13) E. Clementel and C. Villi, Nuovo Cim. **2** (1955) 176
14) A. M. Lane and C. F. Wandel, Phys. Rev. **98** (1955) 1524
15) J. L. Gammel, R. S. Christian and R. M. Thaler, Phys. Rev. **105** (1957) 311
16) W. W. Wada and P. P. Bey, preprint
17) M. L. Goldberger, Phys. Rev. **74** (1948) 1269
18) A. E. Glassgold, Rev. Mod. Phys. **30** (1958) 419
19) K. A. Brueckner and J. L. Gammel, Phys. Rev. **109** (1958) 1023
20) K. A. Brueckner, J. L. Gammel and H. Weitzner, Phys. Rev. **110** (1958) 431
21) B. Lippman and J. Schwinger, Phys. Rev. **79** (1950) 469
22) G. L. Shaw, Bull. Am. Phys. Soc. Vol. 4 (1959) no. 1, p. 49; Annals Phys. **8** (1959) 509; and private communication; after this work was completed also another paper on the same subject appeared: A. K. Kerman, H. Mc Manus and R. M. Thaler, Annals Phys. **8** (1959) 551

2.B

Nuclear Physics **22** (1961) 336—338; ©*North-Holland Publishing Co., Amsterdam*

Not to be reproduced by photoprint or microfilm without written permission from the publisher

THE PERSISTENCE OF NUCLEAR POLARIZATION PRODUCED BY THE CAPTURE OF POLARIZED THERMAL NEUTRONS

A. H. WAPSTRA † and D. W. CONNOR

Argonne National Laboratory, Lemont, Illinois

Received 30 September 1960

Abstract: The relation between observed beta asymmetry and the static magnetic guide field is investigated for the capture of neutrons by ^{7}Li, ^{19}F and ^{27}Al.

Among the early demonstrations of parity nonconservation in beta decay was the observation by Burgy *et al.* [1]) of a directional asymmetry in the beta decay of the ^{8}Li nuclei produced when polarized neutrons were captured by ^{7}Li. The effect, whose observability requires that the nuclear polarization persist for a time comparable to the ^{8}Li half-life, 0.8 sec, was detectable only with fresh samples of the Li_2CO_3 and LiF powders used. The complete attenuation of the observed asymmetry in the course of about 30 minutes irradiation is probably to be explained by the rapid build-up of paramagnetic centres in the sample, due to the fast neutrons and pile gammas with which the polarized beam was contaminated [2]). It is well known from the work of Bloembergen [3]) that paramagnetic impurities can produce relaxation times much less than 1 sec.

Recently Connor has been able to perform a magnetic resonance measurement of the ^{8}Li nuclear magnetic moment [4]) by using the beta asymmetry effect as an indicator of the nuclear polarization. Using a neutron beam which had been polarized by reflection from a magnetized cobalt mirror [5]) and consequently was quite free of contaminating hard radiations, he did not observe the sample aging remarked above.

In both observations of the ^{8}Li decay a static magnetic field at the sample served to decouple the nuclear moments of the polarized ^{8}Li nuclei from those of the surrounding nuclei, and to provide a guide field for the polarized neutrons to prevent their depolarization. We thought it interesting to investigate the relation between the observed beta asymmetry and this magnetic field; also, we tried to find similar effects in other substances that looked promising, especially in ^{19}F and ^{27}Al. The data of interest for these cases are given in table 1.

This table shows that in investigating these two nuclei one should not measure the beta rays during the irradiation as, contrary to the ^{7}Li case, the capture

† On leave from the Institute of Nuclear Physics Research in Amsterdam *and* the Technological University, Delft.

TABLE 1

Relevant data about neutrons capture in ^{7}Li, ^{19}F and ^{27}Al

Target	Nuclear spin		Reaction energy (keV)	Beta decay energy (keV)	Halflife (sec)	Computed Asymmetry	
	Initial	Final				Upper channel spin (%)	Lower channel spin (%)
^{7}Li	$\frac{3}{2}$	1	2033	16002	0.8	11	8
^{19}F	$\frac{1}{2}$	1	6599	7028	11	15	0
^{27}Al	$\frac{3}{2}$	1	7724	4640	140	11	8

gamma rays will give a large background in the beta scintillation counters at any discriminator setting. An automatic shutter system was therefore used to provide alternating irradiation and counting periods of the order of the decay halflives. The alternate irradiations were made with full ($\gtrsim$ 90 %) polarization and with an unpolarized neutron beam.

^{27}Al was investigated as powdered cubic oxyde. No effect was found. Probably, therefore, the relaxation time of ^{28}Al in this material is somewhat shorter than its halflife. Fluorine was used as a monocrystal of CaF_2, and Li in ^{7}LiF as before [4]); the effect of the beta rays of the unwanted activities (^{47}Ca, ^{49}Ca, ^{20}F) was eliminated by proper setting of the discriminator, as checked by following the halflives.

The results of the experiments are shown in fig. 1. The lines drawn through

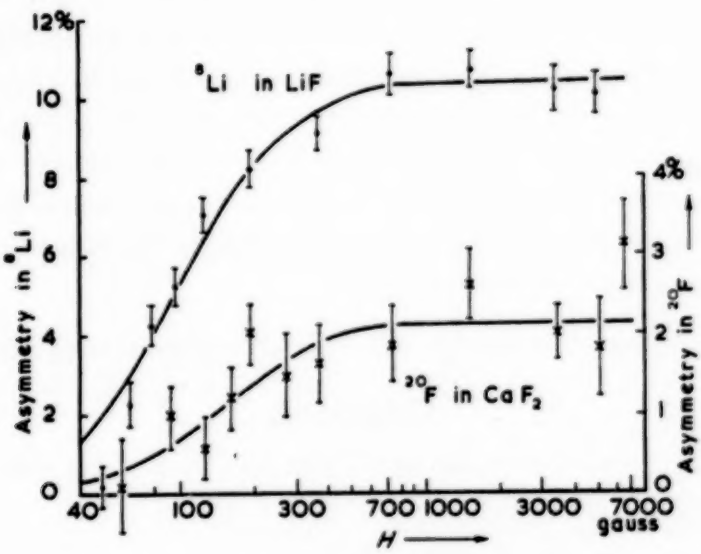

Fig. 1. Relation between the experimental asymmetry in the direction of the nuclear electrons emitted by Li^{8} and ^{20}F samples formed by capture of polarized neutrons, and the magnetic field strength at the samples.

the experimental points are theoretical ones, computed from the assumption that the decrease in the asymmetry observed at lower magnetic fields is due to depolarization of the nuclei with a relaxation time proportional to the square of the magnetic field,

$$\tau_{\text{relax}} = CH^2,$$

as it should be in first approximation if it is determined mainly by dipole interaction. The best values of C following from the above experiments are $(1.1\pm0.1)\times10^{-4}$ sec/Gauss^2 in LiF and $(7\pm3)\times10^{-4}$ sec/Gauss^2 for CaF_2. Since there is a possibility that part of the decrease may be due to depolarization of the neutron beam at lower guide fields, the above values should be considered as lower limits.

The maximum asymmetry in ^{8}Li, 10.4 ± 0.3 %, is somewhat larger than the values obtained before [1,4]) since, due to a better adjustment of the neutron slits, the neutron beam was less contaminated with depolarized or fast neutrons and gamma rays. The above value, compared with the theoretical data in table 1 computed from data given by Shapiro [6]), confirms earlier conclusions [6,7]) that the neutron capture in ^{7}Li occurs mainly, perhaps even exclusively, with channel spin 2. The maximum asymmetry in ^{20}F is 2.2 ± 0.3 %. From this, one can only conclude that channel spin 1 does occur; it may even occur exclusively. A large fraction of the ^{20}F nuclei may have so short a relaxation time that the asymmetry is not detectable, the observed effect being due entirely to a small fraction ($\gtrsim 15$ %) of the nuclei for which τ_r is relatively long. Plausibility is lent to this supposition by the following considerations. Recoil from the capture gamma imparts kinetic energy to the ^{20}F nucleus, 2 keV for the ground state transition and several hundred eV for most cascades. Consequently the typical nucleus is certainly dislodged from its lattice site. A small fraction of the displaced nuclei may come to rest at normal sites, either by occupying vacancies or "bumping" ^{19}F nuclei. The remainder may come to rest in interstitial positions where, since the symmetry is not cubic, the relaxation by quadrupole interaction may be rapid. In the case of ^{8}Li, quadrupole relaxation may be negligible because of the probably small quadrupole moment $Q(^6\text{Li}) \approx -0.002$. Clearly, further experiment will be necessary before the relative importance of the two explanations can be assessed.

It is a pleasure to acknowledge valuable discussions with Dr. T. B. Novey.

References

1) Burgy, Davidon, Novey, Perlow and Ringo, Bull. Am. Phys. Soc. **2** (1957) 206
2) T. B. Novey, private communication
3) N. Bloembergen, Physica **15** (1949) 386
4) D. Connor, Phys. Rev. Lett. **3** (1959) 429
5) D. J. Hughes and M. T. Burgy, Phys. Rev. **81** (1959) 498
6) F. L. Shapiro, Uspekhi Fiz. Nauk **65** (1958) 133
7) D. Kurath, Bull. Am. Phys. Soc. **2** (1957) 206

10.E *Nuclear Physics* **22** (1961) 339; © *North-Holland Publishing Co., Amsterdam*

ERRATUM

In a paper published by us in this journal (**16** (1960) 545) under the title "Nuclear shell model: Hartree-Fock approximation with Gammel-Thaler two-nucleon potential", the definition (1.8) of the $\mathbf{L}\cdot\mathbf{S}$ operator differs from that used by Gammel-Thaler by a factor 2. As a consequence, in our notation, the constants c_0, c_c given in table 2 should have been multiplied by $\frac{1}{2}$.

In the Gammel-Thaler potential employed in that work, there is a strong $\mathbf{L}\cdot\mathbf{S}$ term in the triplet-even potential, and it is pointed out that their triplet-even potential does not fit the deuteron data. This state of affairs has recently been clarified by Gammel and Thaler (Prog. Elementary Particles and Cosmic Ray Physics **5** (1960) 99; it seems that there is no real evidence for a strong $\mathbf{L}\cdot\mathbf{S}$ term in the triplet-even potential, as also found by Signell and Marshak.

If we simply remove the $\mathbf{L}\cdot\mathbf{S}$ term from the triplet-even potential in table 1, we then have, in table 2,

$$c_0+c_c = -\frac{7317.5}{2}\ \text{MeV}, \quad c_0-3c_c = 0$$

and (4.5) becomes

$$V^{LS} = -\frac{9}{2}(c_0+c_c)I_p. \tag{4.5}$$

Now we have $I_p = 3.13\times10^{-4}$, $I_d = 4.33\times10^{-5}$. The corrected results (4.15) to (4.17) now become

$$V^{LS} = \langle A|V^{LS}|A\rangle = 5.15\ \text{MeV}, \tag{4.15}$$

$$^2P_{\frac{3}{2}} - {}^2P_{\frac{1}{2}} = 3\xi V^{LS} = 15.8\ \text{MeV}, \tag{4.16}$$

$$E(^2P_{\frac{1}{2}}, O^{15}) = \bar{\mathscr{H}} - 2\xi V^{LS} = -104.5\ \text{MeV}. \tag{4.17}$$

The doublet separation is now more reasonable, but is still too big by a factor about $\frac{5}{2}$.

The writers are grateful to Dr. A. Azima for calling their attention to the discrepancy mentioned above.

G. E. Tauber and T. Y. Wu

10.E *Nuclear Physics* **22** (1961) 340; © *North-Holland Publishing Co., Amsterdam*

ADDENDUM AND ERRATUM

In an article with the title "On the density of eigenvalues of a random matrix" (this journal, **18** (1960) 420) we estimated the dominant behaviour of the density of eigenvalues of a random matrix of order n when n is large. However, the sum of the squares of the first n oscillator wave functions can be expressed explicitly [see Bateman manuscript project, Higher Transcendental functions, ed. by A. Erdélyi (New York, Toronto, London), Vol. 2, Ch. 10, and Szegö, Orthogonal Polynomials (New York)], so that the equation (36) of our article mentioned above may be replaced by

$$2mP\left(\frac{z}{\sqrt{2}}\right) = \sqrt{2}\left\{(2m-1)u^2_{2m-2}(z) - \sqrt{(2m-2)(2m-1)}\,u_{2m-3}(z)u_{2m-1}(z)\right\} + \sqrt{2m-1}\,u_{2m-1}(z)\int_0^z u_{2m-2}(x)\mathrm{d}x.$$

As asymptotic expansions of $u_n(x)$ for n large are known [apart from those already mentioned, one may see also F. Tricomi, Ann. Mat. Pura. Appl. **28** (1949) 263, and A. Erdélyi in Golden Jubilee Commemoration volume of the Indian Mathematical Society, 1959] for all the three cases according to whether $x > \sqrt{2n}$, $x \approx \sqrt{2n}$ or $x < \sqrt{2n}$, one can get not only the "semi-circle law", but higher terms as well.

A correction to be incorporated in our article: on page 427, twelfth line from above the factor before the bracket should read as

$$\sqrt{2n+2}/2(2n+1-z^2).$$

M. L. Mehta and M. Gaudin

We introduce a

PERSONAL SUBSCRIPTION SCHEME

for

NUCLEAR PHYSICS

8 volumes (1961, vols. 21—28) at the total price of $ 20.00 (£ 7.10.0)

Write for details

NORTH-HOLLAND PUBLISHING COMPANY

P.O. BOX 103 — AMSTERDAM, HOLLAND

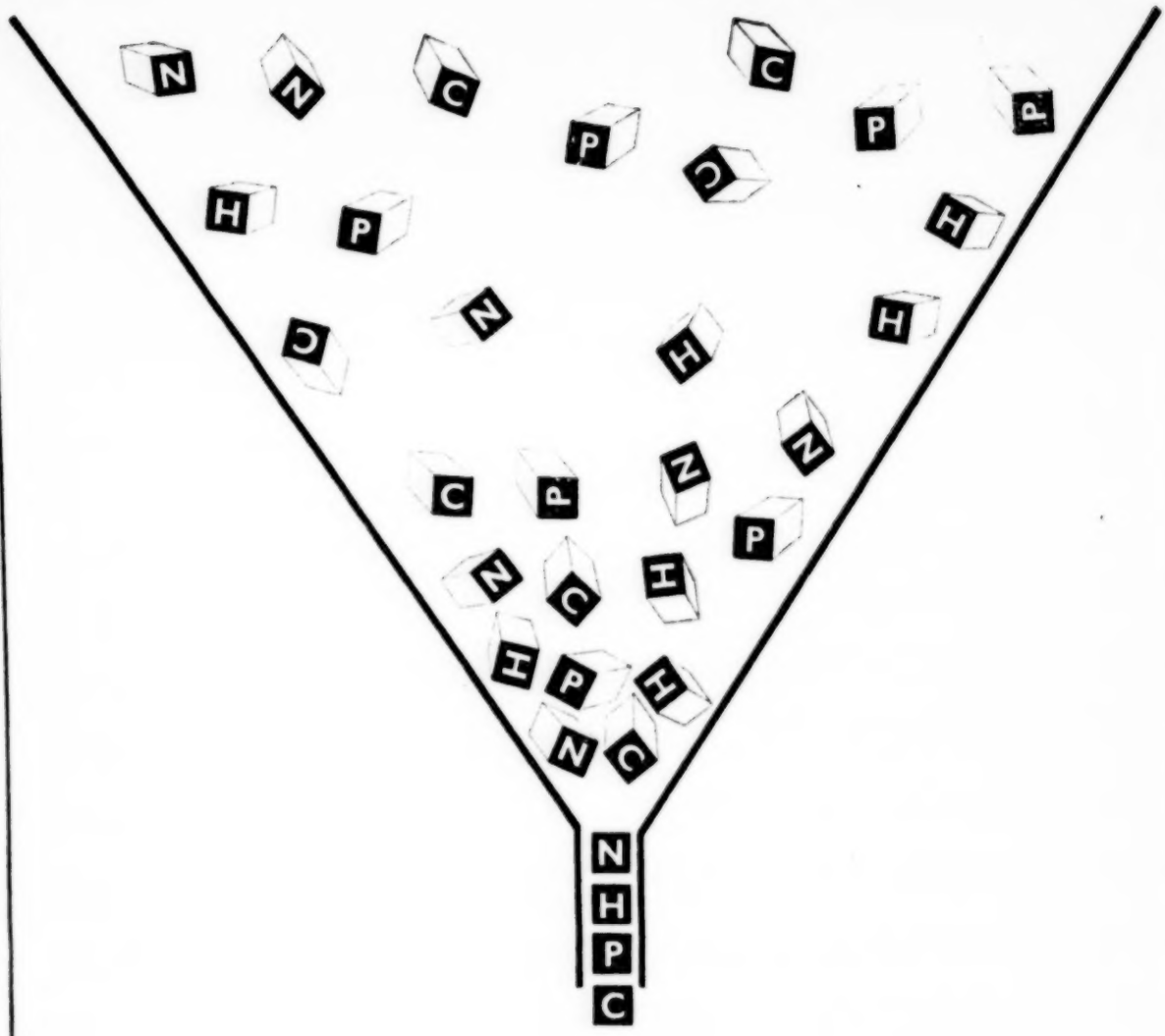

NEW BOOKS

J. L. SYNGE:
Relativity: The general theory

H. G. VAN BUEREN:
Imperfections in crystals

H. JONES:
The theory of Brillouin zones and electronic states in crystals

H. KALLMANN BIJL (Editor):
Space research (Proceedings Nice conference, 1960)

Send your order to your bookseller or directly to:

NORTH-HOLLAND PUBLISHING COMPANY - AMSTERDAM

Sole Agency in the U.S.A.: Interscience Publishers Inc. – New York